frontiers | Research Topics

Neuroimaging insights into the link between sleep disturbances and neuropsychiatric disorders

Edited by
Yuanqiang Zhu, HuaNing Wang, Karen M. von Deneen, Malgorzata Anna Garstka, Jun Chang Su and Tomas Hrbac

Published in
Frontiers in Psychiatry

ISSN 1664-8714
ISBN 978-2-8325-2990-4
DOI 10.3389/978-2-8325-2990-4

About Frontiers

Frontiers is more than just an open access publisher of scholarly articles: it is a pioneering approach to the world of academia, radically improving the way scholarly research is managed. The grand vision of Frontiers is a world where all people have an equal opportunity to seek, share and generate knowledge. Frontiers provides immediate and permanent online open access to all its publications, but this alone is not enough to realize our grand goals.

Frontiers journal series

The Frontiers journal series is a multi-tier and interdisciplinary set of open-access, online journals, promising a paradigm shift from the current review, selection and dissemination processes in academic publishing. All Frontiers journals are driven by researchers for researchers; therefore, they constitute a service to the scholarly community. At the same time, the *Frontiers journal series* operates on a revolutionary invention, the tiered publishing system, initially addressing specific communities of scholars, and gradually climbing up to broader public understanding, thus serving the interests of the lay society, too.

Dedication to quality

Each Frontiers article is a landmark of the highest quality, thanks to genuinely collaborative interactions between authors and review editors, who include some of the world's best academicians. Research must be certified by peers before entering a stream of knowledge that may eventually reach the public - and shape society; therefore, Frontiers only applies the most rigorous and unbiased reviews. Frontiers revolutionizes research publishing by freely delivering the most outstanding research, evaluated with no bias from both the academic and social point of view. By applying the most advanced information technologies, Frontiers is catapulting scholarly publishing into a new generation.

What are Frontiers Research Topics?

Frontiers Research Topics are very popular trademarks of the *Frontiers journals series*: they are collections of at least ten articles, all centered on a particular subject. With their unique mix of varied contributions from Original Research to Review Articles, Frontiers Research Topics unify the most influential researchers, the latest key findings and historical advances in a hot research area.

Find out more on how to host your own Frontiers Research Topic or contribute to one as an author by contacting the Frontiers editorial office: frontiersin.org/about/contact

Neuroimaging insights into the link between sleep disturbances and neuropsychiatric disorders

Topic editors

Yuanqiang Zhu — Fourth Military Medical University, China
HuaNing Wang — Fourth Military Medical University, China
Karen M. von Deneen — Xidian University, China
Malgorzata Anna Garstka — Xi'an Jiaotong University, China
Jun Chang Su — The Fourth Military Medical University
Tomas Hrbac — Neurochirurgická Klinika, Fakultní Nemocnice Ostrava, Czechia

Citation

Zhu, Y., Wang, H., von Deneen, K. M., Garstka, M. A., Su, J. C., Hrbac, T., eds. (2023). *Neuroimaging insights into the link between sleep disturbances and neuropsychiatric disorders*. Lausanne: Frontiers Media SA.
doi: 10.3389/978-2-8325-2990-4

Table of contents

frontiers | Frontiers in Psychiatry

TYPE Editorial
PUBLISHED 29 June 2023
DOI 10.3389/fpsyt.2023.1243486

OPEN ACCESS

EDITED AND REVIEWED BY
Stefan Borgwardt,
University of Lübeck, Germany

*CORRESPONDENCE
Karen M. von Deneen
✉ karen@xidian.edu.cn
Malgorzata A. Garstka
✉ m.garstka@xjtu.edu.cn

RECEIVED 20 June 2023
ACCEPTED 22 June 2023
PUBLISHED 29 June 2023

CITATION
von Deneen KM, Garstka MA, Hrbáč T, Zhu Y, Wang H and Su JC (2023) Editorial: Neuroimaging insights into the link between sleep disturbances and neuropsychiatric disorders. *Front. Psychiatry* 14:1243486. doi: 10.3389/fpsyt.2023.1243486

Editorial: Neuroimaging insights into the link between sleep disturbances and neuropsychiatric disorders

Karen M. von Deneen[1,2]*, Malgorzata A. Garstka[3,4]*, Tomáš Hrbáč[5], Yuanqiang Zhu[6], HuaNing Wang[7] and Jun Chang Su[8]

[1]Center for Brain Imaging, School of Life Science and Technology, Xidian University, Xi'an, Shaanxi, China, [2]International Joint Research Center for Advanced Medical Imaging and Intelligent Diagnosis and Treatment & Xi'an Key Laboratory of Intelligent Sensing and Regulation of Trans-Scale Life Information, School of Life Science and Technology, Xidian University, Xi'an, Shaanxi, China, [3]Core Research Laboratory, Department of Endocrinology, Xi'an, Shaanxi, China, [4]Department of Tumor and Immunology, Precision Medical Institute, Western China Science and Technology Innovation Port, School of Medicine, The Second Affiliated Hospital of Xi'an Jiaotong University, Xi'an, Shaanxi, China, [5]Neurochirurgická Klinika, Fakultní Nemocnice Ostrava, Ostrava, Czechia, [6]Department of Radiology, Xijing Hospital, Fourth Military Medical University, Xi'an, China, [7]Xijing Hospital, Fourth Military Medical University, Xi'an, China, [8]Department of Neurology, Tangdu Hospital, The Fourth Military Medical University, Xi'an, China

KEYWORDS

sleep disorders, neuropsychiatric disorders, neuroimaging, cognition, memory, attention, sleep, brain

Editorial on the Research Topic
Neuroimaging insights into the link between sleep disturbances and neuropsychiatric disorders

Sleep is a fundamental physiological process that plays a crucial role in maintaining overall health and wellbeing. Adequate and quality sleep is essential for cognitive functioning, emotional regulation, and various other aspects of human physiology. Sleep disturbances, on the other hand, have been associated with a wide range of neuropsychiatric disorders, including dementia, Parkinson's disease, major depressive disorder, bipolar disorder, post-traumatic stress disorder, attention deficit hyperactivity disorder, schizophrenia, and anxiety disorders. Despite significant research efforts, the underlying neural mechanisms of sleep, sleep disorders and the neurobiological consequences of sleep deprivation remain partially understood.

In recent years, neuroimaging modalities have provided unique insights into the neural correlates of sleep disturbances and neuropsychiatric disorders. Techniques such as electroencephalography (EEG), magnetoencephalography (MEG), functional magnetic resonance imaging (fMRI), and simultaneous EEG-fMRI studies have allowed researchers to examine the neural dynamics associated with sleep quality and quantity, as well as the structural and functional changes induced by sleep disturbances and neuropsychiatric diseases. These neuroimaging approaches have also facilitated investigations into how the brain adapts to these disorders and the potential consequences for mental health.

We are pleased that our special edition of this journal covers submissions predominantly from China, but also from Taiwan, Switzerland, Netherlands, Italy, Germany, UK, and USA. It brings together a Research Topic of articles that highlight the current state of research on sleep, sleep disturbances, and neuropsychiatric disorders using neuroimaging techniques. The studies cover a wide range of topics based upon the aims and objectives, including the mechanisms of sleep deprivation on cognitive functions and emotional state, the association between sleep disorders and depression, Alzheimer's disease, autism, and epilepsy, the impact of obstructive sleep apnea on mental health, the role of sleep spindles, the consequences of shift-work sleep disorders in the healthy population, and targeted treatments for insomnia and psychiatric diseases.

One area of research that has gained considerable attention is the impact of sleep disturbances on cognitive function and emotional regulation. Specific features of sleep, such as sleep spindles, have been found to be associated with memory consolidation and emotional processing. Neuroimaging findings revealed the neural mechanisms underlying these associations, shedding light on how sleep disturbances may contribute to cognitive and emotional impairments observed in various neuropsychiatric disorders. Patients with insomnia differed from healthy individuals in neural activity, and functional connectivity between the cholinergic and non-cholinergic sub-regions of the basal forebrain, suggesting that the basal forebrain plays an important role in sleep-wake regulation and may be implicated in cortical arousal and activation (Jiang et al.). Awakening was found to be accompanied by an increase in cerebrovascular reactivity and functional connectivity in the thalamus, insula, and primary motor cortex (Hsu et al.). Altered functional connectivity strength in patients with insomnia was associated with neuropsychological performance indicators and specific changes in gut microbiota composition, specifically genera *Alloprevotella, Lachnospiraceae,* and *Faecalicoccus* (Chen et al.). Sleep deprivation can lead to learning and memory impairment, reduced attention, and poor work performance. Individuals suffering from shift work disorder (SWD) displayed alterations in the fundamental architecture of interregional structural connectivity in the brain (Ning et al.). Sleep-deprived rats experienced weakened cognitive functions and memory that were related to impaired conventional protein kinase Cγ (cPKCγ)-neurogranin (Ng) signaling. Activation of the cPKCγ-Ng signal was shown to improve cognitive function and reduce memory impairment caused by sleep deprivation in rats (Xu et al.). Amygdala-based real-time fMRI neurofeedback training employed to treat insomnia patients reshaped neural activity and improved sleep quality in insomnia patients (Li Z. et al.).

Patients with insomnia are known to have a higher depression score, which was also seen in the studies in this Research Topic (Chen et al.; Jiang et al.). Two studies investigated pathophysiology of depression using fMRI. Guo X. et al. found that adolescents with depression had abnormal degree centrality in several brain regions, including the left superior temporal gyrus and right inferior parietal lobule. Patients with melancholic major depressive disorder with insomnia presented abnormal brain functional connectivity in multiple brain regions such as the right middle temporal gyrus, superior temporal gyrus, right middle occipital gyri, superior occipital gyri, right cuneus, bilateral lingual gyrus, and bilateral calcarine compared to healthy controls (Deng et al.). These studies highlight the potential of fMRI as a tool for identifying biomarkers of depression that may inform future research on treatment approaches for depression and could ultimately lead to more personalized and effective interventions. Indeed, fMRI was instrumental in identifying issues with neural activity in patients with depression and suicidal ideation (Tang et al.), postpartum depressive disorder (Zhang et al.), and late-life depression (Li H. et al.). Employing computational approaches, including network analysis and machine learning, the authors selected areas in the brain for treatment by target-transcranial magnetic stimulation (target-TMS) therapy that restored functional network connectivity, and allowed alleviation of depressive clinical symptoms (Tang et al.; Zhang Y. et al.). Brain connectivity in depression could also be improved with mindfulness-based cognitive therapy (MBCT). Patients with late-life depression who underwent MBCT experienced increased connectivity between the middle frontal gyrus and amygdala that corresponded to the reduction in depressive symptoms (Li H. et al.). TMS and MBCT are non-invasive and non-pharmacological interventions, and guided by neuroimaging, they could potentially relieve depression and improve the quality of life.

Besides depression, other psychiatric disorders are also accompanied by sleep disorders including epilepsy, Alzheimer's disease, schizophrenia, or autism. Guo M. et al. aimed to understand the relationship between temporal lobe epilepsy (TLE) and sleep disorders using MRI and diffusion kurtosis imaging. They found that TLE patients with sleep disorders had significantly higher mean diffusivity and radial diffusivity values in the left temporal lobe compared to TLE patients without sleep disorders. These findings suggest that there may be a link between TLE and sleep disorders, which could have implications for diagnosis and treatment.

In the systematic review, Liu et al. summarized studies that investigated structural and functional changes in the brain of Alzheimer's patients with sleep disorders. A range of imaging methods was reported, including MRI, single-photon emission computed tomography, multislice spiral computed tomography perfusion imaging, and 2-deoxy-2-(^{18}F)fluoro-D-glucose positron emission tomography (^{18}F-FDG-PET). They summarized that sleep disorders are common in Alzheimer's patients and may contribute to cognitive decline and other symptoms. The review also highlights several brain regions that are affected by sleep disorders in Alzheimer's patients, including the hippocampus, amygdala, and prefrontal cortex. Zhang A. et al. constructed an fMRI-based whole brain connectivity network to understand the neural mechanisms underlying the core symptoms of autism spectrum disorder (ASD) across different age groups. They identified that functional connectivity (FC) between the left superior occipital lobe and right angular, and the left insula and left caudate was related to the restricted and repetitive behaviors in individuals with ASD, and the decrease in FC between these regions coincided with improvement in autism symptoms.

Dimitrades et al. investigated the differences in sleep spindles between healthy youth and those with schizophrenia or anti-NMDA receptor encephalitis using EEG. They found that patients with schizophrenia or anti-NMDA receptor encephalitis had reduced spindle density and duration compared to healthy young adults. As many individuals with Alzheimer's disease, autism (1), or schizophrenia (2) experience sleep disorders, the findings of these studies should be further explored to address disrupted sleep.

Sleep disturbances are often also seen in other disorders, including hypertension, obesity, type 2 diabetes mellitus, or cardiovascular disease. Neuroimaging methods could be used to reveal the neural mechanisms underlying these associations, and shed light on sleep disturbances in these conditions (3), while computational approaches could enable the identification of distinct subtypes of sleep impairment and provide opportunities for personalized interventions in patients.

Author contributions

All authors listed have made a substantial, direct, and intellectual contribution to the work and approved it for publication.

Acknowledgments

Thanks to the Frontiers editors and peer reviewers who made this special edition possible.

Conflict of interest

The authors declare that the research was conducted in the absence of any commercial or financial relationships that could be construed as a potential conflict of interest.

Publisher's note

References

1. Ballester P, Richdale AL, Baker EK, Peiró AM. Sleep in autism: A biomolecular approach to aetiology and treatment. *Sleep Med Rev.* (2020) 54:101357. doi: 10.1016/j.smrv.2020.101357

2. Ferrarelli F. Sleep abnormalities in schizophrenia: state of the art and next steps. *Am J Psychiatry*. (2021) 178:903–913. doi: 10.1176/appi.ajp.2020.20070968

3. von Deneen KM, Garstka MA. Targeted treatment for type 2 diabetes mellitus and sleep disorders from a clinical and neuroimaging perspective. *Intelligent Med.* (2022) 2:209–220. doi: 10.1016/j.imed.2022.05.003

frontiers in Psychiatry

ORIGINAL RESEARCH
published: 29 October 2021
doi: 10.3389/fpsyt.2021.763032

Effect of the cPKCγ-Ng Signaling System on Rapid Eye Movement Sleep Deprivation-Induced Learning and Memory Impairment in Rats

Shu Xu[1], *Yanbo Zhang*[2]*, *Zhiqing Xu*[3] and *Luping Song*[1,4]*

[1] School of Rehabilitation, Capital Medical University, Neurorehabilitation Center, Beijing Boai Hospital, China Rehabilitation Research Center, Beijing, China, [2] Department of Neurobiology, The Second Affiliation Hospital of Shandong First Medical University, Tai'an, China, [3] Department of Neurobiology, Beijing Key Laboratory of Neural Regeneration and Repair, Capital Medical University, Beijing, China, [4] Department of Rehabilitation Medicine, Shenzhen University General Hospital, Shenzhen, China

OPEN ACCESS

Edited by:
Yuanqiang Zhu,
Fourth Military Medical University, China

Reviewed by:
Wei Xie,
Baotou Medical College, China
Yaoming Xu,
Inner Mongolia Autonomous Region Brucellosis Prevention and Treatment Engineering Technology Research Center, China

***Correspondence:**
Luping Song
songluping882002@aliyun.com
Yanbo Zhang
bbnnbn@163.com

Specialty section:
This article was submitted to Neuroimaging and Stimulation, a section of the journal Frontiers in Psychiatry

Received: 23 August 2021
Accepted: 06 October 2021
Published: 29 October 2021

Citation:
Xu S, Zhang Y, Xu Z and Song L (2021) Effect of the cPKCγ-Ng Signaling System on Rapid Eye Movement Sleep Deprivation-Induced Learning and Memory Impairment in Rats. Front. Psychiatry 12:763032. doi: 10.3389/fpsyt.2021.763032

Objective: Rapid eye movement sleep deprivation (REM-SD) can cause a decline in learning and memory and lead to changes in behavior. Therefore, REM sleep plays a key role in processes that govern learning and memory. However, the mechanism underlying REM-SD-induced learning and memory impairment is unclear and the underlying molecular signaling still needs to be identified. In the present study, we investigated the role of the cPKCγ-Ng signaling pathway in REM-SD-induced learning and memory impairment.

Method: Sixty male rats were divided into Control, REM-SD, REM-SD+cPKCγ activator PMA, REM-SD+cPKCγ inhibitor H-7, and sleep revival (SR) groups. The Morris water maze was used to assess spatial learning and memory. Western blot analysis was used to detect cPKCγ total protein expression and membrane translocation levels, and Ng total protein expression and phosphorylation levels.

Results: The REM-SD group performed worse on the Morris water maze test than the control group. Western blot analysis showed that cPKCγ membrane translocation and Ng phosphorylation levels were significantly lower in the REM-SD group. SR following REM-SD restored learning and memory ability, cPKCγ transmembrane translocation, and Ng phosphorylation levels, but not to levels observed before REM-SD. PMA and H-7 significantly improved/disrupted task ability as well as cPKCγ transmembrane translocation and Ng phosphorylation levels in REM-SD rats.

Conclusion: The REM-SD induced learning and memory impairment in rats and may be associated with the cPKCγ-Ng signaling pathway. Specifically, activation of the cPKCγ-Ng signaling pathway may protect against REM-SD.

Keywords: REM sleep deprivation, learning and memory, cPKCγ, neurogranin, signaling

INTRODUCTION

Sleep deprivation (SD) can cause changes in mood, learning, memory, and immune function, which can lead to physiological, psychological, and even behavioral changes. Although studies have confirmed that SD can cause obvious cognitive impairment (1–3), the underlying mechanisms remain unknown. Studies that focus on the molecular signaling pathways that govern this process will be important for the development of effective therapeutic interventions.

In 2007, the American Academy of Sleep Medicine classified sleep into non-rapid eye movement (NREM) stages 1, 2, and 3 and a rapid eye movement (REM) stage, with each stage being interconnected. Normally, people pass through 4–6 cycles of these sleep stages each night. Compared to a waking state, REM sleep is characterized by low-amplitude, mixed frequency signals as seen on electroencephalograms (EEG), rapid eyeball movement, markedly decreased muscle tone, and increased cerebral blood flow and oxygen consumption. REM-SD can cause a decline in memory and cognitive functions. Therefore, REM sleep plays a key role in learning and memory (4–7). Neuroimaging is a powerful tool to explore the neural mechanism of sleep disorders. Studies have found that some certain diseases, such as optic neuritis, sleep deprivation, etc., can cause changes in the topology of the brain network, which may cause symptoms of cognitive impairment (8). However, it is also of great significance to carry out molecular signal mechanism research. Through the study of molecular signal targets, it may be possible to provide a new perspective for future drug interventions.

Protein kinase C (PKC) was first discovered by Nishizuka in 1977. PKC is a family of serine/threonine kinases that is widely expressed in many bodily systems and is an important intracellular signal transduction molecule. To date, at least 12 subtypes of PKC have been isolated and identified through molecular cloning and enzyme analysis, and these are widely distributed in various tissues and organs. PKC plays an important physiological role in the regulation of neuronal excitability, signal transduction, release of neurotransmitters, synaptic plasticity, learning and memory, cell proliferation, gene expression, cell degeneration, and programmed cell death (9, 10). Under resting conditions, PKC exists in the cytoplasm in an inactive form. When external stimulus exists, PKC is translocated to the cell membrane where it can exert its physiological role (11, 12). There is increasing evidence that PKC also plays an important role in spatial learning and memory (). Inhibition of PKC activity can impair learning and memory abilities, such as that induced by vascular dementia and traumatic brain injury (13–16). PKC activators have also been shown to have memory-enhancing and anti-dementia effects (17). Studies have shown that PKC plays an important role in changes that occur during SD; PKC mRNA levels in the hippocampus and pre-frontal cortex of rats were significantly reduced after periods of SD (18). However, PKC is considered to exert its physiological activities through its translocation, and changes in PKC activity during SD have not been studied, nor has anyone explored the roles that PKC subtypes play in SD-induced learning and memory impairment. cPKCγ is a classical PKC subtype that only exists in neurons of the brain and spinal cord. cPKCγ can regulate synaptic development and plasticity, and can directly affect long-term potentiation and long-term depression (LTD). Thus, cPKCγ has attracted increasing attention. Although some reports have found that cPKCγ is involved in learning and memory (19, 20), the role of cPKCγ in REM-SD-induced learning and memory impairment has been rarely studied. Therefore, in the present study, we investigated the role of cPKCγ in REM-SD-induced learning and memory impairment, and observed changes in its activity in the brain. The results thus contribute to our understanding of the molecular mechanism that underlies REM-SD-induced memory impairment, which is of critical importance in the field of SD.

Neurogranin (Ng) is a newly discovered neuro-specific postsynaptic protein member of the calpacitin protein family that comprises 78 amino acids. Ng is distributed in specific brain regions, including the cerebral cortex, hippocampus, and olfactory bulb, and is a postsynaptic substrate of PKC (21). Ng can be phosphorylated by PKC and participates in the induction of long-term potentiation and long-term depression. Ng gene expression and protein synthesis are synchronized with synapse formation and neuronal differentiation, which indicates that Ng may be involved in physiological processes such as learning, memory, and development of the nervous system. Under certain pathophysiological conditions, such as hypothyroidism, SD, and hypoxic preconditioning, Ng activity plays roles in changing nervous system functions (22–26). One study found that SD resulted in a significant reduction in Ng mRNA levels in the rat hippocampus and pre-frontal cortex (18). Ng exerts its physiological activity after being phosphorylated by PKC, but changes in Ng activity after REM-SD have not been explored, nor have the subtypes of PKC that phosphorylate Ng in REM-SD-induced learning and memory impairment been identified.

Both PKC and Ng play important roles in learning and memory. In the present study, we investigated the role of the PKC-Ng signaling system in REM-SD-induced learning and memory impairment in rats. The key aim was to identify which subtypes of PKC phosphorylate Ng and play crucial roles in learning and memory impairment. Represa et al. found that Ng is widely distributed in the cerebral cortex, thalamus, and striatum, and is scarce in the cerebellum and brain stem, which is consistent with the distribution of cPKCγ in the brain (27). Sato et al. (28) further found that Ng and cPKCγ exhibit similar gene expression patterns during brain development. Neuner-Jehle et al. found that after 24 h of SD, mRNA and expression of Ng differed depending on the brain region. Ng mRNA was significantly reduced in the forebrain and midbrain regions, but did not change in the hippocampus. Ng protein levels were significantly reduced in the cortex, but did not change significantly in other brain regions (29). This suggests that it may be more meaningful to study the changes in the PKC-Ng signaling system in the pre-frontal cortex of animals. Given this theoretical basis, it is important to investigate the cPKCγ-Ng signaling system and its role in REM-SD-induced learning and memory impairment. In the present study, we established a rat model of 72-h REM-SD and 12-h sleep revival

(SR), and identified changes in the cPKCγ-Ng signaling system in the frontal cortex of the rats. Additionally, we measured Ng phosphorylation levels after administration of the cPKCγ activator PMA and the cPKCγ inhibitor H-7 and explored the underlying molecular mechanisms.

MATERIALS AND METHODS

Experimental Animals

Sixty male Sprague Dawley rats (15 weeks old) were used in the experiment [provided by the Experimental Animal Center, Shandong University of Traditional Chinese Medicine, China; License No.: SCXK (Lu) 20050015]. All rats were provided with standard food pellets and tap water and housed in a quiet room set to 18–25°C and 40–60% humidity. The rats were divided into five groups (12 rats/group). Control group: rats were housed in a normal rat cage with a natural 12/12 h light–dark cycle (lights on at 7:00 A.M.), and did not undergo REM-SD. REM-SD group: rats were continuously subjected to a fluorescent lamp for 72 h. After REM-SD was completed, the rats were taken out of the REM-SD box and then returned to their cages. REM-SD+PMA group: during the 72-h continuous REM-SD, 20 μl PMA solution (containing 100 ng PMA, phorbol-12-myristate-13-acetate C2230, Sigma) was injected into the spinal subarachnoid space once every 24 h (three injections overall). The dose of PMA was chosen according to a previous study (11) REM-SD+H-7 group: during the 72-h continuous REM-SD, 20 μl H-7 solution (containing 200 μg H-7, soluble in saline, I6891, Sigma) was injected into the spinal subarachnoid space once every 24 h (three injections overall). The dose of H-7 was chosen according to previous study (11). SR group: after the rats were subjected to 72 h of continuous REM-SD, rats were placed in a cage for 12 h of SR. An overview of the experimental procedure is shown in **Figure 1**.

Catheterization of the Spinal Subarachnoid Space

Rats were anesthetized with sodium pentobarbital (40 mg/kg) intraperitoneally. The skin was incised at the midline of the occipital bone and separated layer by layer. Heads were tilted forward by about 30° and a polyethylene catheter (PE-10) was caudally inserted into the subarachnoid space. After surgery, rats were injected intramuscularly with gentamicin sulfate (40,000 units/rat/day) for 3–5 days. Normal rats without hemiparesis were used for the experiments.

Establishment of the REM-SD Model

REM-SD was induced by the modified multiple platform method as described previously (30, 31). The modified multiple platform method is the most widely used technique mainly for deprivation of REM sleep, but not for deprivation of non-REM sleep (NREM). A self-made REM-SD box (110 × 60 × 40 cm) had 15 small platforms (6.5 cm in diameter and 8.0 cm in height) that were set up at 15-cm intervals. The box was filled with water, and the surface of the water was about 1.0 cm below the surface of the platforms. Water and food were placed on the top of platforms. Rats had free access to food and water and were allowed to move freely between platforms. Due to their instinctive fear of water, rats slept on the platforms and could enter NREM. However, if the rats entered REM sleep and lost their muscle tone, they would fall into the water and awaken, thus being prevented from entering REM sleep. This technique has been validated using electroencephalography and has been shown to eliminate ∼90–95% of REM sleep (32).

The Morris Water Maze

The Morris water maze is a widely used method to assess spatial learning and memory. Maze testing was carried out by the SMART-CS (Panlab, Barcelona, Spain). This maze comprised a circular pool with a 160 cm-diameter and a 55 cm-high wall. The pool was divided into four equal quadrants. Powdered milk was added to make the water opaque, and the water was kept at 22–25°C. A circular transparent platform (12 cm in diameter and 25 cm in height) was located in the center of the third quadrant, hidden 1 cm below the surface of the water. The Morris water maze test was conducted for 5 days, beginning immediately after 72-h REM-SD and 12-h SR, and the navigation probe test was performed within the first 4 days of the experiment. For each trial, a rat was put into the water from the midpoint of each quadrant facing the maze's wall. The rat was allowed to swim for 120 sec to find the hidden platform and climb onto it. If the rat found the platform within 120 sec, the rat was allowed to remain on the platform for 4 sec, then the trial was terminated and the latency was recorded; if the rat had not found the platform in 120 sec, it was guided and placed on the platform for 30 sec by the experimenter, the trial was terminated and latency period was recorded as 120 sec. There was an intertrial interval of 5 min. The position of rats in the pool was tracked using an overhead camera connected to a SMART-CS program. The escape latency, swimming distance, and swimming speed were recorded (average of four trials) to evaluate the spatial learning of rats.

The spatial probe test was performed on day 6 to evaluate the spatial memory of rats. In this test, the platform was removed, the rats were placed into the water from the first quadrant, and were allowed to swim for 120 sec. The time spent in the target quadrant (where the platform had previously been placed) and the other quadrants within 120 sec was recorded.

Western Blot Analysis

The pre-frontal cortices of rats in each group were removed and frozen in liquid nitrogen and stored at −80°C for future use.

Detection of cPKCγ protein expression in cytosolic and membrane fractions: The frozen tissues were thawed and homogenized in Buffer A (10 μl/mg tissue, containing 50 mmol/L Tris-HCl pH 7.5, 2 mmol/L EDTA, 2 mmol/L EGTA, 2 mmol/L DTT, 5 mmol/L Napyrophosphate, 50 mmol/L KF, 5 × 10^{-5} mmol/L Okadaic acid, and 5 ug/ml each of leupeptin, aprotinin, pepstatin A, and chymostatin). After centrifugation at 30,000 g for 30 min at 4°C, the supernatant was collected as cytoplasmic fraction (cytosol) and stored. Then, Buffer B (Buffer A + 0.5% NP-40) was added to the remaining pellet, the procedure described above was performed, and the supernatant

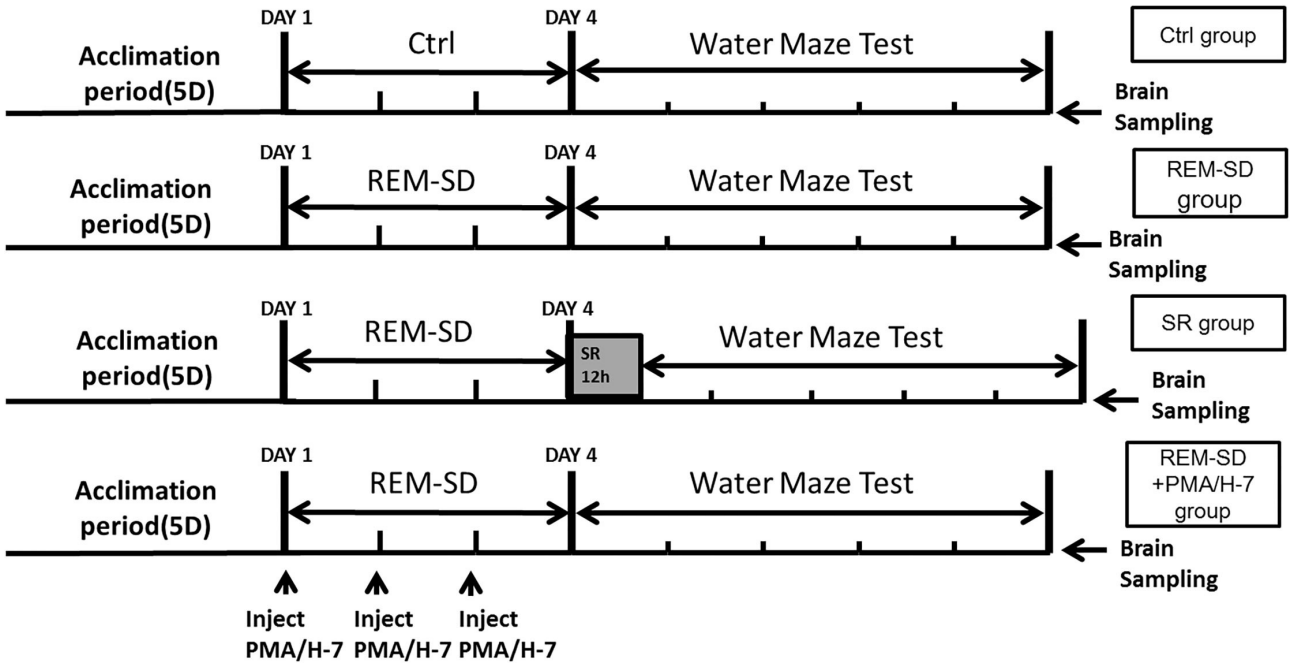

FIGURE 1 | Overview of the experimental procedures.

was collected as a membrane fraction (particulate). *Total cPKCγ protein*: The frozen tissues were thawed and homogenized in Lysis Buffer containing 50 mM Tris-HCl pH 7.5, 5 mM EDTA, 5 mM EGTA, 1.0% SDS, 150 mM NaCl (10 μl/mg tissue). *Ng protein*: The frozen tissues were thawed and homogenized in lysis buffer (10 μl/mg tissue) containing 50 mM Tris-HCl, pH 7.5, 2 mM EDTA, 2 mM EGTA, 2 mM DTT, 5 mM Na pyrophosphate, 50 mM KF, 50 nM Okadaic acid, 5 mg/ml each of leupeptin, aprotinin, pepstatin A, and chymostatin, and 1.0% SDS. Protein concentration was measured using a BCA kit (Pierce Company, Rockford, USA). SDS-PAGE loading buffer was added to the protein samples (3 μg/μL) and the samples were boiled for 5 min and then stored at −80°C for western blot analysis. Antibodies included cPKCγ rabbit polyclonal antibody (1:1000, Santa Cruz, Dallas, Texas), Ng mouse monoclonal antibody (1:1000, Santa Cruz, Dallas, Texas), phosphorylated Ng rabbit monoclonal antibody (1:1000, Merck-Millipore, ABN426), β-actin rabbit polyclonal antibody (1:1000, Santa Cruz, Dallas, Texas), β-actin mouse monoclonal antibody (1:1000, Santa Cruz, Dallas, Texas), Na-K ATPase monoclonal antibody (1:1000, Santa Cruz, Dallas, Texas), goat anti-rabbit secondary antibody (1:5000, Santa Cruz, Dallas, Texas), and goat anti-mouse secondary antibody (1:5000, Santa Cruz, Dallas, Texas). Western blots were developed using the SuperSignal West Pico Chemi-luminescent Substrate kit (Pierce Company, Rockford, USA). After membranes were exposed, the bands were scanned and analyzed using Quantity One 1-D analysis software (Bio-Rad Laboratory, Hercules, CA). The contents of cPKCγ cytoplasmic protein and membrane protein were calculated using β-actin as an internal reference. The cPKCγ membrane translocation level was expressed by the percentage of membrane protein content to total protein (membrane protein + cytoplasmic protein) in each group. The membrane translocation level of the control group was taken as 100%, and the cPKCγ membrane translocation level in each experimental group was expressed using a percentage. Taking β-actin as an internal reference, the total protein contents of cPKCγ and Ng were calculated for each group. The protein expression in the control group was 100%, and the change of protein expression in each group was expressed as a percentage. The Ng phosphorylation level was expressed as the ratio of Ng phosphorylated protein to total protein.

Statistical Analysis

Results were analyzed using a two-way ANOVA and one-way ANOVA using SPSS 22.0 software. For significant results identified by the one-way ANOVA, Tukey's *post hoc* tests were used to compare the differences between multiple groups. A value of $P < 0.05$ was considered statistically significant.

RESULTS

REM-SD- Induced Behavioral and Physiological Changes in Rats

As the length of sleep deprivation increased, behavioral and physiological changes in rats became increasingly obvious. The primary manifestations included increased lassitude, dullness, lack of luster, dryness, disheveled and untidy fur, increased excitability and irritability, and increased alertness, responsiveness, and aggressive behavior in response to environmental stimuli. Some rats even suffered from mucosal

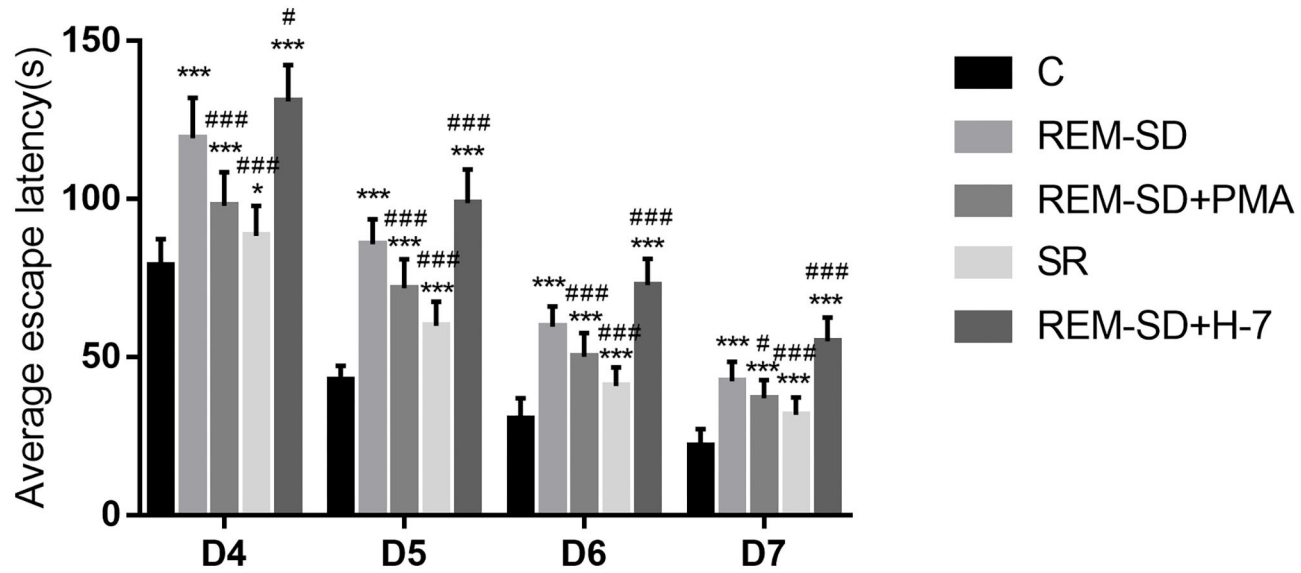

FIGURE 2 | Average escape latency (seconds) for all groups. Compared with the control group (C), the average escape latencies for all other groups were significantly prolonged on each day of training. Compared with the REM-SD group, the average escape latency was significantly shorter in the SR and REM-SD+PMA groups, and was significantly longer in the REM-SD+H-7 group $^{*}P < 0.05$, $^{\#}P < 0.05$ vs. control group, $^{***/\#\#\#}$means $P < 0.001$.

bleeding of the paws due to scratching. These symptoms indicated successful establishment of the rat model of REM-SD.

REM-SD Induced Changes of Morris Water Maze Test in Rats

REM-SD Prolongs the Average Escape Latency in Rats

Results from the place navigation test showed that, for all groups, the average time needed to find the platform gradually shortened during training. However, compared with the control group, the average escape latencies for all other groups were significantly prolonged on each day of training. Compared with the REM-SD group, the average escape latency was significantly shorter in the SR and REM-SD+PMA groups, and was significantly longer in the REM-SD+H-7 group (**Figure 2**).

REM-SD Decreases the Percentage of Time Spent in the Target Quadrant

Results from the spatial probe test showed that, compared with the control group, the percentage of time spent on searching for the target quadrant (where the platform was placed) was significantly lower in the REM-SD, REM-SD+PMA, REM-SD+H-7, and SR groups. Compared with the REM-SD group, this time was significantly higher in the SR and REM-SD+PMA groups and lower in the REM-SD+H-7 group. The REM-SD, REM-SD+PMA, and REM-SD+H-7 groups spent significantly more time in the first quadrant than did the control group, and no significant difference was found between the SR and control groups. Compared with the REM-SD group, the percentage of time spent in the first quadrant was lower in the SR and REM-SD+PMA groups, and higher in the REM-SD+H-7 group (**Figure 3**).

REM -SD Does Not Affect Swimming Speed in Rats

Average swimming speed did not differ across the five groups (**Figure 4**) on the Morris water-maze test.

REM-SD Reduces cPKCγ Protein Expression

Results from Western blot analysis showed that cPKCγ protein expression in the REM-SD, REM-SD+PMA, and REM-SD+H-7 groups was significantly lower than that in the control group. Levels did not differ between the SR and control groups, between the REM-SD and REM-SD+PMA groups, or between the REM-SD and REM-SD+H-7 groups. cPKCγ protein expression in the SR group was significantly higher than that in the REM-SD group (**Figure 5**).

REM-SD Inhibits cPKCγ Membrane Translocation

Results from western blot analysis showed that the level of cPKCγ membrane translocation in the REM-SD, REM-SD+PMA, REM-SD+H-7, and SR groups were all significantly lower than that in the control group. Compared with REM-SD group, levels were higher in the SR and REM-SD+PMA groups and lower in the REM-SD+H-7 group (**Figure 6**).

REM-SD Reduces Ng and Phosphorylated Ng Expression

Western blot analysis showed that Ng protein expression in REM-SD/ REM-SD+PMA/ REM-SD+H-7 experimental groups were significantly lower than in the control group. Compared with the REM-SD group, Ng protein expression was significantly

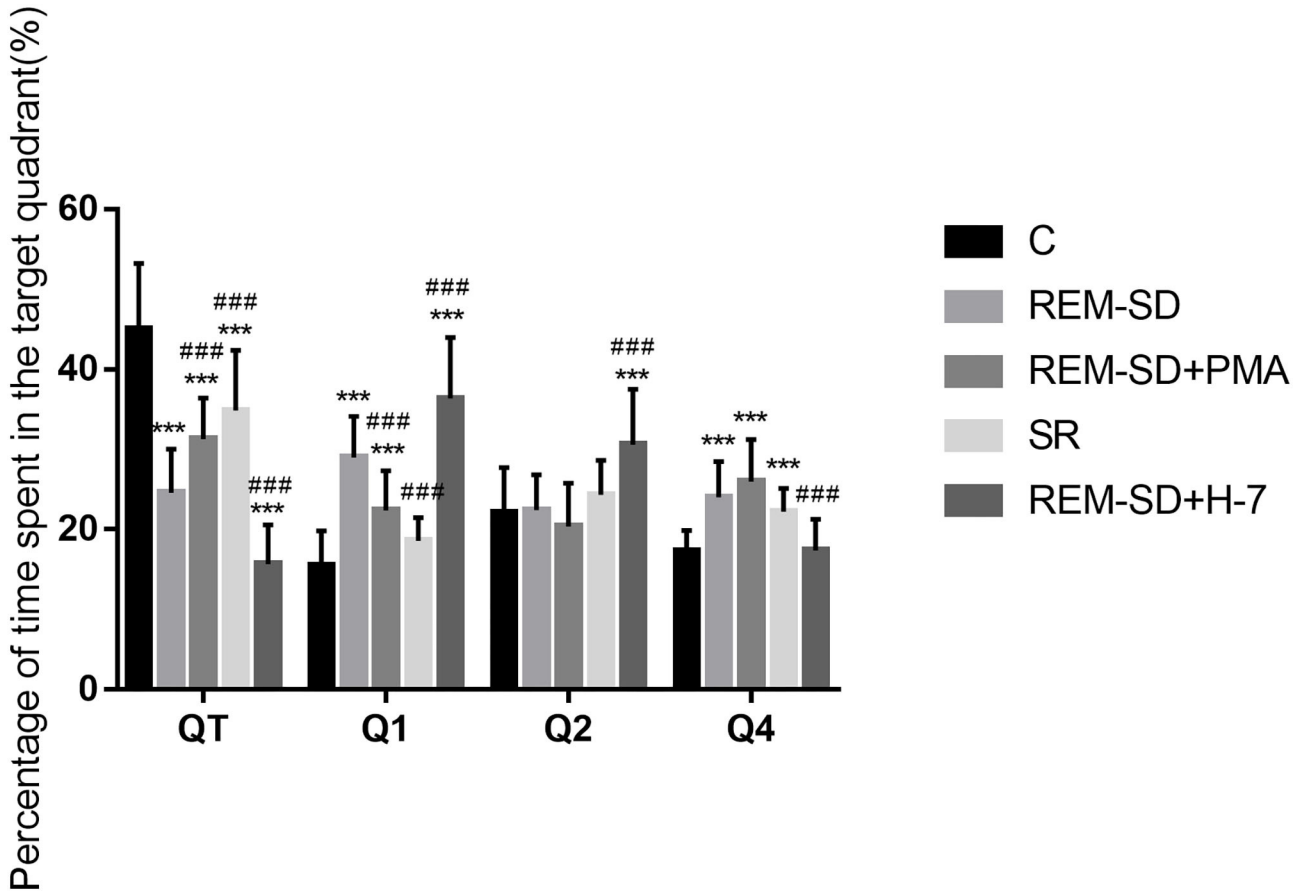

FIGURE 3 | The percentage of time spent in target quadrant for each group. Compared with the control group (C), the percentage of time spent searching the target quadrant (where the platform was placed) was significantly lower in the REM-SD, REM-SD+PMA, REM-SD+H-7, and SR groups. Compared with the REM-SD group, this time was significantly higher in the SR and REM-SD+PMA groups and lower in the REM-SD+H-7 group. ***### means $P < 0.001$.

lower in the REM-SD+H-7 group, tended to be higher in REM-SD+PMA group, and was significantly higher in the SR group (**Figure 7**).

The expression of phosphorylated Ng in all experimental groups was lower than in the control group. Compared with the REM-SD group, expression of phosphorylated Ng was significantly higher in the SR and REM-SD+PMA groups and was significantly lower in the REM-SD+H-7 group (**Figure 7**).

DISCUSSION

In the present study, we confirmed that REM-SD can significantly reduce spatial learning and memory ability in rats. Western blot analysis showed that cPKCγ activity and Ng phosphorylation levels were significantly reduced following REM-SD, which suggests that REM-SD-induced impairments in spatial learning and memory in rats are associated with cPKCγ-Ng signal transduction.

We used a modified multiple platform method to selectively deprive rats of REM sleep. When rats enter REM sleep, they lose their muscle tone and fall into the water, thus waking them up and making rats unable to enter REM sleep. After 72 h of REM-SD, we observed expected symptoms of REM-SD, including increased food intake, lassitude, dullness, lack of luster, dryness, disheveled and untidy fur, increased excitability and irritability, and increased alertness, responsiveness, and aggressive behavior in response to environmental stimuli.

We used the Morris water maze to assess changes in spatial learning and memory. The place navigation test revealed that the average time needed to find the platform (escape latency) was significantly prolonged in the REM-SD group compared with control group, which indicates that REM-SD can significantly impair spatial learning and memory ability in rats. Although escape latency in the SR group was significantly shorter than that of the REM-SD group, it was still longer than that of the control group. This indicates that SR following REM-SD only partially restores learning and memory ability. During the spatial probe test, the percentage of time spent in the target quadrant

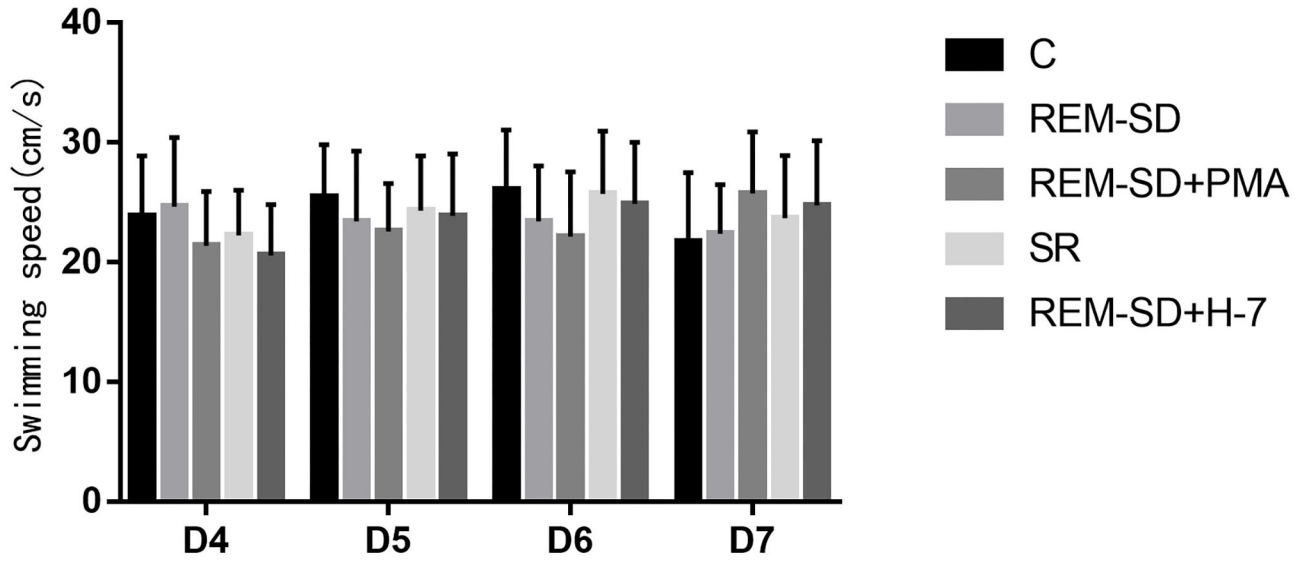

FIGURE 4 | The average swim speed (cm/s) on the Morris water-maze test for each group. No significant difference was found between the five groups with regard to the average swimming speed on the Morris water-maze test.

was significantly shorter in the REM-SD group than that in the control group, which indicates that REM-SD can cause damage to the acquisition and maintenance of spatial memory, which is consistent with previous resultsT. The percentage of time spent in the target quadrant was significantly longer in the SR group compared to the REM-SD group, and was shorter in the SR group than in the control group, which indicates that after 12 h of SR, spatial memory was partially improved. This further validated the results of the place navigation test. We also found that the REM-SD group spent significantly more time in the first quadrant than did the control group, while the SR group spent significantly less time in the first quadrant compared with the REM-SD group, further suggesting that REM-SD can impair spatial learning and memory.

PKC is a family of serine–threonine kinases that is widely expressed in mammalian tissues. PKC is essential for signal transduction involved in sleep/wake regulation and sleep-related behaviors (33–35). Studies focused on cPKCγ have attracted broad attention. Although some reports have found that cPKCγ is involved in learning and memory (19, 20), its role in REM-SD-induced learning and memory impairment is still unknown. In the present study, we found that cPKCγ protein expression was significantly reduced after REM-SD and was increased following SR. However, administration of the cPKCγ activator PMA and the inhibitor H-7 had no effects on cPKCγ protein expression. cPKCγ is present in the cytoplasm in an inactive form when at rest. The regulatory domain interacts with the catalytic domain through a pseudosubstrate sequence and prevents the substrate from entering the catalytic region. cPKCγ is activated upon translocation to the cell membrane under external stimulus conditions (20, 36). We therefore also investigated the degree to which cPKCγ was translocated to the membrane and found that it was markedly lower in the REM-SD group than in the control group. This indicates that REM-SD can significantly inhibit cPKCγ membrane translocation and activation. SR after REM-SD can increase cPKCγ membrane-translocation levels and thus promote cPKCγ activation, although activation levels did not reach pre-SD levels. These results are consistent with the Morris water maze test results. Similarly, administering the cPKCγ activator PMA significantly increased cPKCγ membrane translocation, and thus promoted its activation. In contrast, the cPKCγ inhibitor H-7 significantly reduced cPKCγ membrane translocation and activation. These changes are also consistent with the behavioral results; the REM-SD+PMA group performed better than the REM-SD group on the place navigation and spatial probe tests, whereas the REM-SD+H-7 group performed worse than both untreated and REM-SD rats. These findings indicate that changes in the level of cPKCγ membrane translocation are related to REM-SD-induced learning and memory impairment.

Ng is a natural postsynaptic PKC substrate that is abundantly expressed in brain regions, and which is involved in cognitive function (36). Ng is a key CaM-binding protein that buffers CaM function. Phosphorylation of Ng by PKC at serine 36 (Ser36) reduces its binding to CaM, allowing CaM to bind to calcium and activate CaM-dependent pathways, such as the Ca^{2+}/Calmodulin-Dependent Protein Kinase II (CaMKII) signal cascade, which is involved in learning and memory. Zhong et al. revealed the importance of the PKC signaling system for CaM-Ng-dependent synaptic plasticity; the ratio of phosphorylated/non-phosphorylated Ng can determine the CaMKII- associated LTP/LTD threshold (37). Our western blot analysis results showed that REM-SD significantly reduced cPKCγ membrane translocation and Ng phosphorylation levels,

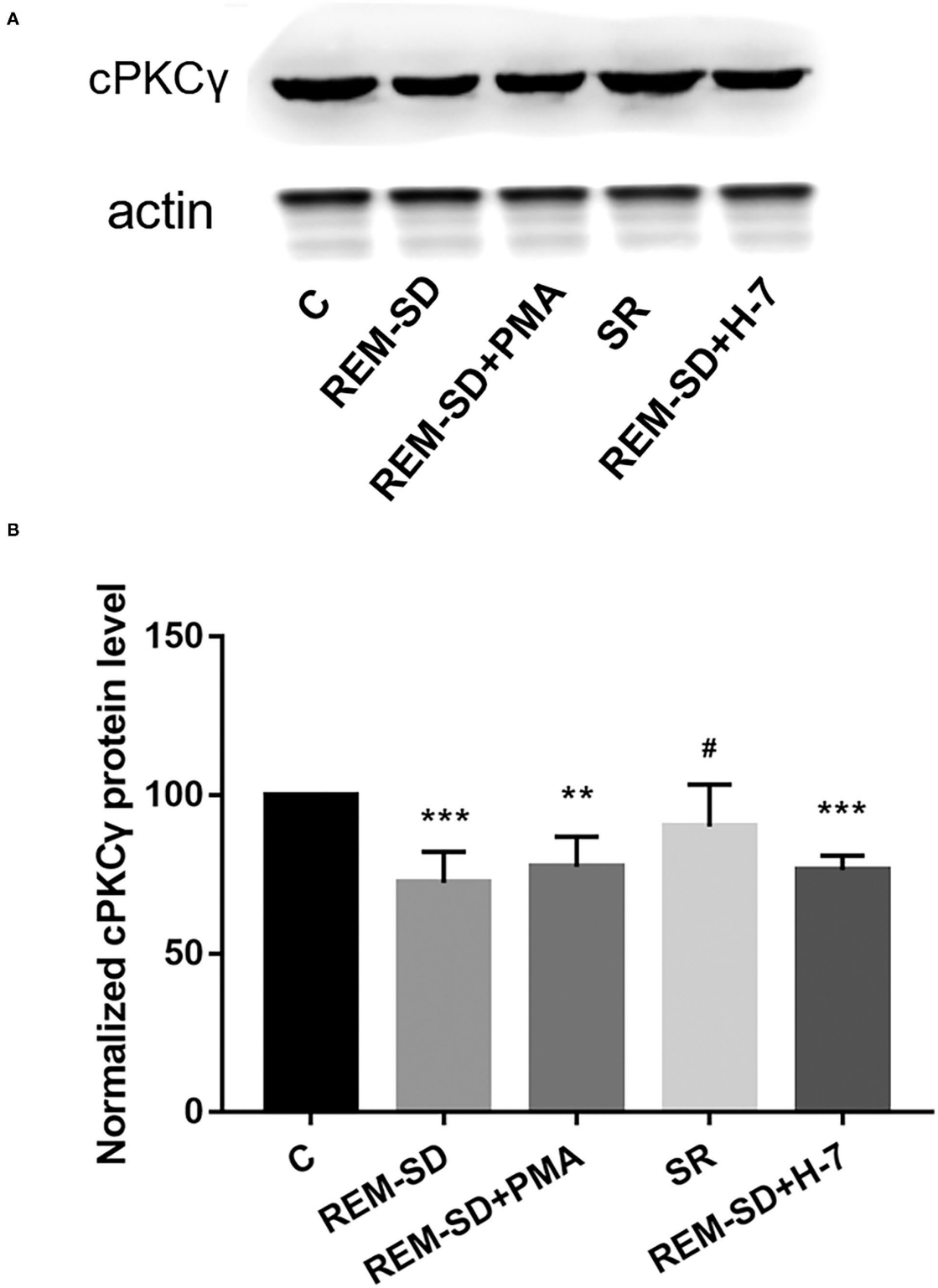

FIGURE 5 | cPKCγ protein expression in the prefrontal cortex of SD rats from each group and control group (C). **(A)** Western blot analysis results. **(B)** The relative protein expression of cPKCγ for each group. $^{**}P < 0.01$, $^{***}P < 0.001$ vs. control group; $^{\#}P < 0.05$ vs. SD group.

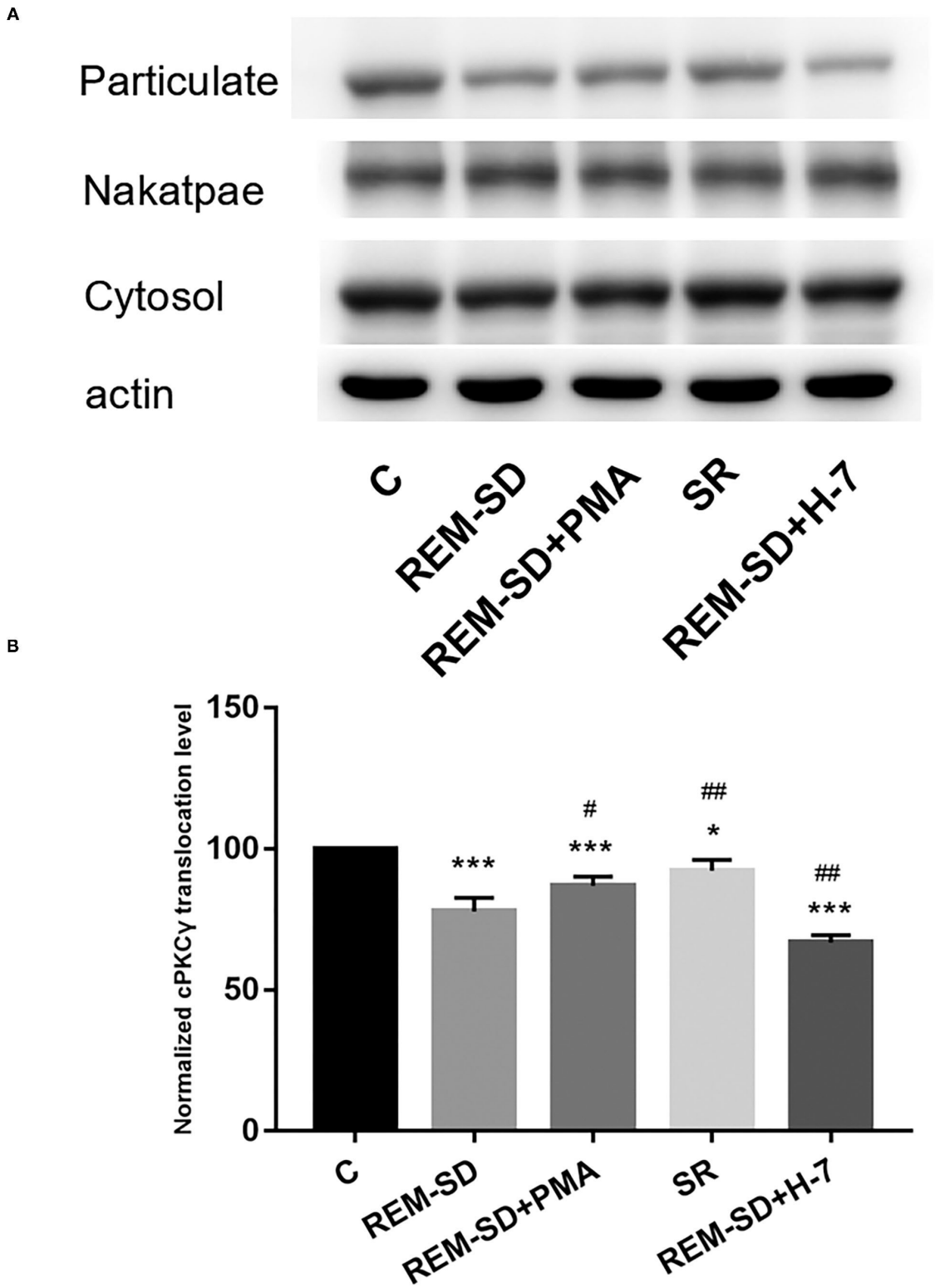

FIGURE 6 | cPKCγ membrane translocation levels in the prefrontal cortex of SD rats from each group and control group (C). **(A)** Western blot analysis results. Cytosol and particulate-represented cytosolic and membrane proteins, respectively. **(B)** cPKCγ membrane translocation levels for each group. $^{*}P < 0.05$, $^{***}P < 0.001$ vs. control; $^{\#}P < 0.05$, $^{\#\#}P < 0.01$, vs. SD group.

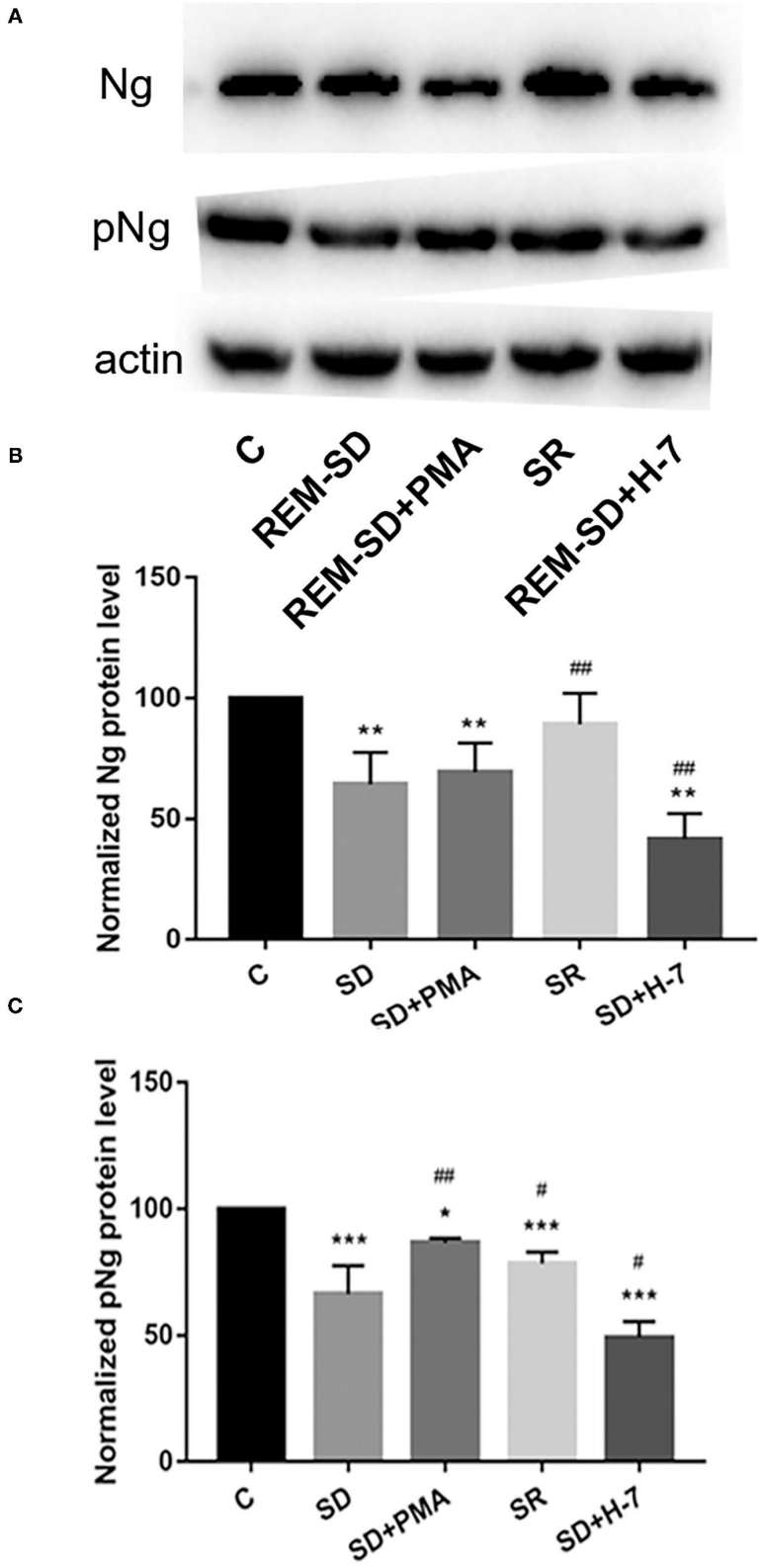

FIGURE 7 | Protein expression for Ng and phosphorylated Ng in the prefrontal cortex of SD rats from each group and control group (C). **(A)** Western blot analysis results. **(B)** Relative protein expression of Ng for each group. **(C)** Relative protein expression of phosphorylated Ng for each group. $^{*}P < 0.05$, $^{**}P < 0.01$, $^{***}P < 0.001$ vs. control; $^{\#}P < 0.05$, $^{\#\#}P < 0.01$ vs. SD group.

which suggests that REM-SD-induced memory impairment is mediated by inhibition of the cPKCγ and Ng signaling-transduction pathway. REM-SD may prevent the buffering effect of non-phosphorylated Ng over CaM, leading to abnormal CaM signaling. Administration of the cPKCγ activator PMA significantly increased Ng phosphorylation levels and the cPKCγ inhibitor H-7 significantly inhibited Ng phosphorylation, which suggests that Ng is downstream of the cPKCγ signaling pathway. The cPKCγ inhibitor H-7 can significantly reduce Ng protein expression and the cPKCγ activator PMA can increase Ng protein expression. Although no statistical difference was found between groups, the results further indicate that cPKCγ not only regulates the activation and phosphorylation of Ng, but can also promote Ng protein expression.

REM sleep plays an important role in the consolidation of long-term memory in the nervous system, which can strengthen the newly-formed connections made during wakefulness, form new connections, and enhance new memories during subsequent wakefulness. Thus, we can hypothesize that the role of the cPKCγ-Ng pathway on REM-SD-induced learning and memory impairment may be associated with it involvement in the establishment of new synaptic connections during the learning and memory consolidation. In future work, we will use neurophysiological methods to perform electrophysiological recordings of the pre-frontal cortex in rats, and investigate the role of cPKCγ-Ng in long-term synaptic plasticity during REM-SD.

There are some limitations to the current study. The main purpose of the modified multiple platform method is used in the present study to investigate REM (30, 31). The EEG results also support this is an effective performance to reduce the 95% of REM (30, 32). However, Alkadhi et al. found that non-REM (NREM) sleep was signficantly reduced by the multiple platform method (38). Therefore, we cannot completely exclude the effects of NREM deprivation on the impairment of spatial lerning and memory. Additionally, it has been reported that expression levels of both Ng mRNA and Ng protein differ across different brain regions after 24 h of SD, and Ng protein levels were significantly reduced in the cortex (29). Based on these findings, we only focused on the pre-frontal cortex. However, the hippocampus is a key area for spatial learning and memory. Further investigations should explore the changes in the PKC-Ng signaling pathway in the hippocampus of rats to confirm our results. Furthermore, due to a lack of specific activators and inhibitors of cPKCγ, we used the non-specific activators and inhibitors of the PKC family, PMA and H-7. Also, it remains unclear without administration of PMA/H-7 will affect the response during water maze test. Administering PMA can promote cPKCγ activation and increase Ng phosphorylation levels, and administering H-7 showed the opposite effect; this result indicates that PMA and H-7 have excitatory and inhibitory effects on cPKCγ, respectively. Other groups' studies have found that many signaling pathways are involved in REM-SD-induced cognitive impairment, including NMDA receptor pathways; 24-h SD impairs NMDAR function in the rat dentate gyrus and 72-h REM-SD also impairs NMDAR function in the rat hippocampal CA1 area (33, 34). Thus, in the future, we will investigate other possible downstream targets of the cPKCγ signaling pathway, or other signaling pathways that could play a role in learning and memory impairment after REM-SD.

In summary, our results showed that the REM-SD can induce learning and memory impairments in rats which are associated with the cPKCγ-Ng signaling pathway. Activation of the cPKCγ-Ng signaling pathway can significantly improve REM-SD-induced learning and memory impairment, which is expected to become a novel molecular target for treatment of REM-SD.

DATA AVAILABILITY STATEMENT

The original contributions presented in the study are included in the article/**Supplementary Material**, further inquiries can be directed to the corresponding authors.

ETHICS STATEMENT

All animal experiments were approved by the Ethics Committee of the Medical School of Capital Medical University.

AUTHOR CONTRIBUTIONS

SX, YZ, ZX, and LS: contributed significantly to this work, and wrote and revised the manuscript. ZX and LS: designed the research study. SX and YZ: performed the research study and extracted and analyzed the data. All authors approved the final version of the manuscript.

FUNDING

This study was supported by the National Science and Technology Support Program in China (2013BAI07B01), the Natural Science Foundation of Shandong Province in China (ZR2012HQ014, ZR2011HM044, ZR2015HL041), and Shandong Province Medical and Health Plan (2014WSB32015), Special Fund of Basic Scientifc Research Service Fee of Central Public Welfare Scientifc Research Institute of China (2015CZ-49, 2019zx-Q9), The National Key Research and Development Program of China (2016YFF0201002).

SUPPLEMENTARY MATERIAL

The Supplementary Material for this article can be found online at: https://www.frontiersin.org/articles/10.3389/fpsyt.2021.763032/full#supplementary-material

REFERENCES

1. Nir Y, Andrillon T, Marmelshtein A, Suthana N, Cirelli C, Tononi G, et al. Selective neuronal lapses precede human cognitive lapses following sleep deprivation. *Nat Med.* (2017) 23:1474–80. doi: 10.1038/nm.4433
2. Ratcliff R, Van Dongen HPA. The effects of sleep deprivation on item and associative recognition memory. *J Exp Psychol Learn Mem Cogn.* (2018) 44:193–208. doi: 10.1037/xlm0000452
3. Saygin M, Ozguner MF, Onder O, Doguc DK, Ilhan I, Peker Y. The impact of sleep deprivation on hippocampal-mediated learning and memory in rats. *Bratisl Lek Listy.* (2017) 118:408–16. doi: 10.4149/BLL_2017_080
4. Santos PD, Targa ADS, Noseda ACD, Rodrigues LS, Fagotti J, Lima MMS. Cholinergic oculomotor nucleus activity is induced by REM sleep deprivation negatively impacting on cognition. *Mol Neurobiol.* (2017) 54:5721–9. doi: 10.1007/s12035-016-0112-z
5. Alzoubi KH. Rababa'h AM, Owaisi A, Khabour OF. L-carnitine prevents memory impairment induced by chronic REM-sleep deprivation. *Brain Res Bull.* (2017) 131:176–82. doi: 10.1016/j.brainresbull.2017.04.004
6. Eydipour Z, Vaezi G, Nasehi M, Haeri-Rouhani SA, Zarrindast MR. Different Role of CA1 5HT3 serotonin receptors on memory acquisition deficit induced by total (TSD) and REM sleep deprivation (RSD). *Arch Iran Med.* (2017) 20:581–8. doi: 10.15171/icnj.2018.04
7. Qureshi MF, Jha SK. Short-term total sleep-deprivation impairs contextual fear memory, and contextual fear-conditioning reduces rem sleep in moderately anxious swiss mice. *Front Behav Neurosci.* (2017) 11:239. doi: 10.3389/fnbeh.2017.00239
8. Song K, Li J, Zhu Y, Ren F, Cao L, Huang ZG. Altered small-world functional network topology in patients with optic neuritis: a resting-state fMRI study. *Dis Markers.* (2021) 2021:9948751. doi: 10.1155/2021/9948751
9. Zhang Y, Wang N, Su P, Lu J, Wang Y. Disruption of dopamine D1 receptor phosphorylation at serine 421 attenuates cocaine-induced behaviors in mice. *Neurosci Bull.* (2014) 30:1025–35. doi: 10.1007/s12264-014-1473-9
10. Yang P, Li ZQ, Song L, Yin YQ. Protein kinase C regulates neurite outgrowth in spinal cord neurons. *Neurosci Bull.* (2010) 26:117–25. doi: 10.1007/s12264-010-1105-y
11. Zhang Y, Gong K, Zhou W, Shao G, Li S, Lin Q, et al. Involvement of subtypes gamma and epsilon of protein kinase C in colon pain induced by formalin injection. *Neurosignals.* (2011) 19:142–50. doi: 10.1159/000328311
12. Zhang YB, Guo ZD Li MY, Fong P, Zhang JG, Zhang CW, et al. Gabapentin effects on PKC-ERK1/2 signaling in the spinal cord of rats with formalin-induced visceral inflammatory pain. *PLoS ONE.* (2015) 10:e0141142. doi: 10.1371/journal.pone.0141142
13. Sajan MP, Hansen BC, Higgs MG, Kahn CR, Braun U, Leitges M, et al. Atypical PKC, PKClambda/iota, activates beta-secretase and increases Abeta1-40/42 and phospho-tau in mouse brain and isolated neuronal cells, and may link hyperinsulinemia and other aPKC activators to development of pathological and memory abnormalities in Alzheimer's disease. *Neurobiol Aging.* (2018) 61:225–37. doi: 10.1016/j.neurobiolaging.2017.09.001
14. Howell KK, Monk BR, Carmack SA, Mrowczynski OD, Clark RE, Anagnostaras SG. Inhibition of PKC disrupts addiction-related memory. *Front Behav Neurosci.* (2014) 8:70. doi: 10.3389/fnbeh.2014.00070
15. Sun MK, Alkon DL. The "memory kinases": roles of PKC isoforms in signal processing. *Prog Mol Biol Transl Sci.* (2014) 122:31–59. doi: 10.1016/B978-0-12-420170-5.00002-7
16. Wang J, Gallagher D, DeVito LM, Cancino GI, Tsui D, He L, et al. Metformin activates an atypical PKC-CBP pathway to promote neurogenesis and enhance spatial memory formation. *Cell Stem Cell.* (2012) 11:23–35. doi: 10.1016/j.stem.2012.03.016
17. Hongpaisan J, Alkon DL. A structural basis for enhancement of long-term associative memory in single dendritic spines regulated by PKC. *Proc Natl Acad Sci USA.* (2007) 104:19571–6. doi: 10.1073/pnas.0709311104
18. Zhang N, Liu HT. Effects of different duration of sleep deprivation on neurogranin, PKC and CaMK II mRNA expression in hippocampus and forebrain of rats. *Zhongguo Bingli Shengli Zazhi.* (2009) 25:1355–9. doi: 10.3321/j.issn:1000-4718.2009.07.020
19. Ma Y, Wang S, Tian Y, Chen L, Li G, Mao J. Disruption of persistent nociceptive behavior in rats with learning impairment. *PLoS ONE.* (2013) 8:e74533. doi: 10.1371/journal.pone.0074533
20. Bohacek J, Farinelli M, Mirante O, Steiner G, Gapp K, Coiret G, et al. Pathological brain plasticity and cognition in the offspring of males subjected to postnatal traumatic stress. *Mol Psychiatry.* (2015) 20:621–31. doi: 10.1038/mp.2014.80
21. Neuner-Jehle M, Denizot JP, Mallet J. Neurogranin is locally concentrated in rat cortical and hippocampal neurons. *Brain Res.* (1996) 733:149–54. doi: 10.1016/0006-8993(96)00786-X
22. Reker AN, Oliveros A, Sullivan JM, Nahar L, Hinton DJ, Kim T, et al. Neurogranin in the nucleus accumbens regulates NMDA receptor tolerance and motivation for ethanol seeking. *Neuropharmacology.* (2018) 131:58–67. doi: 10.1016/j.neuropharm.2017.12.008
23. Casaletto KB, Elahi FM, Bettcher BM, Neuhaus J, Bendlin BB, Asthana S, et al. Neurogranin, a synaptic protein, is associated with memory independent of Alzheimer biomarkers. *Neurology.* (2017) 89:1782–8. doi: 10.1212/WNL.0000000000004569
24. Lista S, Toschi N, Baldacci F, Zetterberg H, Blennow K, Kilimann I, et al. Cerebrospinal fluid neurogranin as a biomarker of neurodegenerative diseases: a cross-sectional study. *J Alzheimers Dis.* (2017) 59:1327–34. doi: 10.3233/JAD-170368
25. Lista S, Hampel H. Synaptic degeneration and neurogranin in the pathophysiology of Alzheimer's disease. *Expert Rev Neurother.* (2017) 17:47–57. doi: 10.1080/14737175.2016.1204234
26. Zhang P, Tripathi S, Trinh H, Cheung MS. Opposing intermolecular tuning of $Ca^{(2+)}$ affinity for calmodulin by neurogranin and CaMKII peptides. *Biophys J.* (2017) 112:1105–19. doi: 10.1016/j.bpj.2017.01.020
27. Represa A, Deloulme JC, Sensenbrenner M, Ben-Ari Y, Baudier J. Neurogranin: immunocytochemical localization of a brain-specific protein kinase C substrate. *J Neurosci.* (1990) 10:3782–92. doi: 10.1523/JNEUROSCI.10-12-03782.1990
28. Sato T, Xiao DM Li H, Huang FL, Huang KP. Structure and regulation of the gene encoding the neuron-specific protein kinase C substrate neurogranin (RC3 protein). *J Biol Chem.* (1995) 270:10314–22. doi: 10.1074/jbc.270.17.10314
29. Neuner-Jehle M, Rhyner TA, Borbely AA. Sleep deprivation differentially alters the mRNA and protein levels of neurogranin in rat brain. *Brain Res.* (1995) 685:143–53. doi: 10.1016/0006-8993(95)00416-N
30. Machado R B, Aa H D S, Tufik S. Sleep deprivation induced by the modified multiple platform technique: quantification of sleep loss and recovery. *Brain Res.* (2004) 1004:45–51. doi: 10.1016/j.brainres.2004.01.019
31. Han Y, Wen XS, Rong F, Chen XM, Ouyang RY, Wu S, et al. Effects of chronic rem sleep restriction on D1 receptor and related signal pathways in rat prefrontal cortex. *Biomed Res Int.* (2015) 2015:978236, doi: 10.1155/2015/978236.
32. Suchecki D, Tufik S. Comparison of REM sleep-deprivation methods: role of stress and validity of use. In: Mallick BN, Pandi-Perumal SR, McCarley RW, Morrison AR, editors. *Rapid Eye Movement Sleep: Regulation and Function*. Cambridge: Cambridge University Press (2011) p. 368–382. doi: 10.1017/CBO9780511921179.039
33. Li SJ, Cui SY, Zhang XQ Yu B, Sheng ZF, Huang YL, et al. PKC in rat dorsal raphe nucleus plays a key role in sleep–wake regulation. *Prog Neuropsychopharmacol Biol Psychiatry.* (2015) 63:47–53. doi: 10.1016/j.pnpbp.2015.05.005
34. Armani F, Andersen ML, Andreatini R, Frussa-Filho R, Tufik S, Galduróz JC. Successful combined therapy with tamoxifen and lithium in a paradoxical sleep deprivation-induced mania model. *CNS Neurosci Ther.* (2012) 18:119–25. doi: 10.1111/j.1755-5949.2010.00224.x
35. Abrial E, Bétourné A, Etiévant A, Lucas G, Scarna H, Lambásseñas L, et al. Protein kinase c inhibition rescues manic-like behaviors and hippocampal cell proliferation deficits in the sleep deprivation model of mania. *Int J Neuropsychopharmacol.* (2014) 18:pyu031. doi: 10.1093/ijnp/pyu031
36. Díez-Guerra FJ. Neurogranin, a link between calcium/calmodulin and protein kinase C signaling in synaptic plasticity. *IUBMB Life.* (2010) 62:597–606. doi: 10.1002/iub.357
37. Kumar V, Chichili VPR, Zhong L, Tang X, Velazquez-Campoy A, Sheu FS, et al. Structural basis for the interaction of unstructured neuron specific substrates neuromodulin and neurogranin with calmodulin. *Sci Rep.* (2013) 3:1392. doi: 10.1038/srep01392

38. Alkadhi K, Zaqaar M, Alhaider I, Salim S, Aleisa A. Neurobiological consequences of sleep deprivation. *Curr Neuropharmacol.* (2013) 11:231–49. doi: 10.2174/1570159X11311030001

Conflict of Interest: The authors declare that the research was conducted in the absence of any commercial or financial relationships that could be construed as a potential conflict of interest.

Publisher's Note: All claims expressed in this article are solely those of the authors and do not necessarily represent those of their affiliated organizations, or those of the publisher, the editors and the reviewers. Any product that may be evaluated in this article, or claim that may be made by its manufacturer, is not guaranteed or endorsed by the publisher.

frontiers in Psychiatry

SYSTEMATIC REVIEW
published: 01 November 2021
doi: 10.3389/fpsyt.2021.772068

Brain Functional and Structural Changes in Alzheimer's Disease With Sleep Disorders: A Systematic Review

Yong-shou Liu[1]*, *Yong-ming Wang*[2]* and *Ding-jun Zha*[1]*

[1] Department of Otolaryngology-Head and Neck Surgery, Xijing Hospital, Air Force Medical University, Xi'an, China,
[2] Department of Psychosis Studies, Institute of Psychiatry, Psychology & Neuroscience, King's College London, London, United Kingdom

Introduction: Sleep disorders (SLD) are supposed to be associated with increased risk and development of Alzheimer's disease (AD), and patients with AD are more likely to show SLD. However, neurobiological performance of patients with both AD and SLD in previous studies is inconsistent, and identifying specific patterns of the brain functional network and structural characteristics in this kind of comorbidity is warranted for understanding how AD and SLD symptoms interact with each other as well as finding effective clinical intervention. Thus, the aims of this systematic review were to summarize the relevant findings and their limitations and provide future research directions.

Methods: A systematic search on brain functional and structural changes in patients with both AD and SLD was conducted from PubMed, Web of Science, and EMBASE databases.

Results: Nine original articles published between 2009 and 2021 were included with a total of 328 patients with comorbid AD and SLD, 367 patients with only AD, and 294 healthy controls. One single-photon emission computed tomography study and one multislice spiral computed tomography perfusion imaging study investigated changes of cerebral blood flow; four structural magnetic resonance imaging (MRI) studies investigated brain structural changes, two of them used whole brain analysis, and another two used regions of interest; two resting-state functional MRI studies investigated brain functional changes, and one 2-deoxy-2-(18F)fluoro-d-glucose positron emission tomography (18F-FDG-PET) investigated 18F-FDG-PET uptake in patients with comorbid AD and SLD. Findings were inconsistent, ranging from default mode network to sensorimotor cortex, hippocampus, brain stem, and pineal gland, which may be due to different imaging techniques, measurements of sleep disorder and subtypes of AD and SLD.

Conclusions: Our review provides a systematic summary and promising implication of specific neuroimaging dysfunction underlying co-occurrence of AD and SLD. However, limited and inconsistent findings still restrict its neurobiological explanation. Further

OPEN ACCESS

Edited by:
Yuanqiang Zhu,
Fourth Military Medical University, China

Reviewed by:
Zhuoya Yang,
Army Medical University, China
Wenfeng Zhu,
Tianjin Normal University, China

***Correspondence:**
Yong-shou Liu
liuysh1980@163.com
Yong-ming Wang
1926418@qq.com
Ding-jun Zha
zhadjun@fmmu.edu.cn

Specialty section:
This article was submitted to Neuroimaging and Stimulation, a section of the journal Frontiers in Psychiatry

Received: *07 September 2021*
Accepted: *01 October 2021*
Published: *01 November 2021*

Citation:
Liu Y-s, Wang Y-m and Zha D-j (2021) Brain Functional and Structural Changes in Alzheimer's Disease With Sleep Disorders: A Systematic Review. Front. Psychiatry 12:772068. doi: 10.3389/fpsyt.2021.772068

studies should use unified standards and comprehensive brain indices to investigate the pathophysiological basis of interaction between AD and SLD symptoms in the development of the disease spectrums.

Keywords: Alzheimer's, sleep disorders, brain function and structure, default mode network, hippocampus

INTRODUCTION

Alzheimer's disease (AD) is a severe neurodegenerative disease, manifested as deterioration in cognition (1), memory (2), thinking, behavior, and the ability to perform everyday activities (3). The World Health Organization reports that, as the most common form of dementia, AD may contribute to 30–35 million patients worldwide and 6–7 million new cases every year. However, there is still no particularly effective treatment for it (3). Finding possible risk or comorbid factors and effective intervention of this disease is warranted.

As one of the most important noxious factors on physical and mental health (4), sleep disorder (SLD) is reported to be closely associated with development of AD (5–7). Some researchers even believe that SLD has decisive effects on AD (2). It is reported that roughly more than 50% of patients with AD have got significant SLD (8), which may include insomnia, obstructive apnea hypopnea syndrome (OSA), rapid eye movement sleep behavior disorder (RBD), sleep apnea, shortened sleep duration, fragmented sleep, slow wave sleep disruption, and misalignment of circadian rhythm (9). Older adults with SLD are more likely to have a diagnosis of AD or cognitive decline (10). Brain chemical changes in OSA patients could further lead to cognitive impairment and early AD clinical performance, and continuous positive airway pressure therapy could modify these AD biomarkers (11). RBD may also lead to cognitive impairment and pathologies of AD (12).

Another 9-year follow-up study found reduced sleep was associated with a two-fold increased risk of AD compared with controls (13). The reasons for this significant correlation could be that the SLD can increase stress reactions and impair attention, episodic memory (14) and cognitive function (15), increase adrenocorticotropin and cortisol secretion, weaken neuronal structures, increase risk of cell death (5). Specifically, SLD could increase beta-amyloid production and deposition (2) and decrease its clearance in the brain (7), further cause synaptic dysfunction (2), and exacerbate the deterioration of AD symptoms, especially when both were severe (9). One review indicates that the treatment of SLD may also alleviate cognitive decline and the risk of AD (2) and be an effective therapy for AD symptoms (9). However, the specific neurobiological basis of the interactive process between AD and SLD symptoms are still controversial.

Neuroimaging technology could help us understand the brain pathophysiology of AD and SLD *in vivo*. Previous review and meta-analysis studies indicate that patients with AD exhibit decreased regional cerebral blood flow in the posterior cingulate cortices (PCC), precuneus, inferior parietal lobules (IPL), dorsolateral prefrontal cortex (DLPFC) (16); decreased gray matter volume in the left parahippocampal gyrus, left PCC, right fusiform gyrus, and right superior frontal gyrus (SFG) (17) and network changes mainly associated with subcortical areas (18) and default mode network (DMN) (19). In particular, the DMN is reported as the first network affected by AD (20). Meanwhile, patients with SLD show decreased brain functional and structural indices in the frontal cortex, temporal gyrus, fusiform gyrus, striatum, cingulate cortex, precentral gyrus, and reduced glucose metabolism in the limbic system as well as increased brain activation and regional homogeneity in the middle frontal gyrus, precunus, cingulate gyrus (21) and overactivation in the hypothalamic-pituitary-adrenal cascade (5). However, one review indicates that cortical hyperarousal other than hypo-arousal activities, as the central feature of SLD, may be located at the temporal cortex and hippocampus and could contribute to both AD and SLD pathogenesis so as to increase their comorbidity rate (8).

Although these findings show some shared and bidirectional interactions of brain disturbances, neurodegeneration, and neuropathology between AD and SLD (9), the key brain changes associated with high comorbidity and their interactions are still controversial and remain to be elucidated. The necessity and merits of this review are that through the conclusions of previous brain functional and structural findings in patients with comorbid AD and SLD, we could find the possibly abnormal SLD-related brain regions or networks that beta-amyloid mainly deposit or neural inflammation led to in these patients. We could also well-understand the specific neurobiological basis of how SLD contributes to the development of AD symptoms and find a possible effective way to delay or prevent the brain alterations and clinical manifestations of AD through effective treatment of

Abbreviations: 18F-FDG-PET, 2-deoxy-2-(18F)fluoro-d-glucose positron emission tomography; AD, Alzheimer's disease; CBF, cerebral blood flow; CCMD-3, Chinese Classification of Mental Disorders version 3; CERAD, consortium to establish a registry for Alzheimer's disease assessment packet clinical assessment battery; dALFF, dynamic amplitude of low-frequency fluctuation; DLPFC, dorsolateral prefrontal cortex; DMN, default mode network; IPL, inferior parietal lobules; MFG, middle frontal gyrus; mPerAF, percent amplitude of fluctuation divided by global mean PerAF; MSCTP, multi-slice spiral computed tomography perfusion imaging; NIAA, National Institute of Aging-Alzheimer's criteria in 2011; NIAAA, National Institute on Aging-Alzheimer's Association workgroups on diagnostic guidelines for Alzheimer's disease; NPI-Q, brief questionnaire form of neuropsychiatric inventory; OSA, obstructive apnea hypopnea syndrome; PCC, posterior cingulate cortices; PerAF, percent amplitude of fluctuation; PSG, polysomnographic recordings; PSQI, Pittsburgh sleep quality index; RBD, rapid eye movement sleep behavior disorder; RBDSQ, rapid eye movement sleep behavior disorder screening questionnaire; ROI, region of interest; rs-fMRI, resting-state functional magnetic resonance imaging; SFG, superior frontal gyrus; SLD, sleep disorder; SMG, supramarginal gyrus; sMRI, structural magnetic resonance imaging (sMRI); sNPI, sleep subscale of neuropsychiatric inventory; SPECT, Single-photon emission computed tomography; STP, superior temporal pole.

SLD symptoms. Furthermore, concluding the specific differences of brain changes in patients with comorbidity of AD and SLD compared with patients with AD alone could also help us find a possible specific subtype of the AD spectrum. For these aims, the present review provides an overview of the specific neuroimaging findings of patients with comorbid AD and SLD, their limitations, and future research directions. In addition, if the number of included studies using the same imaging technologies is >3, then a meta-analysis will be conducted.

Previous studies mainly found abnormal limbic structures, especially hippocampal astrophic (9) and dysfunctional regions in the DMN in patients with AD or SLD (20). Based on these findings, we hypothesize that these brain regions and networks would exhibit relatively consistent abnormality in patients with comorbid AD and SLD in related studies.

METHODS

Search Strategy and Study Selection

A systematic literature search was conducted to identify published studies that examined brain imaging changes in patients with AD and SLD using databases of PubMed, Web of Science, and Embase. The key words were searched using the following terms: (sleep OR insomnia OR apnea hypopnea) AND (Alzheimer's*) AND (MRI OR brain imag*), and the search period ended on August 8, 2021, from the earliest date of the databases. The reference lists of retrieved articles were also searched for identifying potentially relevant studies. There were no other restrictions, such as SLD classification, imaging methods, language, or publication year; i.e., we included all studies of insomnia, OSA, RBD, sleep apnea, shortened sleep duration, fragmented sleep, slow wave sleep disruption, and misalignment of circadian rhythm, etc. All primary studies that reported brain functional or structural changes of the patients with comorbid AD and SLD were included in the review. If values of demographic information or brain changes were unclear, we attempted to contact the authors for clarification. The exclusion criteria were (1) case reports, (2) review or meta-analyses, and (3) non-human studies, and (4) if studies had overlapping samples, only studies with the largest sample were included. Any divergences were resolved by discussion between authors.

Data Extraction

The extracted characteristics of the articles included first author, publish year, sample size, mean age of participants, questionnaires for AD or SLD in the articles, imaging technique, whole brain or regions of interest analysis, country of study, and the main results, which were brain functional or structural or chemical changes in comorbid AD and SLD compared with AD or healthy controls.

RESULTS

Included Studies

A PRISMA flow chart of article choice is presented in **Figure 1**. A total of 1,240 articles were retrieved, 1,231 articles were excluded, and nine studies were finally included in the review. Summary of the included studies is showed in **Table 1**.

Two of them compared brain differences between the comorbidity of AD and SLD groups, the AD group and healthy controls (22, 23); three studies only included the comorbidity group and healthy controls (24–26); four studies recruited the comorbidity group and the AD group (20, 27–29). Published years of articles ranged from 2009 to 2021. Three studies were conducted in China, three in Korea, one in Canada, one in Italy, and one in Japan.

Included patients with comorbid AD and SLD, AD only, and controls in this review were 328, 367, and 294, respectively. Sample size of every group ranged from 14 to 257. Mean age of participants ranged from 71.5 to 81.5.

In these studies, one single-photon emission computed tomography (SPECT) (22) study and one multislice spiral computed tomography perfusion imaging (MSCTP) (26) study investigated changes of cerebral blood flow; two whole-brain structural magnetic resonance imaging (sMRI) studies investigated brain structural changes (27, 28), one sMRI study investigated the brain stem volume (24), and another investigated the pineal gland volume (30); two resting-state functional magnetic resonance imaging (rs-fMRI) studies investigated brain functional changes (23, 29); and one 2-deoxy-2-(18F) fluoro-d-glucose positron emission tomography (18F-FDG-PET) investigated 18F-FDG-PET uptake in patients with comorbid AD and SLD (25).

Evaluation of AD and SLD

Diagnosis and evaluation of AD and SLD are heterogeneous. In AD diagnosis, four studies used National Institute of Neurological and Communicative Disorders and stroke—AD and related disorders association criteria (NINCD) (22–24, 28), one used National Institute on Aging-Alzheimer's Association workgroups on diagnostic guidelines for AD (NIAAA) (25), one used a consortium to establish a registry for AD assessment packet clinical assessment battery (CERAD) (30), one used Chinese Classification of Mental Disorders version 3 (CCMD-3) (26), one used National Institute of Aging-Alzheimer's criteria in 2011 (NIAA) (29), and one did not provide a diagnostic standard (27). In SLD evaluation, three used a sleep subscale of neuropsychiatric inventory (sNPI) (22, 24, 28), three used the Pittsburgh sleep quality index (PSQI) (26, 27, 29), one used polysomnographic recordings (PSG) (25), one used a brief questionnaire form of neuropsychiatric inventory (NPI-Q) (23), one used a rapid eye movement sleep behavior disorder screening questionnaire (RBDSQ) (30).

Brain Changes in Comorbid AD and SLD

All studies found significant brain changes in patients with comorbid AD and SLD compared with patients with only AD or healthy controls.

One region of interest (ROI)-based sMRI study found significant differences of posterior brain stem morphology in the AD and SLD group compared with controls and a negative correlation between the NPI scores and left posterior lateral brain stem volume (24), and another ROI

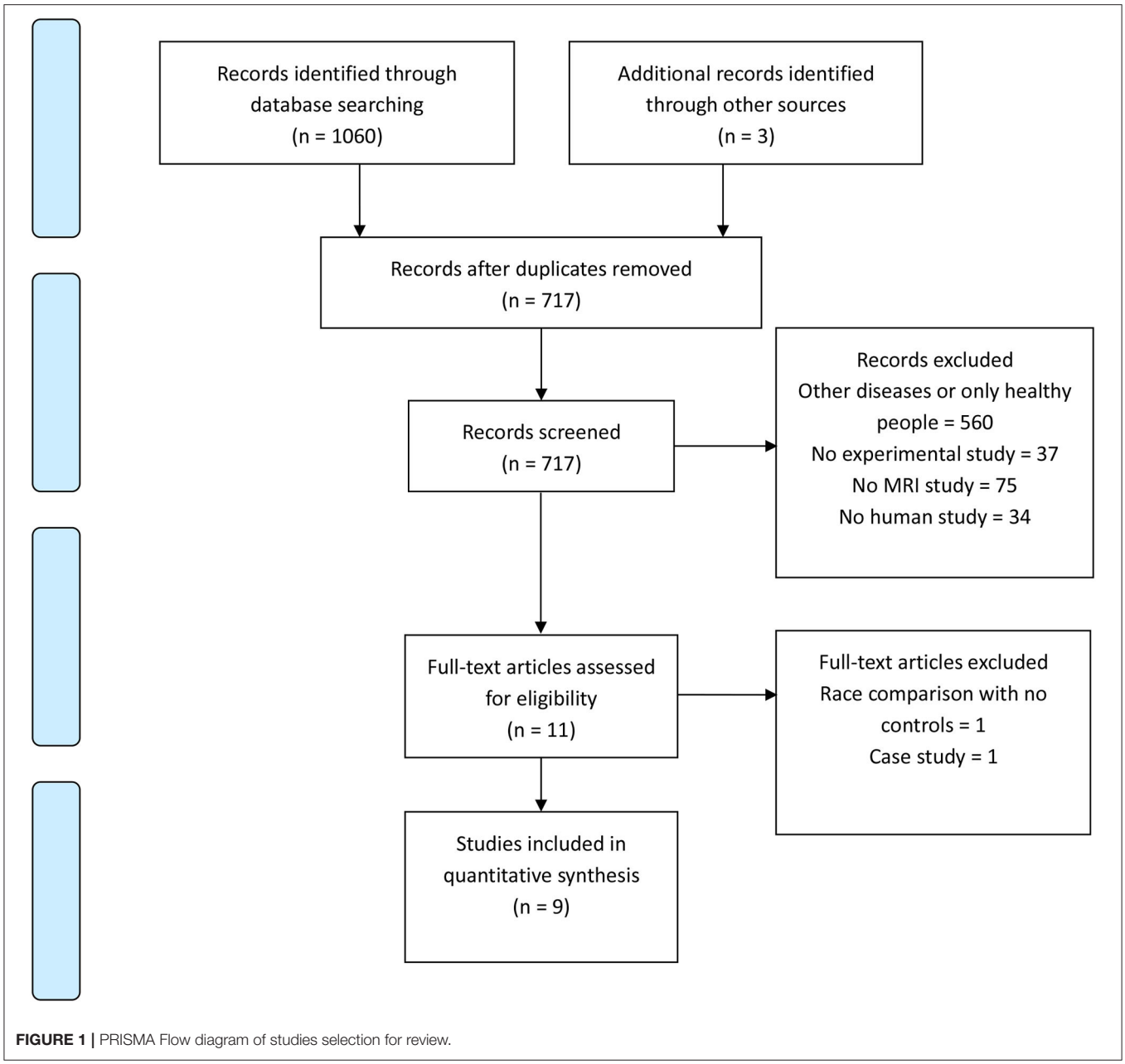

FIGURE 1 | PRISMA Flow diagram of studies selection for review.

study found decreased pineal gland volume in AD and SLD compared with AD, and the pineal gland volume negatively correlated with the severity of SLD (30). One whole brain and hippocampus subfield ROI study found decreased gray matter volume of bilateral cingulate gyrus in poor sleeper AD compared with AD only as well as no significant results in the hippocampus (27). Another whole brain and pineal gland ROI study found decreased gray matter volume of bilateral precuneus in AD patients with sleep disturbance compared with patients with AD only, which negatively correlated with the sNPI scores (28). However, different from the second study, no significant results were found in the pineal gland ROI comparison (28).

Two rs-fMRI studies investigated brain functional changes (23, 29). One of them found increased dynamic amplitude of low-frequency fluctuation (dALFF) variance of right cerebellum, left superior temporal pole (STP), right rectus, right hippocampus, decreased dALFF variance of right supramarginal gyrus (SMG), decreased sALFF of left precentral gyrus, right IPL, and cuneus in patients with AD and SLD compared with AD, and dALFF variance positively correlated with amyloid deposit in regions involved in memory and sleep (23). Another study found a decreased percentage of amplitude of fluctuation (PerAF) and PerAF divided by global mean PerAF (mPerAF) in the left brainstem, left calcarine gyrus, left lingual gyrus; decreased PerAF in the left fusiform gyrus, left parahippocampal gyrus, left

TABLE 1 | Summary of AD&SLD studies included in the meta-analysis.

References	Country	AD and SLD subsets	AD and SLD cases (male/female)	AD cases (male/female)	Controls (male/female)	AD and SLD mean age (SD)	AD mean age (SD)	Controls mean age (SD)	Questionnaire	Imaging technique	ROIs	Main results
Ismail et al. (22)	Canada	AD with or without sleep loss	14/24	7/10	17/20	72.4 (7.4)	74.2 (8.3)	71.5 (6.3)	NINCD, sNPI	SPECT-CBF	WB	Higher perfusion in the right MFG in AD and SLD compared with AD
Lee et al. (24)	Korea	sNPI in AD & SLD	13/31	N.A.	14/26	76.2 (5.7)	N.A.	75.2 (4.7)	NINCD, CDR, sNPI	3T T1-weighted sMRI	Brain stem	Decreased volume in the brain stem; negative correlation between the sNPI scores and left posterior lateral brain stem volume in AD and SLD
Liguori et al. (25)	Italy	Polysomnographic recordings in AD & SLD	8/18	N.A.	7/11	71.56 (3.92)	N.A.	74.11 (2.78)	NIAAA, PSG	18F-FDG-PET	Hypo-thalamus	Interplay between the reduction of sleep efficiency, REM sleep and the reduction of hypothalamic 18F-FDG-PET uptake, which negatively correlated with the index of neurodegeneration in AD and SLD
Yi et al. (27)	Korea	Poor or good sleeper AD	32	14	N.A.	N.A.	N.A.	N.A.	PSQI	3T T1-weighted sMRI	WB and hippo subfields	Decreased gray matter volume in the bilateral cingulate gyrus in poor sleeper AD. No hippo findings.
Matsuoka et al. (28)	Japan	AD with or without sleep disturbance	8/11	11/33	N.A.	81.5 (6.4)	77.8 (6.9)	N.A.	NINCD, ICD-10, sNPI	3T T1-weighted sMRI	WB and pineal gland	Decreased gray matter volume in the bilateral precuneus in AD with sleep disturbance. No pineal gland findings.
Li et al. (23)	China	AD with poor or normal sleep	7/9	9/5	53/70	74.66 (8.50)	70.76 (8.24)	74.02 (7.13)	NINCD, CDR, NPI-Q	rs-fMRI &PET	WB	Increased dALFF variance in the right cerebellum, left STP, right rectus, right hippo, decreased dALFF variance in the right SMG, decreased sALFF in the left precentral gyrus, right IPL and cuneus in AD and SLD compared with AD

(Continued)

TABLE 1 | Continued

References	Country	AD and SLD subsets	AD and SLD cases (male/female)	AD cases (male/female)	Controls (male/female)	AD and SLD mean age (SD)	AD mean age (SD)	Controls mean age (SD)	Questionnaire	Imaging technique	ROIs	Main results
Park et al. (20)	Korea	AD with or without sleep behavior disorder	8/31	79/178	N.A.	76.8 (7.4)	77.4 (7.4)	N.A.	CERAD, RBDSQ	3T T1-weighted sMRI & PET	Pineal gland	Decreased pineal gland volume in AD & SLD compared with AD, and the pineal gland volume negatively correlated with the severity of SLD
Liu et al. (26)	China	AD with sleep disorders	31/45	N.A.	32/44	73.07 (5.41)	N.A.	72.32 (5.28)	CCMD-3, PQSI	MSCTP-CBF	TL, FL, hippo, BG	Decreased CBF in the TL, FL, hippo and BG in AD and SLD
Wang et al. (29)	China	Mild AD with or without sleep disturbances	12/26	8/13	N.A.	73.7 (7.2)	73.6 (8.4)	N.A.	NIAA, CDR, PSQI	rs-fMRI	WB	Decreased mPerAF and PerAF in the left brainstem, left calcarine gyrus, left lingual gyrus; decreased PerAF in the left fusiform gyrus, left parahippocampal gyrus, left precentral gyrus, left postcentral gyrus

18F-FDG-PET, 2-deoxy-2-(18F)fluoro-d-glucose positron emission tomography; AD, Alzheimer's disease; BG, basal ganglia; CBF, cerebral blood flow; CCMD-3, Chinese Classification of Mental Disorders version 3; CDR, clinical dementia rating scale; CERAD, consortium to establish a registry for Alzheimer's disease assessment packet clinical assessment battery; dALFF, dynamic amplitude of low-frequency fluctuation; FL, frontal lobe; hippo, hippocampus; ICD-10, International Classification of Disease version 10; IPL, inferior parietal lobule; MFG, middle frontal gyrus; mPerAF, percent amplitude of fluctuation divided by global mean percent amplitude of fluctuation; MSCTP, multi-slice spiral computed tomography perfusion imaging; N.A., not available; NIAA, National Institute of Aging-Alzheimer's criteria in 2011; NIAAA, National Institute on Aging-Alzheimer's Association workgroups on diagnostic guidelines for Alzheimer's disease; NINCD, National Institute of Neurological and Communicative Disorders and stroke – Alzheimer's disease and related disorders association criteria; NPI-Q, brief questionnaire form of neuropsychiatric inventory; PerAF, percent amplitude of fluctuation; PSQI, Pittsburgh sleep quality index; RBDSQ, rapid eye movement sleep behavior disorder screening questionnaire; PSG, polysomnographic recordings; REM, rapid eye movement; ROI, region of interests; rs-fMRI, resting state functional magnetic resonance imaging; sALFF, static amplitude of low-frequency fluctuation; SD, standard deviation; SLD, sleep disorders; SMG, supramarginal gyrus; sMRI, structural magnetic resonance imaging; sNPI, sleep subscale of neuropsychiatric inventory; SPECT, single-photon emission computed tomography; STP, superior temporal pole; TL, temporal lobe; WB, whole brain.

precentral gyrus, left postcentral gyrus in patients with AD and SLD compared with AD (29).

In the rest of the studies, one MSCTP study investigated changes of cerebral blood flow (CBF) in ROIs, and found decreased CBF of temporal lobe, frontal lobe, hippocampus, and basal ganglia in the AD and SLD group compared with controls (26). One SPECT study found higher CBF in the right middle frontal gyrus (MFG) in the AD and SLD group compared with the AD group (22). One 18F-FDG-PET study investigated 18F-FDG-PET uptake in patients with comorbid AD and SLD and found correlation between the reduction of sleep efficiency, REM sleep, and the reduction of hypothalamic 18F-FDG-PET uptake, which negatively correlated with the index of neurodegeneration in AD and SLD group compared with controls (25).

DISCUSSION

Nine experimental studies, which investigated brain functional and structural changes in patients with both AD and SLD, using rs-fMRI, sMRI, PET, SPECT, or MSCTP scanning, were included in our review. Although many findings showed heterogeneity, which may be due to small sample sizes, different experimental designs, disease assessment and imaging tools, some findings still support our hypothesis.

DMN is a brain network most activated in the resting state and associated with autobiographical and episodic memory (1), consolidating individual experiments, self-referential information processing, and constructing integrated "self" (31). These cognitive domains are believed to be impaired early, and the DMN is the first dysfunctional network affected by increased beta-amyloid deposition in patients with AD (1, 20) as well as in patients with SLD (32, 33). The abnormal DMN, especially the overactivated hippocampus and medial temporal lobe, is reported to associate with dysfunction of emotion (34), memory, and cognition in patients with SLD (15, 35) and could also interact with increased beta-amyloid production and greater local deposition (1) and facilitate the following hypo-activation and atrophy of hippocampus and other DMN regions in patients with AD (8). However, whether overactivation (8, 15), hypo-activation (26, 29), or no change (22, 27) of the hippocampus in the different developmental processes of these two diseases is still controversial. It may be due to different categories of hippocampal subregions, such as previous studies that believe that changed anterior, medial, or posterior parts of the hippocampal volumes could have different changes in patients with AD (36) or abnormal hippocampal subregions of the dentate gyrus (DG), cornu ammonis 1/2/3, and subiculum play distinct roles in memory impairments (37) or due to different neurobiological changes of SLD subtypes, such as OSA or RBD, which need further investigation with high-resolution brain imaging.

Decreased sALFF in the precentral gyrus (23) and decreased PerAF in the precentral and postcentral gyrus were found in the comorbidity of the AD and SLD group (29). These decreased precentral activations may imply increased night awakening, reduced slow-wave activity, and sleep depth linked to sleep disruption (38) as well as impaired sensory and motor function by SLD in the development of AD (29).

Decreased volume (24), mPerAF and PerAF of the brainstem were found in the comorbidity group in previous studies (29). The brainstem is usually unmentioned or not investigated in brain imaging studies. However, it is a key neurobiological basis of sleep regulation, producing and regulating the sleep–wake rhythms (29). Degeneration of it could occur very early in patients with AD and also contribute to the onset of SLD, fragmented sleep, impaired memory consolidation, and cognitive decline (24).

Some researchers believe that the pineal gland is associated with sleep regulation through melatonin synthesis, and beta-amyloid could easily inhibit its function (39), which, in turn, could reduce the protection of cholinergic neurons from amyloid toxicity, increase the risk of both SLD and AD (30). In the included studies, only one found decreased pineal gland volume in the comorbidity group (30). Another ROI-based study (28) and four whole-brain studies did not find any significant results (22, 23, 27, 29). These inconsistent results in previous studies may imply a different presentation of melatonergic systems in different developmental stages or subtypes of the diseases, which need more studies with large sample sizes for further verification (28).

Some other positive results could also be worth considering. One whole-brain study found higher CBF in the dorsal lateral prefrontal cortex (DLPFC) in the comorbidity group compared with the AD group (22). Another ROI-based study found significant decreased brain glucose consumption in the hypothalamus in the comorbidity group, which negatively correlated with the index of neurodegeneration in patients with AD and SLD and a significant interplay between the reduction of sleep efficiency, REM sleep, and the reduction of hypothalamic 18F-FDG-PET uptake (25). The abnormal activation of DLPFC, which may be the result of impaired thalamocortical ascending executive cholinergic pathways, could associated with sleep loss and frequent arousals during sleep (22) and lead to cognitive dysfunction (15). The hypothalamus is associated with homeostasis and the sleep–wake cycle and could be affected by AD pathology leading to some non-cognitive deficits, such as sleep–wake and neuroendocrine disorders and loss of weight (25). Meanwhile, hypothalamic-pituitary-adrenal axis dysregulation and inflammation was also reported to contribute to the development of pathophysiology of both SLD and AD symptoms (8). The knowledge of the hypothalamic circuitry functions in the interaction between AD and SLD symptoms still needs expansion for reliable biomarkers and therapeutic approaches.

There are still many limitations left in current research. First, the clinical manifestation and developmental process of SLD is complicated with high heterogeneity, and the assessment of it is still not unified between studies. Furthermore, many studies did not report the onset time or duration of SLD. Second, neurobiological explanation of comorbidity is still constrained by a lack of magnetic resonance spectroscopy or other microscopic neurobiological studies. Elaborate experiments with solution of these limitations, such as

large, well-characterized, or homogeneous samples; standard assessment; diagnosis; imaging and analysis protocols (40); and longitudinal studies on AD risk management, prevention and intervention from the viewpoint of SLD treatment are warranted (6). Finally, because the number of studies included in our review using the same scanning technology are all not greater than three, meta-analysis was not able to be conducted. It limits the preciseness and generalizability of our research.

Integrating all these studies together, we could conclude that SLD may have induced even decisive effects on the pathological development of AD symptoms. The DMN, especially the hippocampus as well as the sensorimotor cortex, may be the initial neurophysiological basis of interactions between AD and SLD symptoms. These changes could be mainly associated with memory, self-awareness, and sensorimotor deficiencies. Functions of the brainstem and pineal gland in this comorbidity still need further verification. Our study may contribute to a better understanding of the pathophysiology and possible risk of AD in patients with SLD and a suggestion of potential neural biomarkers for the further investigation on the early diagnosis and treatment of SLD patients with AD risk or with the comorbidity of AD and SLD. The facilitated effects of SLD symptoms on AD, and this physiological basis in the AD developmental continuum from subclinical to high-risk population and to patients deserve more attention in the future studies. For example, elaborately task-based fMRI experimental design, technology of magnetic resonance spectroscopy or AD animal models could be introduced. Findings from these studies could further help us to prevent or attenuate cognitive decline and AD symptoms (2), perform targeted early intervention on possible dementia risk and improve senile life quality (5).

DATA AVAILABILITY STATEMENT

The original contributions presented in the study are included in the article/supplementary material, further inquiries can be directed to the corresponding author/s.

AUTHOR CONTRIBUTIONS

Y-sL and Y-mW designed the study, managed the literature searches and the analyses, and wrote the whole manuscript. D-jZ designed the study, interpreted the data, and edited this manuscript. All authors have contributed to approved the final manuscript.

REFERENCES

1. Lucey BP, Bateman RJ. Amyloid-β diurnal pattern: possible role of sleep in Alzheimer's disease pathogenesis. *Neurobiol Aging.* (2014) 35:S29–34. doi: 10.1016/j.neurobiolaging.2014.03.035
2. Sadeghmousavi S, Eskian M, Rahmani F, Rezaei N. The effect of insomnia on development of Alzheimer's disease. *J Neuroinflamm.* (2020) 17:1–20. doi: 10.1186/s12974-020-01960-9
3. World Health Organization. *Dementia.* (2020). Availability online at: https://www.who.int/news-room/fact-sheets/detail/dementia
4. Li L, Wu C, Gan Y, Qu X, Lu Z. Insomnia and the risk of depression: a meta-analysis of prospective cohort studies. *BMC Psychiatry.* (2016) 16:1–16. doi: 10.1186/s12888-016-1075-3
5. de Almondes KM, Costa MV, Malloy-Diniz LF, Diniz BS. Insomnia and risk of dementia in older adults: systematic review and meta-analysis. *J Psychiat Res.* (2016) 77:109–15. doi: 10.1016/j.jpsychires.2016.02.021
6. Hertenstein E, Feige B, Gmeiner T, Kienzler C, Spiegelhalder K, Johann A, et al. Insomnia as a predictor of mental disorders: a systematic review and meta-analysis. *Sleep Med Rev.* (2019) 43:96–105. doi: 10.1016/j.smrv.2018.10.006
7. Sumsuzzman DM, Choi J, Jin Y, Hong Y. Neurocognitive effects of melatonin treatment in healthy adults and individuals with Alzheimer's disease and insomnia: a systematic review and meta-analysis of randomized controlled trials. *Neurosci Biobehav Rev.* (2021) 127:459–73. doi: 10.1016/j.neubiorev.2021.04.034
8. Chappel-Farley MG, Lui KK, Dave A, Chen IY, Mander BA. Candidate mechanisms linking insomnia disorder to Alzheimer's disease risk. *Curr Opin Behav Sci.* (2020) 33:92–8. doi: 10.1016/j.cobeha.2020.01.010
9. Ferini-Strambi L, Hensley M, Salsone M. Decoding causal links between sleep apnea and Alzheimer's disease. *J Alzheimers Dis.* (2021) 80:29–40. doi: 10.3233/JAD-201066
10. Osorio RS, Pirraglia E, Agüera-Ortiz LF, During EH, Sacks H, Ayappa I, et al. Greater risk of Alzheimer's disease in older adults with insomnia. *J Am Geriatr Soc.* (2011) 59:559–62. doi: 10.1111/j.1532-5415.2010.03288.x
11. Liguori C, Mercuri NB, Izzi F, Romigi A, Cordella A, Sancesario G, et al. Obstructive sleep apnea is associated with early but possibly modifiable Alzheimer's disease biomarkers changes. *Sleep.* (2017) 40:zsx011. doi: 10.1093/sleep/zsx011
12. Zhang F, Niu L, Liu X, Liu Y, Li S, Yu H, et al. Rapid eye movement sleep behavior disorder and neurodegenerative diseases: an update. *Aging Dis.* (2020) 11:315–26. doi: 10.14336/AD.2019.0324
13. Hahn EA, Wang HX, Andel R, Fratiglioni L. A change in sleep pattern may predict Alzheimer disease. *Am J Geriatr Psychiatr.* (2014) 22:1262–71. doi: 10.1016/j.jagp.2013.04.015
14. Grau-Rivera O, Operto G, Falcón C, Sánchez-Benavides G, Cacciaglia R, Brugulat-Serrat A, et al. Association between insomnia and cognitive performance, gray matter volume, and white matter microstructure in cognitively unimpaired adults. *Alzheimers Res Ther.* (2020) 12:4. doi: 10.1186/s13195-019-0547-3
15. Pang R, Zhan Y, Zhang Y, Guo R, Wang J, Guo X, et al. Aberrant functional connectivity architecture in participants with chronic insomnia disorder accompanying cognitive dysfunction: a whole-brain, data-driven analysis. *Front Neurosci.* (2017) 11:259. doi: 10.3389/fnins.2017.00259
16. Ma HR, Pan PL, Sheng LQ, Dai ZY, Wang DG, Luo R, et al. Aberrant pattern of regional cerebral blood flow in Alzheimer's disease: a voxel-wise meta-analysis of arterial spin labeling MR imaging studies. *Oncotarget.* (2017) 8:93196–208. doi: 10.18632/oncotarget.21475
17. Wang WY, Yu JT, Liu Y, Yin RH, Wang HF, Wang J, et al. Voxel-based meta-analysis of grey matter changes in Alzheimer's disease. *Transl Neurodegener.* (2015) 4:1–9. doi: 10.1186/s40035-015-0027-z
18. Jacobs HI, Radua J, Lückmann HC, Sack AT. Meta-analysis of functional network alterations in Alzheimer's disease: toward a network biomarker. *Neurosci Biobehav Rev.* (2013) 37:753–65. doi: 10.1016/j.neubiorev.2013.03.009
19. Badhwar A, Tam A, Dansereau C, Orban P, Hoffstaedter F, Bellec P. Resting-state network dysfunction in Alzheimer's disease: a systematic review and meta-analysis. *Alzheimer's & Dement.* (2017) 8:73–85. doi: 10.1016/j.dadm.2017.03.007
20. Greicius MD, Srivastava G, Reiss AL, Menon V. Default-mode network activity distinguishes Alzheimer's disease from healthy aging: evidence from functional MRI. *Proc Natl Acad Sci USA.* (2004) 101:4637–42. doi: 10.1073/pnas.0308627101
21. Wu Y, Zhuang Y, Qi J. Explore structural and functional brain changes in insomnia disorder: a PRISMA-compliant whole brain ALE meta-analysis for multimodal MRI. *Medicine.* (2020) 99:e19151. doi: 10.1097/MD.0000000000019151

22. Ismail Z, Herrmann N, Francis PL, Rothenburg LS, Lobaugh NJ, Leibovitch FS, et al. A SPECT study of sleep disturbance and Alzheimer's disease. *Dement Geriatr Cogn.* (2009) 27:254–59. doi: 10.1159/000203889
23. Li K, Luo X, Zeng Q, Jiaerken Y, Wang S, Xu X, et al. Interactions between sleep disturbances and Alzheimer's disease on brain function: a preliminary study combining the static and dynamic functional MRI. *Sci Rep.* (2019) 9:19064. doi: 10.1038/s41598-019-55452-9
24. Lee JH, Jung WS, Choi WH, Lim HK. Aberrant brain stem morphometry associated with sleep disturbance in drug-naïve subjects with Alzheimer's disease. *Neuropsychiatr Dis Treat.* (2016) 12:2089–93. doi: 10.2147/ndt.S114383
25. Liguori C, Chiaravalloti A, Nuccetelli M, Izzi F, Sancesario G, Cimini A, et al. Hypothalamic dysfunction is related to sleep impairment and CSF biomarkers in Alzheimer's disease. *J Neurol.* (2017) 264:2215–23. doi: 10.1007/s00415-017-8613-x
26. Liu WC, Wu JM, Xia JH. Diagnosis of MSCTP in Alzheimer's disease with sleep disorders as the primary manifestation. *Chin J Prim Med Pharm.* (2020) 27:1707–10. doi: 10.3760/cma.j.issn.1008-6706.2020.14.010
27. Yi H, Lee H. Patterns of gray matter volume loss in Alzheimer's disease with sleep disturbance. *Alzheimers Dement.* (2017) 13:P1042. doi: 10.1016/j.jalz.2017.06.1473
28. Matsuoka T, Imai A, Fujimoto H, Kato Y, Shibata K, Nakamura K, et al. Neural correlates of sleep disturbance in Alzheimer's disease: role of the precuneus in sleep disturbance. *J Alzheimers Dis.* (2018) 63:957–64. doi: 10.3233/jad-171169
29. Wang L, Peng D. Altered intrinsic brain activity in mild Alzheimer's disease patients with sleep disturbances. *Neuroreport.* (2021) 32:942–8. doi: 10.1097/wnr.0000000000001689
30. Park J, Suh SW, Kim GE, Lee S, Kim JS, Kim HS, et al. Smaller pineal gland is associated with rapid eye movement sleep behavior disorder in Alzheimer's disease. *Alzheimer's Res Ther.* (2020) 12:157. doi: 10.1186/s13195-020-00725-z
31. Wang YM, Zou LQ, Xie WL, Yang ZY, Zhu XZ, Cheung EF, et al. Altered functional connectivity of the default mode network in patients with schizo-obsessive comorbidity; A comparison between schizophrenia and obsessive-compulsive disorder. *Schizophr Bull.* (2019) 45:199–210. doi: 10.1093/schbul/sbx194
32. Marques DR, Gomes AA, Caetano G, Castelo-Branco M. Insomnia disorder and brain's default-mode network. *Curr Neurol Neurosci.* (2018) 18:1–4. doi: 10.1007/s11910-018-0861-3
33. Li HJ, Nie X, Gong HH, Zhang W, Nie S, Peng DC. Abnormal resting-state functional connectivity within the default mode network subregions in male patients with obstructive sleep apnea. *Neuropsych Dis Treat.* (2016) 12:203–12. doi: 10.2147/NDT.S97449
34. Song K, Li J, Zhu Y, Ren F, Cao L, Huang ZG. Altered small-world functional network topology in patients with optic neuritis: a resting-state fMRI study. *Dis Markers.* (2020) 2021:9948751. doi: 10.1155/2021/9948751
35. Marques DR, Gomes AA, Clemente V, dos Santos JM, Castelo-Branco M. Default-mode network activity and its role in comprehension and management of psychophysiological insomnia: a new perspective. *New Ideas Psychol.* (2015) 36:30–7. doi: 10.1016/j.newideapsych.2014.08.001
36. Laakso MP, Frisoni GB, Könönen M, Mikkonen M, Beltramello A, Geroldi C, et al. Hippocampus and entorhinal cortex in frontotemporal dementia and Alzheimer's disease: a morphometric MRI study. *Biol Psychiatry.* (2000) 47:1056–63. doi: 10.1016/S0006-3223(99)00306-6
37. Masurkar AV. Towards a circuit-level understanding of hippocampal CA1 dysfunction in Alzheimer's disease across anatomical axes. *Journal of Alzheimer's Dis Parkinson*. (2018) 8:412.
38. Peter-Derex L, Yammine P, Bastuji H, Croisile B. Sleep and Alzheimer's disease. *Sleep Med Rev.* (2015) 19:29–38. doi: 10.1016/j.smrv.2014.03.007
39. Cecon E, Chen M, Marçola M, Fernandes PA, Jockers R, Markus RP. Amyloid β peptide directly impairs pineal gland melatonin synthesis and melatonin receptor signaling through the ERK pathway. *FASEB J.* (2015) 29:2566–82. doi: 10.1096/fj.14-265678
40. Tahmasian M, Noori K, Samea F, Zarei M, Spiegelhalder K, Eickhoff SB, et al. A lack of consistent brain alterations in insomnia disorder: an activation likelihood estimation meta-analysis. *Sleep Med Rev.* (2018) 42:111–18. doi: 10.1016/j.smrv.2018.07.004

Conflict of Interest: The authors declare that the research was conducted in the absence of any commercial or financial relationships that could be construed as a potential conflict of interest.

The handling editor YZ declared a shared affiliation, though no other collaboration, with one of the authors Y-sL and D-jZ at the time of the review.

Publisher's Note: All claims expressed in this article are solely those of the authors and do not necessarily represent those of their affiliated organizations, or those of the publisher, the editors and the reviewers. Any product that may be evaluated in this article, or claim that may be made by its manufacturer, is not guaranteed or endorsed by the publisher.

frontiers in Psychiatry

ORIGINAL RESEARCH
published: 05 November 2021
doi: 10.3389/fpsyt.2021.768819

Clinical Response of Major Depressive Disorder Patients With Suicidal Ideation to Individual Target-Transcranial Magnetic Stimulation

Nailong Tang[1,2†], Chuanzhu Sun[3,4†], Yangtao Wang[3†], Xiang Li[3,5], Junchang Liu[1], Yihuan Chen[1], Liang Sun[3], Yang Rao[3], Sanzhong Li[6], Shun Qi[3,7] and Huaning Wang[1*]*

[1] Department of Psychiatry, Xijing Hospital, Fourth Military Medical University, Xi'an, China, [2] Department of Psychiatry, 907 Hospital of Joint Logistics Team, Nanping, China, [3] Brain Modulation and Scientific Research Center, Xi'an, China, [4] The Key Laboratory of Biomedical Information Engineering, Ministry of Education, Department of Biomedical Engineering, School of Life Science and Technology, Xi'an Jiaotong University, Xi'an, China, [5] The Key Laboratory of Biomedical Information Engineering of Ministry of Education, Institute of Health and Rehabilitation Science, School of Life Science and Technology, Xi'an Jiaotong University, Xi'an, China, [6] Department of Neurosurgery, Xijing Hospital, Fourth Military Medical University, Xi'an, China, [7] Neuromodulation Lab of Brain Science and Humanoid Intelligence Research Center, Xi'an Jiaotong University, Xi'an, China

OPEN ACCESS

Edited by:
Karen M. von Deneen,
Xidian University, China

Reviewed by:
Xiaowei Ma,
Central South University, China
Libo Liu,
Shandong First Medical University, China

***Correspondence:**
Shun Qi
qishun@xjtu.edu.cn
Huaning Wang
13609161341@163.com

[†]These authors have contributed equally to this work and share first authorship

Specialty section:
This article was submitted to Neuroimaging and Stimulation, a section of the journal Frontiers in Psychiatry

Received: 01 September 2021
Accepted: 15 October 2021
Published: 05 November 2021

Citation:
Tang N, Sun C, Wang Y, Li X, Liu J, Chen Y, Sun L, Rao Y, Li S, Qi S and Wang H (2021) Clinical Response of Major Depressive Disorder Patients With Suicidal Ideation to Individual Target-Transcranial Magnetic Stimulation. Front. Psychiatry 12:768819. doi: 10.3389/fpsyt.2021.768819

Suicidal ideation increases precipitously in patients with depression, contributing to the risk of suicidal attempts. Despite the recent advancement in transcranial magnetic stimulation, its effectiveness in depression disorder and its wide acceptance, the network mechanisms of the clinical response to suicidal ideation in major depressive disorder remain unclear. Independent component analysis for neuroimaging data allows the identification of functional network connectivity which may help to explore the neural basis of suicidal ideation in major depressive disorder. Resting-state functional magnetic resonance imaging data and clinical scales were collected from 30 participants (15 major depressive patients with suicidal ideation and 15 healthy subjects). Individual target-transcranial magnetic stimulation (IT-TMS) was then used to decrease the subgenual anterior cingulate cortex activity through the left dorsolateral prefrontal cortex. Thirty days post IT-TMS therapy, seven of 15 patients (46.67%) met suicidal remission criteria, and 12 patients (80.00%) met depression remission criteria. We found that IT-TMS could restore the abnormal functional network connectivity between default mode network and precuneus network, left executive control network and sensory-motor network. Furthermore, the changes in functional network connectivity between the default mode network and precuneus network were associated with suicidal ideation, and depressive symptoms were related to connectivity between left executive control network and sensory-motor network. These findings illustrate that IT-TMS is an effective protocol for the accurate restoration of impaired brain networks, which is consistent with clinical symptoms.

Keywords: individual target-transcranial magnetic stimulation, major depressive disorder, suicidal ideation, functional network connectivity, independent component analysis

INTRODUCTION

Major depressive disorder (MDD) is the most common mental disorder, with 58% of MDD patients having suicidal ideation (SI) and 15% having attempted suicide (1, 2). Although suicide prevention has been thoroughly researched, suicide remains a major cause of morbidity and mortality worldwide (3). The World Health Organization (WHO) reports that approximately 800,000 suicides occur annually across the globe (4), which is a heavy economic burden (5). Only a few treatment options are available for suicidal ideation (e.g., lithium, Emission Computed Tomography) and are only partially effective (6). Individual target-transcranial magnetic stimulation (IT-TMS) represents an original tool that opens new avenues in the treatment of mental disorders, especially MDD (7). However, the clinical responses and neural networks of patients with MDD and SI are unclear.

Brain neural networks are complex systems, and multiple connective networks serve different functions (8, 9). Each functional network controls several brain regions with similar patterns of blood oxygen level-dependent (BOLD) signal changes, whereas each network shows distinct patterns (10–12). In recent years, few studies have investigated the functional network connectivity (FNC) of MDD patients with SI and reported inconsistent results regarding the brain regions associated with resting-state functional alterations (13). Kim et al. researched MDD and MDD patients with SI; FNC between the left superior frontal gyrus and left/right caudate, left superior frontal gyrus and right putamen, left thalamus, left middle frontal gyrus, right thalamus, left postcentral gyrus, etc. were significantly reduced (14). Jung et al. compared the resting-state brain network of MDD patients with suicidal attempts and Health Controls (HCs), and found decreased functional connectivity between the insular network (IN) and default mode network (DMN), as well as the medial prefrontal cortex network (mPFCN) and left frontal-parietal network (LFPN), and increased connectivity between the IN and basal ganglia network (BGN) (15). Chase et al. found that the lower connectivity between the salience network (especially in dACC) and DMN (specifically, dorsal and ventral posterior cingulate cortex) in depression patients with suicidal ideation (16). Although various rest state function Magnetic Resonance Imaging (rsfMRI) studies have revealed functional alterations in brain regions and networks, the network restoration mechanism of IT-TMS rapid action in MDD patients with SI is not yet known.

Traditional TMS spans six consecutive weeks and meets approximately 32% remission and 49% response in depression (17, 18). Stanford accelerated intelligent neuromodulation therapy (SAINT) is a new TMS protocol that is accelerated, safe, tolerable, high-dose, durable, and effective for MDD (19). The core mechanism was subgenual anterior cingulate cortex (sgACC) observed to be hyperactive and its activity was decreased through indirect functional connectivity from the left dorsolateral prefrontal cortex (L-DLPFC) (19–21). However, the L-DLPFC is a large brain area that consists of numerous subunits, which are correlated and some anticorrelated with the sgACC (22). Complex algorithms and precise stimulation of individual anticorrelation subunits have greatly hampered the clinical application of TMS.

In the current study, we try to elucidate intrinsic brain activity and connectivity in MDD patients with SI and HCs by ICA. Firstly, we hypothesized that compared with HCs, depressed patients with suicidal ideation show altered patterns of neural activity, and individual target was generated for the guide intelligent neural navigation system over rsfMRI analysis. Then, the abnormal FNC could repaired after IT-TMS therapy. Finally, we attempted to identify the distinct associated changes in the FNC and clinical scales that assess SI and MDD. A systematic flowchart of the study design is shown in **Figure 1**.

MATERIALS AND METHODS

Participants

Participants were recruited from the Psychiatric Department of Xijing Hospital (Shaanxi, China) between June 2020 and March 2021. All MDD patients were diagnosed with SI using a structured clinical interview from the Diagnostic and Statistical Manual of Mental Disorder (DSM-5). At the time of screening, our enrollment criteria for MDD patients with SI were as follows: (i) right handed; (ii) ages 18–60; (iii) 17-item Hamilton Depression Rating Scale (HAMD) score >17 and Beck Scale for Suicide Ideation-Chinese Version (BSI-CV) score >6; (iv) a nonpsychotic; (v) a negative urine drug screen, and a negative urine pregnancy test if female; (vi) acute suicide behavior (who needed immediate treatment) were excluded by clinical diagnosis and evaluation (vii) no contraindications of TMS and MRI measurement, such as neurological and psychiatric diseases, history of epilepsy, a brain disorder or abnormality, head trauma, metal or electronic instruments (e.g., intracranial metal device, cochlear implants, cardiac pacemakers, and stents) in the body (23–25). For safety, all MDD patients with SI need to take venlafaxine or duloxetine (serotonin and noradrenaline reuptake inhibitor antidepressant) during this study.

Fifteen patients (ages 18–60, 13 females, mean 25.8) and 15 HCs (ages 18–60, 12 females, mean 32.2) were recruited for this study. And the two groups were not statistically significant in sex ($p = 0.62$), age ($p = 0.21$), and education years ($p = 0.07$). None of the HCs currently or previously had psychopathology, and the above exclusion criteria were also applied to them. The protocol of this study was approved by the Xijing Hospital and the procedures were per the Declaration of Helsinki. All of the participants signed an informed consent form before they participated in this study.

MRI Acquisition and Data Processing

MRI scans were done using a 3.0 T-UNITED Discovery 770 scanner equipped with a 32-channel head coil. Earplugs were used to reduce the scanner noise, tight but comfortable enough to reduce the head motion. T1-weighted sagittal anatomical images were obtained. The parameters were: sagittal slices = 192; repetition time (TR) = 7.24 ms; echo time (TE) = 3.10 ms; slice thickness/gap = 0.5/0 mm; in-plane resolution = 512 × 512; inversion time (TI) = 750 ms; flip angle = 10°; field of view

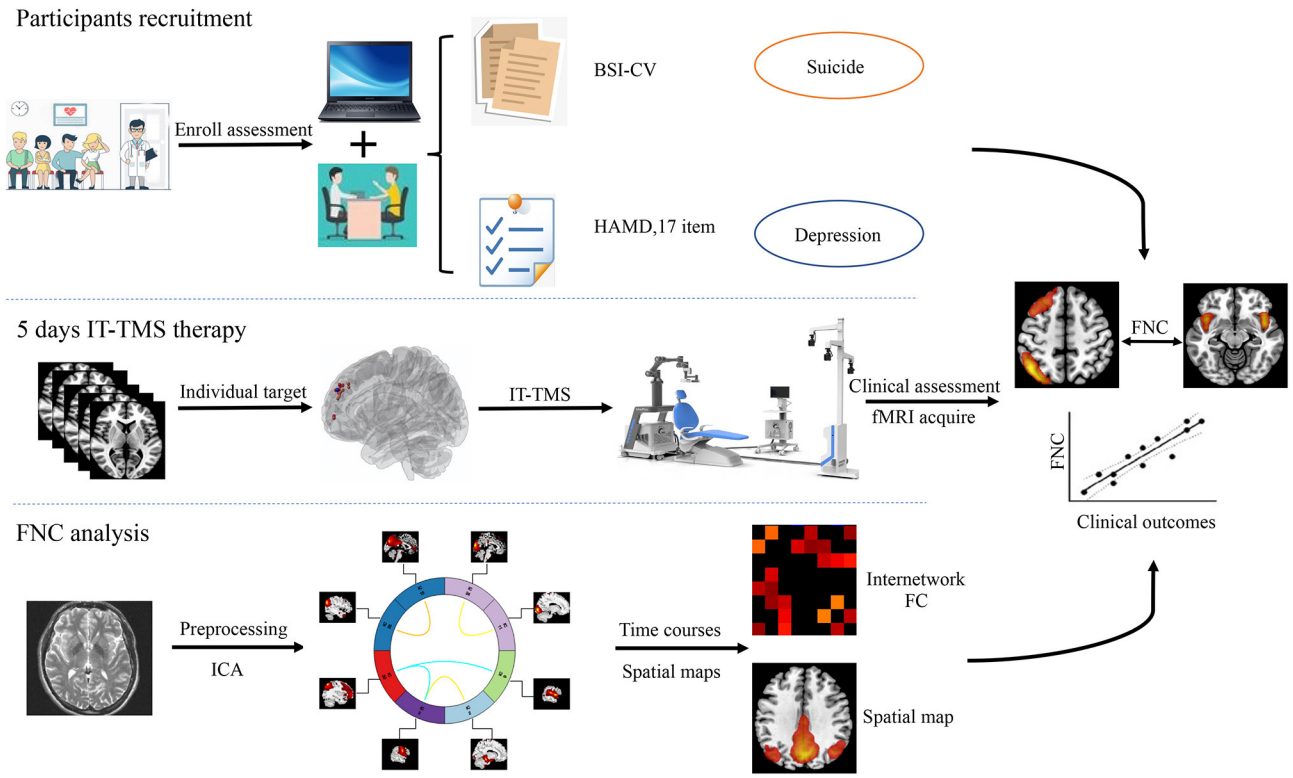

FIGURE 1 | Flowchart of this study design. IT-TMS, Individual Target-Transcranial Magnetic Stimulation; FNC, Functional Network Connectivity; fMRI, Functional Magnetic Resonance Imaging; ICA, Independent Component Analysis; BSI-CV, Beck Scale for Suicidal Ideation—Chinese Version.

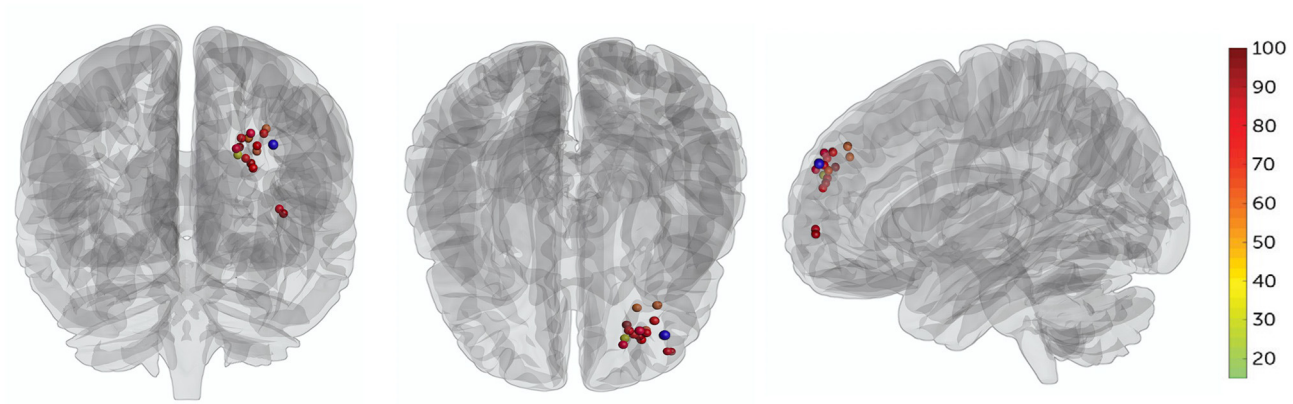

FIGURE 2 | All patients' target locations for IT-TMS therapy. The colors of the targets represent the percentage change in BSI-CV (Beck Scale for Suicidal Ideation—Chinese Version) score after a 5-day therapy, dark red indicating great changes. The F3 location (MNI coordinates−35.3, 49.4, 32.4) is shown in blue.

(FOV) = 256 × 256 mm; voxel size = 0.5× 0.5 × 1 mm. Resting-state fMRI data were acquired using T2-weighted oblique slices aligned to the anterior and posterior commissure, and the parameters were as follows: sagittal slices = 8,400; repetition time (TR) = 2,000 ms; echo time (TE) = 30 ms; slice thickness/gap = 4/0 mm; in-plane resolution = 64 × 64; inversion time (TI) = 1,100 ms; flip angle = 90°; FOV = 224 × 224 mm; voxel size = 3.5 × 3.5 × 4.0 mm^3. During the scan, all participants were instructed to keep their eyes closed, relax, think of nothing in particular, but not fall asleep.

As described in previous work across several independent samples, structure and resting-state BOLD data were preprocessed using REST software (26, 27). First, the initial 10 volumes for each participant were discarded to avoid

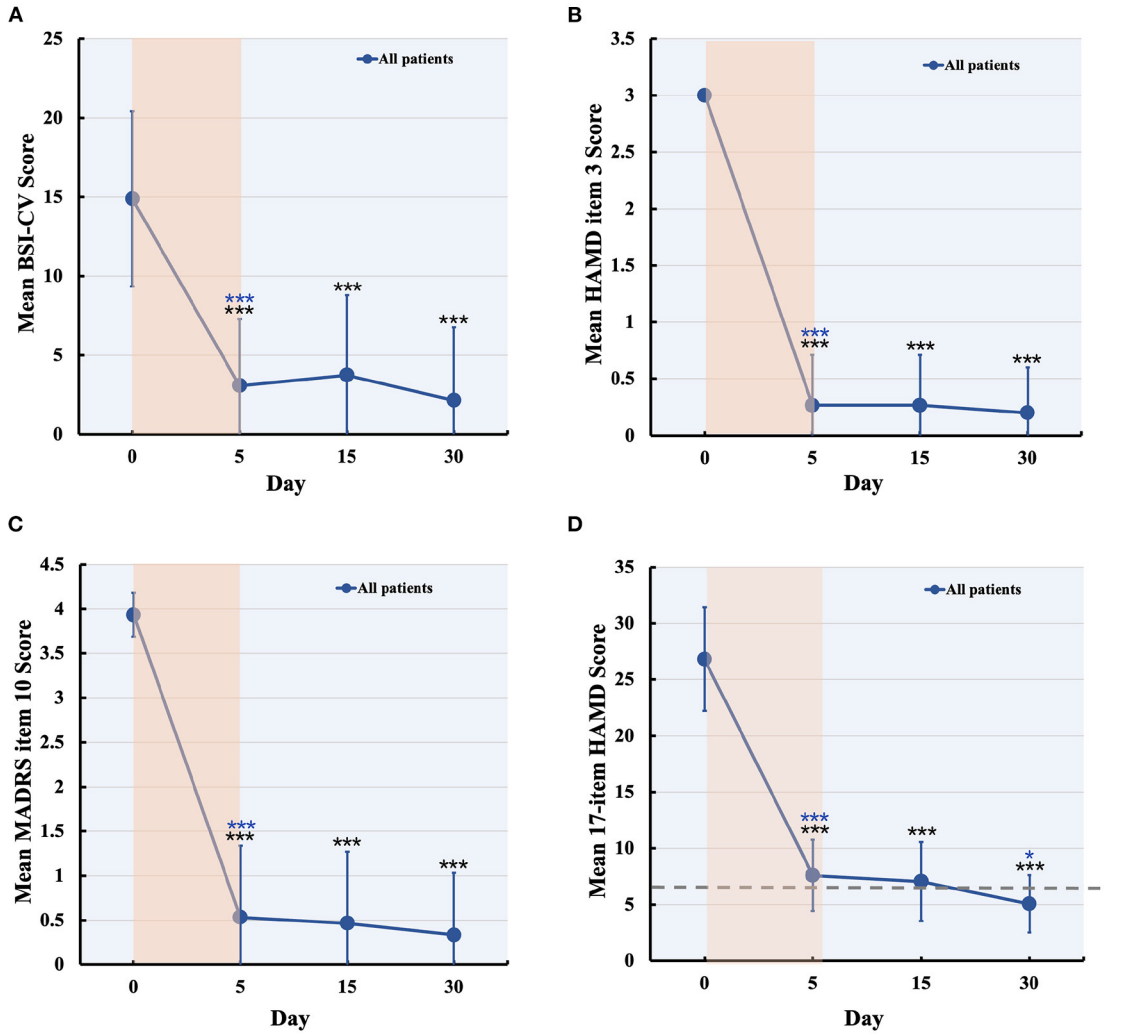

FIGURE 3 | Changes in suicidal and depression score during and after IT-TMS therapy for MDD patients with SI. Panel **(A–C)** shows the suicidal assessment scale of BSI-CV, item 3 of HAMD, and item 10 of MADRS, for patients' baseline (day 0), just post-therapy (5 days), 15, and 30 days post IT-TMS therapy. Panel **(D)** was the mean score of the 17-item HAMD for all patients at baseline (day 0), just post-therapy (5 days), 15, and 30 days post IT-TMS therapy. Black asterisks, significance is compared with baseline; blue asterisks, significance is compared with previous time point. BSI-CV, Beck Scale for Suicide Ideation-Chinese Version; HAMD, Hamilton Depression Rating Score; MADRS, Montgomery–Asberg Depression Rating Scale.

scanning noise, and the remaining 230 volumes were corrected for the acquisition time delay between slices. Then, realigning was used to correct the head motion (<2 mm or 2°) between the time points. Four patients' fMRI data were excluded because of heavy head motion. The effects of nuisance signals and head motion (Friston-24 model) were also regressed out. In the normalization steps, individual structural images were first co-registered with the functional images, segmented, and normalized to the Montreal Neurological Institute (MNI) space using diffeomorphic anatomical registration through the exponentiated lie algebra (28, 29). Finally, the normalized images were smoothed and band-pass filtered (0.01–0.08 Hz).

Individual Target Generation

Patients' targets in the L-DLPFC were set, in which the TMS coil placement was delivered by two separate algorithms (19, 30). First, each patient's L-DLPFC and sgACC were subdivided into numerous functional subunits using a hierarchical agglomerative clustering algorithm. Then, the functional subunits were defined as all voxel pairs being correlated with each other by Spearman's correlation coefficient, and rho $\geq$0.5. For each functional subunit in the L-DLPFC and sgACC, a single time series value was used to find the single voxel time series, most correlated with the median time series. Once a single time series was identified, Spearman correlation coefficients were used to calculate the correlation matrix between the L-DLPFC and sgACC subunits.

Finally, the decision-making algorithm was used to selected most anticorrelation subunit (effective to depression and suicidal symptom), larger size of subunit (easier to target with the IT-TMS coil), and higher spatial concentration (more clustered about the voxels). These three factors are equally weighted for generated individual target, and the numerous individual target location were see in **Figure 2**.

Precision Therapy by IT-TMS

The IT-TMS used in this study was the Black Dolphin Navigation Robot (S-50, China), a sub-millimeter smart system that ensures the same subunit stimulation for repeat therapy. The 3D individual mask was beneficial for locating the subunits in the L-DLPFC. Fifty intermittent theta-burst stimulation (iTBS) sessions (1,800 pulses per session, 50-min intervals) were delivered in 10 daily sessions over 5 consecutive days at a 90% resting motor threshold.

Clinical Assessment and Analysis

Suicidal ideation and depression symptoms were assessed by BSI-CV and a 17-item HAMD scale before and after IT-TMS therapy. Response and remission of suicidal ideation were defined as a reduction of more than 50% compared to the baseline score, and the BSI-CV score was 0 (19). Depression response was defined as a reduction of more than 50% compared to the baseline score, and remission was defined as a Montgomery Asberg Depression Rating Score <11 (31). A neuropsychological test battery was used to assess any neurocognitive side effects after IT-TMS.

SPSS software (version 26) was used for statistical analysis, multiple comparisons were corrected by false discovery rate (FDR) with a corrected significance level of $p = 0.05$ (32). The floor effect of IT-TMS therapy was observed across all clinical scales, and the Shapiro-Wilk residuals of the initial linear mixed model were not normally distributed. Thus, changes in clinical scores were analyzed with a general linear model that used a Satterthwaite approximation of degree of freedom, compound symmetry covariance structure, and robust coefficients excluding violations. All *post-hoc* pairwise comparisons were Bonferroni-corrected.

Defining Functional Networks Using Independent Component Analysis

Group independent component analysis (ICA) was performed to parcellate the preprocessed fMRI data using the GIFT toolbox (33), the number of independent components was set to 25 by automatic estimation. To ensure estimation stability, the infomax algorithm was repeated 20 times in ICASSO (software for investigating the reliability of ICA estimates by clustering and visualization), and the most central run was selected and analyzed further (34). Finally, the time courses and spatial maps of the patients were obtained by reconstruction. Based on the peak activations in gray matter, we focused on the subdivisions of 11 components maybe correlated with the SI in MDD and defined as resting-state brain networks (RSNs). **Figure 4** showed the spatial map of each component.

Our primary aim was to detect the neural differences between HCs and patients (MDD patients with SI) before and after IT-TMS therapy. The resulting whole-brain maps were threshold at $p < 0.005$, and the voxel level with FDR corrected of $p < 0.05$, cluster size >100. Before the function network connectivity analysis, a serous of post-processing steps including de-trending linear, quadratic, cubic trends and de-spiking detected outliers were performed. Then cut off the frequency of 0.15 HZ and transforming to z-score by Fisher's.

For the selected RSNs, two outcomes from the ICA analysis were compared using MANCOVAN (tools for multivariate analysis) with covariates including age and head motion, and the mean temporal correlation across all voxels followed by *post-hoc* t-test ($p < 0.05$). For the outcome measures were correlated with clinical rating score (BSI-CV and HAMD) using Pearson's correlations ($P_{\mathrm{FDR-corrected}} < 0.05$).

RESULTS

Suicidal Ideation

No serious adverse events occurred and no participant dropped out. Two patients experienced scalp numbness and slight pain in the regions of stimulation during IT-TMS therapy. All 15 patients had suicidal ideation at the time of screening for BSI-CV (score >6), and the scores were more than zero on item 3 of the HAMD and item 10 of the MADRS. Changes in suicidal scale scores were assessed using a general linear model with repeated measurement. **Figures 3A–C** show the baseline score and results after IT-TMS therapy, significant reduction in BSI-CV ($F = 38.77$, $df = 3$, $p < 0.001$), item 3 of HAMD ($F = 296.66$, $df = 3$, $p < 0.001$), and item 10 of MADRS ($F = 153.72$, $df = 3$, $p < 0.001$). Thirteen patients (86.67%) met a response in suicidal ideation, and eight patients (53.33%) were in remission on the BSI-CV scale just after 5 days therapy. Fifteen days post-IT-TMS met 80% response and 40% remission. Furthermore, the response and remission rates reached 93.33 and 80%, respectively, 30 days after IT-TMS therapy (**Table 1**). A lower efficacy patient (green dot in **Figure 2**) after 5 days therapy was improved gradually, and arrived the suicidal remission criteria after 30 days post-therapy.

Depression Symptoms

Significant changes in the 17-item HAMD ($F = 143.54$, $df = 3$, $p < 0.001$) by general linear model analysis (**Figure 3D**), and the mean score of all patients was nearly in remission during the 5-day therapy. These scores also steadily decreased after 15 and 30 days, respectively. Finally, we tracked the data at 30 days after therapy and found that the response rate was 100% and remission was 80.00%, which is more efficient in depression. We collected the data of 15 patients after 60 days of IT-TMS therapy, most of them (13 patients, 86.67%) were not depression or suicidal symptom except for two patients. The two patients who relapsed maybe required more days of treatment to achieve the remission criterion, and another 5 days therapy were delivered.

Brain Network Activity

Twenty-five components estimated by ICA and 11 temporal coherent signals confined to the brain were selected as

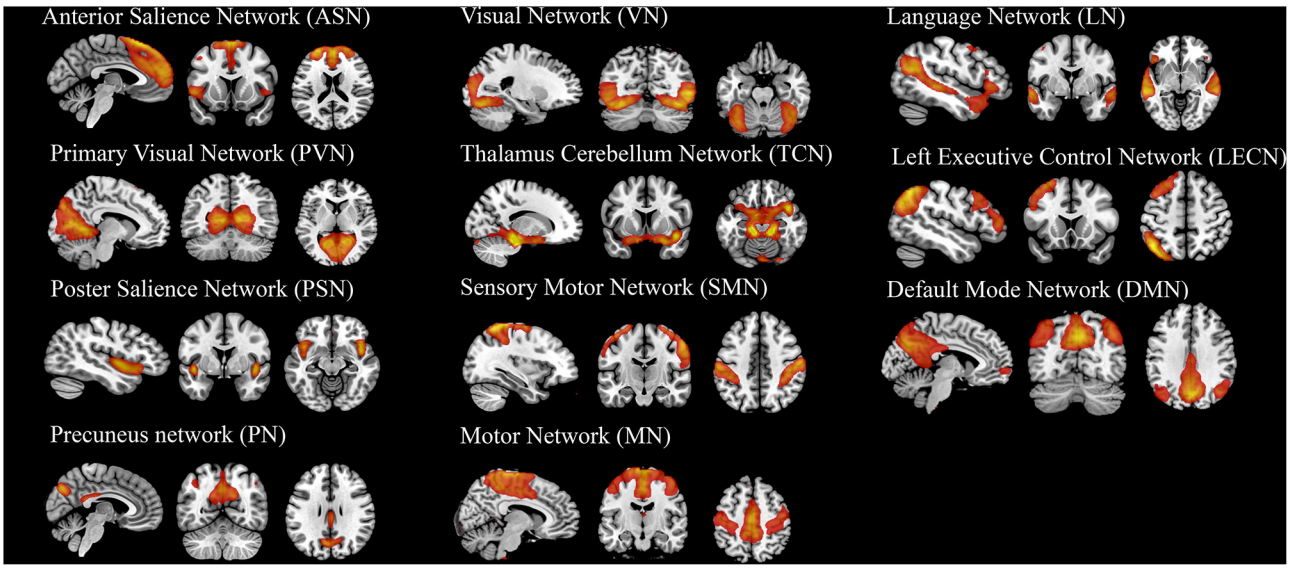

FIGURE 4 | The spatial map of 11 components (RSNs) derived from group ICA analysis. The statistical threshold was set at $T > 20$.

TABLE 1 | Clinical assessment score for patients[a].

Measure	Baseline		Immediately post IT-TMS therapy			15 days post IT-TMS therapy			30days post IT-TMS therapy		
	N	Mean (SD)	Mean (SD)	Response (%)	Remission (%)	Mean (SD)	Response (%)	Remission (%)	Mean (SD)	Response (%)	Remission (%)
Suicidal ideation											
BSI-CV	15	14.8 (5.73)	3.06 (4.35)	86.67	53.33	3.73 (5.24)	80.00	40.00	2.13 (4.77)	93.33	46.67
HAMD, item 3	15	3 (0)	0.26 (0.45)	100.00	73.33	0.26 (0.46)	100.00	73.33	0.20 (0.41)	100.00	80.00
MADRS, item 10	15	3.93 (0.26)	0.53 (0.83)	100.00	66.67	0.47 (0.83)	100.00	73.33	0.33 (0.72)	100.00	80.00
Depression symptoms											
HAMD, 17 items	15	26.8 (4.75)	7.6 (3.29)	93.33	46.67	7.07 (3.63)	100.00	53.33	5.07 (2.63)	100.00	80.00

[a] *Response was defined as a reduction of 50% in score compared to baseline; Remission was defined as a score of zero on the suicidal ideation, and a score <7 on 17 item HAMD. SD, standard deviation; IT-TMS, Individual Target-Transcranial Magnetic Stimulation; BSI-CV, Beck Scale for Suicide Ideation-Chinese Version; HAMD, Hamilton Depression Rating Scale; MADRS, Montgomery–Asberg Depression Rating Scale.*

the RSNs. Here, we labeled the RSNs according to their spatial locations or a previous study described (**Figure 4** and **Supplementary Table S1**) show the spatial map of RSNs: anterior salience network (ASN), primary visual network (PVN), posterior salience network (PSN), precuneus network (PN), visual network (VN), thalamus cerebellum network (TCN), sensory-motor network (SMN), motor network (MN), language network (LN), left executive control network (LECN), and default mode network (DMN).

Functional Network Connectivity

Figure 5A shows a significant difference of three groups on FNC between 11 RSNs, and these results performed *post-hoc* tests. Compared to the HC group, MDD patients with SI exhibited a decreased FNC between DMN and PN, as well as an enhanced FNC in DMN and TCN, DMN and SMN, LECN and SMN, SMN, and PN. Compared to the pre-therapy and post-therapy images, FNC was decreased in SMN and LECN, but increased in LECN and LN. Finally, we explored the post-therapy and HCs and found that the FNC between PSN and SMN, PN and LN were significantly decreased.

Correlation analysis was used to investigate the relationship between FNC and clinical efficacy (**Figures 5B,C**). The FNC between the DMN and PN gradually increased from the pre-therapy (MDD patients with SI) to the post-therapy and from the post-therapy groups to the HCs. The FNC changes in DMN-PN were positively correlated with the 17 item HAMD score ($r = 0.1838$, $P_{\mathrm{FDR-corrected}} = 0.0492$) and BSI-CV scores ($r = 0.5474$, $P_{\mathrm{FDR-corrected}} = 0.0366$). Furthermore, the FNC in LECN and SMN showed a significant correlation with HAMD ($r = 0.5250$, $P_{\mathrm{FDR-corrected}} = 0.0247$), but not with BSI-CV. No other correlations were statistically significant between the HCs, pre-therapy, and post-therapy.

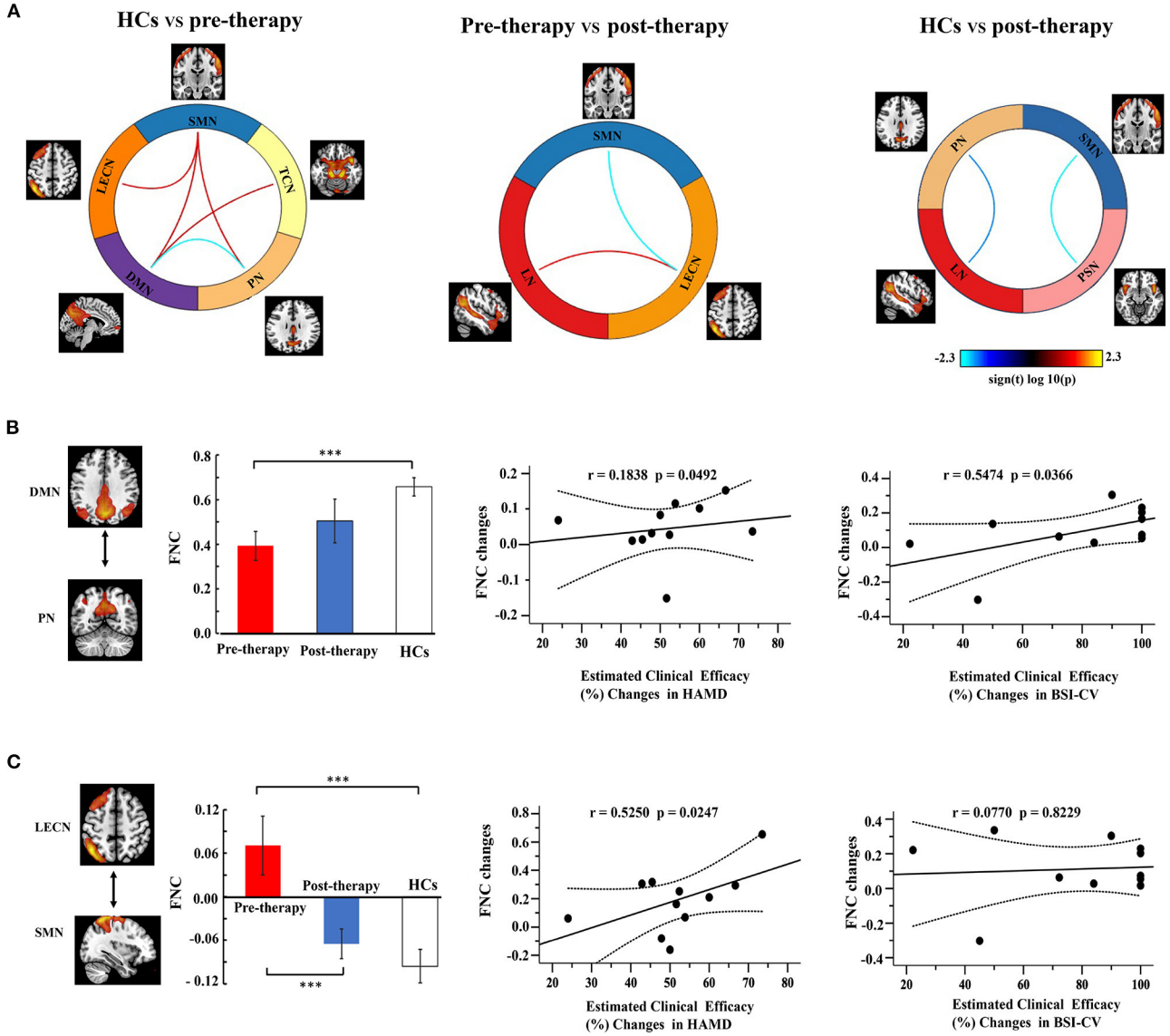

FIGURE 5 | Function network connectivity (FNC) between RSNs. **(A)** FNC differences in the selected FNC. The blue line indicates a decreased FNC and the red lines indicates improved FNC ($P < 0.05$). **(B,C)** shows the relationships between the FNC and clinical efficacy. Error bars indicate the standard error. Dotted lines indicated the significantly changes of groups. $^{*}p < 0.05$. $^{**}p < 0.01$. $^{***}p < 0.001$.

DISCUSSION

IT-TMS is a non-invasive, safe, and effective method for MDD patients with SI (6), but there are only a few systematic research on the FNC mechanism. Here, we found that IT-TMS significantly decreased suicidal ideation and depressive symptoms within five continuous days. Furthermore, suicidal ideation and depressive symptoms were not recurrent 1 month later, and the depression remission rate (80%) of 17 item HAMD was higher than that of SAINT protocol (65%) (19). These differences between the observed and SAINT protocols may be due to the sub-millimeter smart navigate system that ensures the same subunit stimulation for repeat therapy.

Recently, Northoff reported that various depressive and suicidal symptoms can be translated as intrinsic brain activity in spatiotemporal disturbances, which is the organization of the resting-state network activity (35). We found that MDD patients with SI had several significant changes in functional network connections, including LECN-SMN, DMN-SMN, DMN-TCN, SMN-PN, and DMN-PN, compared to HCs. Specifically, DMN and PN showed decreased functional connectivity, but the others improved. These results are compatible with a recent view on the heterogeneity connection of the DMN, ECN, and SMN, which can be reorganized according to specific demands by functional anatomic fractionation (36, 37). Our results illustrate the complex

network imbalance derived from deficits in suicidal ideation and depressive symptoms.

Based on previous research, Serafini et al. proposed that frontal limbic or frontal-parietal cerebellar pathways and DMN connection abnormalities increase emotional dysregulation (self-focus, hopelessness, and suicidal ideation) (13). These results consistent with our study that the functional network connection of MDD patients with SI were significantly changes, especially in DMN, LECN, SMN, TCN, and PN. Moreover, MDD patients with SI showed more alterations in the SMN, LECN, and LN through IT-TMS therapy: increased functional connectivity in LECN-LN and decreased functional connectivity in LECN-SMN. Decreased connections in limbic regions may contribute to suicidal ideation regulation by emotion processing (38, 39), whereas increased connections in the executive and language networks may contribute to depressive symptoms (40). Here, we speculated that the brain responses of MDD patients with SI represent an insufficient compensatory mechanism for network interfering activity, which perhaps modulation by the IT-TMS therapy.

Mechanistic research further revealed that functional connectivity changes in various brain networks are significantly related to suicidal ideation and depression symptoms. It is noteworthy that the core rest-state networks of the DMN and PN decreased connections, suggesting an intimate link to suicidal ideation (41–43). A previous study in MDD patients with SI has also reported that the DMN and PN positive connection benefits depression and suicidal remission (44). These two networks play a key role in emotion and cognitive modulation and show a bias toward self-centered rather than self-other processing (41, 45).

Interestingly, IT-TMN therapy significantly improved patients' anti-connectivity between LECN and SMN, which is related to higher 17 item HAMD score changes. First, the LECN engages in cognitive control to support goal-directed behavior, consistent with depression and suicidal patients' difficulty in regulating emotions (46). Our finding of decreased positive connection between LECN and SMN by IT-TMN was consistent with the evidence for increased functional connectivity in MDD patients (47). The current findings not only may add important literature to potential neurobiological mechanisms, but also have high clinical relevance for exposing the MDD patients with SI neuro-biomarkers.

LIMITATIONS AND CONCLUSION

This study has several limitations. First, the small sample size and the age might not be representative of the general population. Further research with larger sample size and a broader age range may validate our findings. Second, although we identified a meaningful functional network from a range of ICA-derived components through a structural selection procedure, this may have influenced our interpretation. Third, rsfMRI data can be related to the effects of brain activity, but we did not ensure that participants thought of nothing in particular. Finally, the sham stimulation group and only drug group were also required to exclude false-positive results.

To the best of our knowledge, this study is the first to examine multiple brain network interactions after IT-TMS therapy for MDD patients with SI. We demonstrated that widespread but discrete network changes in functional networks and their abnormalities are associated with clinical efficiency. Moreover, DMN-PN and LECN-SMN functional connectivity may act as mediators of suicidal ideation or depressive symptoms. These findings might expand existing knowledge concerning suicidal and depression function network organization. More generally, they may ultimately inform a clinical protocol for the remission of suicidal ideation and depressive symptoms by IT-TMS.

DATA AVAILABILITY STATEMENT

The original contributions presented in the study are included in the article/**Supplementary Material**, further inquiries can be directed to the corresponding author/s.

ETHICS STATEMENT

The studies involving human participants were reviewed and approved by Medical Ethics Committee of the First Affiliated Hospital of PLA Air Force Military Medical University. The patients/participants provided their written informed consent to participate in this study.

AUTHOR CONTRIBUTIONS

HW, SQ, and SL designed the current study. NT, JL, and YC collected the data. XL, LS, and YR analyzed the data. CS and YW wrote the manuscript. All authors read and approved the final manuscript.

FUNDING

This study was financially supported by the National Natural Science Foundation (number 81974215) and Social Development Area in Shaanxi Key Projects (number 2017ZDXM-SF-047).

ACKNOWLEDGMENTS

We would like to thank Editage (www.editage.com) for english language editing. All volunteers are thanked for their participation of the study.

SUPPLEMENTARY MATERIAL

The Supplementary Material for this article can be found online at: https://www.frontiersin.org/articles/10.3389/fpsyt.2021.768819/full#supplementary-material

REFERENCES

1. Sokero TP, Melartin TK, Rytsala HJ, Leskela US, Lestela-Mielonen PS, Isometsa ET. Suicidal ideation and attempts among psychiatric patients with major depressive disorder. *J Clin Psychiatry.* (2003) 64:1094–100. doi: 10.4088/JCP.v64n0916
2. Jeon HJ, Lee J-Y, Lee YM, Hong JP, Won S-H, Cho S-J, et al. Unplanned versus planned suicide attempters, precipitants, methods, and an association with mental disorders in a Korea-based community sample. *J Affect Disord.* (2010) 127:274–80. doi: 10.1016/j.jad.2010.05.027
3. Huang Y, Wang Y, Wang H. Prevalence of mental disorders in China: a cross-sectional epidemiological study (vol 6, pg 211, 2019). *Lancet Psychiatry.* (2019) 6:E11. doi: 10.1016/S2215-0366(19)30074-4
4. World Health Organization. *Suicide Data.* (2016). https://www.who.int/mental_health/prevention/suicide/estimates/en/
5. Chisholm D, Sweeny K, Sheehan P, Rasmussen B, Smit F, Cuijpers P, et al. Scaling-up treatment of depression and anxiety: a global return on investment analysis. *Lancet Psychiatry.* (2016) 3:415–24. doi: 10.1016/S2215-0366(16)30024-4
6. Abdelnaim MA, Langguth B, Deppe M, Mohonko A, Kreuzer PM, Poeppl TB, et al. Anti-suicidal efficacy of repetitive transcranial magnetic stimulation in depressive patients: a retrospective analysis of a large sample. *Front Psychiatry.* (2020) 10:929. doi: 10.3389/fpsyt.2019.00929
7. Tang Y, Jiao X, Wang J, Zhu T, Zhou J, Qian Z, et al. Dynamic functional connectivity within the fronto-limbic network induced by intermittent theta-burst stimulation: a pilot study. *Front Neurosci.* (2019) 13:944. doi: 10.3389/fnins.2019.00944
8. Kang S-G, Na K-S, Choi J-W, Kim J-H, Son Y-D, Lee YJ. Resting-state functional connectivity of the amygdala in suicide attempters with major depressive disorder. *Prog Neuro-Psychopharmacol Biol Psychiatry.* (2017) 77:222–7. doi: 10.1016/j.pnpbp.2017.04.029
9. Holmes SE, Scheinost D, Finnema SJ, Naganawa M, Davis MT, Dellagioia N, et al. Lower synaptic density is associated with depression severity and network alterations. *Nat Commun.* (2019) 10:1–0. doi: 10.1038/s41467-019-09562-7
10. Cuijpers P, Quero S, Noma H, Ciharova M, Miguel C, Karyotaki E, et al. Psychotherapies for depression: a network meta-analysis covering efficacy, acceptability and long-term outcomes of all main treatmenttypes. *World psychiatry: Official J World Psychiatr Assoc (WPA).* (2021) 20:283–93. doi: 10.1002/wps.20860
11. Kadakia A, Dembek C, Heller V, Singh R, Uyei J, Hagi K, et al. Efficacy and tolerability of atypical antipsychotics for acute bipolar depression: a network meta-analysis. *BMC Psychiatry.* (2021) 21:249. doi: 10.1186/s12888-021-03220-3
12. Li H, Cui L, Li J, Liu Y, Chen Y. Comparative efficacy and acceptability of neuromodulation procedures in the treatment of treatment-resistant depression: a network meta-analysis of randomized controlled trials. *J Affect Disord.* (2021) 287:115–24. doi: 10.1016/j.jad.2021.03.019
13. Serafini G, Pardini M, Pompili M, Girardi P, Amore M. Understanding suicidal behavior: the contribution of recent resting-state fMRI techniques. *Front Psychiatry.* (2016) 7. doi: 10.3389/fpsyt.2016.00069
14. Kim K, Kim S-W, Myung W, Han CE, Fava M, Mischoulon D, et al. Reduced orbitofrontal-thalamic functional connectivity related to suicidal ideation in patients with major depressive disorder. *Sci Rep.* (2017) 7:69. doi: 10.1038/s41598-017-15926-0
15. Jung J, Choi S, Han K-M, Kim A, Kang W, Paik J-W, et al. Alterations in functional brain networks in depressed patients with a suicide attempt history. *Neuropsychopharmacology.* (2020) 45:964–74. doi: 10.1038/s41386-019-0560-z
16. Chase HW, Segreti AM, Keller TA, Cherkassky VL, Just MA, Pan LA, et al. Alterations of functional connectivity and intrinsic activity within the cingulate cortex of suicidal ideators. *J Affect Disord.* (2017) 212:78–85. doi: 10.1016/j.jad.2017.01.013
17. Huang YZ, Rothwell JC. The effect of short-duration bursts of high-frequency, low-intensity transcranial magnetic stimulation on the human motor cortex. *Clin Neurophysiol.* (2004) 115:1069–75. doi: 10.1016/j.clinph.2003.12.026
18. Blumberger DM, Vila-Rodriguez F, Thorpe KE. Effectiveness of theta burst versus high-frequency repetitive transcranial magnetic stimulation in patients with depression (THREE-D): a randomised non-inferiority trial (vol 391, pg 1683, 2018). *Lancet.* (2018) 391:E24. doi: 10.1016/S0140-6736(18)30295-2
19. Cole EJ, Stimpson KH, Bentzley BS, Gulser M, Cherian K, Tischler C, et al. Stanford accelerated intelligent neuromodulation therapy for treatment-resistant depression. *Am J Psychiatry.* (2020) 177:716–26. doi: 10.1176/appi.ajp.2019.19070720
20. Drevets WC, Savitz J. The subgenual anterior cingulate cortex in mood disorders. *CNS Spectr.* (2008) 13:663–81. doi: 10.1017/S1092852900013754
21. Koenigs M, Grafman J. The functional neuroanatomy of depression: distinct roles for ventromedial and dorsolateral prefrontal cortex. *Behav Brain Res.* (2009) 201:239–43. doi: 10.1016/j.bbr.2009.03.004
22. Hoshi E. Functional specialization within the dorsolateral prefrontal cortex: a review of anatomical and physiological studies of non-human primates. *Neurosci Res.* (2006) 54:73–84. doi: 10.1016/j.neures.2005.10.013
23. Lefaucheur J-P, Aleman A, Baeken C, Benninger DH, Brunelin J, Di Lazzaro V, et al. Evidence-based guidelines on the therapeutic use of repetitive transcranial magnetic stimulation (rTMS): An update (2014–2018). *Clin Neurophysiol.* (2020) 131:474–528. doi: 10.1016/j.clinph.2019.11.002
24. Rocchi L, Di Santo A, Brown K, Ibanez J, Casula E, Rawji V, et al. Disentangling EEG responses to TMS due to cortical and peripheral activations. *Brain Stimul.* (2021) 14:4–18. doi: 10.1016/j.brs.2020.10.011
25. Rossi S, Antal A, Bestmann S, Bikson M, Brewer C, Brockmoller J, et al. Safety and recommendations for TMS use in healthy subjects and patient populations, with updates on training, ethical and regulatory issues: Expert Guidelines. *Clin Neurophysiol.* (2021) 132:269–306. doi: 10.1016/j.clinph.2020.10.003
26. Wang D, Buckner RL, Fox MD, Holt DJ, Holmes AJ, Stoecklein S, et al. Parcellating cortical functional networks in individuals. *Nat Neurosci.* (2015) 18:1853–60. doi: 10.1038/nn.4164
27. Xu Y, Yu P, Zheng J, Wang C, Hu T, Yang Q, et al. Classifying vulnerability to sleep deprivation using resting-state functional MRI graph theory metrics. *Front Neurosci.* (2021) 15:660365. doi: 10.3389/fnins.2021.660365
28. Asami T, Bouix S, Whitford TJ, Shenton ME, Salisbury DF, Mccarley RW. Longitudinal loss of gray matter volume in patients with first-episode schizophrenia: DARTEL automated analysis and ROI validation. *Neuroimage.* (2012) 59:986–96. doi: 10.1016/j.neuroimage.2011.08.066
29. Liu S, Wang S, Zhang M, Xu Y, Shao Z, Chen L, et al. Brain responses to drug cues predict craving changes in abstinent heroin users: A preliminary study. *Neuroimage.* (2021) 237:118169. doi: 10.1016/j.neuroimage.2021.118169
30. Fox MD, Buckner RL, White MP, Greicius MD, Pascual-Leone A. Efficacy of transcranial magnetic stimulation targets for depression is related to intrinsic functional connectivity with the subgenual cingulate. *Biol Psychiatry.* (2012) 72:595–603. doi: 10.1016/j.biopsych.2012.04.028
31. Hengartner MP, Jakobsen JC, Sorensen A, Ploederl M. Efficacy of new-generation antidepressants assessed with the Montgomery-Asberg depression rating scale, the gold standard clinician rating scale: A meta-analysis of randomised placebo-controlled trials. *PLoS ONE.* (2020) 15:e0229381. doi: 10.1371/journal.pone.0229381
32. Song K, Li J, Zhu Y, Ren F, Cao L, Huang Z-G. (2020). Altered small-world functional network topology in patients with optic neuritis: A resting-state fMRI study. *Dis Markers.* (2021) 2021:9948751. doi: 10.1101/2020.06.09.141432
33. Shi Y, Zeng W, Wang N. SCGICAR: spatial concatenation based group ICA with reference for fMRI data analysis. *Comput Methods Programs Biomed.* (2017) 148:137–51. doi: 10.1016/j.cmpb.2017.07.001
34. Himberg J, Hyvarinen A, Esposito F. Validating the independent components of neuroimaging time series *via* clustering and visualization. *Neuroimage.* (2004) 22:1214–22. doi: 10.1016/j.neuroimage.2004.03.027
35. Northoff G. Spatiotemporal psychopathology I: no rest for the brain's resting state activity in depression? Spatiotemporal psychopathology of depressive symptoms. *J Affect Disord.* (2016) 190:854–66. doi: 10.1016/j.jad.2015.05.007
36. Andrews-Hanna JR, Reidler JS, Sepulcre J, Poulin R, Buckner RL. Functional-anatomic fractionation of the brain's default network. *Neuron.* (2010) 65:550–62. doi: 10.1016/j.neuron.2010.02.005

37. Camilleri JA, Mueller VI, Fox P, Laird AR, Hoffstaedter F, Kalenscher T, et al. Definition and characterization of an extended multiple-demand network. *Neuroimage.* (2018) 165:138–47. doi: 10.1016/j.neuroimage.2017.10.020
38. Lu Y, Liang H, Han D, Mo Y, Li Z, Cheng Y, et al. The volumetric and shape changes of the putamen and thalamus in first episode, untreated major depressive disorder. *Neuroimage-Clinical.* (2016) 11:658–66. doi: 10.1016/j.nicl.2016.04.008
39. Khosravani V, Berk M, Sharifi Bastan F, Samimi Ardestani SM, Wrobel A. The effects of childhood emotional maltreatment and alexithymia on depressive and manic symptoms and suicidal ideation in females with bipolar disorder: emotion dysregulation as a mediator. *Int J Psychiatry Clin Pract.* (2021) 25:90–102. doi: 10.1080/13651501.2021.1879867
40. Backes H, Dietsche B, Nagels A, Stratmann M, Konrad C, Kircher T, et al. Increased neural activity during overt and continuous semantic verbal fluency in major depression: mainly a failure to deactivate. *Eur Arch Psychiatry Clin Neurosci.* (2014) 264:631–45. doi: 10.1007/s00406-014-0491-y
41. Ordaz SJ, Goyer MS, Ho TC, Singh MK, Gotlib IH. Network basis of suicidal ideation in depressed adolescents. *J Affect Disord.* (2018) 226:92–9. doi: 10.1016/j.jad.2017.09.021
42. Schmaal L, Van Harmelen A-L, Chatzi V, Lippard ETC, Toenders YJ, Averill LA, et al. Imaging suicidal thoughts and behaviors: a comprehensive review of 2 decades of neuroimaging studies. *Mol Psychiatry.* (2020) 25:408–27. doi: 10.1038/s41380-019-0587-x
43. Auerbach RP, Pagliaccio D, Allison GO, Alqueza KL, Alonso MF. Neural correlates associated with suicide and nonsuicidal self-injury in youth. *Biol Psychiatry.* (2021) 89:119–33. doi: 10.1016/j.biopsych.2020.06.002
44. Martens M, Filippini N, Masaki C, Godlewska BR. Functional connectivity between task-positive networks and the left precuneus as a biomarker of response to lamotrigine in bipolar depression: a pilot study. *Pharmaceuticals.* (2021) 14:534. doi: 10.3390/ph14060534
45. Malhi GS, Das P, Outhred T, Bryant RA, Calhoun V, Mann JJ. Default mode dysfunction underpins suicidal activity in mood disorders. *Psychol Med.* (2020) 50:1214–23. doi: 10.1017/S0033291719001132
46. Gould MS, Greenberg T, Velting DM, Shaffer D. Youth suicide risk and preventive interventions: A review of the past 10 years. *J Am Acad Child Adolesc Psychiatry.* (2003) 42:386–405. doi: 10.1097/01.CHI.0000046821.95464.CF
47. Chin Fatt CR, Jha MK, Minhajuddin A, Mayes T, Ballard ED, Trivedi MH. Dysfunction of default mode network is associated with active suicidal ideation in youths and young adults with depression: Findings from the T-RAD study. *J Psychiatr Res.* (2021) 142:258–62. doi: 10.1016/j.jpsychires.2021.07.047

Conflict of Interest: The authors declare that the research was conducted in the absence of any commercial or financial relationships that could be construed as a potential conflict of interest.

frontiers in Psychiatry

ORIGINAL RESEARCH
published: 01 February 2022
doi: 10.3389/fpsyt.2021.802830

Attention Performance Correlated With White Matter Structural Brain Networks in Shift Work Disorder

Yanzhe Ning[1,2†], Meng Fang[1,2†], Yong Zhang[3], Sitong Feng[1], Zhengtian Feng[1], Xinzi Liu[1], Kuangshi Li[3] and Hongxiao Jia[1,2*]*

[1] The National Clinical Research Center for Mental Disorders & Beijing Key Laboratory of Mental Disorders, Beijing Anding Hospital, Capital Medical University, Beijing, China, [2] Advanced Innovation Center for Human Brain Protection, Capital Medical University, Beijing, China, [3] Dongzhimen Hospital, Beijing University of Chinese Medicine, Beijing, China

Neuroimaging studies have revealed that shift work disorder (SWD) affected the functional connectivity in specific brain regions and networks. However, topological disruptions in the structural connectivity of the white matter (WM) networks associated with attention function remain poorly understood. In the current study, we recruited 33 patients with SWD and 29 matched healthy subjects. The attention network test (ANT) was employed to investigate the efficiency of alerting, orienting, and executive control networks. The diffusion tensor imaging (DTI) tractography was used to construct the WM structural networks. The graph theory analysis was applied to detect the alterations of topological properties of structural networks. Our results showed lower alerting effect and higher executive effect for patients with SWD. Using the link-based analysis, 15 altered connectivity matrices (lower fiber numbers) were found between the two groups. Meanwhile, the graph theoretical analysis showed that the global efficiency and characteristic path length within SWD patients declined in contrast with the healthy controls. Furthermore, a significantly negative correlation was found between the executive effect and global network efficiency. Our findings provide the new insights into the fundamental architecture of interregional structural connectivity underlying attention deficits in SWD, which may be a potential biomarker for SWD.

Keywords: attention, shift work disorder, structural brain network, graph analysis, diffusion tensor imaging (DTI)

OPEN ACCESS

Edited by:
Yuanqiang Zhu, Fourth Military Medical University, China

Reviewed by:
Lin Liu, Peking University Health Science Centre, China
Kiyotaka Nemoto, University of Tsukuba, Japan

***Correspondence:**
Kuangshi Li
likuangshi89@hotmail.com
Hongxiao Jia
jhxlj@ccmu.edu.cn

† These authors have contributed equally to this work

Specialty section:
This article was submitted to Neuroimaging and Stimulation, a section of the journal Frontiers in Psychiatry

Received: *27 October 2021*
Accepted: *15 December 2021*
Published: *01 February 2022*

Citation:
Ning Y, Fang M, Zhang Y, Feng S, Feng Z, Liu X, Li K and Jia H (2022) Attention Performance Correlated With White Matter Structural Brain Networks in Shift Work Disorder. Front. Psychiatry 12:802830. doi: 10.3389/fpsyt.2021.802830

INTRODUCTION

Shift work disorder (SWD), involving circadian rhythm disorders, is characterized by the difficulty in falling asleep, sufficient sleep, and daytime fatigue, which result in the altered cognitive performance (1). One study has shown that the exposure duration of shift work was negatively associated with impaired cognition (2). Another study on the effects of shift work nurses on sleep and cognitive function has shown impaired attention for SWD (3). However, the knowledge about underlying mechanisms of the cognitive impairments on SWD is limited.

Attention network test (ANT), developed by Fan et al. (4), provides an easy way to distinguish three independent attentional components within one integrated task. It is widely used to measure the attentional performance of healthy individuals and mental patients (5–7). The ANT study on sleep deprivation has shown an overall slowing of reaction times in the nocturnal session, along with impairments in orientation and executive function (8). However, the abnormal attention on SWD *via* the ANT is still unknown.

To date, numerous studies on functional abnormalities in SWD have been detected *via* functional magnetic resonance imaging (fMRI) (9, 10). One study on night shift nurses has shown higher ReHo in the bilateral occipital lobe and left parietal lobe and lower regional homogeneity (ReHo) in the bilateral cerebellar hemisphere in contrast with the day shift nurses (10). Another study on SWD has revealed disrupted functional connectivity between default mode network and sensorimotor network, left frontoparietal network, and salience network (9). Nevertheless, there is no study focusing on structural changes in SWD. The diffusion tensor imaging (DTI) opens a window to investigate the brain structural connectivity *in vivo* (11). In combination with a graph theoretical method, this advanced technique can offer insight into the brain's structural connection patterns. In recent years, graph theory has been widely used to analyze large-scale brain networks across the whole brain. Previous neuroimaging studies have brought the analysis of structural large-scale brain networks to healthy subjects (12), primary insomnia (13), and so on. One study on patients with depression has revealed the decreased shortest path length and clustering coefficient and increased global and local efficiency (14). Another study on primary insomnia has suggested that the insomnia patients showed increased local efficiency and decreased global efficiency (13). However, to our knowledge, the structural large-scale brain networks on SWD remain unexplored.

In the current study, we applied DTI tractography in combination with graph theory to examine the neuroanatomical substrates of the three attention systems measured by ANT in 33 patients with SWD and 29 healthy subjects. First, white matter connectivity, assessed with diffusion tensor imaging deterministic tractography, was modeled as a structural network comprising 148 nodes defined by the Destrieux atlas. Then, we calculated global, local, and regional efficiencies of structural brain networks for each subject. Finally, we conducted the linear regression analyses to investigate the relationship between the network efficiency and the three attentional effects.

MATERIALS AND METHODS

The Beijing Anding Hospital of Ethics Committee approved this study. All participants signed informed consents prior to participation.

Participants

Thirty-three right-handed participants (two male, aged 28.06 ± 2.28 years) were diagnosed with SWD in accordance with the International Classification of Sleep Disorders (2nd Edition) by the American Sleep Disorders Association; nursing staff at Beijing Anding Hospital; 20–40 years old, right-handed; working regular night shift for at least 1 year and at least two shifts per week; with no history of prophylactic or therapeutic medicine in the past 3 months; and no history of long-term analgesic use. The exclusion criteria were as follows: being pregnant or breastfeeding, having a history of neurological or psychiatric disorders, participating in cognitive experiments within 1 year, any mental or physical impairments that may interfere with participation, any brain structure damage or abnormalities identified by MRI examinations, any history of alcohol or drug dependence, and any MRI contraindications.

Another 29 healthy subjects (three male, aged 27.17 ± 2.25 years) were recruited meeting the following inclusion criteria: relative regularity of sleep in the past 12 months; aged 20–40 years, right-handed; sleeping <3 times per month after 2,300 h, and working the night shift <3 times per month in the past year.

ANT Assessment

ANT, a cognitive task designed by Fan et al. (4) investigated the efficiency of alerting, orienting, and executive control networks involved in attention. All recruited participants were ordered to press a button as accurately and rapidly as possible to determine the direction of the target. Participants were presented with the target and flankers until they made a response or 2,000 ms had elapsed. A cue would be presented for 200 ms prior to the target. The task used three cue conditions: no cue, center cue, and spatial cue. Each participant completed three blocks in this experiment, each block lasting for 5 min and 42 s and consisting of 36 trials, plus two buffer trials at the start. In each block, a total of six trial types were presented in a counterbalanced order. All subjects were trained before the formal experiment. Stimuli were presented, and behavioral responses were recorded using E-Prime 2.0 software. Three attention networks were evaluated by calculating ratio scores of alerting, orienting, and EC issues. The formulas were as follows:

Alerting effect = no cue response – center cue response.
Orienting effect = center cue response – spatial cue response.
Executive effect = incongruent target response – congruent target response.

A higher executive effect score reflected a relatively poorer executive function. The total accuracy of each subject was calculated, and those with over 20% error rates should be excluded from this study. The trials with incorrect responses or with response time (RT) longer than 1,500 ms or shorter than 200 ms were also excluded to avoid the influence of the outliers. The procedure of ANT is shown in **Figure 1**.

MRI Acquisition

The MRI scan was acquired using a 3.0-T MRI scanner (Siemens, Prisma Germany) at Anding Hospital, Beijing, China. Participants were instructed to rest for 30 min before scanning, stay still, stay focused, keep their eyes closed, and refrain from falling asleep during the scan. Earplugs were worn to reduce scanner noise. The foam head holders were immobilized to minimize head movements during scanning.

Prior to the DTI scanning, a standard 3D T1-weight high-resolution structural image was acquired with the following parameters: voxel size = 1 mm^3, TR = 2,530 ms, TE = 3.39 ms, flip angle = 90°, matrix = 256 × 256, field of view =256 mm × 256 mm, slice thickness = 1 mm. The DTI data lasted 12 min and 30 s with a single-shot, echo-planar imaging sequence. The diffusion sensitizing gradients were applied along 64 non-collinear directions (b = 1,000 s/mm^2) with an acquisition without diffusion weighting (b = 0 s/mm^2). In addition, specific

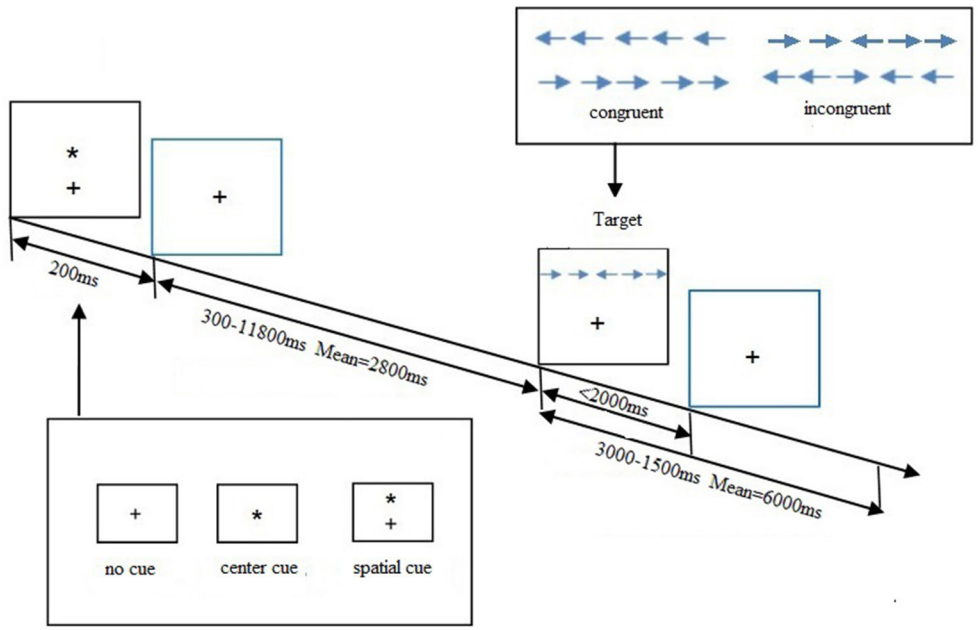

FIGURE 1 | Attention network test (ANT) schematic showing the time and different conditions for each trial. A trial starts *via* presenting one cue condition for 200 ms. A variable delay period of 300–11,800 ms elapses before one target condition is displayed. The target disappears after 2,000 ms had elapsed or until they made a response. From the moment, the target appears the trial continues for a variable delay period of 3,000–15,000 ms.

parameters were as follow: TR= 11,000 ms, TE = 98 ms, matrix = 128 × 128, field of view = 256 mm × 256 mm, slice thickness = 2.0 mm with no gap.

T1 Data Preprocessing

All T1 data were preprocessed by the Freesurfer 6.0 (http://surfer.nmr.mgh.harvard.edu) with the basic method of recon-all to remove the nonbrain structure. Moreover, 5ttgen from MRtrix was applied to generate five-tissue-type image, including cortical gray matter, subcortical gray matter, white matter, cerebrospinal fluid, and pathological tissues. Then, the parcellation of cortical ribbon was segmented into 148 different regions by the Destrieux atlas (15, 16). After that, MRtrix was used to convert the parcellated image for producing 164 nodes, which was prepared for connectome analysis.

DTI Data Preprocessing and Tractography

First, the noise was removed in the original DTI data by the dwidenoise from MRtrix, which implemented dMRI noise level estimation and denoising based on random matrix theory (17, 18). Second, the dwifslpreproc script of MRtrix, which comprises FSL's eddy and top-up tools, was used to correct the eddy current-induced distortion, motion distortion, and susceptibility-induced distortion. Third, DWI bias field correction was performed on data processed in the previous step using the N4 algorithm (19) as provided in ANTs. Fourth, the processed DTI data and the preprocessed T1 image were registered by ANTs (https://github.com/ANTsX) software, and the alignment matrix was obtained. Meanwhile, the alignment matrix was applied into the DTI data. Fifth, applying fiber constrained spherical deconvolution algorithm, orientation distributions were calculated by estimating multitissue response function (20). The whole-brain tractgrams were produced by five-tissue-type segmented T1 image and anatomically constrained tractography. Finally, a 164 × 164 connectivity matrix was produced by mapping the tracks into the 164 nodes. Each contribution to the connectivity was decided by the inverse of the two node volumes, which applied link-based analysis to explore individual connections between any node pair within a network. The procedure is shown in **Figure 2**.

Connectivity and Small Network Analysis

Gretna 2.0 was applied for graph theory analysis. In this study, the correlation coefficient matrix is processed into an undirected binary matrix by the sparsity threshold method. The topological organization changes in the whole brain functional network are described by analyzing small-world metrics and network efficiency. The main small-world parameters included the clustering coefficient (Cp) and characteristic path length (Lp), which reflected the mean clustering coefficient and characteristic path length of 100 random networks. The Cp is defined as the average clustering coefficient over all nodes, meanwhile the Lp is defined as the average of all shortest path lengths between all over anode pairs. The network efficiency included global efficiency (Eg), and the mean is the mean local efficiency over all nodes in the network (21). Eg is defined as the inverse of the harmonic mean of the shortest path lengths of each pair of nodes, reflecting the capacity for communications throughout the entire network,

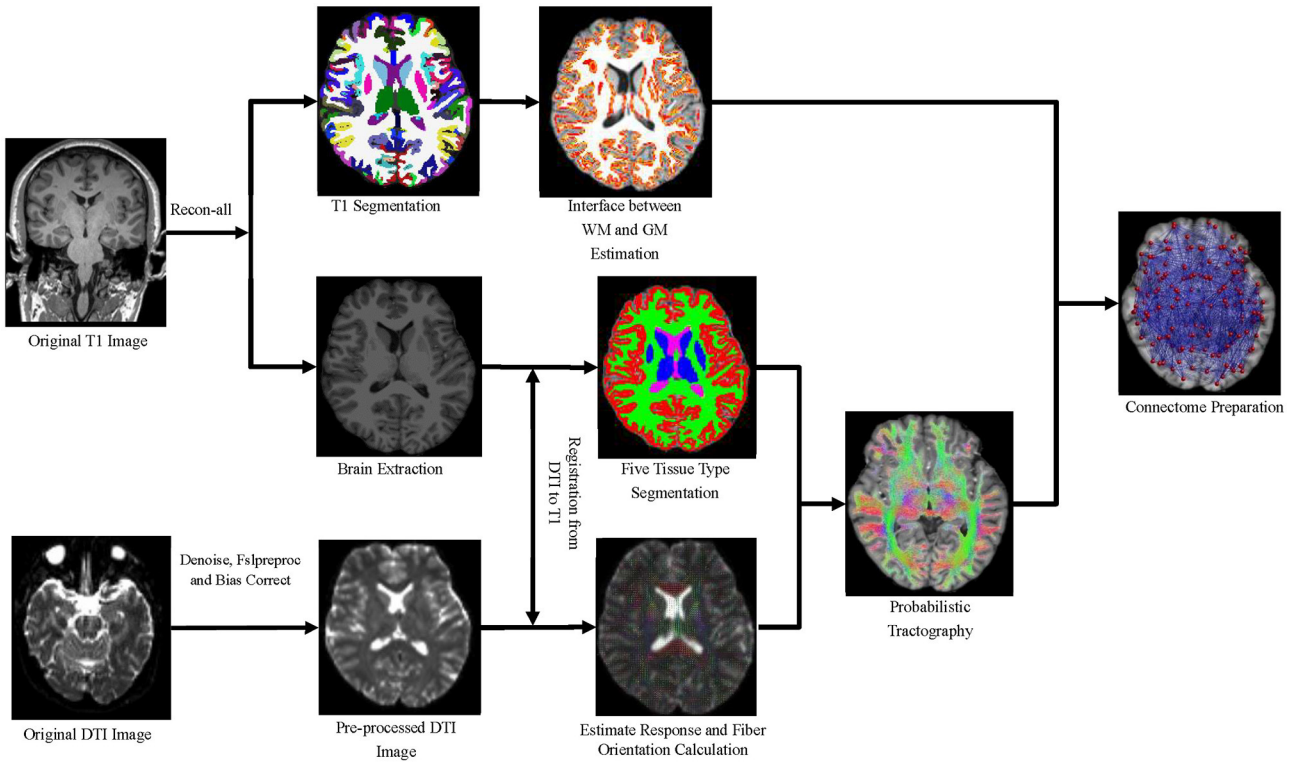

FIGURE 2 | A flowchart of white matter network construction.

while the local efficiency is the mean local efficiency over all nodes in the network. Small-world brain network and network efficiency index between the two groups were compared with two sample *t*-test. The network-based statistic (NBS) was used to identify the group of connections. A total of 5,000 permutations were generated to estimate *p*-values (edge $p < 0.001$, component $p < 0.05$). Meanwhile, a correlation analysis was implemented between the three attentional effects and network efficiency.

RESULTS

Demographic and Clinical Information

Socio-demographic characteristics and ANT scores of all recruited subjects are shown in **Table 1**. **Table 1** also shows that the age of patients with SWD distributed between 24 and 33 years old, which can eliminate aging impact on changes in tolerance to shift work. There were also no significant differences in gender and educational level between the two groups.

The ANT effects between the two groups were conducted *via* two sample t-test analysis or non-parameter test. Compared with healthy controls, patients with SWD showed lower alerting effects and higher executive effects, which suggested declines in alerting and executive functions. No significant differences were observed on orienting effect, overall mean RT, and accuracy between the two groups.

Group Differences in Connectivity Matrix

After accumulating 164 × 164 connectivity matrix, we found 15 significant differences in individual graph components between patients with SWD and healthy controls. The results were corrected by NBS (edge $p < 0.001$, component $p < 0.05$). Significant components for patients with SWD showed lower fiber numbers than healthy controls concerned connections between the left proper thalamus and left middle frontal gyrus, between the left proper thalamus and left postcentral gyrus, between the right temporal pole and left parieto-occipital, between the left temporal pole and left occipital pole, between the left caudate and left middle frontal gyrus, between the right middle frontal gyrus and right putamen, between the right superior frontal gyrus and left superior frontal gyrus, between the left superior frontal gyrus and left anterior middle cingulate, between the left occipital pole and left occipital temporal lateral fusiform, between the right middle frontal gyrus and right caudate, between the right superior frontal gyrus and right caudate, between the left circular superior insula and left long insular, between the left suborbital and left subcallosal, between the left lat fissure post and left paracentral, and between the right occipital superior and transversalis and right calcarine (**Table 2**; **Figure 3**). No connectivity matrix was found for higher fiber numbers on patients with SWD in contrast with healthy controls.

TABLE 1 | The demographic information and ANT between patients with SWD and healthy controls.

Item	SWD $N = 33$	HC $N = 29$	$\chi^2/t/z$	p
Gender (male/female)	2/31	3/26	0.38 (χ^2)	0.54
Age range (min, max)/years	24, 33	24, 33	NA	NA
Age [M(IQR)]/years	28 (4)	27 (3.5)	−1.66 (z)	0.10
Educational level [M(IQR)]/years	16 (3)	16 (3)	−0.56 (z)	0.58
Alerting effect [mean(SD)]/ms	39.79 (3.94)	50.34 (3.36)	−2.01 (t)	0.049
Orienting effect [M(IQR)]/ ms	44 (23.5)	44 (25)	−0.36 (z)	0.72
Executive conflict effect [M(IQR)]/ms	125 (43)	108 (14.5)	−2.44 (z)	0.02
Overall mean RT [M(IQR)]/ms	616 (89)	598 (65)	−1.35 (z)	0.18
Accuracy [M(IQR)]/%	97 (2.5)	98 (1)	−1.76 (z)	0.08

HC, healthy control; IQR, interquartile range; M, median; RT, reaction time; SD, standard deviation; SWD, shift work disorder.

TABLE 2 | Significant components in connectivity matrix between the two groups.

Components (HC > SWD)	t	p
Left proper thalamus–left middle frontal gyrus	3.51	0.03
Left proper thalamus–left postcentral gyrus	3.61	0.03
Right temporal pole–left parieto-occipital	3.65	0.03
Left temporal pole–left occipital pole	4.08	0.01
Left caudate–left middle frontal gyrus	3.62	0.03
Right middle frontal gyrus–right putamen	3.33	0.03
Right superior frontal gyrus–left superior frontal gyrus	3.63	0.03
Left superior frontal gyrus–left anterior middle cingulate	3.5	0.03
Left occipital pole–left occipital temporal lateral fusiform	3.88	0.02
Right middle frontal gyrus–right caudate	3.74	0.02
Right superior frontal gyrus–right caudate	3.84	0.02
Left circular superior insula–left long insular	3.59	0.03
Left suborbital–left subcallosal	3.9	0.02
Left lat fissure post–left paracentral	3.41	0.04
Right occipital superior and transversalis–right calcarine	3.41	0.04

HC, healthy control; SWD, shift work disorder; –, represents the link between the two brain regions.
The results were corrected by NBS (edge $p < 0.001$, component $p < 0.05$).

Group Differences in Small-World Parameters and Network Efficiency

The matrices were constructed with a wide range of sparsity (0.05–0.5) in all enrolled subjects. The small-world parameters were calculated and further compared between the patients with SWD and healthy controls. The Lp values of the patients with SWD had a significant reduction in contrast with healthy controls ($0.1 \leq Sp \leq 0.25$), which is shown in **Figure 4A**. After accumulating the global network efficiency, the result revealed that the patients with SWD exhibited notably lower Eg than the healthy controls on certain sparsity thresholds ($0.1 \leq Sp \leq 0.25$), which is shown in **Figure 4B**. However, no significant differences between the two groups were revealed in regard to the local efficiency.

Correlation Analysis Between ANT Effects and Network Efficiency

The correlation analysis was conducted between the three attentional effects and the global network efficiency. A significant negative correlation ($R^2 = 0.123$, $p = 0.045$) was found between the executive effect and global network efficiency (**Figure 5**).

DISCUSSION

To our knowledge, this is the first study exploring WM structural connectivity and associations with ANT in patients with SWD. Our results revealed lower alerting effects and higher executive effects for patients with SWD. Using link-based analysis, significant group differences were found for 15 links. Meanwhile, the graph theoretical analysis showed that the patients with SWD displayed declines on the Eg and Lp in contrast with the healthy controls. Moreover, the Eg value was negatively correlated with the executive effect. This study primarily demonstrated the disrupted WM structural brain networks underlying the abnormal characteristic of ANT in SWD.

In our study, we first conducted the comparisons between patients with SWD and healthy controls on efficiency of attentional networks. The lower alerting effects and higher executive effects were found on patients with SWD, which suggested declines in alerting and executive functions. Our results were in line with previous studies. One study on healthcare works showed impaired alertness and performance for night shifts due to circadian misalignment (22). Another study on shift work nurses showed that nurses after working night shifts performed worse concentration and more fatigue compared with after working day shifts (23). Furthermore, it was reported that healthy subjects with mental fatigue impairs pre-attentive processing (24). Hence, we speculated that the fatigue might explain the reasons for declines in alerting and executive functions.

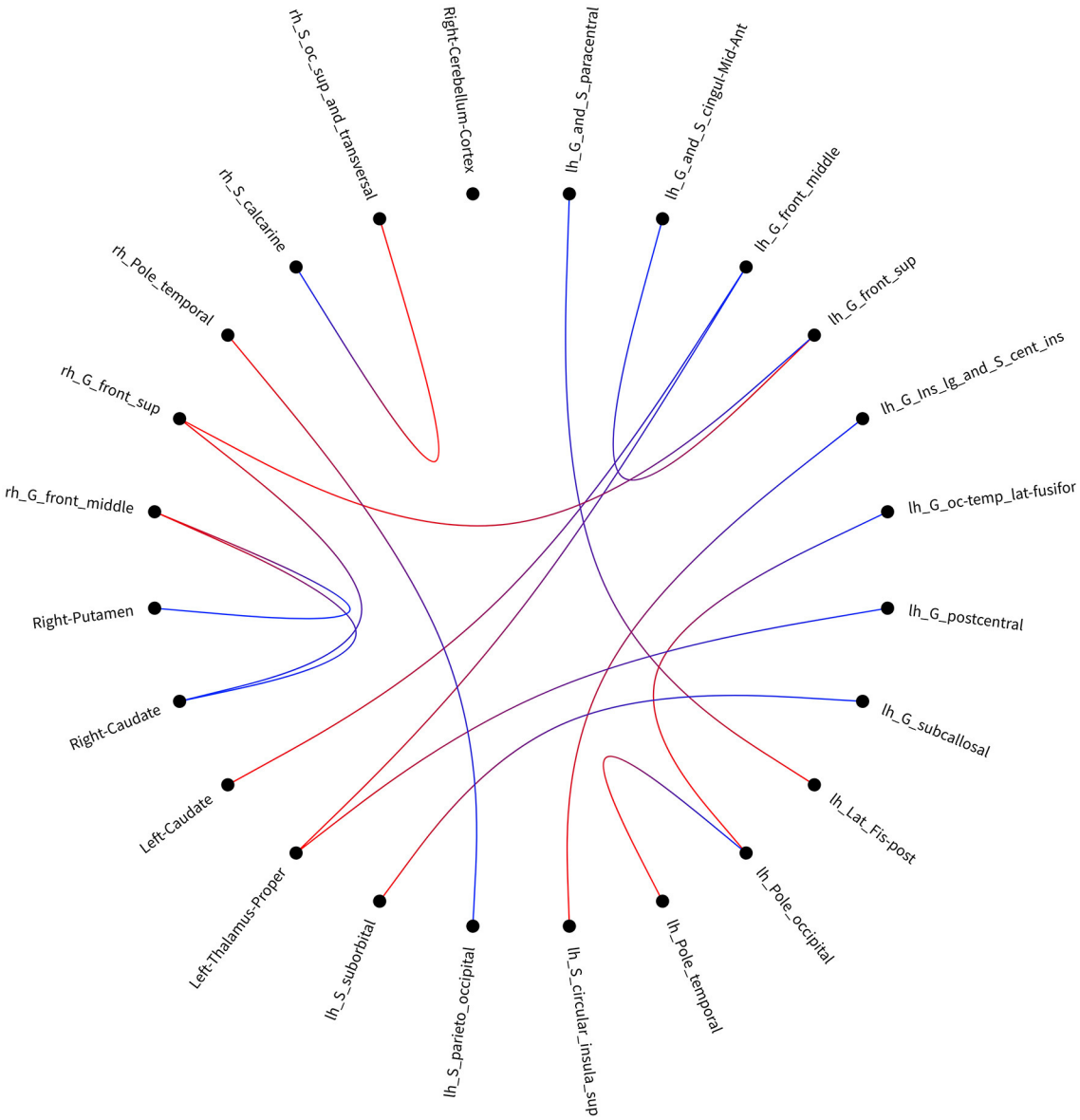

FIGURE 3 | Visualization of the disrupted connectivity matrix found in the group comparison when using link-based analysis. lh, left hemisphere; rh, right hemisphere.

The results from the link-based analysis showed 15 altered connectivity matrices (lower fiber numbers) in patients with SWD compared with healthy controls. The brain regions of disrupted structural connectivity were mainly involved in the frontal gyrus, putamen, and caudate. The frontal gyrus is known to be responsible for emotion processing, working memory, attention, and executive functions (25). One working memory task-related fMRI study on insomnia patients revealed deactivations in the frontal regions (26). In addition, the resting-state fMRI study on insomnia patients showed decreased amplitude of low-frequency fluctuation values in the right middle frontal gyrus and the left orbitofrontal cortex (27). The putamen and caudate belong to the corpus striatum, which forms multisynaptic loops with cortical regions and is associated with motor, memory, and learning. One study on morphological changes in subcortical structures showed that the volume loss of the putamen was associated with impaired cognitive function in patients with chronic insomnia (28). Another study on patients with depression showed disrupted structural connections between the right orbitofrontal cortex and the right putamen, caudate, and inferior temporal gyrus (14). It is possible that the disrupted structural connectivity between frontal gyrus and subcortical nuclei underlies cognitive impairments in patients with SWD. Moreover, we also found lower structural connectivity between the left proper thalamus and left middle frontal gyrus, between the left proper thalamus

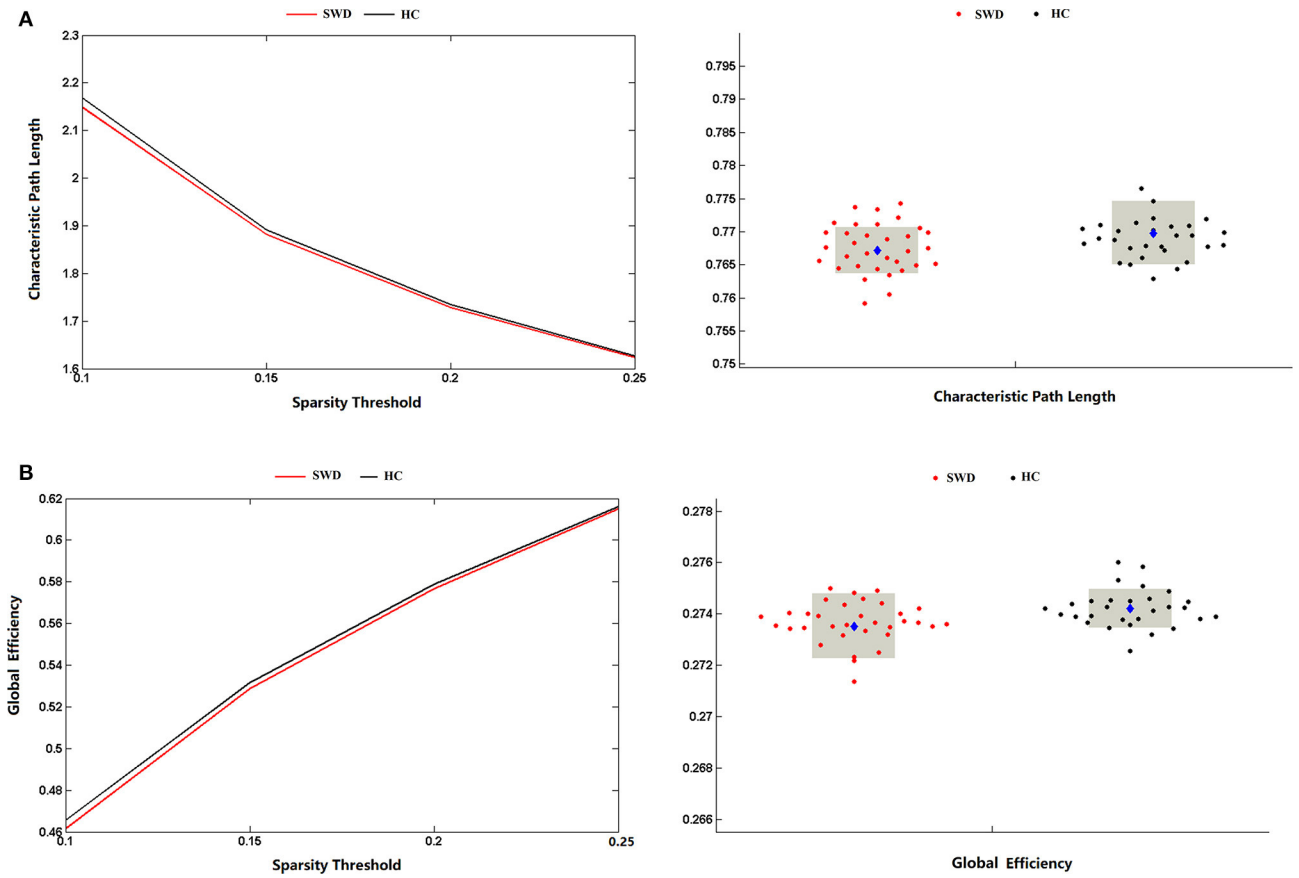

FIGURE 4 | Group comparison of global network topological properties (Lp and Eg) between the patients with SWD and healthy controls. **(A)** The Lp values of the patients with SWD had a significant reduction in contrast with HCs on certain sparsity thresholds ($0.1 \leq Sp \leq 0.25$). **(B)** The result revealed that the patients with SWD exhibited notably lower Eg than the HCs on certain sparsity thresholds ($0.1 \leq Sp \leq 0.25$). Eg, global efficiency; HC, healthy control; Lp, characteristic path length; SWD, shift work disorder.

and left postcentral gyrus. The thalamus is recognized to be involved in maintaining alertness and vigilant attention, which is also a key hub of the cortical attention network (29). The study on sleep deprivation revealed increased thalamic activation after total sleep deprivation, which suggested that increased thalamic activation may compensate for the attention in order to complete the task (30). Notably, the more positive connectivity between the thalamus and cortical regions in patients with insomnia was found in comparison with the healthy controls, which also supported the hyperarousal hypothesis (31). In conclusion, these explorative findings may explain the structural connectivity mechanisms underlying the reduced alertness and executive function in patients with SWD.

The graph theoretical method of structural networks have indicated the shortest paths between brain regions and high clustering of connections, which balanced between the global integration and local specialization. In line with previous studies on structural and functional networks, our results also showed decline on the Eg and Lp between the two groups, which represented the disrupted small-world organization of the structural brain networks. Global network efficiency mainly reflected the capacity for network-wide communication and was regarded as the basis of integrative processing for cognitive functions. Patients with AD (32), primary insomnia (13), and attention deficit hyperactivity disorder (ADHD) (33, 34) all exhibited a decreased global efficiency of the whole WM networks compared with healthy subjects. Nevertheless, the study on sleep deprivation showed the enhanced small-world property, which suggested a possible compensatory effect on the human brain (35). Moreover, the global network efficiency was negatively correlated with the executive effect, which meant the poorer executive function with the lower global efficiency of WM networks. One study on hypertension patients (36) exhibited the executive function impairment underlying a decreased global efficiency of the WM networks. Another study on healthy subjects (12) also showed a significant negative correlation between global efficiency of WM brain network and the executive effect. Hence, we speculated that the declined Eg and Lp may reflect the impaired WM structural network underlying the deficit of attention.

However, there were still some limitations. First, we applied the Destrieux atlas to divide the human brain. However, recent

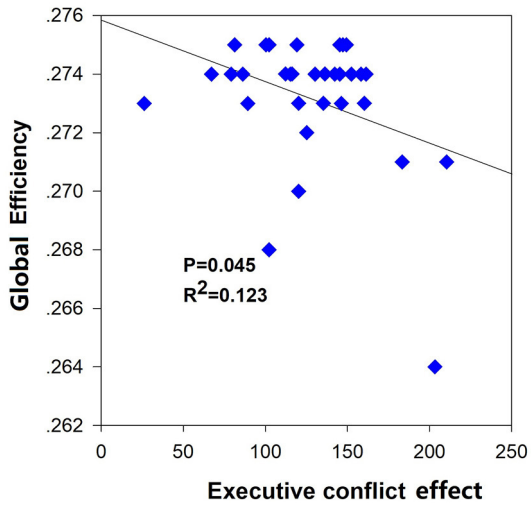

FIGURE 5 | Significant negative correlation between global efficiency and executive conflict effect.

studies have shown that higher-spatial-resolution networks of up to 10,240 parcels (37, 38) could supply an increased sensitivity to local properties. Further studies with higher-spatial-resolution networks may help provide more results on local properties. Second, the enrolled patients in our study only included two male subjects, which failed to analyze the difference in WM structural networks in gender.

CONCLUSION

To the best of our knowledge, this is the first study to explore the topological organization of WM structural network connectivity in SWD. Our findings provide new insights into the fundamental architecture of interregional structural connectivity underlying attention deficits in SWD, which may be a potential biomarker for SWD.

DATA AVAILABILITY STATEMENT

The original contributions presented in the study are included in the article/supplementary material, further inquiries can be directed to the corresponding author/s.

ETHICS STATEMENT

The studies involving human participants were reviewed and approved by Beijing Anding Hospital of Ethics Committee. The patients/participants provided their written informed consent to participate in this study.

AUTHOR CONTRIBUTIONS

HJ provided his expertise in shift work disorder, managed the data collection, and contributed to the writing of the manuscript. KL and YN conceived the idea and methodology for the study, designed the study, and contributed to the writing of the manuscript. YN and MF managed data analyses and wrote the manuscript. YZ, SF, ZF, and XL was contributed to conducting the research and the graph display. All authors contributed to the article and approved the submitted version.

FUNDING

This study was supported by Beijing Hospitals Authority Youth Program (Grant No. QML20201901), National Natural Science Foundation (Grant No. 81904120 and 82004437), Beijing Natural Science Foundation (Grant No. 7204277), Beijing Hospitals Authority Clinical Medicine Development of Special Funding (Grant No. ZYLX202129), Beijing Hospitals Authority's Ascent Plan (Grant No. DFL20191901), and Talents Training Fund of Beijing (Grant No. 2018000021469G292).

REFERENCES

1. Cheng P, Drake C. Shift work disorder. *Neurol Clin.* (2019) 37:563–77. doi: 10.1016/j.ncl.2019.03.003
2. Marquie JC, Tucker P, Folkard S, Gentil C, Ansiau D. Chronic effects of shift work on cognition: findings from the VISAT longitudinal study. *Occup Environ Med.* (2015) 72:258–64. doi: 10.1136/oemed-2013-101993
3. Donmezdil S, Arac S. Effect of shift work in intensive care on attention disorder in nurses. *Int J Clin Pract.* (2021) 75:e13774. doi: 10.1111/ijcp.13774
4. Fan J, McCandliss BD, Fossella J, Flombaum JI, Posner MI. The activation of attentional networks. *Neuroimage.* (2005) 26:471–9. doi: 10.1016/j.neuroimage.2005.02.004
5. Fan J, Bernardi S, Van Dam NT, Anagnostou E, Gu X, Martin L, et al. Functional deficits of the attentional networks in autism. *Brain Behav.* (2012) 2:647–60. doi: 10.1002/brb3.90
6. Joseph RM, Fricker Z, Keehn B. Activation of frontoparietal attention networks by non-predictive gaze and arrow cues. *Soc Cogn Affect Neurosci.* (2015) 10:294–301. doi: 10.1093/scan/nsu054
7. Spagna A, Dong Y, Mackie MA, Li M, Harvey PD, Tian Y, et al. Clozapine improves the orienting of attention in schizophrenia. *Schizophr Res.* (2015) 168:285–91. doi: 10.1016/j.schres.2015.08.009
8. Martella D, Casagrande M, Lupianez J. Alerting, orienting and executive control: the effects of sleep deprivation on attentional networks. *Exp Brain Res.* (2011) 210:81–9. doi: 10.1007/s00221-011-2605-3
9. Ning Y, Li K, Zhang Y, Chen P, Yin D, Zhu H, et al. Assessing Cognitive Abilities of Patients With Shift Work Disorder: Insights From RBANS and Granger Causality Connections Among Resting-State Networks. *Front Psychiatry.* (2020) 11:780. doi: 10.3389/fpsyt.2020.00780
10. Wu X, Bai F, Wang Y, Zhang L, Liu L, Chen Y, et al. Circadian rhythm disorders and corresponding functional brain abnormalities in young female nurses: a preliminary study. *Front Neurol.* (2021) 12:664610. doi: 10.3389/fneur.2021.664610
11. Guo W, Liu F, Liu Z, Gao K, Xiao C, Chen H, et al. Right lateralized white matter abnormalities in first-episode, drug-naive paranoid schizophrenia. *Neurosci Lett.* (2012) 531:5–9. doi: 10.1016/j.neulet.2012.09.033
12. Xiao M, Ge H, Khundrakpam BS, Xu J, Bezgin G, Leng Y, et al. Attention performance measured by attention network test is correlated with global and regional efficiency of structural brain networks. *Front Behav Neurosci.* (2016) 10:194. doi: 10.3389/fnbeh.2016.00194
13. Lu FM, Dai J, Couto TA, Liu CH, Chen H, Lu SL, et al. Diffusion tensor imaging tractography reveals disrupted white matter structural connectivity

network in healthy adults with insomnia symptoms. *Front Hum Neurosci.* (2017) 11:583. doi: 10.3389/fnhum.2017.00583
14. Long Z, Duan X, Wang Y, Liu F, Zeng L, Zhao JP, et al. Disrupted structural connectivity network in treatment-naive depression. *Prog Neuropsychopharmacol Biol Psychiatry.* (2015) 56:18–26. doi: 10.1016/j.pnpbp.2014.07.007
15. Fischl B, van der Kouwe A, Destrieux C, Halgren E, Segonne F, Salat DH, et al. Automatically parcellating the human cerebral cortex. *Cereb Cortex.* (2004) 14:11–22. doi: 10.1093/cercor/bhg087
16. Desikan RS, Segonne F, Fischl B, Quinn BT, Dickerson BC, Blacker D, et al. An automated labeling system for subdividing the human cerebral cortex on MRI scans into gyral based regions of interest. *Neuroimage.* (2006) 31:968–80. doi: 10.1016/j.neuroimage.2006.01.021
17. Veraart J, Fieremans E, Novikov DS. Diffusion MRI noise mapping using random matrix theory. *Magn Reson Med.* (2016) 76:1582–93. doi: 10.1002/mrm.26059
18. Veraart J, Novikov DS, Christiaens D, Ades-Aron B, Sijbers J, Fieremans E. Denoising of diffusion MRI using random matrix theory. *Neuroimage.* (2016) 142:394–406. doi: 10.1016/j.neuroimage.2016.08.016
19. Tustison NJ, Avants BB, Cook PA, Zheng Y, Egan A, Yushkevich PA, et al. N4ITK: improved N3 bias correction. *IEEE Trans Med Imaging.* (2010) 29:1310–20. doi: 10.1109/TMI.2010.2046908
20. Jeurissen B, Tournier JD, Dhollander T, Connelly A, Sijbers J. Multi-tissue constrained spherical deconvolution for improved analysis of multi-shell diffusion MRI data. *Neuroimage.* (2014) 103:411–26. doi: 10.1016/j.neuroimage.2014.07.061
21. Maslov S, Sneppen K. Specificity and stability in topology of protein networks. *Science.* (2002) 296:910–3. doi: 10.1126/science.1065103
22. Ganesan S, Magee M, Stone JE, Mulhall MD, Collins A, Howard ME, et al. The Impact of Shift Work on Sleep, Alertness and Performance in Healthcare Workers. *Sci Rep.* (2019) 9:4635. doi: 10.1038/s41598-019-40914-x
23. Imes CC, Chasens ER. Rotating Shifts Negatively Impacts Health and Wellness Among Intensive Care Nurses. *Workplace Health Saf.* (2019) 67:241–9. doi: 10.1177/2165079918820866
24. Yang B, Xiao W, Liu X, Wu S, Miao D. Mental fatigue impairs pre-attentive processing: a MMN study. *Neurosci Lett.* (2013) 532:12–6. doi: 10.1016/j.neulet.2012.08.080
25. Baddeley A. Working memory: looking back and looking forward. *Nat Rev Neurosci.* (2003) 4:829–39. doi: 10.1038/nrn1201
26. Drummond SP, Walker M, Almklov E, Campos M, Anderson DE, Straus LD. Neural correlates of working memory performance in primary insomnia. *Sleep.* (2013) 36:1307–16. doi: 10.5665/sleep.2952
27. Zhou F, Huang S, Zhuang Y, Gao L, Gong H. Frequency-dependent changes in local intrinsic oscillations in chronic primary insomnia: A study of the amplitude of low-frequency fluctuations in the resting state. *Neuroimage Clin.* (2017) 15:458–65. doi: 10.1016/j.nicl.2016.05.011
28. Koo DL, Shin JH, Lim JS, Seong JK, Joo EY. Changes in subcortical shape and cognitive function in patients with chronic insomnia. *Sleep Med.* (2017) 35:23–6. doi: 10.1016/j.sleep.2017.04.002
29. Schiff ND. Central thalamic contributions to arousal regulation and neurological disorders of consciousness. *Ann N Y Acad Sci.* (2008) 1129:105–18. doi: 10.1196/annals.1417.029
30. Ma N, Dinges DF, Basner M, Rao H. How acute total sleep loss affects the attending brain: a meta-analysis of neuroimaging studies. *Sleep.* (2015) 38:233–40. doi: 10.5665/sleep.4404
31. Zou G, Li Y, Liu J, Zhou S, Xu J, Qin L, et al. Altered thalamic connectivity in insomnia disorder during wakefulness and sleep. *Hum Brain Mapp.* (2021) 42:259–70. doi: 10.1002/hbm.25221
32. Lo CY, Wang PN, Chou KH, Wang J, He Y, Lin CP. Diffusion tensor tractography reveals abnormal topological organization in structural cortical networks in Alzheimer's disease. *J Neurosci.* (2010) 30:16876–85. doi: 10.1523/JNEUROSCI.4136-10.2010
33. Cao Q, Shu N, An L, Wang P, Sun L, Xia MR, et al. Probabilistic diffusion tractography and graph theory analysis reveal abnormal white matter structural connectivity networks in drug-naive boys with attention deficit/hyperactivity disorder. *J Neurosci.* (2013) 33:10676–87. doi: 10.1523/JNEUROSCI.4793-12.2013
34. Sidlauskaite J, Caeyenberghs K, Sonuga-Barke E, Roeyers H, Wiersema JR. Whole-brain structural topology in adult attention-deficit/hyperactivity disorder: Preserved global - disturbed local network organization. *Neuroimage Clin.* (2015) 9:506–12. doi: 10.1016/j.nicl.2015.10.001
35. Liu H, Li H, Wang Y, Lei X. Enhanced brain small-worldness after sleep deprivation: a compensatory effect. *J Sleep Res.* (2014) 23:554–63. doi: 10.1111/jsr.12147
36. Li X, Ma C, Sun X, Zhang J, Chen Y, Chen K, et al. Disrupted white matter structure underlies cognitive deficit in hypertensive patients. *Eur Radiol.* (2016) 26:2899–907. doi: 10.1007/s00330-015-4116-2
37. Zalesky A, Fornito A, Harding IH, Cocchi L, Yucel M, Pantelis C, et al. Whole-brain anatomical networks: does the choice of nodes matter? *Neuroimage.* (2010) 50:970–83. doi: 10.1016/j.neuroimage.2009.12.027
38. Khundrakpam BS, Tohka J, Evans AC, Brain Development Cooperative G. Prediction of brain maturity based on cortical thickness at different spatial resolutions. *Neuroimage.* (2015) 111:350–9. doi: 10.1016/j.neuroimage.2015.02.046

Conflict of Interest: The authors declare that the research was conducted in the absence of any commercial or financial relationships that could be construed as a potential conflict of interest.

frontiers in Psychiatry

ORIGINAL RESEARCH
published: 14 February 2022
doi: 10.3389/fpsyt.2022.841461

Mindfulness-Based Cognitive Therapy Regulates Brain Connectivity in Patients With Late-Life Depression

Hui Li[1†], Wei Yan[1†], Qianwen Wang[1†], Lin Liu[1†], Xiao Lin[1], Ximei Zhu[1], Sizhen Su[1], Wei Sun[1], Manqiu Sui[2], Yanping Bao[3], Lin Lu[1,3,4], Jiahui Deng[1*] and Xinyu Sun[1*]*

[1] Peking University Sixth Hospital, Peking University Institute of Mental Health, NHC Key Laboratory of Mental Health (Peking University), National Clinical Research Center for Mental Disorders (Peking University Sixth Hospital), Beijing, China, [2] Beijing Xi Cheng District Pingan Hospital, Beijing, China, [3] National Institute on Drug Dependence and Beijing Key Laboratory of Drug Dependence, Peking University, Beijing, China, [4] Peking-Tsinghua Center for Life Sciences and PKU-IDG/McGovern Institute for Brain Research, Peking University, Beijing, China

Late-life depression (LLD) is an important public health problem among the aging population. Recent studies found that mindfulness-based cognitive therapy (MBCT) can effectively alleviate depressive symptoms in major depressive disorder. The present study explored the clinical effect and potential neuroimaging mechanism of MBCT in the treatment of LLD. We enrolled 60 participants with LLD in an 8-week, randomized, controlled trial (ChiCTR1800017725). Patients were randomized to the treatment-as-usual (TAU) group or a MBCT+TAU group. The Hamilton Depression Scale (HAMD) and Hamilton Anxiety Scale (HAMA) were used to evaluate symptoms. Magnetic resonance imaging (MRI) was used to measure changes in resting-state functional connectivity and structural connectivity. We also measured the relationship between changes in brain connectivity and improvements in clinical symptoms. HAMD total scores in the MBCT+TAU group were significantly lower than in the TAU group after 8 weeks of treatment ($p < 0.001$) and at the end of the 3-month follow-up ($p < 0.001$). The increase in functional connections between the amygdala and middle frontal gyrus (MFG) correlated with decreases in HAMA and HAMD scores in the MBCT+TAU group. Diffusion tensor imaging analyses showed that fractional anisotropy of the MFG-amygdala significantly increased in the MBCT+TAU group after 8-week treatment compared with the TAU group. Our study suggested that MBCT improves depression and anxiety symptoms that are associated with LLD. MBCT strengthened functional and structural connections between the amygdala and MFG, and this increase in communication correlated with improvements in clinical symptoms.

Randomized Controlled Trial; Follow-Up Study; fMRI; Brain Connectivity

Keywords: late-life depression, mindfulness-based cognitive therapy, magnetic resonance imaging, functional connection, amygdala, middle frontal gyrus

OPEN ACCESS

Edited by:
Yuanqiang Zhu, Fourth Military Medical University, China

Reviewed by:
Zhaowen Liu, Massachusetts General Hospital and Harvard Medical School, United States
Wen-Jun Wu, Fourth Military Medical University, China

***Correspondence:**
Lin Lu
linlu@bjmu.edu.cn
Xinyu Sun
sunxinyu@bjmu.edu.cn
Jiahui Deng
jiahuideng2012@bjmu.edu.cn

[†]These authors have contributed equally to this work

Specialty section:
This article was submitted to Neuroimaging and Stimulation, a section of the journal Frontiers in Psychiatry

Received: *22 December 2021*
Accepted: *19 January 2022*
Published: *14 February 2022*

Citation:
Li H, Yan W, Wang Q, Liu L, Lin X, Zhu X, Su S, Sun W, Sui M, Bao Y, Lu L, Deng J and Sun X (2022) Mindfulness-Based Cognitive Therapy Regulates Brain Connectivity in Patients With Late-Life Depression. Front. Psychiatry 13:841461. doi: 10.3389/fpsyt.2022.841461

INTRODUCTION

Depression that occurs after 60–65 years of age is typically referred to as late-life depression (LLD), with a lifetime prevalence of 16% (1, 2). Late-life depression is an important public health concern among the aging population, severely affecting psychological, social, and biological functions (3). According to data from the World Health Organization, LDD is currently the leading cause of disability worldwide (4). The most common treatments for LLD are antidepressants, but side effects and other limitations can hamper their efficacy. Older adults are considered a vulnerable population because they are more likely to suffer from chronic medical conditions and are sensitive to adverse effects of antidepressants (5). Risks of drug interactions and undesirable side effects increase because of metabolic abnormalities that occur with aging and multiple prescribed medications that are taken for comorbidities (5). Older patients with depression require extra care from clinical professionals because of high rates of relapse and recurrence (6). Psychotherapy can play a significant role in the treatment of psychiatric disorders. Psychotherapy helps patients with mood disorders deal with maladaptive thinking and develop a positive mindset (6, 7). The combination of psychotherapy and pharmacotherapy was shown to be an effective approach to treat the acute phase of depression and preventing relapse and recurrence (7).

Mindfulness-based cognitive therapy (MBCT) is an evidence-based psychotherapeutic intervention that integrates several essential elements of cognitive behavioral therapy with mindfulness meditation (8). Mindfulness training focuses on the progressive acquisition of mindful awareness to ameliorate stress and reduce negative feelings and thoughts. Thus, MBCT may be a good option to treatment stress-related disease. MBCT is currently recommended by several national clinical guidelines as a prophylactic treatment for recurrent major depressive disorder (9, 10), and it is considered a cost-effective intervention. MBCT usually consists of 8-week group sessions and individual daily homework between sessions. Since the first edition of the MBCT manual was published in 2002, mounting interest in MBCT and its clinical potential has been seen in treating depressive disorders (11). Previous studies demonstrated that MBCT is an effective nonpharmacological approach to reduce the risk of depression relapse/recurrence in young adults with major depression (12) and patients with LLD in primary care (13, 14). However, unknown are whether and how specific circuits are affected by MBCT.

Many studies indicate that abnormal structural and functional alterations of the brain underlie the pathophysiology of LDD (15–17). Negative correlations were found between a greater number of depressive episodes and a reduction of hippocampal volume (18), with thinning of the medial prefrontal cortex (mPFC) (19). Illness duration also correlated with a volume reduction of the hippocampus, putamen, insula, and mPFC (20–22). Resting-state functional magnetic resonance imaging (fMRI) studies reported a reduction of connectivity between the amygdala and dorsal frontal regions in LLD patients (23), with disruptions of the fronto-parietal network (24). Brain connectivity between the fronto-parietal network and regions that are involved in sensory information processing were restored after MBCT in patients with major depression (25). Additionally, meditation training is a vital part of MBCT that induces brain network changes in functional and structural connectivity, such as the fronto-parietal network, default mode network, and salience network (26, 27). Prior studies that investigated neural mechanisms of emotion regulation reported that meditation training heightened functional connectivity between the amygdala and mPFC (28). Some attempts have been made to provide initial evidence of a decrease in structural brain connectivities in MDD (29, 30). A decrease in fractional anisotropy (FA) of the white matter tract that connects the subgenual anterior cingulate cortex and amygdala was observed in adolescents with depression (30). However, an increase in radial diffusivity of the right uncinate fasciculus was also reported in patients with MDD (29). Still unclear, however, is how MBCT affects brain structure and function to improve symptoms of LDD.

The present study explored whether MBCT as an adjunctive treatment to treatment as usual (TAU) in LDD patients has superior outcomes compared with TAU alone. Brain imaging was performed to evaluate the possible mechanism of adjunctive MBCT in LDD patients by analyzing brain connectivity and potential biological correlates. We also investigated whether white matter integrity between the amygdala and MFG (i.e., two brain regions that have shown to be important in MDD) supports abnormal functional connectivity between these two brain regions (31, 32). Diffusion-weighted images were collected, and the FA of fiber tracts that connect the amygdala and MFG was compared between patients who received MBCT combined with TAU or TAU alone. Our findings may contribute to new non-pharmaceutical strategies for the treatment of elderly patients with LLD.

MATERIALS AND METHODS

Participants

We recruited outpatients with depression who were over 60 years of age, with no upper age limit, from May 2018 to June 2019. This study was approved by the Ethics Committee of Peking University Sixth Hospital. All patients provided written informed consent to participate in the study. All of the subjects were diagnosed with depression by two experienced psychiatrists using the *Diagnostic and Statistical Manual of Mental Disorders*, 4th edition (DSM-IV), and Structured Clinical Interview for the DSM (SCID). The severity of depression was assessed using the 24-item Hamilton Depression Scale (HAMD). The severity of anxiety was assessed using the Hamilton Anxiety Scale (HAMA). Overall cognitive function was rated using the Mini-Mental State Examination (MMSE). For all of the subjects, the exclusion criteria included the following: (1) current or previous diagnosis of schizophrenia, bipolar disorder, substance abuse, substance-induced depression, or dementia, (2) MMSE score < 26, (3) severe somatic disease (e.g., brain tumors, metastatic cancer, or unstable cardiac, hepatic, or renal disease), (4) treatment with antidepressants (except selective

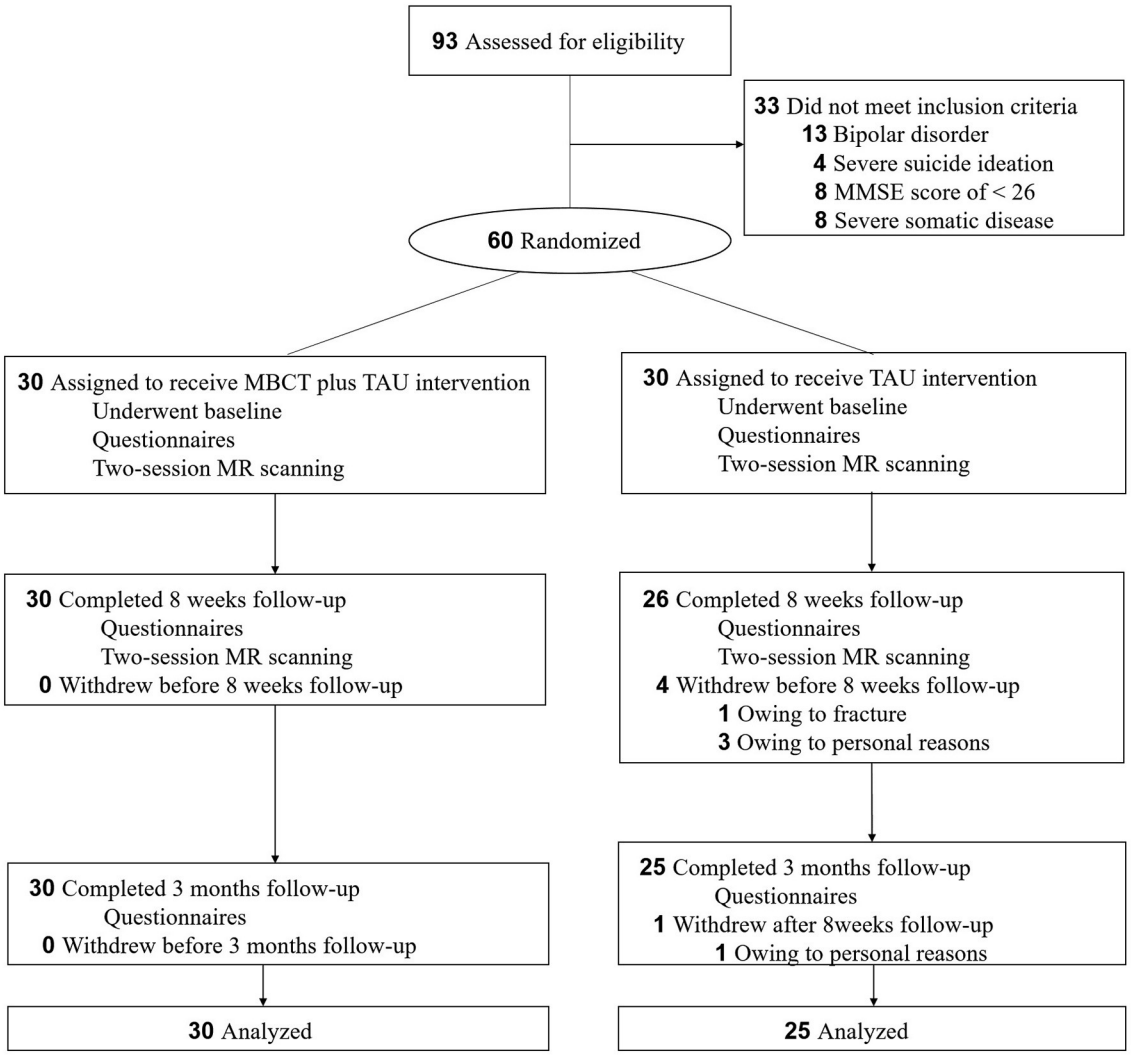

FIGURE 1 | Flow chart of the study.

serotonin reuptake inhibitors [SSRIs] and selective serotonin-norepinephrine reuptake inhibitors [SNRIs]), (5) current suicidal ideation, (6) left handed, and (7) any contraindication to fMRI (e.g., having a pacemaker or implanted metal). In this study, participants were informed about assignment while assessors remained blind.

Study Design

This was a single-center, randomized, parallel-group, controlled trial that was registered with ClinicalTrials.gov (no. ChiCTR1800017725). The study consisted of three phases: screening phase, 8-week treatment phase, and up to a 3-month follow-up phase. Following baseline measure completion, eligible patients were randomly divided into the MBCT+TAU group or TAU group. The MBCT+TAU group was given 8 weeks of the MBCT intervention with current antidepressant treatments. The TAU group continued to receive their usual antidepressant treatments only (**Figure 1**). In the MBCT+TAU group, 22 patients received SSRIs (15 escitalopram, 20 mg/day; 5 sertraline, 150-200 mg/day; 2 fluoxetine, 20 mg/day), and eight patients received SNRIs (5 duloxetine, 60–90 mg/day; 3 venlafaxine, 150–225 mg/day). In the TAU group, 23 patients received SSRIs (16 escitalopram, 20 mg/day; 7 sertraline, 150–200 mg/day), and seven received SNRIs (3 duloxetine, 60–90 mg/day; 4 venlafaxine, 150–225 mg/day).

The MBCT protocol was based on a manualized 8-week meditation-based skills-training group program (8) and adapted to be more suitable for elderly individuals with depression. MBCT was adapted to cater older adults' physical condition and prevent them falls. Furthermore, we would provide online support offers for them to better understanding MBCT program. During 8-week treatment, the guided meditations ranged from 60 to 90 min once weekly. Mindfulness were supervised 45 min daily by themselves. Patients were recommended to

practice mindfulness voluntarily at home. The time of voluntary mindfulness practice were recorded per day by a mindfulness practice log. We visited patients in the TAU group weekly to ask about adverse events. The TAU group did not receive any other psychotherapy. We evaluated changes in depressive and anxiety symptoms using the 24-item HAMD as the primary outcome and HAMA as the secondary outcome at baseline, at the end of 8 weeks of treatment, and at the 3-month follow-up.

Functional Magnetic Resonance Imaging

To further explore possible mechanisms of MBCT, fMRI was performed to measure changes in brain function during the resting state (33, 34) in LLD patients before and after treatment at baseline (pre-test) and 8 weeks (post-test). fMRI data for all participants were acquired using a research-dedicated 3.0 T GE EXCITE HD scanner (GE Medical Systems, Milwaukee, WI, USA) at Peking University Sixth Hospital with an 8-channel head coil. For each participant, high-resolution T1-weighted structural images were acquired using the following parameters: field of view (FOV) = 25.6 cm^3, flip angle = 12°. Eight-min resting-state fMRI scans were performed using a gradient-echo echo-planar imaging (EPI) sequence (FOV = 22.0 cm^3, TR = 2,000 ms, TE = 30 ms, flip angle = 90°, number of slices = 43, total scans = 240). We then performed diffusion tensor imaging (DTI) scans by a gradient-echo EPI sequence (FOV = 22.0 cm^3, TR = 2,000 ms, TE = 30 ms, flip angle = 90°, number of slices = 43, total scans = 240). To reduce motion artifacts, the participant's head was fixed with foam pads on the scanner bed. Each participant was instructed to stay still and awake during data acquisition.

Diffusion Tensor Imaging Data

Diffusion tensor imaging data were processed using tools that are included in the Functional MRI of the Brain (FMRIB) Software Library (FSL), which is used for motion and eddy-current correction. A diffusion tensor model was fit at each voxel using DTIFIT. For individual FA images, the FMRIB Diffusion Toolbox (FDT) was used to fit a diffusion tensor to raw diffusion data, and the brain was extracted using the Brain Extraction Tool (BET). All subjects' FA images were aligned into a common space using the FNIRT nonlinear registration tool. The threshold of the mean FA skeleton image was 0.2.

Data preprocessing and FA values for each white matter tract were calculated using automated whole-brain atlas-based tractography with above method. Preprocessing was performed using the FSL. First, non-brain tissue was deleted with the brain extraction tool from eddy current-corrected diffusion MRI data. Diffusion indices, such as FA, tensors, and the first eigenvector, were calculated using the FMRIB Diffusion Toolbox. Finally, linear and non-linear registrations were conducted using the FMRIB Linear Image Registration Tool, followed by the FMRIB Nonlinear Image Registration Tool. Automated fiber tracking with the tensor deflection method was performed with 54 white matter parcels, which were prescribed based on the Johns Hopkins University Diffusion Tensor Imaging-based white-matter atlas. The FA value at each stepping point (stepping width: 0.5 mm) along each fiber was calculated by interpolation using volume data for the center points of the nearest eight voxels around the stepping point. The terminate criteria were FA < 0.25 and flip angle $> 45°$. Fiber tracking procedures were performed using MATLAB R2015b for Windows (MathWorks, Natick, MA, USA).

Data Analysis

Functional image preprocessing was performed using CONN software (http://web.mit.edu/swg/software.htm). Briefly, after excluding the first 10 images to ensure signal equilibrium, functional images were corrected for head motion and temporal differences. A subject was excluded if any translation or rotation parameters in this subject's dataset exceeded $\pm$ 2.5 mm and/or $\pm$ 2.5°. The corrected functional images were first co-registered to each subject's T1 images without re-slicing. T1 images were then normalized to Montreal Neurological Institute (MNI) space, which generated a transformed matrix from native space to MNI space. Functional images were then transformed to MNI space using this matrix and resampled at $3 \times 3 \times 3$ mm^3. Outlier detection was performed on the normalized images. Finally, all images were smoothed with a 6 mm full width at half maximum Gaussian kernel.

An Anatomical Automatic Labeling cortical and sub-cortical atlas was used to segment the whole brain into 116 anatomical regions of interest (ROIs). For each subject, each ROI time series was extracted as the average time series across all voxels within that region. To remove spurious sources of variance, all ROI time series underwent the following steps: (1) linear detrending, (2) regressing out the six head motion parameters and their first-level derivative, the averaged cerebrospinal fluid and white matter signals, and the scrubbing signal from the time series, and (3) 0.01–0.1 Hz band-pass filtering. All of these steps were accomplished using CONN software. Finally, Pearson correlation coefficients were calculated between each pair of preprocessed ROI time series, and a temporal correlation matrix was generated for each subject. We analyzed changes in the functional connectivity of these ROIs between the two groups before and after treatment. Functional connectivity with significant group $\times$ time interactions in the two groups was investigated.

DTI data preprocessing was performed using FSL package. To compare between-group differences in white matter integrity of the uncinate fasciculus in both the right and left hemispheres, four seed regions (two seeds for each hemisphere) that represented the amygdala and MFG were defined as volumetric regions based on the anatomical automatic labeling atlas that is available within the FSL package (https://fsl.fmrib.ox.ac.uk/fsldownloads_registration). These seeds were selected to anchor the endpoint of tracks that constituted the uncinate fasciculus. For each hemisphere and each subject/visit, the uncinate fasciculus mean summary values (i.e., FA, mean diffusivity, axial diffusivity, and radial diffusivity) were extracted using TrackVis software (http://www.trackvis.org/). Finally, two-sample *t*-tests were performed to investigate white matter integrity of the uncinate fasciculus within the two groups. Significant changes in FA at baseline were correlated with neuropsychological data to investigate whether individual differences in white matter integrity were associated with the extent of depression. We

reanalyzed the brain images using the false discovery rate (FDR) for multiple comparison correction.

Statistical Analysis

Demographic and clinical characteristics were analyzed for between-group differences using two-sample *t*-tests for continuous variables and the χ^2 test for categorical variables. The total time of voluntary mindfulness practice was summed by daily homework practice time (in hour). Repeated-measures analysis of variance (ANOVA) was used to analyze differences in clinical measures, with group (MBCT+TAU vs. TAU) and time (Pre vs. Post) as factors. Pearson correlation analyses were performed to assess correlations between significant functional connectivity findings and the clinical variables, including HAMD scores and HAMA scores, in each group separately. The tests were two-tailed. Values of $p < 0.05$ were considered statistically significant.

RESULTS

Demographic Results

A total of 60 patients were recruited and randomly assigned to the MBCT+TAU group ($n = 30$; age [mean ± SD] = 62.33 ± 7.26 years) or TAU group ($n = 30$; age [mean ± SD] = 61.96 ± 5.56 years). **Table 1** shows the baseline characteristics and demographics of these patients. In the randomized treatment phase, complete data were available from 30 participants (30/30, 100%) in the MBCT+TAU group. Of the 30 participants in the TAU group, 25 participants (25/30, 83.33%) had two-session MR scanning and follow-up data, four withdrew at 8-week follow-up, and one dropped out at 3 months (**Figure 1**). No significant differences were found between the two groups in age ($t = 0.285$, $p = 0.776$), sex ratio ($\chi^2 = 0.373$, $p = 0.761$), Body Mass Index ($t = -1.773$, $p = 0.082$), age at onset of depression ($t = 0.220$, $p = 0.827$), duration of depression ($t = -0.196$, $p = 0.846$), or number of episodes ($t = -0.643$, $p = 0.523$).

TABLE 1 | Demographic and clinical characteristics of the participants.

	MBCT+TAU group ($n = 30$)	TAU group ($n = 30$)	t/χ^2	*p*
Age (years)	67.66 ± 5.93	67.22 ± 5.78	0.285	0.776
Sex (% male)	6 (20%)	8 (26.7%)	0.373	0.761
Education (years)	13.73 ± 2.66	12.5 ± 3.08	1.658	0.103
Body mass index	22.64 ± 2.42	23.63 ± 1.83	−1.773	0.082
Onset age (years)	62.33 ± 7.26	61.96 ± 5.56	0.220	0.827
Duration (months)	48.23 ± 43.36	50.23 ± 35.41	−0.196	0.846
Number of episodes	2.36 ± 1.77	2.66 ± 1.84	−0.643	0.523
Current type of medication				
SSRIs	22	23	0.089	0.766
SNRIs	8	7	0.089	0.766

The results are expressed as mean ± standard deviation. SSRIs, selective serotonin reuptake inhibitors; SNRIs, serotonin and norepinephrine reuptake inhibitors.

HAMD and HAMA Scores

For our primary outcome, changes in HAMD scores after 8 weeks of treatment and 3 months later were analyzed. For patients with adjunctive MBCT treatment, HAMD scores decreased from baseline (17.67 ± 6.68) to 8-week follow-up (5.83 ± 4.92). In the TAU group, mean HAMD scores were 18.56 ± 7.00) and 11.00 ± 5.29 at baseline and 8-week follow-up, respectively. There were no significant differences between the two groups in HAMD at baseline ($p = 0.631$). The repeated-measures ANOVA revealed main effects of time [$F_{(2,106)} = 98.48$, $p < 0.001$) and group [$F_{(1,53)} = 12.43$, $p = 0.001$] and a significant time × group interaction [$F_{(2,106)} = 3.38$, $p = 0.038$; **Figure 2A**]. We found evidence of a greater reduction of depressive symptoms both after 8 weeks of treatment ($p < 0.001$) and at the end of the 3-month follow-up ($p < 0.001$), as measured by the HAMD in the MBCT+TAU group compared with the TAU group.

We also analyzed correlations between the time of voluntary mindfulness practice and improvements in depressive symptoms after treatment. **Figure 2B** shows that the time of voluntary mindfulness practice in the MBCT+TAU group was significantly negatively correlated with HAMD total scores at the end of treatment ($r = -0.374$, $p = 0.042$).

The repeated-measures ANOVA of HAMA scores showed main effects of time [$F_{(2,106)} = 110.77$, $p < 0.001$] and group [$F_{(1,53)} = 4.18$, $p = 0.046$] but no time × group interaction [$F_{(2,106)} = 1.99$, $p = 0.142$; **Figure 2C**]. Patients in both groups exhibited reductions of anxiety symptoms after treatment.

Resting-State Functional Connectivity

We found that after 8 weeks of treatment, functional connectivity of the right MFG-right amygdala, right amygdala-right frontal pole, and left supraoccipital lateral cortex-left cerebellum VII significantly increased in the MBCT+TAU group compared with the TAU group. The degree of functional connectivity of the left insula-left precentral gyrus, left insula-right cerebellum VII, and left hippocampus-right intracalcarine cortex significantly decreased (**Figure 3A**). Correlation analysis was used to explore the relationship between changes in functional connectivity directly and improvements in symptoms. The results showed that changes in functional connectivity of the right MFG-right amygdala in the MBCT+TAU group significantly positively correlated with changes in HAMD scores ($r = 0.52$, $p = 0.004$ after FDR corrected) and changes in HAMA scores ($r = 0.49$, $p = 0.006$ after FDR corrected), whereas no significant correlations were found in the TAU group (**Figure 3B**).

Diffusion Tensor Imaging Measures

One participant in each group was excluded because of poor image quality for the DTI analysis. **Figure 4** shows FA of the MFG-amygdala before and after therapy in the two groups. The repeated-measures ANOVA showed significant time × group [$F_{(1,51)} = 4.829$, $p = 0.033$] and time × hemisphere [$F_{(1,51)} = 27.524$, $p < 0.001$] interactions and significant main effects of

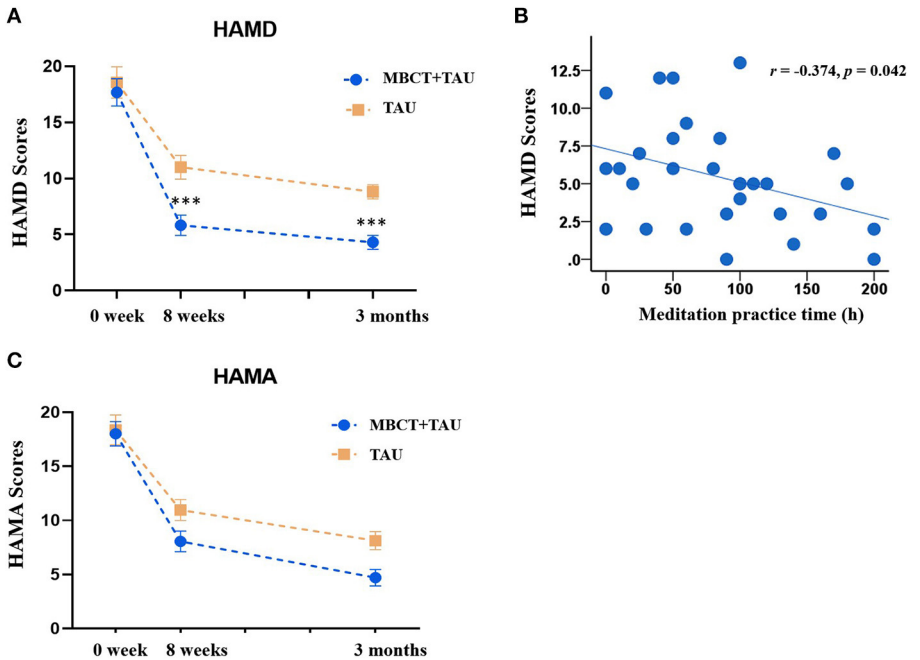

FIGURE 2 | Clinical measures from baseline to endpoints in the two groups. **(A)** Changes in HAMD scores in the MBCT+TAU group and TAU group. **(B)** Correlation between meditation practice time and HAMD scores. **(C)** Changes in HAMD scores in the MBCT+TAU group and TAU group. ***$p < 0.001$.

time [$F_{(1,51)} = 34.757$, $p < 0.001$] and hemisphere [$F_{(1,51)} = 5.800$, $p = 0.02$] but no hemisphere × group [$F_{(1,51)} = 0.029$, $p = 0.866$] or time × hemisphere region × group [$F_{(1,51)} = 0.335$, $p = 0.565$] interaction and no main effect of group [$F_{(1,54)} = 6.30$, $p = 0.015$]. Considering the significant time × group interaction, we performed a simple-effect analysis. The results showed that FA of the MFG-amygdala in the MBCT+TAU group increased more than in the TAU group after 8 weeks of treatment, especially in the right hemisphere. All the results were corrected using FDR.

DISCUSSION

The present study investigated MBCT as an adjunctive treatment to TAU to reduce depression symptoms in patients with LLD and its underlying neuroimaging mechanisms. We found that 8 weeks of adjunctive MBCT with TAU resulted in superior improvement in depressive symptoms in patients with LLD. We also found that MBCT increased functional and structural connectivity between the right MFG and right amygdala, and the increase in brain connectivity positively correlated with improvements in clinical symptoms.

Depressive symptoms significantly decreased after 8 weeks of MBCT, which is consistent with previous studies (35–38). A previous study reported that patients who received MBCT experienced the significant relief of depressive symptoms, whereas the TAU group did not exhibit a significant reduction of depressive symptoms (36). An 8-week course of MBCT was more effective than sertraline monotherapy in patients with acute depression (37). Patients with LDD often experience a greater rate of anxiety symptoms, which hampers recovery (35, 39). Our findings indicated that MBCT alleviated both anxiety and depressive symptoms, achieving better outcomes than drug monotherapy. At the 3-month follow-up, a persistent decrease in depressive symptoms was observed, and HAMD scores were significantly lower in the MBCT+TAU group compared with the TAU group. These results indicate that MBCT maintained a long-term therapeutic effect in elderly individuals with LLD. We also found a positive correlation between the duration of mindfulness practice and mental health at the 3-month follow-up, which was consistent with a previous study (40). Therefore, MBCT appears to be a viable treatment option for aging patients with depression, especially individuals who suffer from undesirable side effects that are caused by pharmacotherapy.

To clarify the mechanism of MBCT, we explored changes in brain communication that were induced by MBCT using fMRI. Changes in functional connectivity of the right MFG-right amygdala in the MBCT+TAU group and improvements in HAMD scores and HAMA scores were significantly positively correlated. These results were partially consistent with previous studies that investigated neuro-mechanisms in depression patients, which also found abnormalities in connectivity in the amygdala, frontal region, insula, and hippocampus (41, 42). The amygdala is considered to be involved in affective modulation (43, 44) and has been implicated in LLD pathophysiology (45). A previous study found that responses of the amygdala were

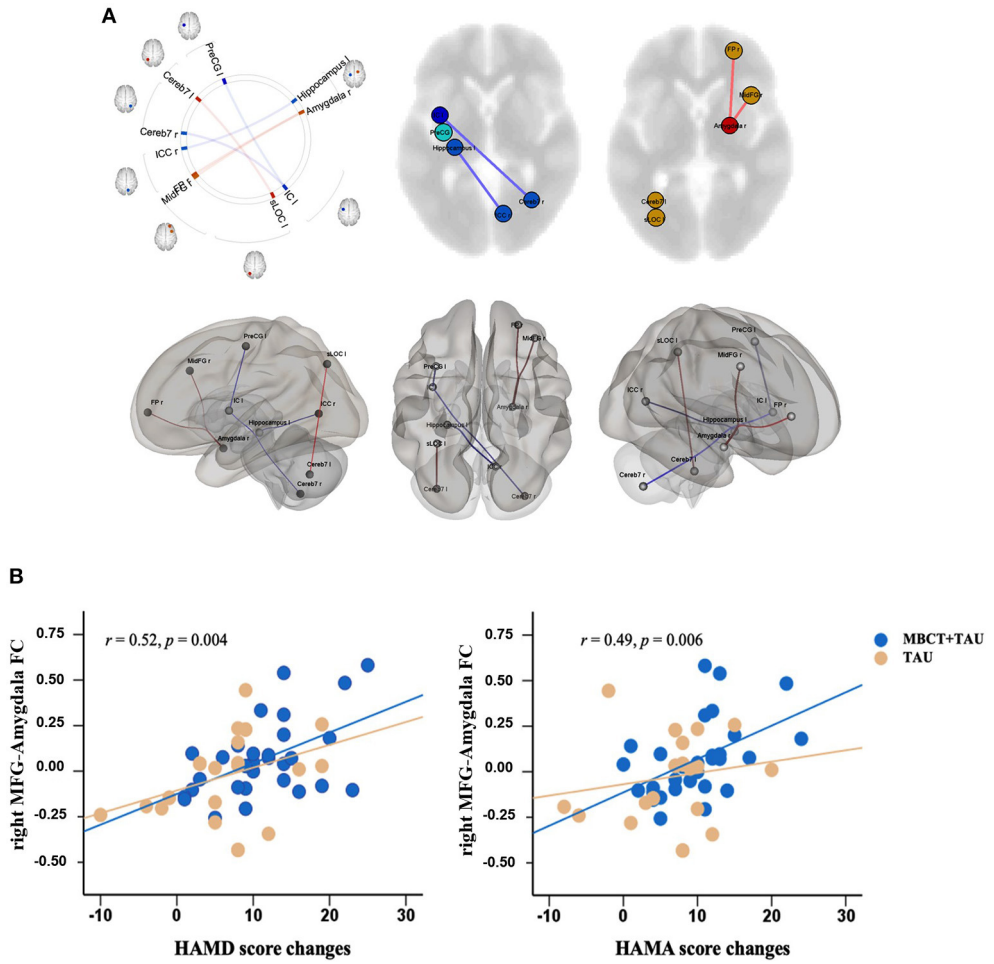

FIGURE 3 | Differences in changes in resting-state functional connectivity and correlations. **(A)** Difference in changes in resting-state functional connectivity in the two groups. **(B)** Correlation between resting-state functional connectivity and clinical measures.

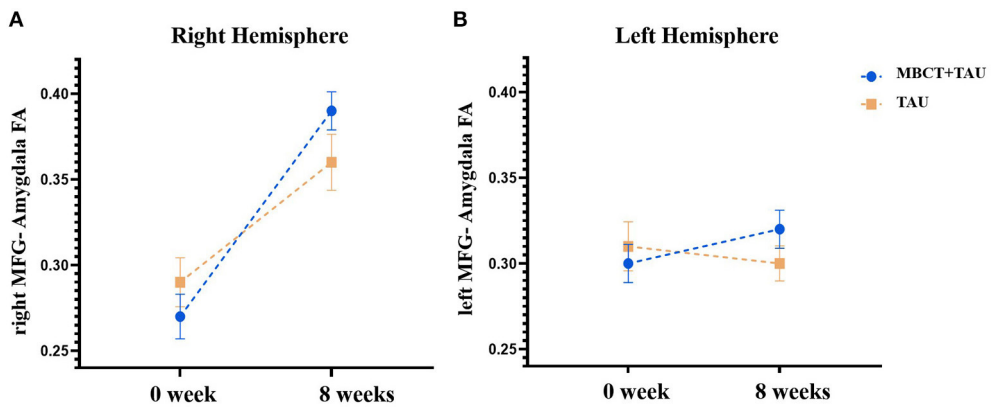

FIGURE 4 | Fractional anisotropy of the MFG-amygdala before and after therapy in the two groups. **(A)** Fractional anisotropy of the right MFG-amygdala before and after therapy in the two groups. **(B)** Fractional anisotropy of the left MFG-amygdala before and after therapy in the two groups.

modulated by subjective experience and may reflect variations in the ability to regulate mood (46). In the present study, the increase in functional and structural connectivity between the right MFG and right amygdala could reflect or underlie alterations of the involvement of brain areas in conscious and cognitively controlled emotion processing in LLD patients after MBCT. Furthermore, functional and microstructural changes in the MFG have been shown to play a crucial role in depression (47–49). The increase in FA of the MFG correlated with a decrease in depressive symptoms (50). Our results were similar to a recent study (51) that found that patients with anxious depression exhibited lower functional connectivity between the right centromedial/laterobasal amygdala and right MFG relative to patients with non-anxious depression (51). Other studies showed that improvements in mood positively correlated with an increase in amygdala-MFG connectivity strength (52). These results indicate that MBCT may strengthen brain communication between the right MFG and right amygdala and further alleviate both anxiety and depression symptoms in LLD patients.

During 8 weeks of MBCT, meditation appeared to play an important role in improving symptoms. The time of voluntary mindfulness practice significantly negatively correlated with the severity of depressive symptoms. A previous study showed that meditation altered brain structure and neuronal plasticity (53). Cortical thickness and the activity of several specific brain regions increased during meditation, such as the hippocampus, whereas a decrease in activity was found in the amygdala (54–57). Stronger functional connectivity was found between the posterior cingulate, dorsal anterior cingulate, and prefrontal cortices was observed in experienced meditators (58, 59). Future studies are needed to explore changes in brain function and structure in patients with LLD during meditation.

Limitations of the present study should be noted. The most obvious limitation was the relatively small sample size, which may have influenced statistical power. Additionally, although we attempted to control for antidepressant use, the inclusion of patients who used medication may have confounded our findings. Furthermore, the absence of a health education control to evaluate the placebo effect of MBCT was also a limitation. Large-sample, intervention-controlled, randomized trials should be conducted to investigate the effects and underlying neural mechanisms of MBCT in patients with LDD.

CONCLUSION

In conclusion, the present study provided efficacy outcomes of adjunctive MBCT with antidepressants in LLD patients. Our data indicate that changes in right MFG-amygdala connectivity were related to improvements in clinical symptoms of LLD after MBCT.

DATA AVAILABILITY STATEMENT

The original contributions presented in the study are included in the article/supplementary material, further inquiries can be directed to the corresponding authors.

ETHICS STATEMENT

The studies involving human participants were reviewed and approved by Ethics Committee of Peking University Sixth Hospital. The patients/participants provided their written informed consent to participate in this study.

AUTHOR CONTRIBUTIONS

HL, XS, LLu, JD, and WY contributed to the study design. HL, XZ, WS, JD, SS, and MS performed the search and collected the data. HL, LLi, XL, and YB performed the statistical analysis. QW, LLiu, JD, and WY drafted the manuscript. All authors reviewed the results and approved the final version of the paper.

FUNDING

This work was supported in part by the National Natural Science Foundation of China (nos. 82171524, 31800897, 82171477, 81821092, and 81761128036), National Key Research and Development Program of China (no. 2019YFA0706200), Capital Characteristic Project (no. Z161100000516129), and Postdoctoral Fellowship of Peking-Tsinghua Center for Life Sciences (LLiu).

ACKNOWLEDGMENTS

The authors thank all of the study participants for their willingness to participate in the study. We also thank all members of the study team for their efforts.

REFERENCES

1. Kessler RC, Aguilar-Gaxiola S, Alonso J, Chatterji S, Lee S, Ormel J, et al. The global burden of mental disorders: an update from the WHO World Mental Health (WMH) surveys. *Epidemiol Psichiatr Soc.* (2009) 18:23. doi: 10.1017/s1121189x00001421
2. Alexopoulos GS. Depression in the elderly. *Lancet.* (2005) 365:1961–70. doi: 10.1016/s0140-6736(05)66665-2
3. Han LKM, Aghajani M, Clark SL, Chan RF, Hattab MW, Shabalin AA, et al. Epigenetic aging in major depressive disorder. *Am J Psychiatry.* (2018) 175:774–82. doi: 10.1176/appi.ajp.2018.17060595
4. WHO. *World Health Organization Depression Fact Sheet No. 369*. World Health Organization (2012).
5. Nyer M, Doorley J, Durham K, Yeung AS, Freeman MP, Mischoulon D. What is the role of alternative treatments in late-life depression? *Psychiatr Clin North Am.* (2013) 36:577–96. doi: 10.1016/j.psc.2013.08.012
6. Bottino CM, Barcelos-Ferreira R, Ribeiz SR. Treatment of depression in older adults. *Curr Psychiatry Rep.* (2012) 14:289–97. doi: 10.1007/s11920-012-0281-z
7. DeRubeis RJ, Siegle GJ, Hollon SD. Cognitive therapy versus medication for depression: treatment outcomes and neural mechanisms. *Nat Rev Neurosci.* (2008) 9:788–96. doi: 10.1038/nrn2345

8. Segal ZV, Williams M, Teasdale J. *Mindfulness-Based Cognitive Therapy for Depression*. 2nd ed. New York, NY: Guilford Press (2012)
9. Mathew KL, Whitford HS, Kenny MA, Denson LA. The long-term effects of mindfulness-based cognitive therapy as a relapse prevention treatment for major depressive disorder. *Behav Cogn Psychother*. (2010) 561–76. doi: 10.1017/S135246581000010X
10. Kuyken W, Warren FC, Taylor RS, Whalley B, Crane C, Bondolfi G, et al. Efficacy of mindfulness-based cognitive therapy in prevention of depressive relapse: an individual patient data meta-analysis from randomized trials. *JAMA Psychiatry*. (2016) 73:565–74. doi: 10.1001/jamapsychiatry.2016.0076
11. Williams JMG, Kuyken W. Mindfulness-based cognitive therapy: a promising new approach to preventing depressive relapse. *Br J Psychiatry*. (2012) 200:359–60. doi: 10.1192/bjp.bp.111.104745
12. Teasdale JD, Segal ZV, Williams JM, Ridgeway VA, Soulsby JM, Lau MA. Prevention of relapse/recurrence in major depression by mindfulness-based cognitive therapy. *J Consult Clin Psychol*. (2000) 68:615–23. doi: 10.1037//0022-006x.68.4.615
13. Torres-Platas SG, Escobar S, Belliveau C, Wu J, Sasi N, Fotso J, et al. Mindfulness-based cognitive therapy intervention for the treatment of late-life depression and anxiety symptoms in primary care: a randomized controlled trial. *Psychother Psychosom*. (2019) 88:254–6. doi: 10.1159/000501214
14. Dikaios E, Escobar S, Nassim M, Su CL, Torres-Platas SG, Rej S. Continuation sessions of mindfulness-based cognitive therapy (MBCT-C) vs. treatment as usual in late-life depression and anxiety: an open-label extension study. *Int J Geriatr Psychiatry*. (2020) 35:1228–32. doi: 10.1002/gps.5360
15. Kaiser RH, Andrews-Hanna JR, Wager TD, Pizzagalli DA. Large-scale network dysfunction in major depressive disorder: a meta-analysis of resting-state functional connectivity. *JAMA Psychiatry*. (2015) 72:603–11. doi: 10.1001/jamapsychiatry.2015.0071
16. Williams LM. Precision psychiatry: a neural circuit taxonomy for depression and anxiety. *Lancet Psychiatry*. (2016) 3:472–80. doi: 10.1016/S2215-0366(15)00579-9
17. Schmaal L, Hibar D, Sämann PG, Hall G, Baune B, Jahanshad N, et al. Cortical abnormalities in adults and adolescents with major depression based on brain scans from 20 cohorts worldwide in the ENIGMA Major Depressive Disorder Working Group. *Mol Psychiatry*. (2017) 22:900–9. doi: 10.1038/mp.2016.60
18. Videbech P, Ravnkilde B. Hippocampal volume and depression: a meta-analysis of MRI studies. *Am J Psychiatry*. (2004) 161:1957–66. doi: 10.1176/appi.ajp.161.11.1957
19. Treadway MT, Waskom ML, Dillon DG, Holmes AJ, Park MTM, Chakravarty MM, et al. Illness progression, recent stress, and morphometry of hippocampal subfields and medial prefrontal cortex in major depression. *Biol Psychiatry*. (2015) 77:285–94. doi: 10.1016/j.biopsych.2014.06.018
20. Sheline YI, Gado MH, Kraemer HC. Untreated depression and hippocampal volume loss. *Am J Psychiatry*. (2003) 160:1516–8. doi: 10.1176/appi.ajp.160.8.1516
21. Serra-Blasco M, Portella MJ, Gomez-Anson B, de Diego-Adelino J, Vives-Gilabert Y, Puigdemont D, et al. Effects of illness duration and treatment resistance on grey matter abnormalities in major depression. *Br J Psychiatry*. (2013) 202:434–40. doi: 10.1192/bjp.bp.112.116228
22. Lacerda AL, Nicoletti MA, Brambilla P, Sassi RB, Mallinger AG, Frank E, et al. Anatomical MRI study of basal ganglia in major depressive disorder. *Psychiatry Res Neuroimaging*. (2003) 124:129–40. doi: 10.1016/S0925-4927(03)00123-9
23. Leaver AM, Yang H, Siddarth P, Vlasova RM, Krause B, St Cyr N, et al. Resilience and amygdala function in older healthy and depressed adults. *J Affect Disord*. (2018) 237:27–34. doi: 10.1016/j.jad.2018.04.109
24. Li H, Lin X, Liu L, Su S, Zhu X, Zheng Y, et al. Disruption of the structural and functional connectivity of the frontoparietal network underlies symptomatic anxiety in late-life depression. *Neuroimage Clin*. (2020) 28:102398. doi: 10.1016/j.nicl.2020.102398
25. Lifshitz M, Sacchet MD, Huntenburg JM, Thiery T, Fan Y, Gärtner M, et al. Mindfulness-based therapy regulates brain connectivity in major depression. *Psychother Psychosom*. (2019) 88:375–7. doi: 10.1159/000501170
26. Fox KC, Dixon ML, Nijeboer S, Girn M, Floman JL, Lifshitz M, et al. Functional neuroanatomy of meditation: a review and meta-analysis of 78 functional neuroimaging investigations. *Neurosci Biobehav Rev*. (2016) 65:208–28. doi: 10.1016/j.neubiorev.2016.03.021
27. Fox KC, Nijeboer S, Dixon ML, Floman JL, Ellamil M, Rumak SP, et al. Is meditation associated with altered brain structure? A systematic review and meta-analysis of morphometric neuroimaging in meditation practitioners. *Neurosci Biobehav Rev*. (2014) 43:48–73. doi: 10.1016/j.neubiorev.2014.03.016
28. Kral TRA, Schuyler BS, Mumford JA, Rosenkranz MA, Lutz A, Davidson RJ. Impact of short- and long-term mindfulness meditation training on amygdala reactivity to emotional stimuli. *Neuroimage*. (2018) 181:301–13. doi: 10.1016/j.neuroimage.2018.07.013
29. Zhang A, Leow A, Ajilore O, Lamar M, Yang S, Joseph J, et al. Quantitative tract-specific measures of uncinate and cingulum in major depression using diffusion tensor imaging. *Neuropsychopharmacology*. (2012) 37:959–67. doi: 10.1038/npp.2011.279
30. Cullen KR, Klimes-Dougan B, Muetzel R, Mueller BA, Camchong J, Houri A, et al. Altered white matter microstructure in adolescents with major depression: a preliminary study. *J Am Acad Child Adolesc Psychiatry*. (2010) 49:173–83.e1. doi: 10.1097/00004583-201002000-00011
31. Ma X, Liu J, Liu T, Ma L, Wang W, Shi S, et al. Altered resting-state functional activity in medication-naive patients with first-episode major depression disorder vs. healthy control: a quantitative meta-analysis. *Front Behav Neurosci*. (2019) 13:89. doi: 10.3389/fnbeh.2019.00089
32. Peters AT, Burkhouse K, Feldhaus CC, Langenecker SA, Jacobs RH. Aberrant resting-state functional connectivity in limbic and cognitive control networks relates to depressive rumination and mindfulness: a pilot study among adolescents with a history of depression. *J Affect Disord*. (2016) 200:178–81. doi: 10.1016/j.jad.2016.03.059
33. Lin X, Li W, Dong G, Wang Q, Sun H, Shi J, et al. Characteristics of multimodal brain connectomics in patients with schizophrenia and the unaffected first-degree relatives. *Front Cell Dev Biol*. (2021) 9:631864. doi: 10.3389/fcell.2021.631864
34. Lin X, Deng J, Dong G, Li S, Wu P, Sun H, et al. Effects of chronic pharmacological treatment on functional brain network connectivity in patients with schizophrenia. *Psychiatry Res*. (2021) 295:113338. doi: 10.1016/j.psychres.2020.113338
35. Foulk MA, Ingersoll-Dayton B, Kavanagh J, Robinson E, Kales HC. Mindfulness-based cognitive therapy with older adults: an exploratory study. *J Gerontol Soc Work*. (2014) 57:498–520. doi: 10.1080/01634372.2013.869787
36. Barnhofer T, Crane C, Hargus E, Amarasinghe M, Winder R, Williams JM. Mindfulness-based cognitive therapy as a treatment for chronic depression: A preliminary study. *Behav Res Ther*. (2009) 47:366–73. doi: 10.1016/j.brat.2009.01.019
37. Eisendrath SJ, Gillung E, Delucchi K, Mathalon DH, Yang TT, Satre DD, et al. A preliminary study: efficacy of mindfulness-based cognitive therapy versus sertraline as first-line treatments for major depressive disorder. *Mindfulness*. (2015) 6:475–82. doi: 10.1007/s12671-014-0280-8
38. Eisendrath SJ, Gillung E, Delucchi KL, Segal ZV, Nelson JC, McInnes LA, et al. A randomized controlled trial of mindfulness-based cognitive therapy for treatment-resistant depression. *Psychother Psychosom*. (2016) 85:99–110. doi: 10.1159/000442260
39. Fiske A, Wetherell JL, Gatz M. Depression in older adults. *Annu Rev Clin Psychol*. (2009) 5:363–89. doi: 10.1146/annurev.clinpsy.032408.153621
40. Chiesa A, Castagner V, Andrisano C, Serretti A, Mandelli L, Porcelli S, et al. Mindfulness-based cognitive therapy vs. psycho-education for patients with major depression who did not achieve remission following antidepressant treatment. *Psychiatry Res*. (2015) 226:474–83. doi: 10.1016/j.psychres.2015.02.003
41. Pannekoek JN, Van Der Werff S, Meens PH, van den Bulk BG, Jolles DD, Veer IM, et al. Aberrant resting-state functional connectivity in limbic and salience networks in treatment-naive clinically depressed adolescents. *J Child Psychol Psychiatry*. (2014) 55:1317–27. doi: 10.1111/jcpp.12266
42. Luking KR, Repovs G, Belden AC, Gaffrey MS, Botteron KN, Luby JL, et al. Functional connectivity of the amygdala in early-childhood-onset depression. *J Am Acad Child Adolesc Psychiatry*. (2011) 50:1027–41. e3. doi: 10.1016/j.jaac.2011.07.019
43. Gallagher M, Chiba AA. The amygdala and emotion. *Curr Opin Neurobiol*. (1996) 6:221–7. doi: 10.1016/s0959-4388(96)80076-6

44. Murray EA. The amygdala, reward and emotion. *Trends Cogn Sci.* (2007) 11:489–97. doi: 10.1016/j.tics.2007.08.013
45. Burke J, McQuoid DR, Payne ME, Steffens DC, Krishnan RR, Taylor WD. Amygdala volume in late-life depression: relationship with age of onset. *Am J Geriatr Psychiatry.* (2011) 19:771–6. doi: 10.1097/JGP.0b013e318211069a
46. Dyck M, Loughead J, Kellermann T, Boers F, Gur RC, Mathiak K. Cognitive versus automatic mechanisms of mood induction differentially activate left and right amygdala. *Neuroimage.* (2011) 54:2503–13. doi: 10.1016/j.neuroimage.2010.10.013
47. Yang Q, Huang X, Hong N, Yu X. White matter microstructural abnormalities in late-life depression. *Int Psychogeriatr.* (2007) 19:757–66. doi: 10.1017/S1041610207004875
48. Taylor WD, MacFall JR, Payne ME, McQuoid DR, Provenzale JM, Steffens DC, et al. Late-life depression and microstructural abnormalities in dorsolateral prefrontal cortex white matter. *Am J Psychiatry.* (2004) 161:1293–6. doi: 10.1176/appi.ajp.161.7.1293
49. Dutta A, McKie S, Deakin JF. Resting state networks in major depressive disorder. *Psychiatry Res.* (2014) 224:139–51. doi: 10.1016/j.pscychresns.2014.10.003
50. Peng H, Zheng H, Li L, Liu J, Zhang Y, Shan B, et al. High-frequency rTMS treatment increases white matter FA in the left middle frontal gyrus in young patients with treatment-resistant depression. *J Affect Disord.* (2012) 136:249–57. doi: 10.1016/j.jad.2011.12.006
51. Qiao J, Tao S, Wang X, Shi J, Chen Y, Tian S, et al. Brain functional abnormalities in the amygdala subregions is associated with anxious depression. *J Affect Disord.* (2020) 276:653–9. doi: 10.1016/j.jad.2020.06.077
52. Bershad AK, Preller KH, Lee R, Keedy S, Wren-Jarvis J, Bremmer MP, et al. Preliminary report on the effects of a low dose of LSD on resting-state amygdala functional connectivity. *Biol Psychiatry Cogn Neurosci Neuroimaging.* (2020) 5:461–7. doi: 10.1016/j.bpsc.2019.12.007
53. Afonso RF, Kraft I, Aratanha MA, Kozasa EH. Neural correlates of meditation: a review of structural and functional MRI studies. *Front Biosci.* (2020) 12:92–115. doi: 10.2741/s542
54. Luders E, Thompson PM, Kurth F, Hong JY, Phillips OR, Wang Y, et al. Global and regional alterations of hippocampal anatomy in long-term meditation practitioners. *Hum Brain Mapp.* (2013) 34:3369–75. doi: 10.1002/hbm.22153
55. Lazar SW, Bush G, Gollub RL, Fricchione GL, Khalsa G, Benson H. Functional brain mapping of the relaxation response and meditation. *Neuroreport.* (2000) 11:1581–5. doi: 10.1097/00001756-200005150-00041
56. Davanger S, Ellingsen O, Holen A, Hugdahl K. Meditation-specific prefrontal cortical activation during acem meditation: an fMRI study. *Percept Mot Skills.* (2010) 111:291–306. doi: 10.2466/02.04.22.PMS.111.4.291-306
57. Doll A, Holzel BK, Mulej Bratec S, Boucard CC, Xie X, Wohlschlager AM, et al. Mindful attention to breath regulates emotions via increased amygdala-prefrontal cortex connectivity. *Neuroimage.* (2016) 134:305–13. doi: 10.1016/j.neuroimage.2016.03.041
58. Brewer JA, Worhunsky PD, Gray JR, Tang YY, Weber J, Kober H. Meditation experience is associated with differences in default mode network activity and connectivity. *Proc Natl Acad Sci USA.* (2011) 108:20254–9. doi: 10.1073/pnas.1112029108
59. Berkovich-Ohana A, Harel M, Hahamy A, Arieli A, Malach R. Alterations in task-induced activity and resting-state fluctuations in visual and DMN areas revealed in long-term meditators. *Neuroimage.* (2016) 135:125–34. doi: 10.1016/j.neuroimage.2016.04.024

Conflict of Interest: The authors declare that the research was conducted in the absence of any commercial or financial relationships that could be construed as a potential conflict of interest.

frontiers in Psychiatry

ORIGINAL RESEARCH
published: 15 March 2022
doi: 10.3389/fpsyt.2022.859453

Improved Interhemispheric Functional Connectivity in Postpartum Depression Disorder: Associations With Individual Target-Transcranial Magnetic Stimulation Treatment Effects

Yao Zhang[1†], *Yunfeng Mu*[2†], *Xiang Li*[3,4,5,6], *Chuanzhu Sun*[4,5], *Xiaowei Ma*[7], *Sanzhong Li*[8], *Li Li*[9], *Zhaohui Zhang*[10,11*] *and Shun Qi*[3,12*]

[1] *Xijing Hospital, The Air Force Military Medical University, Xi'an, China,* [2] *Department of Gynecological Oncology, Shaanxi Provincial Cancer Hospital, Xi'an, China,* [3] *Research Center for Brain-Inspired Intelligence, Xi'an Jiaotong University, Xi'an, China,* [4] *The Key Laboratory of Biomedical Information Engineering of Ministry of Education, Institute of Health and Rehabilitation Science, School of Life Science and Technology, Xi'an Jiaotong University, Xi'an, China,* [5] *The Key Laboratory of Neuro-informatics & Rehabilitation Engineering of Ministry of Civil Affairs, Xi'an, China,* [6] *Xi'an Solide Brain Control Medical Technology Company, Xi'an, China,* [7] *Department of Nuclear Medicine, The Second Xiangya Hospital, Central South University, Changsha, China,* [8] *Department of Neurosurgery, Xijing Hospital, The Air Force Military Medical University, Xi'an, China,* [9] *Center of Treatment and Rehabilitation of Severe Neurological Disorders, Xi'an International Medical Center Hospital, Xi'an, China,* [10] *Henan Key Laboratory of Neurorestoratology, The First Affiliated Hospital of Xinxiang Medical University, Weihui, China,* [11] *Henan Engineering Research Center of Physical Diagnostics and Treatment Technology for the Mental and Neurological Diseases, The Second Affiliated Hospital of Xinxiang Medical University, Xinxiang, China,* [12] *Shaanxi Brain Modulation and Scientific Research Center, Xi'an, China*

Postpartum depression (PPD) is a depressive condition that is associated with a high risk of stressful life events, poor marital relationships, and even suicide. Neuroimaging techniques have enriched our understanding of cerebral mechanisms underlying PPD; namely, abnormalities in the amygdala-insula-frontal circuit might contribute to the pathogenesis of PPD. Stanford Accelerated Intelligent Neuromodulation Therapy (SAINT) is a recently validated neuroscience-informed accelerated intermittent theta-burst stimulation repetitive transcranial magnetic stimulation (rTMS) protocol. It has been shown to be effective, safe, tolerable, and rapid acting for treating treatment-resistant depression, and may be a valuable tool in the treatment of PPD. The purpose of the current study was to detect inter-hemispheric connectivity changes and their relationship with the clinical treatment effects of rTMS. Resting-state fMRI data from 32 patients with PPD treated with SAINT were collected and compared with findings from 32 age matched healthy controls. Voxel-mirrored homotopic connectivity (VMHC) was used to analyze the patterns of interhemispheric intrinsic functional connectivity in patients with PPD. Scores on the 17-item Hamilton Depression Rating Scale, Edinburgh Postnatal Depression Scale (EPDS) scores, and the relationships between these clinical characteristics and VMHC were the primary outcomes. Patients with PPD at baseline showed reduced VMHC in the amygdala, insula, and medial frontal gyrus compared with the HCs. These properties showed a renormalization after individualized rTMS treatment. Furthermore, increased

OPEN ACCESS

Edited by:
Karen M. von Deneen, Xidian University, China

Reviewed by:
Xueyu Wang, Shandong Provincial Hospital, China
Libo Liu, The Second Affiliated Hospital of Shandong First Medical University, China

***Correspondence:**
Zhaohui Zhang
zzhui816@126.com
Shun Qi
qishunjob@163.com

[†] *These authors have contributed equally to this work*

Specialty section:
This article was submitted to Neuroimaging and Stimulation, a section of the journal Frontiers in Psychiatry

Received: *21 January 2022*
Accepted: *14 February 2022*
Published: *15 March 2022*

Citation:
Zhang Y, Mu Y, Li X, Sun C, Ma X, Li S, Li L, Zhang Z and Qi S (2022) Improved Interhemispheric Functional Connectivity in Postpartum Depression Disorder: Associations With Individual Target-Transcranial Magnetic Stimulation Treatment Effects. Front. Psychiatry 13:859453. doi: 10.3389/fpsyt.2022.859453

connectivity between the left and right insula after SAINT was significantly correlated with the improvement of EPDS scores. Our results reveal the disruptions in the intrinsic functional architecture of interhemispheric communication in patients with PPD, and provide evidence for the pathophysiological mechanisms and the effects of rTMS.

Keywords: postpartum depression, repetitive transcranial magnetic stimulation, voxel-mirrored homotopic connectivity, treatment effects, fMRI

INTRODUCTION

Postpartum depression (PPD) is characterized by a series of symptoms, such as depression, agitation, and even suicide, and affects 13% of women who have just given birth (1). Psychotherapy, psychotropic medications, and electroconvulsive therapy are the primary and commonly used treatments for PPD (2, 3). Although the efficacy of these treatments has been documented, each has its limitations and shortcomings. For example, psychotherapy requires a long treatment duration and is costly (4). Women who are breastfeeding may be concerned that their infant will be exposed to psychotropic medications, and worried about the long-term developmental effects of this exposure (5). Electroconvulsive therapy is strongly recommended for the treatment of major depression, but is associated with acute adverse effects such as memory disorder and headaches (6). As such, there is an urgent need for new therapies for PPD that have minimal side effects and can be used over long durations. Repetitive transcranial magnetic stimulation (rTMS) is an effective FDA-approved treatment for major depression and is a promising treatment for PPD (7). The mechanism of rTMS in the treatment include activation of neurotransmitter systems, modulation of neural circuits and brain networks, and synaptic plasticity.

Previous studies using resting-state functional magnetic resonance imaging (fMRI) have found that patients with PPD show decreased activities in several brain regions, including the dorsolateral prefrontal cortex (DLPFC), anterior cingulate cortex, amygdala, and hippocampus, as well as attenuated cortico-cortical and cortico-limbic connectivity (8, 9). Functional network studies have also demonstrated that connectivity between the posterior cingulate cortex and right amygdala was disrupted in patients with PPD (10). Task-related fMRI studies have revealed reduced activity in the orbitofrontal cortex, dorsomedial prefrontal cortex, amygdala and striatum in patients with PPD (11). Furthermore, a diffusion tensor imaging (DTI) study found evidence of aberrant integrity of the corpus callosum, which connects the bilateral hemispheres (12). These results indicate that amygdala-insula-frontal circuit abnormality might contribute to the pathogenesis of PPD.

The DLPFC is the key TMS targeting area for treating major depressive disorder (13). Stanford Accelerated Intelligent Neuromodulation Therapy (SAINT) is an accelerated, fMRI-guided intermittent theta-burst stimulation (iTBS) protocol that has recently been shown to be effective, safe, tolerable, and rapid acting for treating treatment-resistant depression (7, 13). Whether this protocol also has promising treatment effects in patients with PPD has yet to be examined. In the current study, we applied SAINT in patients with PPD and used the voxel-mirrored homotopic connectivity (VMHC) method to investigate how SAINT influenced interhemispheric connectivity (14). We hypothesized that core regions within the amygdala-insula-frontal circuit would show normalized connectivity after SAINT protocol administration.

MATERIALS AND METHODS

Subjects

Patients with PPD were recruited from the First Affiliated Hospital of Xinxiang Medical University. All patients were diagnosed with major depression with a puerperal onset according to the DSM-IV diagnostic criteria. No participants were receiving any pharmacological treatment. Women were excluded from the study if they had a past or current diagnosis of bipolar disorder, post-traumatic stress disorder, or other psychosis. Age matched healthy controls (HCs) were recruited from the local community. Exclusion criteria for both groups were as follows: (1) history or presence of significant neurological or medical illnesses; (2) body mass index (BMI) $\geq$ 30; (3) history of alcohol, drug, or smoking abuse; (4) contraindications for 3T MRI, such as claustrophobia, metal implants, and pacemakers.

MRI Data Collection

A 3.0-T UNITED Discovery 770 MRI scanner was used for all MRI acquisitions. Participants were required to keep still and stay awake during the entire session. The resting-state functional images were obtained with the following parameters: field of view (FOV) = 224 × 224 mm, data matrix = 64 × 64, echo time (TE) = 30 ms, repetition time (TR) = 2,000 ms, slice thickness = 4 mm, flip angle = 90° and voxel size = 3.5 × 3.5 × 40 mm^3. For anatomical reference, a high-resolution T1-weighted image was also acquired with the following parameters: TR = 7.24 ms, TE = 3.10 ms, FOV = 256 × 256 mm, flip angle = 10°, slice thickness = 0.5 mm, and and voxel size = 0.5 × 0.5 × 1 mm^3. The same parameters were used for follow-up scans of the patients with PPD and healthy controls.

fMRI Data Preprocessing

The resting-state fMRI images were preprocessed using the Data Processing & Analysis for Brain imaging (DPABI, http://rfmri.org/dpabi) software. The first 10 images were removed for magnetization equilibrium, and the remaining 200 images were subjected to motion realignment and slice timing, during which the mean frame-wise displacement (FD) was calculated. Subjects with more than 2 mm of maximal translation or 2° of maximal rotation were excluded. Then, the Friston-24 model

was used to regress head motion effects and nuisance signals from cerebrospinal fluid white matter and head motions. Then, the fMRI data were normalized into the MNI space using the diffeomorphic anatomical registration through exponentiated lie algebra (DARTEL) method; the resulting images were finally smoothed with a Gaussian kernel of 6 mm full width at half-maximum and band-pass filtered (0.01–0.08 Hz). Before calculation of the VMHC, all preprocessed rs-fMRI data were transformed into the group-specific symmetric template; then, VMHC was computed as Pearson's correlation coefficient between each voxel's residual time series and that of the corresponding voxel in the opposite hemisphere. Subsequently, the correlation values were converted to z-values using Fisher's r-to-z transformation to enhance the normality of the values.

Treatment

Repetitive transcranial magnetic stimulation was delivered by a commercially available magnetic stimulator (Black Dolphin Navigation Robot). Individual L-DLPFC stimulation target was determined according to a previous study (13). First, a hierarchical agglomerative clustering algorithm was applied to divide the DLPFC and subgenual anterior cingulate cortex (sgACC) into numerous functional subunits, which were defined as voxel pairs to be correlated. For each functional subunit, a single time-series value was identified, which was defined as the time-series that was most strongly correlated with the median time series. Then, Spearman's correlation coefficients were used to calculate the correlation matrix. Finally, the optimal target in DLPFC was determined considering the anticorrelation, size, spatial concentration, and dispersion of subunits. Fifty intermittent theta-burst stimulation (iTBS) sessions (1,800 pulses per session, 50-min interval) were delivered in 10 daily sessions over 5 consecutive days at 90% resting motor threshold.

Statistical Analysis

Demographic characteristics were compared between patients with PPD and HCs using Student's *t*-tests in SPSS (IBM SPSS Statistics for Windows, version 18.0, IBM Corp.). Two-sample *t*-tests (HCs vs. patients with PPD at baseline; HCs vs. patients with PPD at follow-up) or paired *t*-tests (baseline vs. follow-up) were used to identify interhemispheric FC changes. The threshold for significance was $P < 0.05$, corrected with the FDR criterion. Age, and mean FD calculated during the preprocessing step were accounted for by including them as covariates. We extracted the mean VMHC values of the brain regions exhibiting significant differences (baseline vs. follow-up); then, Pearson's correlation coefficient was used to examine the associations between the changes in VMHC and clinical scores in SPSS. Significance was set at a threshold of $P < 0.05$, Bonferroni-corrected. Correction for multiple comparisons was accomplished using the FDR criterion with the "mafdr" script implemented in MATLAB.

RESULTS

Demographic Information

All participants (patients with PPD and healthy controls) were right-handed. There were no significant differences in age, body mass index, education levels and length of pregnancy between women with PPD and HCs. As expected, the patients with PPD exhibited significantly higher EPDS scores ($P < 0.001$) and HAMD scores ($P < 0.001$) than the HCs. After rTMS treatment, all scores showed a significant improvement ($P < 0.01$ for EPDS, $P < 0.01$ for HAMD). Detailed information is listed in **Table 1**. The head motion indicated by mean FD did not differ significantly between baseline and follow-up in patients with PPD ($p > 0.05$; mean FD $= 0.142 \pm 0.035$ for baseline, mean FD $= 0.135 \pm 0.029$ for follow-up), or between patients with PPD and HCs (all $p > 0.05$; mean FD $= 0.108 \pm 0.041$ for HCs).

TABLE 1 | Demographic and clinical characteristics of participants.

Characteristics	PPD (31)	HCs (31)	*p*
Age (years)	31.5 ± 3.4	31.7 ± 6.3	0.91
Education (years)	13.7 ± 2.5	14.1 ± 2.9	0.65
BMI	24.3 ± 4.5	23.9 ± 4.2	0.55
Length of pregnancy(days)	281.2 ± 17.3	280.4 ± 16.9	0.76
EPDS	16.7 ± 4.6	4.75 ± 2.2	<0.01
HAMD	32.6 ± 5.2	8.64 ± 3.8	<0.01
Characteristics	**PI at baseline**	**PI at follow-up**	
EPDS	16.7 ± 4.6	7.88 ± 2.4	<0.01
HAMD	32.6 ± 5.2	12.1 ± 4.5	<0.01

PPD, Postpartum depression; HCs, healthy controls; BMI, body mass index; EPDS, Edinburgh Postnatal Depression Scale; HAMD, 24-Item Hamilton Depression Scale.

VMHC Differences Between Groups

Significant VMHC differences were found between patients with PPD and healthy controls at baseline, whereby patients with PPD showed reduced VMHC in the bilateral insula, bilateral amygdala, bilateral medial frontal gyrus, bilateral putamen, bilateral pallidum, bilateral anterior cingulate cortex, and bilateral middle cingulate cortex. After rTMS treatment, compared with baseline values, patients with PPD at follow-up showed increased VMHC in these regions, in addition, bilateral middle temporal gyrus. No significant differences were found between patients with PPD at follow-up and healthy controls. The detailed results are shown in **Figures 1**, **2** and **Table 2**.

To clearly demonstrate the dynamic changes in VMHC values after TMS treatment, the VMHC values within those brain regions were extracted across the three groups, as shown in **Figure 3**. A renormalization of VMHC changes was found in patients with PPD after TMS treatment.

Correlation Results

The changes of VMHC values after TMS treatment (baseline–follow-up) were extracted, and correlations with the clinical features in patients with PPD were assessed. A significant negative correlation was found between EPDS score changes and VMHC value changes in the left and right insula ($r = -0.47$, $P < 0.001$). The correlation results are shown in **Figure 4**. No significant correlations were found for HAMD and VMHC metrics.

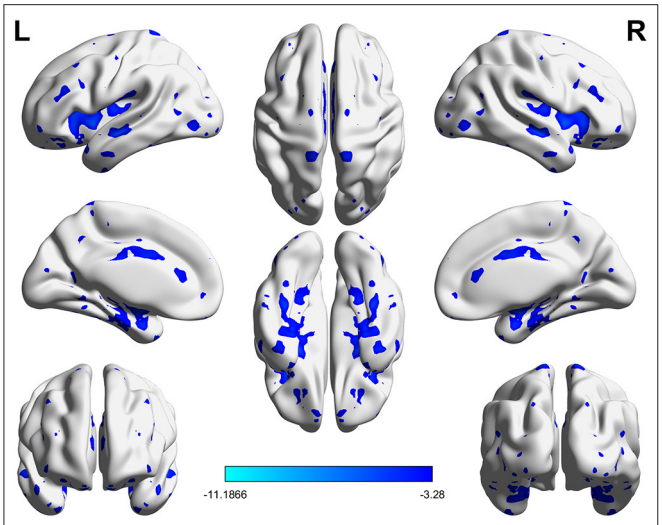

FIGURE 1 | Significant differences of VMHC between PPD patients at baseline and HCs ($P < 0.05$, FDR corrected).

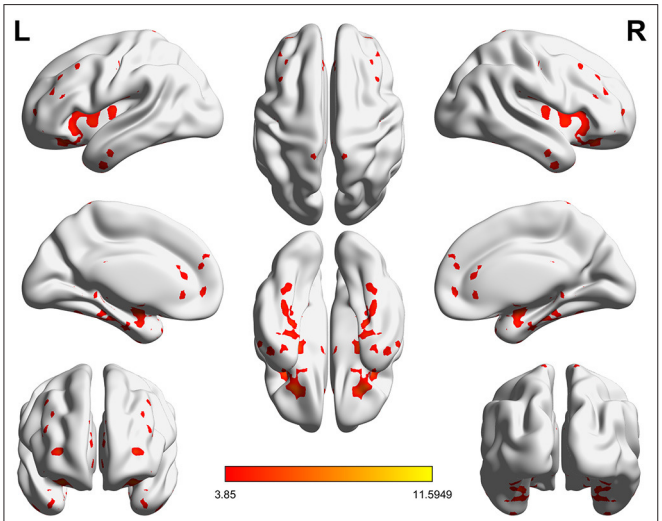

FIGURE 2 | Significant differences of VMHC between PPD patients at baseline and PPD patients at follow-up ($P < 0.05$, FDR corrected).

TABLE 2 | Significantly altered VMHC across the three groups.

	voxels	Peak Coordinates (MNI)			*t*-value
		x	*y*	*z*	
Baseline < HC Right insula	202	42	9	0	−11.19
Left insula	202	−42	9	0	−11.19
Right amygdala	39	27	−3	−12	−7.84
Left amygdala	39	−27	−3	−12	−7.84
Right medial frontal cortex	32	24	36	−12	−4.95
Left medial frontal cortex	32	−24	36	−12	−4.95
Right putamen	152	21	21	3	−5.99
Left putamen	152	−21	21	3	−5.99
Right pallidum	40	24	−3	6	−6.01
Left pallidum	40	−24	−3	6	−6.01
Right anterior cingulate cortex	39	9	33	15	−4.39
Left anterior cingulate cortex	39	−9	33	15	−4.39
Right middle cingulate cortex	60	3	9	30	−5.21
Left middle cingulate cortex	60	−3	9	30	−5.21
Follow-up > Baseline					
Right insula	186	42	9	0	10.59
Left insula	186	−42	9	0	10.59
Right amygdala	30	27	−3	−12	7.15
Left amygdala	30	−27	−3	−12	7.15
Right medial frontal cortex	43	18	48	6	3.72
Left medial frontal cortex	43	−18	48	6	3.72
Right putamen	134	21	21	3	5.46
Left putamen	134	−21	21	3	5.46
Right pallidum	23	24	−6	6	4.95
Left pallidum	23	−24	−6	6	4.95
Right middle temporal gyrus	25	60	−6	−24	3.65
Left middle temporal gyrus	25	−60	−6	−24	3.65

DISCUSSION

In the current study, we found that SAINT applied to patients with PPD significantly reduced depressive symptoms. Increased inter-hemispheric connectivity was found in the amygdala-insula-frontal circuit after SAINT administration. Furthermore, the increased connectivity between the left and right insula after SAINT was significantly correlated with the improvement of the Edinburgh Postnatal Depression Scale score. Our study is the first to demonstrate that SAINT could be a promising TMS protocol for treating patients with PPD.

Multiple fMRI studies have improved our understanding of the neural mechanisms of patients with PPD. Task-related fMRI studies have indicated that during exposure to emotional stimuli, patients with PPD have increased activity in the amygdala (15) and reduced activity in the middle frontal gyrus (MFG) and inferior frontal gyrus (IFG). Resting-state fMRI studies have reported significant disruption of the posterior cingulate cortex (PCC)–right amygdala functional coupling in patients with PPD (16). Another resting-state study using regional homogeneity (ReHo) analysis found that PPD is characterized by decreased ReHo in the left DLPFC, right insular right ventral temporal cortex, amygdala, and hippocampus (17). The MFC, IFC, and PCC constitute the so-called default mode network (DMN), which is active at rest and involved in monitoring the external and internal environment (18); the right insula is a core region of the salience network (SN), which is crucial for detecting salient external stimuli and internal mental events (19). Consistent with previous studies, our findings suggest that disrupted activity within the amygdala, DMN, and SN is important for the pathophysiology of PPD.

Owing to the potential impact of medication side effects on their newborn infant or the perceived risk of breastfeeding while on medication, many mothers do not consider using psychotropic medication to treat their PPD. Compared with other depression therapies, repetitive TMS is unique in that

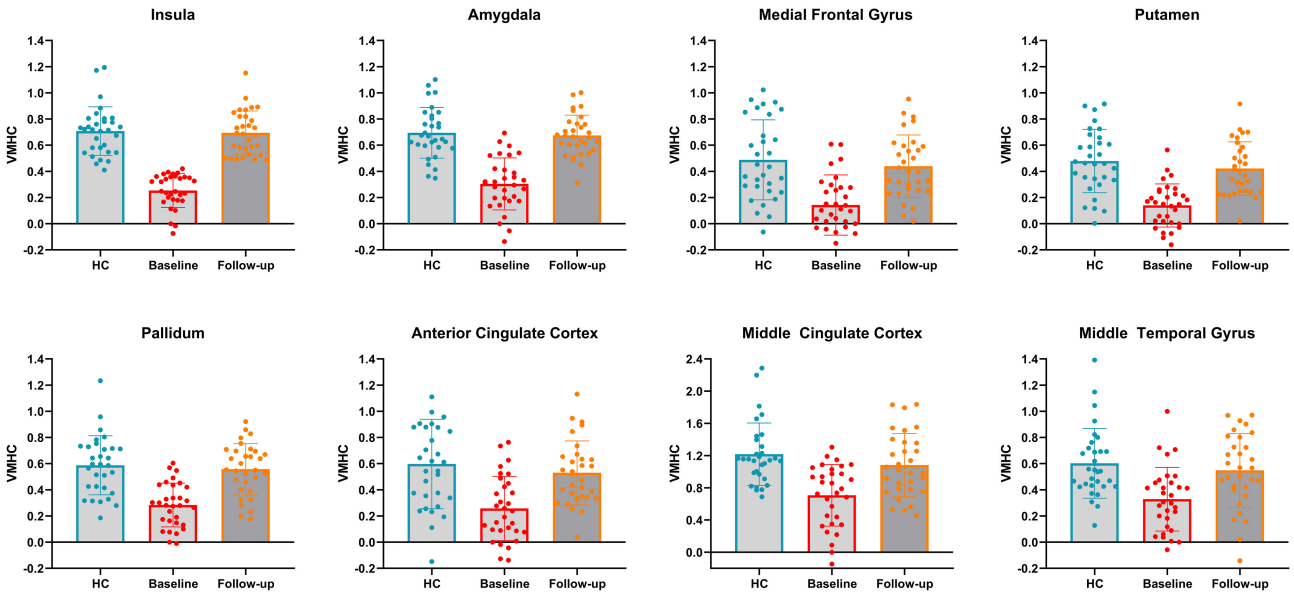

FIGURE 3 | VMHC values in bilateral insula, bilateral amygdala, bilateral medial frontal gyrus, bilateral putamen, bilateral pallidum, bilateral anterior cingulate cortex, bilateral middle cingulate cortex and bilateral middle temporal gyrus across the three groups. HC, healthy controls.

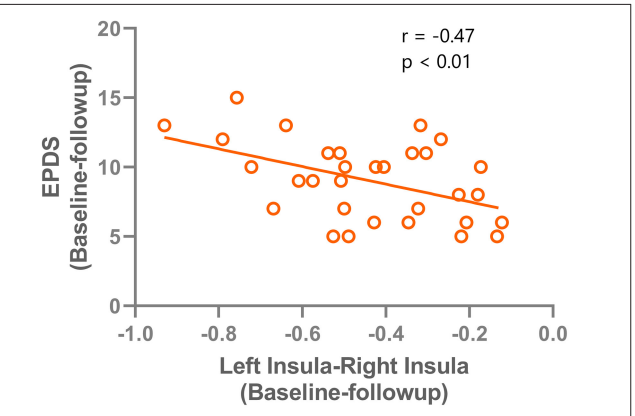

FIGURE 4 | correlation results between the VMHC change (left insula - right insula) and the Edinburgh Postnatal Depression Scale improvements after rTMS treatment.

it has no systemic side effects that would interfere with child care. Previous studies have indicated that the improvement of EPDS scores were higher in the rTMS group than the control group. As reported in previous studies, standard rTMS protocols provide marginal effects in improving the depressive mood and cognitive function of patients with PPD compared with the control group (20, 21). SAINT, however, has several advantages in improving treatment effects, such as individual DLPFC targeting, long intersession intervals to produce cumulative effects on synaptic strengthening, individualized resting motor threshold, and the use of 1,800 pulses rather than the typical 600 pulses per iTBS session.

After SAINT, increased interhemispheric connectivity was found in the amygdala, insula, and frontal gyrus, which suggests that SAINT exerts its effects by increasing interhemispheric communication. Interestingly, we found that the increased connectivity between the left and right insula was correlated with the improvement of depressive symptoms (indicated by a reduced Edinburgh Postnatal Depression Scale score). These findings are consistent with those of previous studies that have highlighted the importance of the salience network in the pathogenesis of depressive disorders. The salience network (SN) is involved in monitoring salient events and processing emotions (19). The deficient role of the insula might disrupt the cross-network interactions between the SN network, DMN, and limbic network, and SAINT might normalize these interactions to improve the clinical manifestations.

This study has several limitations that should be noted. First, this study had a small sample size. In the future, a larger sample size is needed to enhance the generalizability of the present findings. Second, we only explored interhemispheric functional connectivity and did not consider brain structural connectivity, other statis, or dynamic functional connectivity; examining these factors in future work will provide more important information. Third, not all PPD patients showed great improvement after SAINT administration, the underlying mechanism should be further studied in the future.

DATA AVAILABILITY STATEMENT

The raw data supporting the conclusions of this article will be made available by the authors, without undue reservation.

ETHICS STATEMENT

Written informed consent was obtained from the individual(s) for the publication of any potentially identifiable images or data included in this article.

AUTHOR CONTRIBUTIONS

YZ, YM, and XM performed all data analysis and wrote the manuscript. SQ and ZZ raised the conception of the study. XL and CS contributed to the collection of MRI data. SL and LL contributed to the manuscript revision. All authors have read and approved the submitted version.

FUNDING

This study was supported by the Natural Science Basic Research Program of Shaanxi (2020JQ-954).

ACKNOWLEDGMENTS

We thank Nia Cason, Ph.D., from Liwen Bianji (Edanz) (www.liwenbianji.cn/), for editing the English text of a draft of this manuscript.

REFERENCES

1. Deligiannidis KM, Fales CL, Kroll-Desrosiers AR, Shaffer SA, Villamarin V, Tan Y, et al. Resting-state functional connectivity, cortical GABA, and neuroactive steroids in peripartum and peripartum depressed women: a functional magnetic resonance imaging and spectroscopy study. *Neuropsychopharmacology*. (2019) 44:546–54. doi: 10.1038/s41386-018-0242-2
2. Rundgren S, Brus O, Båve U, Landén M, Lundberg J, Nordanskog P, et al. Improvement of postpartum depression and psychosis after electroconvulsive therapy: a population-based study with a matched comparison group. *J Affect Disord.* (2018) 235:258–64. doi: 10.1016/j.jad.2018.04.043
3. Yator O, John-Stewart G, Khasakhala L, Kumar M. Preliminary effectiveness of group interpersonal psychotherapy for young kenyan mothers with HIV and depression: a pilot trial. *Am J Psychother*. (2021) 20200050. doi: 10.1176/appi.psychotherapy.20200050
4. Mohr DC, Lattie EG, Tomasino KN, Kwasny MJ, Kaiser SM, Gray EL, et al. A randomized noninferiority trial evaluating remotely-delivered stepped care for depression using internet cognitive behavioral therapy (CBT) and telephone CBT. *Behav Res Ther.* (2019) 123:103485. doi: 10.1016/j.brat.2019.103485
5. Ward HB, Fromson JA, Cooper JJ, De Oliveira G, Almeida M. Recommendations for the use of ECT in pregnancy: literature review and proposed clinical protocol. *Arch Women's Mental Health.* (2018) 21:715–22. doi: 10.1007/s00737-018-0851-0
6. Di Iorio R, Rossi S, Rossini PM. One century of healing currents into the brain from the scalp: From electroconvulsive therapy to repetitive transcranial magnetic stimulation for neuropsychiatric disorders. *Clinical Neurophysiol.* (2022) 133:145–51. doi: 10.1016/j.clinph.2021.10.014
7. Cole EJ, Stimpson KH, Bentzley BS, Gulser M, Cherian K, Tischler C, et al. Stanford accelerated intelligent neuromodulation therapy for treatment-resistant depression. *Am J Psychiatry*. (2020) 177:716–26. doi: 10.1176/appi.ajp.2019.19070720
8. Stickel S, Wagels L, Wudarczyk O, Jaffee S, Habel U, Schneider F, et al. Neural correlates of depression in women across the reproductive lifespan–an fMRI review. *J Affect Disord.* (2019) 246:556–70. doi: 10.1016/j.jad.2018.12.133
9. Mao N, Che K, Xie H, Li Y, Wang Q, Liu M, et al. Abnormal information flow in postpartum depression: A resting-state functional magnetic resonance imaging study. *J Affect Disord.* (2020) 277:596–602. doi: 10.1016/j.jad.2020.08.060
10. Zhang S, Wang W, Wang G, Li B, Chai L, Guo J, et al. Aberrant resting-state interhemispheric functional connectivity in patients with postpartum depression. *Behav Brain Res.* (2020) 382:112483. doi: 10.1016/j.bbr.2020.112483
11. Ntow KO, Krzeczkowski JE, Amani B, Savoy CD, Schmidt LA, Van Lieshout RJ. Maternal and infant performance on the face-to-face still-face task following maternal cognitive behavioral therapy for postpartum depression. *J Affect Disord.* (2021) 278:583–91. doi: 10.1016/j.jad.2020.09.101
12. Sasaki Y, Ito K, Fukumoto K, Kawamura H, Oyama R, Sasaki M, et al. Cerebral diffusion kurtosis imaging to assess the pathophysiology of postpartum depression. *Sci Rep.* (2020) 10:1–9. doi: 10.1038/s41598-020-72310-1
13. Cole, E.J., Phillips, A.L., Bentzley, B.S., Stimpson, K.H., Nejad, R., Barmak, F., et al. (2021). Stanford Neuromodulation Therapy (SNT): a double-blind randomized controlled trial. *Am J Psychiatry*. 179:132–41. doi: 10.1176/appi.ajp.2021.20101429
14. Zhu Y, Feng Z, Xu J, Fu C, Sun J, Yang X, et al. Increased interhemispheric resting-state functional connectivity after sleep deprivation: a resting-state fMRI study. *Brain Imaging Behav.* (2016) 10:911–9. doi: 10.1007/s11682-015-9490-5
15. Silverman ME, Loudon H, Liu X, Mauro C, Leiter G, Goldstein MA. The neural processing of negative emotion postpartum: a preliminary study of amygdala function in postpartum depression. *Arch Women's Mental Health.* (2011) 14:355–9. doi: 10.1007/s00737-011-0226-2
16. Chase HW, Moses-Kolko EL, Zevallos C, Wisner KL, Phillips ML. Disrupted posterior cingulate–amygdala connectivity in postpartum depressed women as measured with resting BOLD fMRI. *Soc Cogn Affect Neurosci.* (2014) 9:1069–75. doi: 10.1093/scan/nst083
17. Zheng J-X, Chen Y-C, Chen H, Jiang L, Bo F, Feng Y, et al. Disrupted spontaneous neural activity related to cognitive impairment in postpartum women. *Front Psychol.* (2018) 9:624. doi: 10.3389/fpsyg.2018.00624
18. Bak Y, Nah Y, Han S, Lee S-K, Shin N-Y. Altered neural substrates within cognitive networks of postpartum women during working memory process and resting-state. *Sci Rep.* (2020) 10:1–12. doi: 10.1038/s41598-020-66058-x
19. Phillips ML, Schmithorst VJ, Banihashemi L, Taylor M, Samolyk A, Northrup JB, et al. Patterns of infant amygdala connectivity mediate the impact of high caregiver affect on reducing infant smiling: discovery and replication. *Biol Psychiatry.* (2021) 90:342–52. doi: 10.1016/j.biopsych.2021.03.026
20. Myczkowski ML, Dias M, Luvisotto T, Arnaut D, Bellini BB, Mansur CG, et al. Effects of repetitive transcranial magnetic stimulation on clinical, social, and cognitive performance in postpartum depression. *Neuropsychiatr Dis Treat.* (2012) 8:491. doi: 10.2147/NDT.S33851
21. Peng L, Fu C, Xiong F, Zhang Q, Liang Z, Chen L, et al. Effects of repetitive transcranial magnetic stimulation on depression symptoms and cognitive function in treating patients with postpartum depression: a systematic review and meta-analysis of randomized controlled trials. *Psychiatry Res.* (2020) 290:113124. doi: 10.1016/j.psychres.2020.113124

Conflict of Interest: XL was employed by Xi'an Solide Brain Control Medical Technology Company.

The remaining authors declare that the research was conducted in the absence of any commercial or financial relationships that could be construed as a potential conflict of interest.

Publisher's Note: All claims expressed in this article are solely those of the authors and do not necessarily represent those of their affiliated organizations, or those of the publisher, the editors and the reviewers. Any product that may be evaluated in this article, or claim that may be made by its manufacturer, is not guaranteed or endorsed by the publisher.

frontiers in Psychiatry

ORIGINAL RESEARCH
published: 25 March 2022
doi: 10.3389/fpsyt.2022.874090

Connectivity-Based Brain Network Supports Restricted and Repetitive Behaviors in Autism Spectrum Disorder Across Development

Anyi Zhang[1], *Lin Liu*[1,2], *Suhua Chang*[1], *Le Shi*[1], *Peng Li*[1], *Jie Shi*[2], *Lin Lu*[1,3]*, *Yanping Bao*[2,4]* and *Jiajia Liu*[5]*

[1] Peking University Sixth Hospital, Peking University Institute of Mental Health, NHC Key Laboratory of Mental Health (Peking University), National Clinical Research Center for Mental Disorders (Peking University Sixth Hospital), Peking University, Beijing, China, [2] National Institute on Drug Dependence and Beijing Key Laboratory on Drug Dependence Research, Peking University, Beijing, China, [3] Peking-Tsinghua Centre for Life Sciences and PKU-IDG/McGovern Institute for Brain Research, Peking University, Beijing, China, [4] School of Public Health, Peking University, Beijing, China, [5] School of Nursing, Peking University, Beijing, China

OPEN ACCESS

Edited by:
Yuanqiang Zhu,
Fourth Military Medical University, China

Reviewed by:
Jie Gong,
Xidian University, China
Zhaowen Liu,
Massachusetts General Hospital and Harvard Medical School, United States

***Correspondence:**
Jiajia Liu
liujiajia_sdu@bjmu.edu.cn
Yanping Bao
baoyp@bjmu.edu.cn
Lin Lu
linlu@bjmu.edu.cn

Specialty section:
This article was submitted to Neuroimaging and Stimulation, a section of the journal Frontiers in Psychiatry

Received: 11 February 2022
Accepted: 04 March 2022
Published: 25 March 2022

Citation:
Zhang A, Liu L, Chang S, Shi L, Li P, Shi J, Lu L, Bao Y and Liu J (2022) Connectivity-Based Brain Network Supports Restricted and Repetitive Behaviors in Autism Spectrum Disorder Across Development. Front. Psychiatry 13:874090. doi: 10.3389/fpsyt.2022.874090

Introduction: Autism spectrum disorder (ASD) is a lifelong condition. Autistic symptoms can persist into adulthood. Studies have reported that autistic symptoms generally improved in adulthood, especially restricted and repetitive behaviors and interests (RRBIs). We explored brain networks that are related to differences in RRBIs in individuals with ASDs among different ages.

Methods: We enrolled 147 ASD patients from the Autism Brain Imaging Data Exchange II (ABIDEII) database. The participants were divided into four age groups: children (6–9 years old), younger adolescents (10–14 years old), older adolescents (15–19 years old), and adults (≥20 years old). RRBIs were evaluated using the Repetitive Behaviors Scale-Revised 6. We first explored differences in RRBIs between age groups using the Kruskal–Wallis test. Associations between improvements in RRBIs and age were analyzed using a general linear model. We then analyzed RRBIs associated functional connectivity (FC) links using the network-based statistic method by adjusting covariates. The association of the identified FC with age group, and mediation function of the FC on the association of age-group and RRBI were further analyzed.

Results: Most subtypes of RRBIs improved with age, especially stereotyped behaviors, ritualistic behaviors, and restricted behaviors ($p = 0.012$, 0.014, and 0.012, respectively). Results showed that 12 FC links were closely related to overall RRBIs, 17 FC links were related to stereotyped behaviors. Among the identified 29 FC links, 15 were negatively related to age-groups. The mostly reported core brain regions included superior occipital gyrus, insula, rolandic operculum, angular, caudate, and cingulum. The decrease in FC between the left superior occipital lobe and right angular (effect = −0.125 and −0.693, respectively) and between the left insula and left caudate (effect = −0.116 and −0.664, respectively) might contribute to improvements in multiple RRBIs with age.

Conclusion: We identified improvements in RRBIs with age in ASD patients, especially stereotyped behaviors, ritualistic behaviors, and restricted behaviors. The decrease

in FC between left superior occipital lobe and right angular and between left insula and left caudate might contribute to these improvements. Our findings improve our understanding of the pathogenesis of RRBIs and suggest potential intervention targets to improve prognosis in adulthood.

Keywords: autism spectrum disorder, brain networks, network-based statistic, restricted and repetitive behaviors, mediation analysis

INTRODUCTION

Autism spectrum disorder (ASD) comprises a set of lifelong neurodevelopmental disorders that develop in early childhood, characterized by such core symptoms as social deficits and restricted and repetitive behaviors and interests [RRBIs; (1)]. The prevalence of ASD is estimated to be 1 in 59, which has dramatically increased in recent decades and caused numerous public health and social burdens worldwide (2). The onset of ASD symptoms among toddlers appears around 18–24 months of age, and a reliable diagnosis is typically made at 3–4 years of age (3). The early onset of deficits in joint attention and verbal or non-verbal communication contribute to early identification (1). Early screening and intervention usually indicate a better outcome in adulthood. Importantly, ASD is a lifelong condition. Its clinical symptoms might persist into adulthood (4). The developmental trajectory of autistic symptoms is largely unknown. Although autism was considered a "devastating condition," subsequent studies reported that autistic symptoms generally improved in adulthood, especially RRBIs that might decrease over time (5–7). According to the finding in typically developing children, the higher-order RRBIs decreased later than lower-order RRBIs (8). Generally, the improvement of RRBIs in autistic children was similar to that in typically developing children, but happened later (5).

There are several subtypes of RRBIs, including stereotyped or repetitive motor movements, insistence on sameness, highly restricted and fixated interests, and hyper- or hyporeactivity to sensory input, according to the *Diagnostic and Statistical Manual of Mental Disorders*, 5th edition (1). As a core symptom of ASD, RRBIs might first be found at 2 years of age, expressed as repetitively playing with specific toys or abnormal sensory interests, and gradually increased with age before 6 years old (9). The severity of repetitive motor movements and rigid routines is highest at preschool age and then decreases during school age and adolescence (10).

Children's brains are rapidly growing and developing systems. Recent studies identified atypical developmental trajectories of brain connectivity in individuals with ASD. These alterations might contribute to different autistic symptoms throughout life (11). Brain connectomics analyses in ASD patients identified an atypical age-associated trajectory of connectivity in the default mode network [DMN; (12)]. Studies of developmental changes in large-scale brain networks indicated that within and between network connectivity were not uniform at different ages (13). A previous review proposed a developmental model to explain age-related connectivity in ASD patients, including hyperconnectivity in childhood and hypoconnectivity in adulthood (14). These findings indicate atypical developmental trajectories in ASD patients over time, which might contribute to different clinical characteristics at different developmental stages.

According to studies of brain mechanisms that underlie RRBIs, structural abnormalities of the striatum might be involved in RRBIs in autism (15). Little is known about connectivity-based brain characteristics of age-related developmental trends of RRBIs. The present study explored brain network organization that is related to RRBIs in ASD patients of different ages. We expected to generate a comprehensive model of age-related brain network features that support RRBIs in ASD. Our findings will help understand the pathogenesis of age-related changes in RRBIs and provide crucial clues to aid the development of new treatments and interventions at early stages of ASD and improve prognosis in adulthood.

MATERIALS AND METHODS

Participants

Participants were recruited from the Autism Brain Imaging Data Exchange II (ABIDEII; http://fcon_1000.projects.nitrc.org/indi/abide/). There were 1,144 subjects who were 5-64 years old in the ABIDEII database, including 521 individuals with ASD [diagnosed by Autism Diagnostic Observation Scale (ADOS) and/or Autism Diagnostic Interview-Revised (ADI-R)] and 593 controls (16). Participants were included if they (1) were $\geq$ 6 years old, (2) were diagnosed with ASD, (3) had complete data from the Repetitive Behaviors Scale-Revised 6 (RBSR-6), and (4) were right-handed. The exclusion criteria were (1) missing data on age, sex, full intelligence quotient (FIQ), and current medication status, (2) no functional or structural imaging data, and (3) large head motions (3.0 mm translation or 3.0° rotation). The final sample included 147 ASD patients (123 males and 24 females) from nine sites: Barber National Institute (BNI), Institut Pasteur (IP), Kennedy Krieger Institute (KKI), Katholieke Universiteit Leuven (KUL), New York University (NYU), San Diego State University (SDSU), Trinity College Dublin (TCD), and University College Dublin (UCD). The ASD patients were classified into four groups according to the World Health Organization classification: (1) children (6–10 years old; 31 subjects), (2) younger adolescents (11–14 years old; 52 subjects), (3) older adolescents (15-19 years old; 33 subjects), and (4) adults ($\geq$20 years old; 31 subjects) (17).

Ethics

The data in the present study was extracted from an open online database (http://fcon_1000.projects.sitrc.org/indi/abide/).

All participants and their caregivers signed informed consent forms at each site.

Measures

RBSR-6

The RBSR-6 is a widely used questionnaire that evaluates RRBIs. It includes 43 items that are grouped into six RRBI subtypes: stereotyped behaviors, self-injurious behaviors, compulsive behaviors, ritualistic behaviors, sameness behaviors, and restricted behaviors. Every item is ranked on a 4-point Likert-type scale, from 0 (do not occur) to 3 (very serious) (18). The assessment of RRBIs using the RBSR-6 is usually based on observations by parents, caregivers, teachers, or others who know the patient. This questionnaire has excellent reliability and validity (19).

Covariates

We further extracted age, sex, handedness, FIQ, eye-status during scan, and current medication status from the online database (http://fcon_1000.projects.sitrc.org/indi/abide/). Handedness was grouped into three categories: right-handed, left-handed, and mixed-handed. Only right-handed patients were enrolled in the study. Measurements of FIQ were different across sites: Kaufman Brief Intelligence Test at BNI, Wechsler Intelligence Scale for Children at IP and KKI, Wechsler Adult Intelligence Scale at KUL, and Wechsler Abbreviated Scale of Intelligence at NYU, SDSU, TCD, and UCD. The results of the different measurements were comparable (20, 21). Eye-status during scan was grouped into two categories: open and closed. Medication status about whether the participants currently took medications within 3 months before the scan was also extracted from the database. These data were controlled as covariates in the analysis.

Brain Imaging Processing

Imaging data were preprocessed using the Data Processing Assistant for Resting-State Functional Magnetic Resonance Imaging (DPARSF) in MATLAB (22). The first 10 volumes for each subject were removed for magnetization equilibrium. The remaining volumes were slice-time corrected, head-motion realigned, co-registered to structural scans, normalized to $3 \times 3 \times 3$ mm^3 voxels with a bounding box of [−90 −126 −72; 90 90 108], smoothed with a Gaussian kernel with a full-width half maximum of 6 mm, and bandpass filtered (0.01–0.1 Hz). The detailed scan parameters were presented in **Supplementary Table 1**.

After preprocessing, we constructed a whole-brain functional connectivity (FC) network for each participant in DPARSF. The whole brain was segmented into 116 brain regions based on the Anatomical Automatic Labeling atlas, and regional signals were extracted by averaging blood oxygen level-dependent signals of every voxel in the brain region. We then calculated FC between every two brain regions using the Pearson correlation between regional signals (116 × 116 brain regions with 13,456 edges for all of them).

Statistical Analysis

Demographic characteristics are presented as percentages for categorical variables and means, standard deviations (SDs) or medians, and interquartile ranges (IQRs) for continuous variables. Comparisons of RRBIs in the different age groups were conducted using the Kruskal–Wallis test. We additionally compared the subscales evaluating restricted/repetitive behaviors in ADOS and ADI-R among different age-group using the Kruskal–Wallis test, and results were presented in **Supplementary Table 2**. Associations between age groups and RRBIs were further investigated using a general linear model (GLM) after adjusting for sex, age, FIQ, and current medication status. These analyses were performed using Statistical Package for the Social Sciences (SPSS) 23.0 software.

The network-based statistic (NBS) was applied to investigate functional networks that were associated with RRBIs in ASD patients after controlling for age, sex, FIQ, eye-status during rest scan, and medication status (23). The NBS process was conducted as the following: (1) conduct a linear regression model to explore every edge associated with RRBIs after controlling covariates, and further perform *t*-tests for those associated components, (2) identify connected components that were suprathreshold (threshold = 3.0) links, and (3) compute the family-wise error-corrected *p*-value for each connected components using 5,000 random permutations. Correlations between RRBIs-related FC links and age groups were then investigated using Pearson correlation analysis by controlling for sex, age, FIQ, eye-status during scan, and medication status.

Shared FC links that were related to the RRBI subscales and age groups might simultaneously contribute to developmental changes in RRBIs with age in ASD patients. We conducted a mediation analysis to explore whether shared FC links might mediate the relationship between developmental stages and RRBIs. We used Model 4 in PROCESS, and $N = 10{,}000$ was used for the bootstrap. The level of significance was set at $p < 0.05$ (two-tailed).

RESULTS

Demographic Characteristics

Demographic characteristics are presented in **Table 1**. Included participants were between 6 and 64 years of age, and the median age was 17 years old. Most participants in our study were male (83.67%). The FIQ of the subjects ranged from 66 to 146. Most patients had high-functioning autism (IQ > 70).

RRBIs at Different Developmental Stages

Figure 1 shows the severity of RRBI subtypes in the different age groups. The trajectories of each subtype showed similar developmental patterns, in which children had the highest scores, which then gradually decreased with age. According to the results of the Kruskal–Wallis test, improvements in stereotyped behaviors, ritualistic behaviors, and restricted behaviors were statistically significant ($p = 0.012$, 0.014, and 0.012, respectively). The *post-hoc* tests showed significant differences between children and the older age groups. Detailed RRBI subtype scores in the different age groups are presented in **Table 2**.

TABLE 1 | Demographic characteristics ($n = 147$).

Item	Description
Male [*n* (%)]	123 (83.67%)
Age (years) (median, IQR)	17.37 ± 11.57
Age-group [*n* (%)]	
Children	31 (21.09%)
Younger adolescents	52 (35.37%)
Older adolescents	33 (22.45%)
Adults	31 (21.09%)
FIQ (mean ± SD)	104.56 ± 15.00
Currently taking medication [*n* (%)]	39 (26.5%)
RBSR-6 total raw score (median, IQR)	20.00, 22.00
Stereotyped behaviors	3.00, 4.00
Self-injurious behaviors	0.00, 2.00
Compulsive behaviors	2.00, 4.00
Ritualistic behaviors	4.00, 5.00
Sameness behaviors	6.00, 7.00
Restricted behaviors	3.00, 4.00
Eyes opened during scanning [*n* (%)]	102 (69.39%)

IQR, interquartile range; SD, standard deviation; RBSR-6, Repetitive Behaviors Scale-Revised 6.

Associations between the severity of RRBIs and age groups are shown in **Table 3**. Because this was an observational study, GLM analysis showed that age was negatively associated with the severity of stereotyped behaviors, ritualistic behaviors, restricted behaviors, and overall RRBIs. Associations with other RRBI subtypes were not statistically significant (**Table 3**).

Functional Connectivity Links Associated With RRBI Subtypes

We explored FC links that were associated with stereotyped behaviors, ritualistic behaviors, restricted behaviors, and overall RRBIs. For stereotyped behaviors, the underlying functional network included 17 edges between 13 brain regions (**Table 4**, **Figures 2A,B**). We did not find FC links that were associated with ritualistic behaviors or restricted behaviors. For overall RRBIs, the correlated connectivity network included 12 edges between 12 brain regions (**Table 4**, **Figures 2C,D**). We then extracted the 17 and 12 FC links for each individual, and the association between FC links and age were also calculated. It was found that 15 out of the 29 FC links were negatively related to age, meaning that FC between these 13 brain regions decreased with age (**Table 4**).

FC Links Mediated the Association Between Age and RRBIs

As shown in **Table 5**, FC between left superior occipital lobe and right angular, left superior occipital lobe and left angular, left cuneus and right angular, left insula and left caudate, left caudate and right caudate mediated improvements in stereotyped behaviors with age. Interestingly, all these forementioned FC links negatively mediated the difference of stereotyped behaviors and overall RRBIs among age groups, which meant that the FC between these brain regions were decreased with age, and the decreased connectivities might further contribute to the improvement of different domains of BBRIs in ASD patients. Moreover, FC between left superior occipital lobe and right angular, left insula and left caudate were related to improvements in total RRBIs with age simultaneously, which might indicate that FC links between the left superior occipital lobe and right angular, left insula and left caudate might contribute to developmental changes in multiple RRBIs in patients with ASD.

DISCUSSION

We identified improvements in RRBIs with age, especially stereotyped behaviors, ritualistic behaviors, and restricted behaviors. Furthermore, FC between the left superior occipital lobe and right angular and between the left insula and left caudate, which are responsible for visual integration, motor function, and sensorimotor process, might contribute to developmental changes in multiple RRBIs in patients with ASD. To our knowledge, this was the first study to analyze neuroimaging-based features that support trajectories of RRBIs in ASD patients. These core brain regions might have implications for future intervention targets.

Our results indicated that the RRBI subscales had different improvement trajectories. Stereotyped behaviors, ritualistic behaviors, and restricted behaviors improved greatly after childhood. These finding corroborated previous studies that reported a broad range of trajectories of RRBIs in ASD patients (8–10, 24). For children, RRBIs are relatively stable between 2 and 7 years of age (9). Richler et al. reported discrepant trajectories between different subtypes of RRBIs, in which repetitive sensory motor behaviors (i.e., repetitive motor movements) and the repetitive usage of objects would increase while the insistence of sameness (i.e., adherence to daily routines) would decrease during a 7-year follow-up period (10). Moreover, RRBIs also manifest in typically developing children, and developmental changes of RRBIs in healthy toddlers suggest that higher-order RRBIs (e.g., insistence on sameness) decrease later than lower-order RRBIs (e.g., stereotype behaviors; (8). In summary, the trajectory of autistic symptoms in ASD patients suggests stable improvements in RRBIs over time. We were able to measure age-related improvements in stereotyped behaviors, ritualistic behaviors, and restricted behaviors in the present study. The present GLM analysis indicated that compulsive behaviors greatly improved after younger adolescence, which occurred slightly later than improvements in stereotyped behaviors, which was consistent with a previous study (8).

Atypical neurodevelopment has been previously reported to contribute to autism-related symptoms. Previous brain development studies mostly focused on cortical volume, gray matter thickness, or white matter volume (25). We found that significant reductions of FC among brain regions in the temporal lobe, occipital lobe, and cingulate might contribute to the trajectory of RRBIs over time, especially stereotyped behaviors and overall RRBIs (evaluated by the RBSR-6). Previous studies that examined associations between cortical thickness and RRBI severity over time found that gray matter thickness of

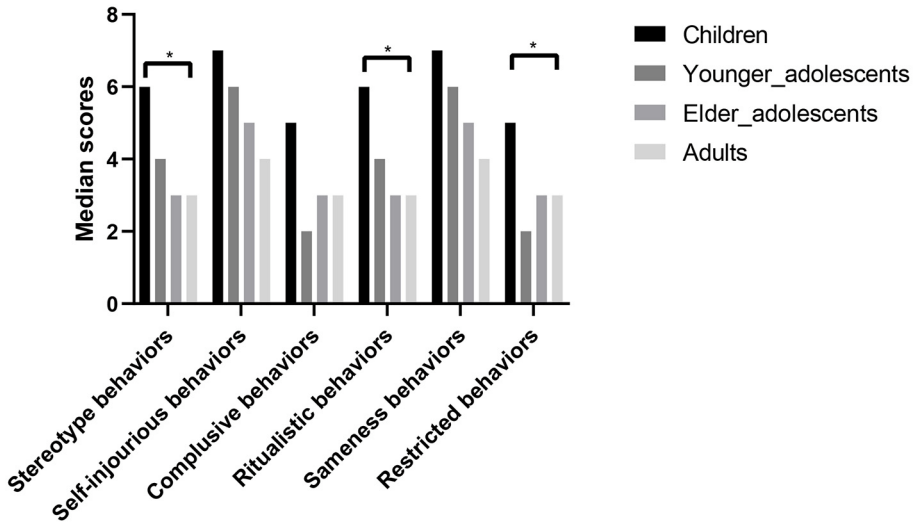

FIGURE 1 | RRBI subtype scores at different developmental stages ($n = 147$). Median scores are shown for six subtypes of RRBIs (stereotyped behaviors, self-injurious behaviors, compulsive behaviors, ritualistic behaviors, sameness behaviors, and restricted behaviors) in four age groups: children (6–9 years old), younger adolescents (10–14 years old), older adolescents (15–19 years old), and adults (≥20 years old). Comparisons of median scores among different age groups were performed using the Kruskal–Wallis test. Children had the highest scores, and then their scores for every subtype gradually decreased with age. The decreases in stereotyped behaviors, ritualistic behaviors, and restricted behaviors were statistically significant. *$p < 0.05$.

TABLE 2 | Description of RRBIs in different age groups ($n = 147$).

Item	(1) Children ($n = 31$)	(2) Younger adolescents ($n = 52$)	(3) Older adolescents ($n = 33$)	(4) Adults ($n = 31$)	*H*	*p*	*p* in *post-hoc* test					
							(2)–(1)	(3)–(1)	(4)–(1)	(3)–(2)	(4)–(2)	(4)–(3)
RBSR-6 total raw score	32.77, 21.54	23.40, 17.69	22.42, 16.68	20.48, 14.48	7.89	0.048	0.020	0.036	0.014	0.967	0.630	0.693
Stereotyped behaviors	4.81, 3.46	3.31, 2.84	3.42, 3.24	2.32, 1.99	10.75	0.013	0.026	0.060	0.001	0.918	0.159	0.176
Self-injurious behaviors	2.23, 3.47	1.92, 2.75	1.52, 2.69	0.94, 1.71	5.22	0.157	NA	NA	NA	NA	NA	NA
Compulsive behaviors	5.19, 4.98	3.42, 3.76	3.12, 4.20	3.65, 3.77	7.08	0.070	NA	NA	NA	NA	NA	NA
Ritualistic behaviors	6.77, 4.40	4.94, 3.90	3.97, 3.89	3.87, 3.26	10.28	0.016	0.054	0.004	0.008	0.209	0.288	0.881
Sameness behaviors	9.03, 7.18	6.79, 6.44	7.15, 6.28	6.94, 6.04	4.56	0.207	NS.	NS.	NS.	NS.	NS.	NS.
Restricted behaviors	4.74, 3.30	2.98, 2.51	3.24, 2.67	2.77, 2.43	9.20	0.027	0.006	0.066	0.011	0.498	0.888	0.471

RRBIs, restricted and repetitive behaviors and interests; IQR, interquartile range; RBSR-6, Repetitive Behaviors Scale-Revised 6; NA, not applicable. Post-hoc tests were conducted to explore differences between age groups. In the post-hoc test, (1) refers to children, (2) refers to younger adolescents, (3) refers to older adolescents, and (4) refers to adults.

TABLE 3 | Association between age and severity of RRBIs based on GLM ($n = 147$).

Age group	Total raw score	Stereotyped behaviors	Self-injurious behaviors	Compulsive behaviors	Ritualistic behaviors	Sameness behaviors	Restricted behaviors
Children (reference)	1	1	1	1	1	1	1
Younger adolescents	−9.37* (−17.16, −1.58)	−1.50* (−2.78, −0.22)	−0.30 (−1.50, 0.90)	−1.77 (−3.59, 0.05)	−1.83* (−3.54, −0.13)	−2.24 (−5.09, 0.60)	−1.76* (−2.95, −0.57)
Older adolescents	−10.35* (−18.93, −1.77)	−1.38 (−2.80, 0.03)	−0.71 (−2.03, 0.61)	−2.07* (−4.08, −0.07)	−2.80* (−4.68, −0.93)	−1.88 (−5.02, 1.26)	−1.50* (−2.81, −0.19)
Adults	−12.29* (−21.01, −3.57)	−2.48* (−3.92, −1.05)	−1.29 (−2.63, 0.05)	−1.55 (−3.59, 0.49)	−2.90* (−4.81, −1.00)	−2.10 (−5.28, 1.09)	−1.97* (−2.95, −0.57)

*The statistics show β and 95% confidence interval. RRBIs, restricted and repetitive behaviors and interests. The models adjusted for sex, age, FIQ, eye status during scan and current medication status. * $p < 0.05$.*

TABLE 4 | Functional connectivity associated with stereotyped behaviors and overall RRBIs and correlation between FC and age ($n = 147$).

Dependent variable	Brain region 1	Brain region 2	Connection strength	Correlation with age
Stereotyped behaviors	Occipital_sup_L	Angular_R	3.39	−0.35**
	Occipital_sup_L	Caudate_L	3.18	−0.16
	Occipital_sup_L	Cingulum_ant_R	3.04	−0.20*
	Occipital_sup_L	Caudata_R	3.60	−0.16
	Occipital_sup_L	Angular_L	3.02	−0.35**
	Cuneus_L	Angular_R	3.41	−0.38**
	Insula_R	Occipital_mid_L	3.08	−0.13
	Insula_L	Occipital_mid_L	3.04	−0.13
	Insula_L	Caudate_L	3.18	−0.189*
	Insula_L	Caudate_R	3.15	−0.21*
	Insula_L	Cingulum_ant_L	3.22	−0.26*
	Insula_L	Rolandic_oper_L	3.59	−0.20*
	Angular_L	Heschl_L	3.10	−0.26*
	Cingulum_ant_L	Heschl_L	3.03	−0.23*
	Rolandic_oper_L	Caudate_R	3.27	−0.23*
	Rolandic_oper_L	Cingulum_ant_L	3.05	−0.29**
	Rolandic_oper_L	Cingulum_ant_R	3.16	−0.31*
Overall RRBIs	Occipital_sup_R	Caudate_R	3.31	−0.14
	Cuneus_R	Caudate_R	3.00	−0.15
	Occipital_sup_L	Angular_R	3.10	−0.35**
	Occipital_sup_L	Insula_R	3.36	−0.07
	Occipital_sup_L	Caudate_R	4.02	−0.16
	Occipital_sup_L	Caudate_L	3.50	−0.16
	Occipital_sup_L	Cingulum_ant_R	3.43	−0.20*
	Occipital_sup_L	Cingulum_ant_L	3.12	−0.19*
	Insula_R	Hippocampus_L	3.01	−0.25*
	Insula_R	Cingulum_ant_L	3.10	−0.25*
	Occipital_mid_L	Caudate_R	3.30	−0.18
	Insula_L	Caudate_L	3.03	−0.19*

RRBIs, restricted and repetitive behaviors and interests; NBS, network-based statistic; R, right hemicerebrum; L, left hemicerebrum. The models adjusted for sex, age, FIQ, eye status during scan and current medication status. $^{*}p < 0.05$, $^{**}p < 0.001$.

the orbital frontal cortex and middle frontal cortex correlated with self-injurious behaviors in adolescent patients (24). In the present study, core brain regions that were responsible for stereotyped behaviors included the superior occipital gyrus, insula, rolandic operculum, angular, caudate, and cingulum. Importantly, these FC links declined with age at the same time. In ASD patients, neurobiology studies found that the most reported brain regions that were responsible for RRBIs were located in corticostriatal circuits, including the orbitofrontal cortex, anterior cingulate cortex, caudate, putamen, pallidum. These brain regions that are associated with goal-directed behaviors, alterations of growth rate, abnormalities in cortical thickness or volume, decreases or increases in FC between brain regions, and changes in neuro-metabolism might contribute to atypical behaviors, including RRBIs (15, 26, 27). The present study supported the implication of these brain regions. We also found that stereotyped behaviors were related to alterations of FC between the superior occipital gyrus, angular, insula, rolandic operculum, and Heschl gyrus, which are mostly related to sensory processing and integration.

The superior occipital gyrus is important for visual processing and fluid reasoning (27, 28). Nebel et al. found that atypical FC between the superior occipital gyrus and motor cortex might contribute to visual-motor disfunction in school-age ASD patients (29). Thus, alterations of FC of the superior occipital gyrus might have been responsible for sensorial stereotyped behaviors that are related to visual processes in the present study.

The angular gyrus is in the parietal lobe and part of the DMN (30). Dysfunction of the angular gyrus has been reported to be involved in pathophysiological social cognition and social deficits in ASD patients (31). The angular gyrus is also an important hub that converts multisensorial messages and manages multicognition processes (32). With regard to RRBIs, abnormal FC of the angular gyrus might be an attempt to correct atypical FC in corticostriatal circuits (15, 30).

The insular cortex is located at the base of the lateral sulcus, consisting of three subregions that are based on distinct functions: dorsal anterior insular (involved in cognitive control), ventral insula (involved in emotion and affective processing), and posterior insula (involved in sensorimotor processing) (33, 34).

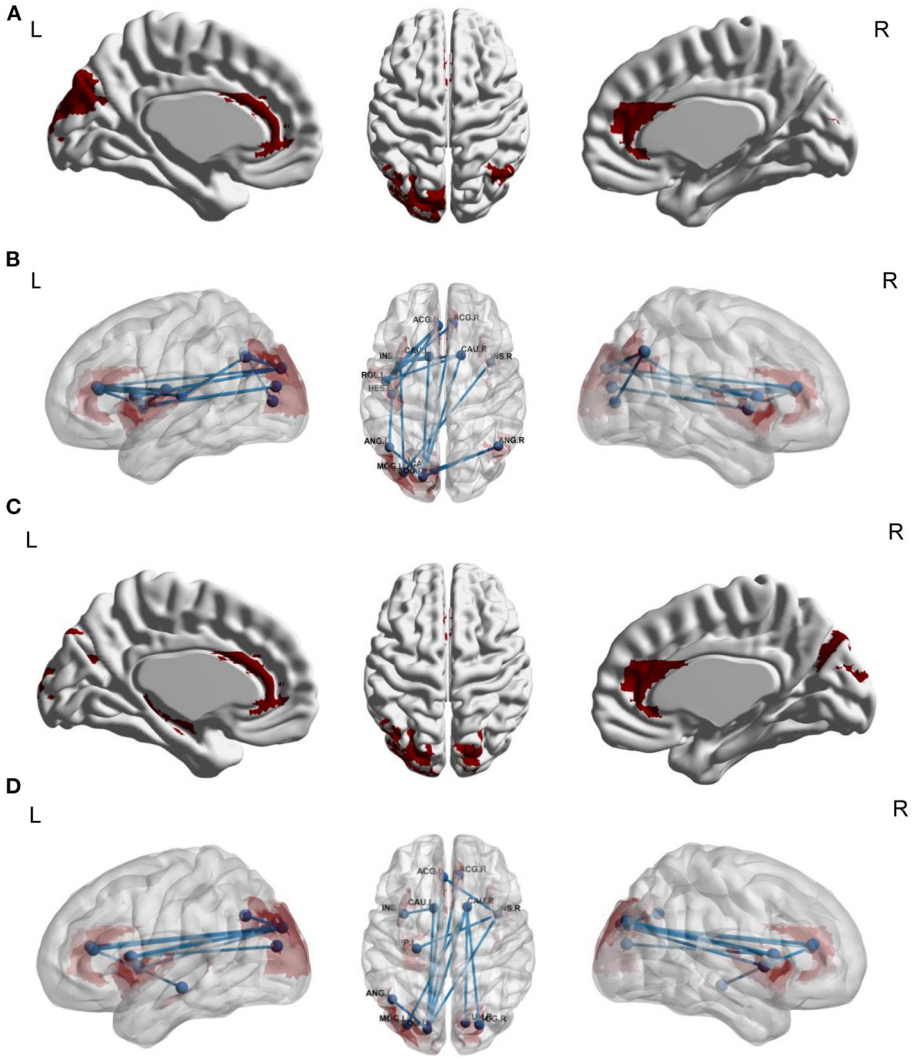

FIGURE 2 | Functional connectivity links associated with stereotyped behaviors **(A,B)** and overall RRBIs **(C,D)** ($n = 147$). **(A,B)** Network-based statistic results for stereotyped behaviors in ASD patients. The underlying functional network included 17 edges between 13 brain regions. **(C,D)** Network-based statistic results for overall RRBIs. The correlated connectivity network included 12 edges between 12 brain regions. In the NBS analysis, we adjusted several covariates, including sex, age, FIQ, eye-status during scan, and medication status. ACG_L, left anterior cingulate gyrus; ACG_R, right anterior cingulated gyrus; CAU_L, left caudate; CAU_R, right caudate; INS_L, left insular; INS_R, right insular; ROL_L, left rolandic operculum; HES_L, left heschl's gyrus; ANG_L, left angular; ANG_R, right angular; MOG_L, left middle occipital gyrus; SOG_L, left superior occipital gyrus; CAL_L, left calcarine; ACG_L, left anterior cingulate gyrus; ACG_R, right anterior cingulate gyrus; HIP_L, left hippocampus; CUN_R, right cuneus; SOG_R, right superior occipital gyrus.

Structural and functional abnormalities of the insula have been reported to contribute to social and non-social cognitive impairments in ASD patients (34). The volume of the caudate, the density of caudate nuclei, and atypical structural or FC between frontal-striatal circuits have been reported to underlie RRBIs (15, 35, 36).

The operculum covers the insula, which is related to emotional processing and facial expressions (37, 38). Zhou et al. found that RRBIs in ASD patients were closely related to a decrease in FC between the rolandic operculum and anterior cingulum cortex (39). The rolandic operculum is also an important part of the sensorimotor network, and a decrease in connectivity of the rolandic operculum might contribute to deficits in sensory processing and motor function. Moreover, ASD patients were suggested to engage in stereotyped or compulsive behaviors to produce sensory self-stimulation, reflecting a sensory processing deficit (39, 40).

The Heschl gyrus is part of the temporal lobe, located mainly at the primary auditory cortex (41). In ASD patients, bottom-up sensorimotor network dysfunction is common. The Heschl gyrus plays an important role in auditory-motor integration (42, 43). The early onset of auditorial processing abnormalities might further affect subsequent higher-order sensorial perception (44). In preschool children with ASD, alterations of FC of the Heschl gyrus was positively related to ASD symptoms (45). Moreover, reductions of gray matter volume of the

TABLE 5 | Functional connectivity that mediated associations between age and stereotyped behaviors/overall RRBIs ($n = 147$).

X	M	Y	Mediation effect			
			Effect	SE	LLCI	ULCI
Age groups	Occipital_sup_L+Angular_R	Stereotyped behaviors	−0.125	0.074	−0.292	−0.003
	Occipital_sup_L+Angular_L		−0.110	0.069	−0.270	−0.001
	Cuneus_L+ Angular_R		−0.136	0.077	−0.312	−0.012
	Insula_L+Caudate_L		−0.116	0.075	−0.288	−0.003
	Insula_L+Caudate_R		−0.118	0.077	−0.295	−0.005
Age groups	Occipital_sup_L+Angular_R	Overall RRBIs	−0.693	0.408	−1.605	−0.027
	Insula_L+Caudate_L		−0.664	0.435	−1.672	−0.015

RRBIs, restricted and repetitive behaviors and interests; X, independent variables; M, mediators; Y, dependent variables; SE, standard error; LLCI, lower level of 95% confidence interval; ULCI, upper level of 95% confidence interval; R, right hemicerebrum; L, left hemicerebrum.

Heschl gyrus were suggested to contribute to delays in spoken language (44).

Furthermore, we found that two FC links mediated the development of multiple RRBIs at different ages: between the left superior occipital lobe and right angular and between the left insula and left caudate. As a subregion of the striatum, the caudate was notably associated with RRBIs (46). Previous FC studies of the striatum found that RRBIs were associated with imbalanced corticostriatal connectivity, involving the striatum, frontal lobe, and parietal lobe (46–48). In the present study, FC between the left superior occipital lobe and right angular and between the left insula and left caudate decreased with age, which might contribute to the improvements of RRBIs. The angular gyrus was reported to be involved in semantic processing, word reading and comprehension, attention, and spatial cognition, and atypical structural and functional development of this region might contribute to autistic symptoms (30). As described in previous studies, alterations of FC of the angular gyrus were reported to be related to tactile disorders in ASD patients (49). Increases in volume of the angular gyrus were shown to be involved in motor impairments (30, 50). The insula and caudate were responsible for social cognitive and movement accordingly (15, 34–36). In the present study, we found that alterations of FC between the insula and caudate might further exacerbate impairments in social function and stereotyped behaviors.

The present study explored connectivity-based brain network features that supported RRBIs in ASD patients across development, but several limitations should be noted. First, this was a cross-sectional study with participants of different ages. The results should be cross-validated in a longitudinal analysis of subjects with follow-up. Second, the ASD patients mostly had high-functioning ASD. Future studies should also focus on low-functioning ASD patients. Third, we did not find FC links that were related to trajectories of self-injurious behaviors, compulsive behaviors, ritualistic behaviors, sameness behaviors, or restricted behaviors, which might be related to our limited sample size or cross-sectional study design. Thus, longitudinal studies with larger sample sizes are needed. Last but not the least, most participants in our study were boys, which might be a potential source of heterogeneity. Future studies with more girls are needed to test the generalizability of our findings.

In conclusion, the present study identified improvements in RRBIs in ASD patients with age, especially stereotyped behaviors, ritualistic behaviors, and restricted behaviors. The decrease in FC between the left superior occipital lobe and right angular and between the left insula and left caudate might contribute to improvements in multiple RRBIs in patients with ASD.

DATA AVAILABILITY STATEMENT

The datasets presented in this study can be found in online repositories. The names of the repository/repositories and accession number(s) can be found below: Data in present study was extracted from the open online database at http://fcon_1000.projects.nitrc.org/indi/abide/.

ETHICS STATEMENT

Data in present study was extracted from the open online database. All participants and their caregivers have signed the contents at every sites. Written informed consent to participate in this study was provided by the participants' legal guardian/next of kin.

AUTHOR CONTRIBUTIONS

LLu, YB, and JL proposed the topic and main idea. AZ wrote the initial draft of manuscript with contributions from LLi, JL, and YB. AZ conducted the data analyses with help from LLi. JS, YB, JL, LLi, SC, LS, PL, and LLu critically revised the manuscript. All authors approved the results and final version of the manuscript.

FUNDING

This study was supported by the National Natural Science Foundation of China (Nos. 81761128036, 81821092, and 82171514), Beijing Municipal Science and Technology Commission (Z181100001518005), the Fundamental Research Funds for the Central Universities (No. 71006Y2557), and PKU-Baidu Fund (No. 2020BD011). LLu was supported in part by the Postdoctoral Fellowship of Peking-Tsinghua Center for Life Sciences.

ACKNOWLEDGMENTS

The authors thank all the patients and their parents for participating in the ABIDEII project and all researchers at each sites.

SUPPLEMENTARY MATERIAL

The Supplementary Material for this article can be found online at: https://www.frontiersin.org/articles/10.3389/fpsyt.2022.874090/full#supplementary-material

REFERENCES

1. Lai MC, Lombardo MV, Baron-Cohen S. Autism. *Lancet.* (2014) 383:896–910. doi: 10.1016/S0140-6736(13)61539-1
2. Baio J, Wiggins L, Christensen DL, Maenner MJ, Daniels J, Warren Z, et al. Prevalence of autism spectrum disorder among children aged 8 years - autism and developmental disabilities monitoring Network, 11 sites, United States, 2014. *MMWR Surveill Summ.* (2018) 67:1–23. doi: 10.15585/mmwr.ss6706a1
3. Hyman SL, Levy SE, Myers SM. Identification, evaluation, and management of children with autism spectrum disorder. *Pediatrics.* (2020) 145. doi: 10.1542/peds.2019-3447
4. Bathelt J, Koolschijn PC, Geurts HM. Age-variant and age-invariant features of functional brain organization in middle-aged and older autistic adults. *Mol Autism.* (2020) 11:9. doi: 10.1186/s13229-020-0316-y
5. Harrop C, McConachie H, Emsley R, Leadbitter K, Green J. Restricted and repetitive behaviors in autism spectrum disorders and typical development: cross-sectional and longitudinal comparisons. *J Autism Dev Disord.* (2014) 44:1207–19. doi: 10.1007/s10803-013-1986-5
6. Pickles A, McCauley JB, Pepa LA, Huerta M, Lord C. The adult outcome of children referred for autism: typology and prediction from childhood. *J Child Psychol Psychiatry.* (2020) 61:760–7. doi: 10.1111/jcpp.13180
7. Howlin P. Adults with autism: changes in understanding since DSM-111. *J Autism Dev Disord.* (2021) 51:4291–308. doi: 10.1007/s10803-020-04847-z
8. Sifre R, Berry D, Wolff JJ, Elison JT. Longitudinal change in restricted and repetitive behaviors from 8-36 months. *J Neurodev Disord.* (2021) 13:7. doi: 10.1186/s11689-020-09335-0
9. Joseph L, Thurm A, Farmer C, Shumway S. Repetitive behavior and restricted interests in young children with autism: comparisons with controls and stability over 2 years. *Autism Res.* (2013) 6:584–95. doi: 10.1002/aur.1316
10. Richler J, Huerta M, Bishop SL, Lord C. Developmental trajectories of restricted and repetitive behaviors and interests in children with autism spectrum disorders. *Dev Psychopathol.* (2010) 22:55–69. doi: 10.1017/S0954579409990265
11. Ecker C, Bookheimer SY, Murphy DG. Neuroimaging in autism spectrum disorder: brain structure and function across the lifespan. *Lancet Neurol.* (2015) 14:1121–34. doi: 10.1016/S1474-4422(15)00050-2
12. Wiggins JL, Peltier SJ, Ashinoff S, Weng SJ, Carrasco M, Welsh RC, et al. Using a self-organizing map algorithm to detect age-related changes in functional connectivity during rest in autism spectrum disorders. *Brain Res.* (2011) 1380:187–97. doi: 10.1016/j.brainres.2010.10.102
13. Nomi JS, Uddin LQ. Developmental changes in large-scale network connectivity in autism. *Neuroimage Clin.* (2015) 7:732–41. doi: 10.1016/j.nicl.2015.02.024
14. Uddin LQ, Supekar K, Menon V. Reconceptualizing functional brain connectivity in autism from a developmental perspective. *Front Hum Neurosci.* (2013) 7:458. doi: 10.3389/fnhum.2013.00458
15. Langen M, Bos D, Noordermeer SD, Nederveen H, van Engeland H, Durston S. Changes in the development of striatum are involved in repetitive behavior in autism. *Biol Psychiatry.* (2014) 76:405–11. doi: 10.1016/j.biopsych.2013.08.013
16. Di Martino A, O'Connor D, Chen B, Alaerts K, Anderson JS, Assaf M, et al. Enhancing studies of the connectome in autism using the autism brain imaging data exchange II. *Sci Data.* (2017) 4:170010. doi: 10.1038/sdata.2017.10
17. World Health Organization. *Adolescent Mental Health.* (2021). Available online at: https://www.who.int/news-room/fact-sheets/detail/adolescentmental-health (accessed January 15, 2022).
18. Bodfish JW, Symons FJ, Parker DE, Lewis MH. Varieties of repetitive behavior in autism: comparisons to mental retardation. *J Autism Dev Disord.* (2000) 30:237–43. doi: 10.1023/A:1005596502855
19. Bishop SL, Hus V, Duncan A, Huerta M, Gotham K, Pickles A, et al. Subcategories of restricted and repetitive behaviors in children with autism spectrum disorders. *J Autism Dev Disord.* (2013) 43:1287–97. doi: 10.1007/s10803-012-1671-0
20. Scott WC, Austin DW, Reid DS. Investigation of the WISC-III and WASI in clinical child populations: a framework for further exploration. *Can J Sch Psychol.* (2007) 22:249–54. doi: 10.1177/0829573507308162
21. Kuriakose S. Concurrent validity of the WISC-IV and DAS-II in children with autism spectrum disorder. *J Psychoeducl Assess.* (2014) 32:283–94. doi: 10.1177/0734282913511051
22. Yan CG, Zang YF. DPARSF: a MATLAB toolbox for "pipeline" data analysis of resting-state fMRI. *Front Syst Neurosci.* (2010) 4:13. doi: 10.3389/fnsys.2010.00013
23. Zalesky A, Fornito A, Bullmore ET. Network-based statistic: identifying differences in brain networks. *Neuroimage.* (2010) 53:1197–207. doi: 10.1016/j.neuroimage.2010.06.041
24. Bieneck V, Bletsch A, Mann C, Schäfer T, Seelemeyer H, Herøy N, et al. Longitudinal changes in cortical thickness in adolescents with autism spectrum disorder and their association with restricted and repetitive behaviors. *Genes.* (2021) 12:2024. doi: 10.3390/genes12122024
25. Mann C, Bletsch A, Andrews D, Daly E, Murphy C, Murphy D, et al. The effect of age on vertex-based measures of the grey-white matter tissue contrast in autism spectrum disorder. *Mol Autism.* (2018) 9:49. doi: 10.1186/s13229-018-0232-6
26. Shukla DK, Keehn B, Müller RA. Tract-specific analyses of diffusion tensor imaging show widespread white matter compromise in autism spectrum disorder. *J Child Psychol Psychiatry.* (2011) 52:286–95. doi: 10.1111/j.1469-7610.2010.02342.x
27. Hegarty IJ, Lazzeroni LC, Raman MM, Hallmayer JF, Cleveland SC, Wolke ON, et al. Genetic and environmental influences on corticostriatal circuits in twins with autism. *J Psychiatry Neurosci.* (2020) 45:188–97. doi: 10.1503/jpn.190030
28. Simard I, Luck D, Mottron L, Zeffiro TA, Soulières I. Autistic fluid intelligence: increased reliance on visual functional connectivity with diminished modulation of coupling by task difficulty. *Neuroimage Clin.* (2015) 9:467–78. doi: 10.1016/j.nicl.2015.09.007
29. Nebel MB, Eloyan A, Nettles CA, Sweeney KL, Ament K, Ward RE, et al. Intrinsic visual-motor synchrony correlates with social deficits in autism. *Biol Psychiatry.* (2016) 79:633–41. doi: 10.1016/j.biopsych.2015.08.029
30. Liu J, Yao L, Zhang W, Xiao Y, Liu L, Gao X, et al. Gray matter abnormalities in pediatric autism spectrum disorder: a meta-analysis with signed differential mapping. *Eur Child Adolesc Psychiatry.* (2017) 26:933–45. doi: 10.1007/s00787-017-0964-4
31. Assaf M, Jagannathan K, Calhoun VD, Miller L, Stevens MC, Sahl R, et al. Abnormal functional connectivity of default mode sub-networks in autism spectrum disorder patients. *Neuroimage.* (2010) 53:247–56. doi: 10.1016/j.neuroimage.2010.05.067
32. Seghier ML. The angular gyrus: multiple functions and multiple subdivisions. *Neuroscientist.* (2013) 19:43–61. doi: 10.1177/1073858412440596
33. Chang LJ, Yarkoni T, Khaw MW, Sanfey AG. Decoding the role of the insula in human cognition: functional parcellation and large-scale reverse inference. *Cereb Cortex.* (2013) 23:739–49. doi: 10.1093/cercor/bhs065

34. Nomi JS, Molnar-Szakacs I, Uddin LQ. Insular function in autism: update and future directions in neuroimaging and interventions. *Prog Neuropsychopharmacol Biol Psychiatry.* (2019) 89:412–26. doi: 10.1016/j.pnpbp.2018.10.015
35. Langen M, Leemans A, Johnston P, Ecker C, Daly E, Murphy CM, et al. Fronto-striatal circuitry and inhibitory control in autism: findings from diffusion tensor imaging tractography. *Cortex.* (2012) 48:183–93. doi: 10.1016/j.cortex.2011.05.018
36. Foster NE, Doyle-Thomas KA, Tryfon A, Ouimet T, Anagnostou E, Evans AC, et al. Structural gray matter differences during childhood development in autism spectrum disorder: a multimetric approach. *Pediatr Neurol.* (2015) 53:350–9. doi: 10.1016/j.pediatrneurol.2015.06.013
37. Gebauer L, Skewes J, Westphael G, Heaton P, Vuust P. Intact brain processing of musical emotions in autism spectrum disorder, but more cognitive load and arousal in happy vs. *sad music Front Neurosci.* (2014) 8:192. doi: 10.3389/fnins.2014.00192
38. Sutoko S, Atsumori H, Obata A, Funane T, Kandori A, Shimonaga K, et al. Lesions in the right Rolandic operculum are associated with self-rating affective and apathetic depressive symptoms for post-stroke patients. *Sci Rep.* (2020) 10:20264. doi: 10.1038/s41598-020-77136-5
39. Zhou Y, Shi L, Cui X, Wang S, Luo X. Functional connectivity of the caudal anterior cingulate cortex is decreased in autism. *PLoS ONE.* (2016) 11:e0151879. doi: 10.1371/journal.pone.0151879
40. Liss M, Saulnier C, Fein D, Kinsbourne M. Sensory and attention abnormalities in autistic spectrum disorders. *Autism.* (2006) 10:155–72. doi: 10.1177/1362361306062021
41. Jao Keehn RJ, Sanchez SS, Stewart CR, Zhao W, Grenesko-Stevens EL, Keehn B, et al. Impaired downregulation of visual cortex during auditory processing is associated with autism symptomatology in children and adolescents with autism spectrum disorder. *Autism Res.* (2017) 10:130–43. doi: 10.1002/aur.1636
42. Sharda M, Tuerk C, Chowdhury R, Jamey K, Foster N, Custo-Blanch M, et al. Music improves social communication and auditory-motor connectivity in children with autism. *Transl Psychiatry.* (2018) 8:231. doi: 10.1038/s41398-018-0287-3
43. Thye MD, Bednarz HM, Herringshaw AJ, Sartin EB, Kana RK. The impact of atypical sensory processing on social impairments in autism spectrum disorder. *Dev Cogn Neurosci.* (2018) 29:151–67. doi: 10.1016/j.dcn.2017.04.010
44. Prigge MD, Bigler ED, Fletcher PT, Zielinski BA, Ravichandran C, Anderson J, et al. Longitudinal Heschl's gyrus growth during childhood and adolescence in typical development and autism. *Autism Res.* (2013) 6:78–90. doi: 10.1002/aur.1265
45. Kim D, Lee JY, Jeong BC, Ahn JH, Kim JI, Lee ES, et al. Overconnectivity of the right Heschl's and inferior temporal gyrus correlates with symptom severity in preschoolers with autism spectrum disorder. *Autism Res.* (2021) 14:2314–29. doi: 10.1002/aur.2609
46. Abbott AE, Linke AC, Nair A, Jahedi A, Alba LA, Keown CL, et al. Repetitive behaviors in autism are linked to imbalance of corticostriatal connectivity: a functional connectivity MRI study. *Soc Cogn Aff.* (2018) 13:32–42. doi: 10.1093/scan/nsx129
47. Padmanabhan A, Lynn A, Foran W, Luna B, O'Hearn K. Age related changes in striatal resting state functional connectivity in autism. *Front Hum Neurosci.* (2013) 7:814. doi: 10.3389/fnhum.2013.00814
48. Jaspers E, Balsters JH, Kassraian Fard P, Mantini D, Wenderoth N. Corticostriatal connectivity fingerprints: probability maps based on resting-state functional connectivity. *Hum Brain Mapp.* (2017) 38:1478–91. doi: 10.1002/hbm.23466
49. Spitoni GF, Pireddu G, Cimmino RL, Galati G, Priori A, Lavidor M, et al. Right but not left angular gyrus modulates the metric component of the mental body representation: a tDCS study. *Exp Brain Res.* (2013) 228:63–72. doi: 10.1007/s00221-013-3538-9
50. Yang X, Si T, Gong Q, Qiu L, Jia Z, Zhou M, et al. Brain gray matter alterations and associated demographic profiles in adults with autism spectrum disorder: a meta-analysis of voxel-based morphometry studies. *Aust N Z J Psychiatry.* (2016) 50:741–53. doi: 10.1177/0004867415623858

Conflict of Interest: The authors declare that the research was conducted in the absence of any commercial or financial relationships that could be construed as a potential conflict of interest.

frontiers | Frontiers in Psychiatry

ORIGINAL RESEARCH
published: 26 May 2022
doi: 10.3389/fpsyt.2022.885477

Diffusion Abnormality in Temporal Lobe Epilepsy Patients With Sleep Disorders: A Diffusion Kurtosis Imaging Study

*Min Guo[1], Boxing Shen[1], Jinhong Li[1], Xiaoqi Huang[1], Jie Hu[1], Xiaocheng Wei[2], Shaoyu Wang[3], Ruohan Yuan[1], Chengcheng He[1] and Yanjing Li[1]**

[1] Department of Radiology, Yanan University Affiliated Hospital, Yanan, China, [2] MR Research China, GE Healthcare, Beijing, China, [3] MR Scientific Marketing, Siemens Healthineers, Shanghai, China

OPEN ACCESS

Edited by:
Yuanqiang Zhu,
Fourth Military Medical University, China

Reviewed by:
Haihua Bao,
Affiliated Hospital of Qinghai University, China
Guihua Jiang,
Guangdong Second Provincial General Hospital, China
Guanmin Quan,
Second Hospital of Hebei Medical University, China

***Correspondence:**
Yanjing Li
lixiang_068@163.com

Specialty section:
This article was submitted to Neuroimaging and Stimulation, a section of the journal Frontiers in Psychiatry

Received: 28 February 2022
Accepted: 13 April 2022
Published: 26 May 2022

Citation:
Guo M, Shen B, Li J, Huang X, Hu J, Wei X, Wang S, Yuan R, He C and Li Y (2022) Diffusion Abnormality in Temporal Lobe Epilepsy Patients With Sleep Disorders: A Diffusion Kurtosis Imaging Study. Front. Psychiatry 13:885477. doi: 10.3389/fpsyt.2022.885477

Background: Patients with temporal lobe epilepsy (TLE) frequently complain of poor sleep quality, which is a condition that clinicians are typically neglecting. In this study, Epworth Sleepiness Scale (ESS), Pittsburgh Sleep Quality Index (PSQI), and Athens Insomnia Scale (AIS) were used to assess the sleep status of patients with temporal lobe epilepsy (TLE). Simultaneously diffusion kurtosis imaging (DKI) was applied to examine the white matter microstructure abnormalities in patients with TLE and sleep disorders.

Methods: TLE patients who have been diagnosed in the cardio-cerebrovascular ward of the Yanan University Affiliated Hospital from October 2020 to August 2021 were recruited. Finally, 51 patients and 30 healthy controls were enrolled in our study, with all subjects completing the sleep evaluation questionnaire and undergoing a DKI examination. Using independent sample *t*-test, analysis of variance (ANOVA), and Mann-Whitney U test to compare groups.

Results: Thirty patients (58.82%) complained of long-term sleep difficulties. The overall differences among the evaluation of AIS, ESS, and PSQI are significant ($P = 0.00$, $P = 0.00$, $P = 0.03$). The scores of AIS, ESS in Left and Right-TLE (L/R-TLE) with sleep disorders, as well as PSQI in L-TLE, are statistically higher than the control group ($P = 0.00$, $P = 0.00$, $P = 0.00$, $P = 0.00$, $P = 0.02$). L-TLE with sleep disorders showed decreased MK on affected sides ($P = 0.01$). However, statistical differences in MD and FA have not been observed ($P = 0.34$, $P = 0.06$); R-TLE with sleep disorders showed significantly decreased MK and increased MD on affected sides ($P = 0.00$, $P = 0.00$), but FA's statistical difference has not been observed ($P = 0.20$).

Conclusions: TLE patients with sleep disorders have different DKI parameters than individuals who do not have sleep issues. During this process, the kurtosis parameter (MK) was more sensitive than the tensor parameters (MD, FA) in detecting the patient's aberrant white matter diffusion. DKI may be a better choice for *in vivo* investigation of anomalous craniocerebral water diffusion.

Keywords: diffusional kurtosis imaging (DKI), temporal lobe epilepsy (TLE), sleep disorders, sleep questionnaires, abnormal white matter structure

INTRODUCTION

The most prevalent intractable focal epilepsy is temporal lobe epilepsy (TLE), which is frequently linked with hippocampal sclerosis (HS) (1). Moreover, the location of TLE tissue damage followed a specific anatomical and functional pattern, with the sections directly or indirectly related to the medial temporal lobe being the most affected (2). Seizures affect patients' cognitive abilities and quality of life (3) and negatively affect sleep structure. Previous studies discovered that poor sleep quality would affect peoples' memory formation and life wellbeing (4). Although the interaction between seizures and sleep issues is still under research, sleep disorders have become a common but often overlooked problem in patients with epilepsy by neurologists. Sleep disorders are common comorbidities in epilepsy, such as obstructive sleep apnea syndrome (OSA), restless legs syndrome, and chronic insomnia. Sleep deficit, poor sleep quality, and daytime sleepiness are common complaints among clinical TLE patients (5). According to statistics, about 50% of patients have chronic insomnia (6).

Early identification of the comorbidity can help ameliorate patients' epilepsy burden and improve their quality of life. Yaranagula (7) found that although surgery can control the frequency of seizures, the sleep quality of the patients did not improve. The sleep quality scores before and after surgery were lower, so the purpose of epilepsy treatment should not be limited to controlling the frequency, but also to treat the disease on the adverse effects on the patient, such as sleep, are minimized. Rapid eye movement (REM) has a protective effect on seizures (8). Previous studies have used polysomnography (PSG) to investigate the sleep structure of TLE patients and compared the sleep status of patients without seizures during the day with the patients after seizures, finding that nighttime REM sleep was significantly reduced after seizures and that reductions were more pronounced after nighttime seizures than daytime seizures, patients also experienced significantly lower sleep efficiency, and the effect of L-TLE on REM was more significant after nighttime seizures than daytime seizures (9).

The anomalous diffusion of cerebral water molecules was discovered in researches that used diffusion tensor imaging (DTI) to examine patients with primary insomnia (PI) (10). Jensen first introduced diffusional kurtosis imaging (DKI) in 2005, which expands traditional DTI by estimating the kurtosis of the water diffusion probability distribution function. DKI can provide both kurtosis parameters and tensor parameters. Many researchers have used DKI to assess microscopic white matter abnormalities in patients with various types of epilepsy using the region of interest (ROI), voxel analysis, and automated fiber quantification (AFQ) and have discovered abnormal brain regions and extensive anomalies in brain networks (1, 11, 12). Nonetheless, this approach has hardly been used in studies to identify subtle structural abnormalities in TLE patients with sleep disturbances. Furthermore, in clinical work, sleep questionnaires are frequently used to examine the subjective sleep experience of TLE patients.

Our purpose is to use the DKI to analyze microstructural abnormalities in white matter in TLE patients with subjective sleep issues and to measure patients' subjective sleep quality by delivering sleep questionnaires. We also looked into the differences in sleep scores between sick and healthy controls.

SUBJECTS AND METHODS

Participants

The local institutional review board of the Yanan University Affiliated Hospital approved this prospective study (number: YAS-S01-202106001), and informed consent was obtained from all participants. From October 2020 to August 2021, patients suspected of having unilateral TLE were recruited for this study. Inclusion criteria were as follows: (1) in line with the International League Against Epilepsy (ILAE) and the International Bureau for Epilepsy (IBE) (13) diagnostic criteria for TLE; (2) younger than 50 years old, since previous research have suggested that adults over 50 had different sleep habits than younger people (14); (3) had no seizures within 24 h before MR examination and (4) had complete DKI-MRI data and sleep status data available. Of the 57 patients initially enrolled, 6 were excluded (2 with obvious image artifacts, 1 with concomitant white matter lesions grade III, 1 is encephalitis secondary epilepsy, and 2 with concomitant traumatic brain injury). Finally, 51 patients with unilateral TLE were enrolled. Another 30 healthy volunteers with no neurological abnormalities were also recruited to form a control group.

Neurologists referred to the International Classification of Sleep Disorders-third edition (ICSD-3) and screened patients for underlying sleep disorders, such as insomnia, somnolence, sleep-related breathing disorders or movement disorders (restless legs syndrome), etc. (15), based on their main complaints. Then allocated subjects to 3 subgroups, consisting of TLE patients with sleep disorders, without sleep disorders and the control group. A flow chart is shown in **Figure 1**.

Sleep Questionnaires Evaluation

Epworth Sleepiness Scale

Excessive daytime sleepiness (EDS) is described as a recent three-month inability to stay awake during the primary awake part of the day. The Epworth Sleepiness Scale (ESS) (16) is a questionnaire that assesses a person's daytime sleepiness. Participants were asked to rate their chances of nodding off in various situations. It can determine the likelihood of dozing off in eight situations that we encounter daily, which spans from 0 (never dozing off) points to 3 (frequently dozing off). Previous research (17) validated the construct validity and internal consistency of the score. An ESS score of more than ten is seen as abnormal (7, 18).

Pittsburgh Sleep Quality Index

The Pittsburgh Sleep Quality Index (PSQI) (19) was compiled in 1989 to assess sleep quality during the previous month. It consists of 19 self-evaluated questions and five roommate-evaluated questions, with the last five items being used

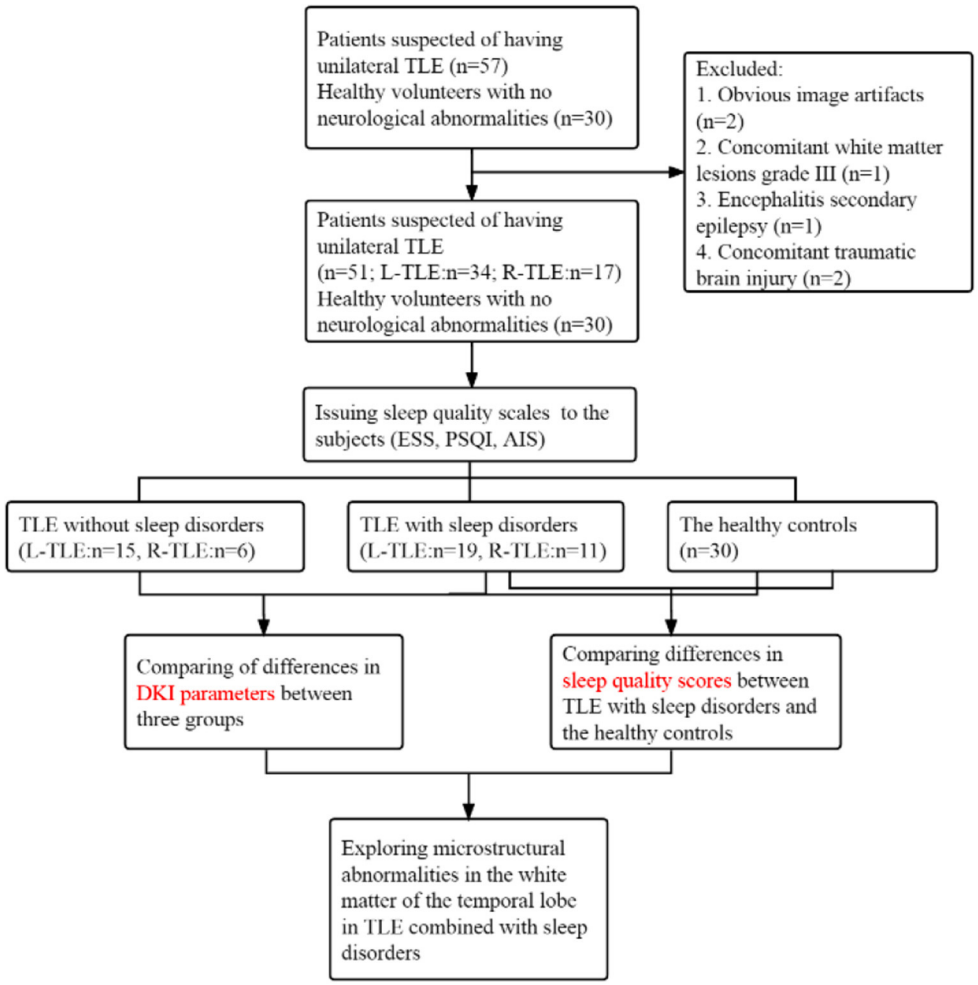

FIGURE 1 | A flow chart is used to show the implementation method of the study.

solely for clinical data. These 19 self-assessment questions look at a variety of sleep-related characteristics, such as sleep length and latency estimates, as well as the frequency and severity of specific sleep-related issues. These 19 items are separated into seven components, and the scores from the seven components are summed together to provide a PSQI score (0–21). The higher the score, the poorer the sleep quality. The sleep quality scale measures subjective sleep quality, sleep latency, and sleep length, among other things. A PSQI score of more than five is considered abnormal (7).

Athens Insomnia Scale

The Athens Insomnia Scale (AIS) (20) is an eight-item self-assessment of sleep status with a total score of 0–24, with 1–5 questions evaluating sleep status and 6–8 items evaluating daytime mental state, an AIS score of more than six are considered abnormal (21). The Chinese version (22) of AIS has been proven to be reliable and effective in adolescents and adults.

Magnetic Resonance Imaging Acquisition and Data Analysis

Images acquisition were performed on a 3T MRI scanner (Magnetom Verio, Siemens Healthineers, Erlangen, Germany) equipped with an 8-channel head coil. The conventional MRI protocols included the following sequences: axial T1-weighted, axial T2-weighted, and axial FLAIR images. The detail parameters about DKI imaging were: TR = 11000 ms, TE = 96 ms, field- of- view = 230 × 230 mm^2, matrix size = 100 × 100, scanning slice thickness = 2 mm, b = 0, 1,000 and 2,000 s/mm^2, using 30 different diffusion coding directions totally.

The images were double-blind analyzed by two neuroimaging physicians who have worked for over 10 years and the average of the two was taken as the final result. The diffusional kurtosis estimator software (https://www.nitrc.org/projects/dke/Version2.6) was used to analyze raw diffusion images and calculate DKI's parametric maps, specifically maps of mean diffusivity (MD), fractional anisotropy (FA), and mean kurtosis (MK). **Figure 2** shows a representation of DKI's major

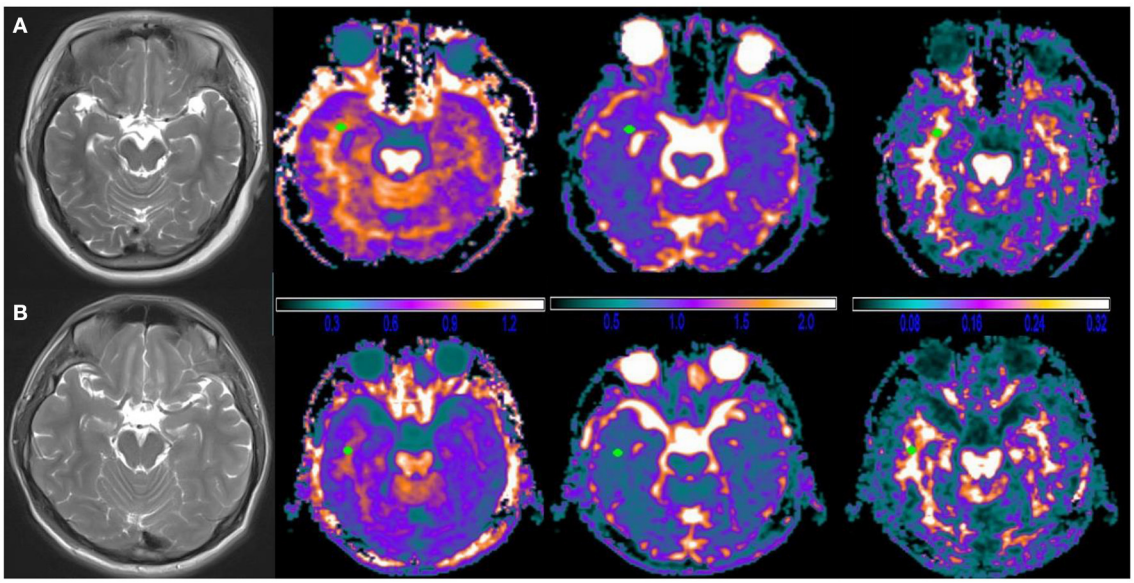

FIGURE 2 | Typical diffusional kurtosis imaging (DKI)-derived parametric maps in a case brain. **(A)** Female, 27 years old, R-TLE with sleep disorder, **(B)** Male, 35 years old, R-TLE without sleep disorder; from left to right are T2WI images, mean kurtosis (MK) maps, mean diffusivity (MD) maps and fractional anisotropy (FA) maps. No clear abnormalities were seen on T2WI images and DKI images in both patients, which could be detected by measurement of DKI parameters. Note: the unit of MD is μm^2/ms, and FA, MK are dimensionless.

TABLE 1 | The demographic and clinical characteristics in subjects of the study.

Characteristics	L-TLE ($n = 34$)	R-TLE ($n = 17$)	HC ($n = 30$)	$F/\chi^2/z$	*P* value
Age (years)	23.52 ± 11.10	27.45 ± 8.51	28.52 ± 11.53	1.29	0.28[a]
Duration (years)	3 (0.42,8)	1.2 (1.0,6.7)	/	−1.30	0.19[b]
Gender (male/female)	16/18	7/10	11/19	0.71	0.70[c]
Sleep disorder (with/not)	19/15	11/6	0/30	28.41	0.00[c]
Type of AED:					
Levetiracetam	17	6	/	1.37	0.71[c]
Lamotrigine	6	5	/		
Valproate sodium	8	4	/		
No medication	3	2	/		

L-TLE, Left-TLE; R-TLE, Right-TLE; HC, The healthy control group.
[a]Analysis of variance (ANOVA) [b]Mann-Whitney U-test [c]Chi-square test.

parametric maps. Using the T1WI image as a reference, one circular ROI was drawn in the white matter of the temporal lobe on the affected side of patients and matched side of control group through MRIcron software (https://www.nitrc.org/projects/mricron/Version1.0.20190902), avoiding the sulci, split-brain, and ventricle. The ROI would be no <25 mm^2, and the average would be taken by measuring at the same point on three consecutive levels of MK, MD, and FA graphs (23).

Statistical Analysis

SPSS software was used to analyze the data (version 20.0). Continuous variables utilize mean±standard deviation (m±SD), while categorical variables use frequency. An independent sample *t*-test, analysis of variance (ANOVA), and Mann-Whitney U test were used to compare between groups, depending on the normality of the data. *Post-hoc* pairwise comparisons were performed using *LSD-t* test. The Chi-square test and Fisher-Freeman-Halton test were used to study the association between categorical variables. A $P < 0.05$ is considered significant.

RESULTS

Demographic and Clinical Characteristics of Subjects

After screening, 51 TLE were finally enrolled (23 males and 28 females). Video EEG revealed unusual temporal lobe discharge on one side, including 34 cases of Left-TLE (L-TLE) and 17 cases of Right-TLE (R-TLE). **Table 1** shows demographic information and clinical traits. Thirty patients (58.82%) complained of

TABLE 2 | The score of self-evaluation sleep questionnaire in subjects of the study.

Items	AIS(score)	ESS(score)	PSQI(score)	Number		
				score of AIS≥6	score of ESS≥10	score of PSQI>5
L-TLE ($n = 19$)	6.21 ± 2.66	5.84 ± 2.58	5.16 ± 2.60	10	2	5
R-TLE ($n = 11$)	5.81 ± 2.35	6.27 ± 2.53	4.46 ± 1.97	6	1	3
HC ($n = 30$)	2.38 ± 1.28	3.15 ± 1.31	3.34 ± 1.77	0	0	0
F/χ^2	18.79	3.62	3.96	0.25		
P value	0.00[a]	0.00[a]	0.03[a]	1.00[b]		

[a]*Analysis of variance (ANOVA)* [b]*Fisher-Freeman-Halton test (n < 40).*

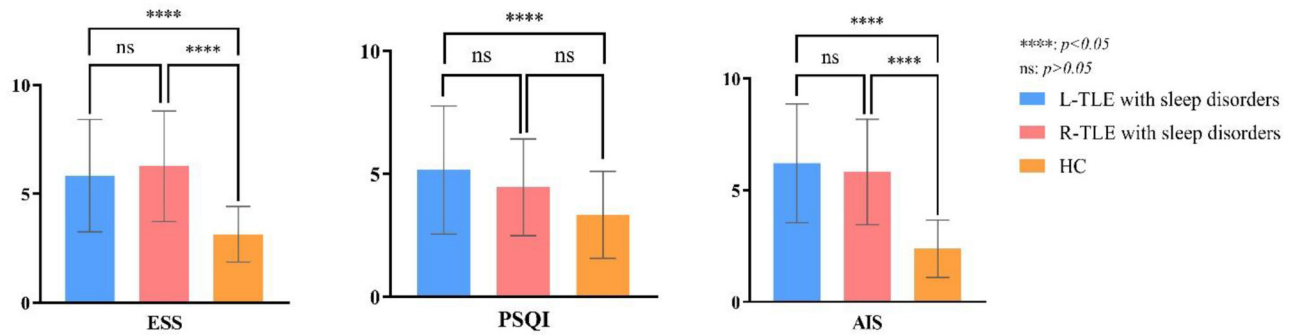

FIGURE 3 | *Post-hoc* multiple comparison in sleep scores of TLE with sleep disorders and the healthy controls.

long-term sleep difficulties, while 21 thought sleep quality was satisfactory. Five patients (9.80%) did not take any medications; the others took the single antiepileptic therapy (AED).

Results of Self-Evaluation Sleep Questionnaire

Table 2 compares the overall differences in AIS, ESS, and PSQI scores between TLE with sleep disorders and the control group. The AIS, ESS, and PSQI total differences are statistically significant ($P = 0.00$, $P = 0.00$, $P = 0.03$). **Figure 3** shows the pairwise comparison: the scores of L/R-TLE in AIS, ESS, and PSQI in L-TLE are statistically higher than the control group ($P = 0.00$, $P = 0.00$, $P = 0.00$, $P = 0.00$, $P = 0.02$). Although the difference in PSQI between R-TLE and the control group was not statistically significant, the mean value was higher than the control group. The number of patients with abnormal scores (AIS≥6, ESS≥10, and PSQI>5) was few, and no statistical difference was detected.

MK, MD and FA Values in White Matter of the Temporal Lobe on Subjects

Nineteen combined with sleep disorders and 15 without in L-TLE, as illustrated in **Table 3**. We compared the DKI parameters in three groups: L-TLE with sleep disorders, L-TLE without sleep disorders, and the control group. We manually delineated the ROI and quantified the MK, MD, and FA values on the afflicted side (left) of a patient and matched the side of the control group (left). **Table 3** and **Figure 4** demonstrate the results.

TABLE 3 | ANOVA of DKI parameters between L-TLE with or without sleep disorders and the healthy controls.

DKI parameters	L-TLE ($n = 34$)		
	MK	MD	FA
With sleep disorder ($n = 19$)	0.8112 ± 0.12	1.0550 ± 0.16	0.2401 ± 0.08
Without sleep disorder ($n = 15$)	0.9374 ± 0.13	1.0011 ± 0.16	0.3041 ± 0.11
HC-L ($n = 30$)	1.0299 ± 0.15	0.9049 ± 0.13	0.3655 ± 0.08
F	15.61	6.33	13.32
P value	0.00	0.00	0.00

The overall difference in MK, MD, and FA between these three groups was statistically significant ($P = 0.00$). The FA, MK of TLE decreased, and the MD increased compared to the control group, regardless of whether sleep disturbance was combined (FA: $P = 0.00$, $P = 0.01$; MD: $P = 0.00$, $P = 0.04$; MK: $P = 0.00$, $P = 0.03$). Especially MK was significantly lower in the sleep disorder group than without sleep disorder ($P = 0.01$). FA was also lower, though not statistically significant ($P = 0.06$). We did not observe a significant difference in MD between the sleep disorder group and those without ($P = 0.30$).

In R-TLE, eleven combined with sleep disorders and six without, as illustrated in **Table 4**. As with L-TLE, we compared DKI parameters between these three groups in the patient's afflicted side (right) and matched side of the control group (right): R-TLE with sleep disorders, R-TLE without

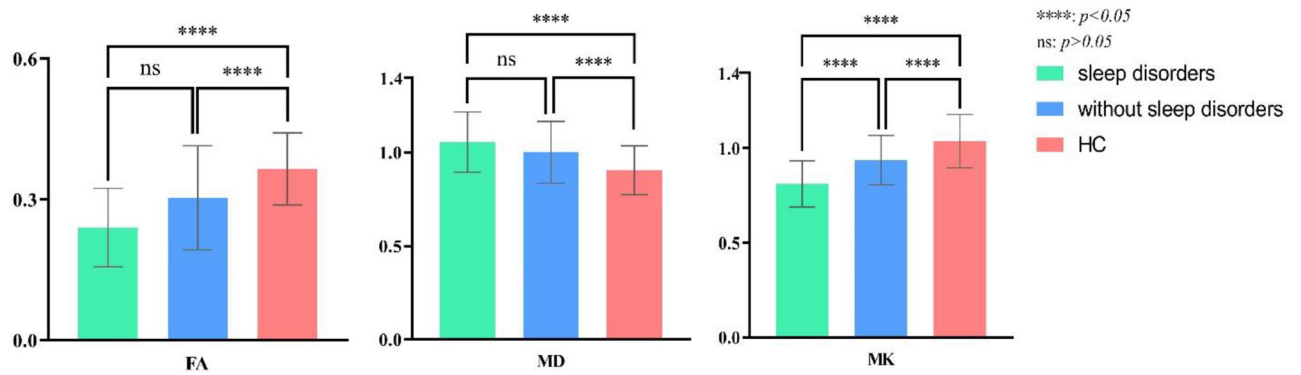

FIGURE 4 | *Post-hoc* multiple comparison in DKI parameters of L-TLE with or without sleep disorders and the healthy controls.

TABLE 4 | ANOVA of DKI parameters between R-TLE with or without sleep disorders and the healthy controls.

DKI parameters	R-TLE (n = 17)		
	MK	MD	FA
With sleep disorder (n = 11)	0.7924 ± 0.12	1.2568 ± 0.11	0.2494 ± 0.06
Without sleep disorder (n = 6)	1.0401 ± 1.13	0.9459 ± 0.21	0.2863 ± 0.04
HC-R (n = 30)	1.1312 ± 0.15	0.8280 ± 0.13	0.3701 ± 0.09
F	22.35	39.24	9.81
P value	0.00	0.00	0.00

sleep disorders, and the control group. **Table 4** and **Figure 5** demonstrate the results.

The overall difference in MK, MD, and FA between these three groups was statistically significant ($P = 0.00$). The FA, MK of TLE with sleep disorders reduced, and the MD increased than that of the control group (FA: $P = 0.00$; MD: $P = 0.00$; MK: $P = 0.00$). There were only six individuals in R-TLE without sleep disorders, so only FA was found to be reduced in without sleep disorder group than the control group ($P = 0.00$), and we did not found difference in MK and MD between them (MD: $P = 0.06$; MK: $P = 0.17$).

The sleep disorder group found significantly higher MD and lower MK patients (MD: $P = 0.00$; MK: $P = 0.00$). The difference in FA between the sleep disorder group and those without has not been observed ($P = 0.39$).

DISCUSSION

Our study's combination of sleep disorders with DKI is a significant advantage, which previous investigations hardly used. Another advantage is the homogeneity of subjects; we controlled for factors that might affect sleep quality, such as age and the amount of medication.

Mechanisms of the interaction between seizures and sleep have been under investigation. Abnormal electrical discharges between seizures can lead to sleep disruption (6), and the disruption of a patient's normal sleep would exacerbate the seizures. Sleep quality also affects the type and likelihood of a patient's seizures, and the association between sudden unexpected death in epilepsy (SUDEP) and sleep is also gradually being recognized.

Our research grouped the sleep condition of patients with TLE and investigated the microstructure through DKI. Meanwhile, we evaluated the sleep quality scores between patients with sleep disorders and the control group by sleep questionnaires. We discovered that TLE with sleep difficulties are pretty common (58.82% in this study), and the values of DKI's parameters also have anomalies.

The diffusion environment of water molecules is affected in TLE due to injured nerve fiber bundles, disrupted white matter integrity, and proliferation of irregular glial cells. Therefore, differences exist in DKI parameters between TLE and the controls. The preliminary results of the present study are also close to our previous works on the microstructure of TLE. However, we aimed to apply the DKI technique to subgroup further comparisons between comorbid sleep disorders and non-comorbid sleep disorders. We want to obtain more information about comorbidities and support individualized treatment of patients with sleep problems.

TLE patients frequently experience insomnia, poor sleep quality, and excessive daytime drowsiness. The prescription of AEDs mainly focused on reducing seizures, and it is easy to overlook other mental and sleep disorders that patients may be experiencing. Our study only included individuals who used one AED to minimize the effects of AEDs on sleep. Drugs have a significant impact on the sleep quality of PWE, prior investigations have reported that combining numerous AEDs can result in a decrease in sleep quality in patients (24).

Twenty-three patients (50%) utilized Levetiracetam in our investigation. Studies (25) have shown that large-dose levetiracetam use caused excessive drowsiness during the day. Patients with sleep disorders had a higher ESS score could be related to their medication. Furthermore, daytime sleepiness in patients may be related to other multiple factors, such

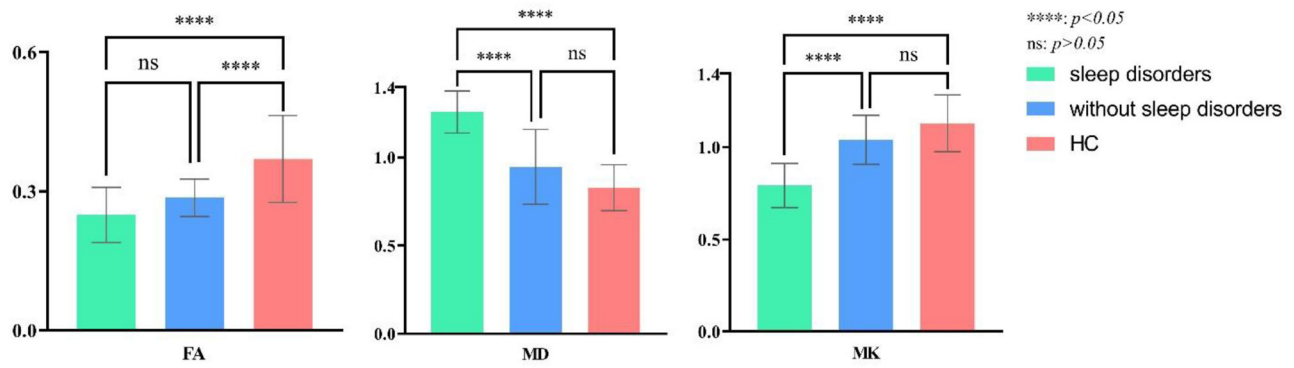

FIGURE 5 | *Post-hoc* multiple comparison in DKI parameters of R-TLE with or without sleep disorders and the healthy controls.

as nocturnal seizures, sedative effects of AEDs, and sleep deprivation at night. However, the number of abnormal ESS scale scores was lower, probably because excessive daytime sleepiness was more common in frontal lobe epilepsy than TLE (26). Lamotrigine and valproate sodium were the other two medicines the patients took in this study. Foldvary (27) compared lamotrigine to several older antiepileptic medicines and concluded that lamotrigine users rarely have significant daytime sleepiness or night sleeplessness. As Foldvary's article indicates, valproate sodium also has no substantial effect on sleep structure (28).

White matter plays a vital role in regulating brain activity and the coupling between brain regions and behavioral regulation (29). Previous studies have found that the proportion of fiber bundles in the left striatum and hippocampus of insomnia patients reduced through DTI technology (30), which may mean the abnormal reduction of white matter fiber tracts in insomnia patients. To further explore the microstructure abnormalities of TLE with sleep disorders, our study used DKI for patients' brain imaging and analysis. Compared with DTI, DKI can describe higher-order diffusion dynamics and more complex diffusion distribution. DKI could detect complex and crossed white matter fiber bundles and provide more comprehensive quantitative parameters, which will help improve the disease detection rate of white matter abnormalities (1). Although the number of studies related to abnormal white matter structure in sleep disorders is lacking, it has confirmed that abnormal changes in microstructure and brain networks exist in the brain of this group, and this abnormality spreads from the limbic system to the entire brain (31).

Numerous previous studies have demonstrated that sleep plays an essential role in the brain. Neuroimaging found sleep disturbances associated with functional deficits as measured by fMRI or atrophy of the cerebral cortex, and the integrity of the white matter microstructure may underlie these associations. Poor sleep may disrupt axonal integrity and degenerate white matter, but white matter pathology may also precede sleep disturbance (32).

Voldsbekk et al. (33) combined spherical mean technique (SMT) and diffusion imaging to inquire into differences between sleep deprivation and normal sleep-wake-cycle (SWC) group. He discovered that sleep deprivation was associated with extensive white matter changes and had an abnormal intracranial diffusion coefficient. Vyas (34) utilized DKI to brain microstructural changes in OSA and detected abnormalities in kurtosis parameters in several brain regions of the patients. They indicated that kurtosis parameters are more sensitive to abnormalities shown at the microcosmic structure level before detectable abnormalities appear in conventional MRI or other imaging modalities.

As a classic parameter of DKI, MK is related to the microstructure changes of many diseases and is sensitive to more subtle brain changes. The increase in the myelin sheath of white matter fibers, dense accumulation of axons and fiber bundles, and decreases in the permeability of the axon membrane caused increases in kurtosis parameters. MK decreased in the sleep disorder comorbidity group in our study. It could be due to a net loss of microscopic tissue complexity caused by damage to the myelin barrier and other microscopic cell structures in these areas, such as the loss of nerve synapses. Which results in decreased cell connections, decreased tissue integrity, and increased extracellular gap (35), and is also consistent with pathological denervation (1). Epilepsy activity and long-term parasomnia may make water molecules in the brain more susceptible to spreading toward synchrony. In an immunohistochemistry investigation of Huntington's disease (36), the number of fibers that can be stained and arranged orderly reduced in regions with decreased kurtosis values.

The present study differs from Tummala's study on OSA (37), which found increased kurtosis parameters in several intracranial regions. They suggested that the hypoxic and ischemic damage caused by OSA may cause swelling of neurons and axons, leading to acute axonal and myelin tissue damage. This study also proposed that the mechanism for the increased kurtosis parameter in acute disease may be the incremental extracellular fluid due to degeneration of axons and myelin sheaths, the more pronounced the non-Gaussian nature of water molecule

diffusion. In contrast, in chronic disease, for instance, epilepsy, the diffusion of water molecules tends to be more Gaussian in distribution due to the decrease in axons, myelin, neurons, and glial cells and the increase in extracellular gaps.

MD variations linked to the activity dynamics of epileptic seizures according to the previous research (38, 39): in the hyper-acute phase after protracted convulsions or status epilepticus, MD decreases due to cytotoxic edema. MD gradually develops during the sub-acute attack period (∼5 days), which is linked to angioedema, while the chronic phase of neuron loss and gliosis leading to an increase in interstitial water content will further lead to an increase in MD.

In our study, the MD of TLE with sleep disorders also tended to higher than patients without sleep disorders. This difference is significant in R-TLE, which may also be consistent with reports of increased MD in the sub-acute state because all patients included in this study had no seizures within 24 h before the scanning. The finding also supports the notion of extensive axonal and neuronal damage. Our results were consistent with research on Rapid eye movement (REM) sleep behavior disorder (RBD), which found the increased MD value in many brain regions (40).

FA is the most often used parameter in daily work and scientific research in neuroimaging and represents water molecules' degree of anisotropic diffusion. The degree of dispersion more noticeable, the bigger the FA. Although the difference in FA in our study was not significant, a downward trend can still be seen, particularly in L-TLE. A decrease in FA reflects the blockage of water molecule transport in the lesion area. The variations in axon density and the integrity of the myelin membrane frequently disrupted water diffusion, the transient increase in diffusion rate generated by the start of angioedema may enhance the probability of water molecules encountering the barrier (41, 42). Our results are similar to Kang's article. He discovered differences in white matter tract spread measures on white matter connections in the left thalamus and inferior frontal gyrus in insomniacs. Insomniacs had compromised white matter integrity, and FA reduced compared with healthy controls. The results may also provide new evidence for decreased connectivity in the thalamic-frontal regions of insomnia patients in functional imaging studies (43). In the future, increasing the sample size may result in more statistically significant findings.

We did not overemphasize the causal relationship between TLE and sleep disorders, which may lead to inappropriate treatment of sleep disorders. Some neurologists may focus on resolving sleep disorders by controlling the primary disease, thus neglecting to correct the patient's sleep problems alone. However, treating the primary disease and sleep disorders should be carried out simultaneously and curing sleep problems also promotes the effectiveness of treatment of the primary disease (15).

However, we still have some limitations: First and foremost, since we have no obtained histology specimens, we must rely on past research to make assumptions. We should collect more longitudinal data from patients to investigate the disease's unique mechanisms. Second, to avoid drug effects on sleep quality, the patients we studied all used only one AED, which may leave out the group of patients treated with a mix of medicines and could have more specific abnormalities in diffusion parameters. Third, our study is a cross-sectional study, and we have not yet obtained a causal relationship from it. So it is unclear whether the abnormality in the observed white matter microstructure is the cause or the result. We hope that future studies with longitudinal designs will identify causal directionality. Fourth, the study's sample size was small (especially in R-TLE), and future continued expansion of the sample size will hopefully lead to more meaningful results.

CONCLUSIONS

To summarize, our research discovered the abnormal DKI parameters in TLE with sleep disorders. The kurtosis parameter (MK) is more sensitive than the tensor parameters (MD, FA) in detecting aberrant white matter diffusion in the patient during this procedure. The DKI properties revealed in our study may represent the underlying pathophysiological mechanism of TLE with sleep disorders, which will need verifying in future investigations.

DATA AVAILABILITY STATEMENT

The original contributions presented in the study are included in the article/supplementary material, further inquiries can be directed to the corresponding author.

ETHICS STATEMENT

The studies involving human participants were reviewed and approved by Ethics Committee of the Yanan University Affiliated Hospital. Written informed consent to participate in this study was provided by the participants' legal guardian/next of kin.

AUTHOR CONTRIBUTIONS

MG and YL proposed the article concept and wrote the manuscript. BS, JH, and JL conducted data collection and analysis. RY and CH conducted the statistical analysis. XW and SW supported the MR technology for this article. XH, MG, and YL supervised the whole research and received funding. All authors have read and approved the final version of the article.

FUNDING

The Red Cross Foundation of China funded the study (approval number: XM_HR_ICON_2020_10_07).

ACKNOWLEDGMENTS

Sincere thanks to all the patients and volunteers who participated in this study, and the engineers of Siemens AG of Germany who provided technical support, the study was completed with the cooperation of everyone.

REFERENCES

1. Glenn GR, Jensen JH, Helpern JA, Spampinato MV, Kuzniecky R, Keller SS, et al. Epilepsy-related cytoarchitectonic abnormalities along white matter pathways. *J Neurol Neurosurg Psychiatry.* (2016) 87:930–6. doi: 10.1136/jnnp-2015-312980
2. Coan AC, Appenzeller S, Bonilha L, Li LM, Cendes F. Seizure frequency and lateralization affect progression of atrophy in temporal lobe epilepsy. *Neurology.* (2009) 73:834–42. doi: 10.1212/WNL.0b013e3181b783dd
3. Hampton T. Experts describe "spectrum" of epilepsy. *JAMA.* (2010) 303:313–4. doi: 10.1001/jama.2009.1977
4. van Schalkwijk FJ, Ricci M, Nikpour A, Miller LA. The impact of sleep characteristics and epilepsy variables on memory performance in patients with focal seizures. *Epilepsy Behav.* (2018) 87:152–8. doi: 10.1016/j.yebeh.2018.06.034
5. de Weerd A, de Haas S, Otte A, Trenité DK, van Erp G. Cohen A, et al. Subjective sleep disturbance in patients with partial epilepsy: a questionnaire-based study on prevalence and impact on quality of life. *Epilepsia.* (2004) 45:1397–404. doi: 10.1111/j.0013-9580.2004.46703.x
6. Moore JL, Carvalho DZ, St Louis EK, Bazil C. Sleep and epilepsy: a focused review of pathophysiology, clinical syndromes, co-morbidities, and therapy. *Neurotherapeutics.* (2021) 18:170–80. doi: 10.1007/s13311-021-01021-w
7. Yaranagula SD, Asranna A, Nagappa M, Nayak CS, Pratyusha PV, Mundlamuri RC, et al. Sleep profile and Polysomnography in patients with drug-resistant temporal lobe epilepsy (TLE) due to hippocampal sclerosis (HS) and the effect of epilepsy surgery on sleep-a prospective cohort study. *Sleep Med.* (2021) 80:176–83. doi: 10.1016/j.sleep.2020.12.016
8. Ng M, Pavlova M. Why are seizures rare in rapid eye movement sleep? Review of the frequency of seizures in different sleep stages. *Epilepsy Res Treat.* (2013) 2013:932790. doi: 10.1155/2013/932790
9. Nakamura M, Jin K, Kato K, Itabashi H, Iwasaki M, Kakisaka Y, et al. Differences in sleep architecture between left and right temporal lobe epilepsy. *Neurol Sci.* (2017) 38:189–92. doi: 10.1007/s10072-016-2731-6
10. Sanjari Moghaddam H, Mohammadi E, Dolatshahi M, Mohebi F, Ashrafi A, Khazaie H, et al. White matter microstructural abnormalities in primary insomnia: a systematic review of diffusion tensor imaging studies. *Prog Neuropsychopharmacol Biol Psychiatry.* (2021) 105:110132. doi: 10.1016/j.pnpbp.2020.110132
11. Gao J, Feng ST, Wu B, Gong N, Lu M, Wu PM, et al. Microstructural brain abnormalities of children of idiopathic generalized epilepsy with generalized tonic-clonic seizure: a voxel-based diffusional kurtosis imaging study. *J Magn Reson Imaging.* (2015) 41:1088–95. doi: 10.1002/jmri.24647
12. Sinha N, Peternell N, Schroeder GM, de Tisi J, Vos SB, Winston GP, et al. Focal to bilateral tonic-clonic seizures are associated with widespread network abnormality in temporal lobe epilepsy. *Epilepsia.* (2021) 62:729–41. doi: 10.1111/epi.16819
13. Fisher RS, van Emde Boas W, Blume W, Elger C, Genton P, Lee P, et al. Epileptic seizures and epilepsy: definitions proposed by the International League Against Epilepsy (ILAE) and the International Bureau for Epilepsy (IBE). *Epilepsia.* (2005) 46:470–2. doi: 10.1111/j.0013-9580.2005.66104.x
14. Reyner LA, Horne JA, Reyner A. Gender- and age-related differences in sleep determined by home-recorded sleep logs and actimetry from 400 adults. *Sleep.* (1995) 18:127–34.
15. Sateia MJ. International classification of sleep disorders-third edition: highlights and modifications. *Chest.* (2014) 146:1387–94. doi: 10.1378/chest.14-0970
16. Johns MW. A new method for measuring daytime sleepiness: the Epworth sleepiness scale. *Sleep.* (1991) 14:540–5. doi: 10.1093/sleep/14.6.540
17. Sap-Anan N, Pascoe M, Wang L, Grigg-Damberger M, Andrews N, Foldvary-Schaefer NJE, et al. The Epworth Sleepiness Scale in epilepsy: Internal consistency and disease-related associations. *Epilepsy Behav.* (2021) 121:108099. doi: 10.1016/j.yebeh.2021.108099
18. Miner B, Gill TM, Yaggi HK, Redeker NS, Van Ness PH, Han L, et al. The Epidemiology of Patient-Reported Hypersomnia in Persons With Advanced Age. *J Am Geriatr Soc.* (2019) 67:2545–52. doi: 10.1111/jgs.16107
19. Buysse DJ, Reynolds CF 3rd, Monk TH, Berman SR, Kupfer DJ. The Pittsburgh Sleep Quality Index: a new instrument for psychiatric practice and research. *Psychiatry Res.* (1989) 28:193–213. doi: 10.1016/0165-1781(89)90047-4
20. Bastien CH, Vallières A, Morin CM. Validation of the Insomnia Severity Index as an outcome measure for insomnia research. *Sleep Med.* (2001) 2:297–307. doi: 10.1016/s1389-9457(00)00065-4
21. Soldatos CR, Dikeos DG, Paparrigopoulos TJ. The diagnostic validity of the Athens Insomnia Scale. *J Psychosom Res.* (2003) 55:263–7. doi: 10.1016/S0022-3999(02)00604-9
22. Chung KF, Kan KK, Yeung WF. Assessing insomnia in adolescents: comparison of insomnia severity index, athens insomnia scale and sleep quality index. *Sleep Med.* (2011) 12:463–70. doi: 10.1016/j.sleep.2010.09.019
23. Park CH, Ohn SH. A challenge of predicting seizure frequency in temporal lobe epilepsy using neuroanatomical features. *Neurosci Lett.* (2019) 692:115–21. doi: 10.1016/j.neulet.2018.11.005
24. Chakravarty K, Shukla G, Poornima S, Agarwal P, Gupta A, Mohammed A, et al. Effect of sleep quality on memory, executive function, and language performance in patients with refractory focal epilepsy and controlled epilepsy versus healthy controls - a prospective study. *Epilepsy Behav.* (2019) 92:176–83. doi: 10.1016/j.yebeh.2018.12.028
25. Jain SV, Glauser TA. In response: Effects of epilepsy treatments on sleep architecture and daytime sleepiness: an evidence-based review of objective sleep metrics. *Epilepsia.* (2014) 55:778. doi: 10.1111/epi.12597
26. Oldani A, Ferini-Strambi L, Zucconi M. Symptomatic nocturnal frontal lobe epilepsy. *Seizure.* (1998) 7:341–3. doi: 10.1016/S1059-1311(98)80030-7
27. Foldvary N, Perry M, Lee J, Dinner D, Morris HH. The effects of lamotrigine on sleep in patients with epilepsy. *Epilepsia.* (2001) 42:1569–73. doi: 10.1046/j.1528-1157.2001.46100.x
28. Foldvary-Schaefer N, Grigg-Damberger M. Sleep and epilepsy: what we know, don't know, and need to know. *J Clin Neurophysiol.* (2006) 23:4–20. doi: 10.1097/01.wnp.0000206877.90232.cb
29. Bi Y, Yuan K, Yu D, Wang R, Li M, Li Y, et al. White matter integrity of central executive network correlates with enhanced brain reactivity to smoking cues. *Hum Brain Mapp.* (2017) 38:6239–49. doi: 10.1002/hbm.23830
30. Chen L, Shao Z, Xu Y, Wang S, Zhang M, Liu S, et al. Disrupted frontostriatal connectivity in primary insomnia: a DTI study. *Brain Imaging Behav.* (2021) 15:2524–31. doi: 10.1007/s11682-021-00454-3
31. Spiegelhalder K, Regen W, Prem M, Baglioni C, Nissen C, Feige B, et al. Reduced anterior internal capsule white matter integrity in primary insomnia. *Hum Brain Mapp.* (2014) 35:3431–8. doi: 10.1002/hbm.22412
32. Kocevska D, Cremers LGM, Lysen TS, Luik AI, Ikram MA, Vernooij MW, et al. Sleep complaints and cerebral white matter: A prospective bidirectional study. *J Psychiatr Res.* (2019) 112:77–82. doi: 10.1016/j.jpsychires.2019.02.002
33. Voldsbekk I, Groote I, Zak N, Roelfs D, Geier O, Due-Tønnessen P, et al. Sleep and sleep deprivation differentially alter white matter microstructure: A mixed model design utilising advanced diffusion modelling. *Neuroimage.* (2021) 226:117540. doi: 10.1016/j.neuroimage.2020.117540
34. Vyas S, Singh P, Khandelwal N, Govind V, Aggarwal AN, Mohanty M. Evaluation of cerebral microstructural changes in adult patients with obstructive sleep apnea by MR diffusion kurtosis imaging using a whole-brain atlas. *Indian J Radiol Imaging.* (2019) 29:356–63. doi: 10.4103/ijri.IJRI_326_19
35. Garza-Villarreal EA, Chakravarty MM, Hansen B, Eskildsen SF, Devenyi GA, Castillo-Padilla D, et al. The effect of crack cocaine addiction and age on the microstructure and morphology of the human striatum and thalamus using shape analysis and fast diffusion kurtosis imaging. *Transl Psychiatry.* (2017) 7:e1122. doi: 10.1038/tp.2017.92
36. Blockx I, De Groof G, Verhoye M, Van Audekerke J, Raber K, Poot D, et al. Microstructural changes observed with DKI in a transgenic Huntington rat model: evidence for abnormal neurodevelopment. *Neuroimage.* (2012) 59:957–67. doi: 10.1016/j.neuroimage.2011.08.062
37. Tummala S, Roy B, Vig R, Park B, Kang DW, Woo MA, et al. Non-Gaussian Diffusion Imaging Shows Brain Myelin and Axonal Changes in Obstructive Sleep Apnea. *J Comput Assist Tomogr.* (2017) 41:181–189. doi: 10.1097/RCT.0000000000000537

38. Scott RC, King MD, Gadian DG, Neville BG, Connelly A. Prolonged febrile seizures are associated with hippocampal vasogenic edema and developmental changes. *Epilepsia.* (2006) 47:1493–8. doi: 10.1111/j.1528-1167.2006.00621.x
39. Concha L, Kim H, Bernasconi A, Bernhardt BC, Bernasconi N. Spatial patterns of water diffusion along white matter tracts in temporal lobe epilepsy. *Neurology.* (2012) 79:455–62. doi: 10.1212/WNL.0b013e31826170b6
40. Lee DA, Lee HJ, Kim HC, Park KM. Application of machine learning analysis based on diffusion tensor imaging to identify REM sleep behavior disorder. *Sleep Breath*. (2021) 1–8. doi: 10.1007/s11325-021-02434-9
41. Wu Q, Butzkueven H, Gresle M, Kirchhoff F, Friedhuber A, Yang Q, et al. MR diffusion changes correlate with ultra-structurally defined axonal degeneration in murine optic nerve. *Neuroimage.* (2007) 37:1138–47. doi: 10.1016/j.neuroimage.2007.06.029
42. Concha L, Livy DJ, Beaulieu C, Wheatley BM, Gross DW. In vivo diffusion tensor imaging and histopathology of the fimbria-fornix in temporal lobe epilepsy. *J Neurosci.* (2010) 30:996–1002. doi: 10.1523/JNEUROSCI.1619-09.2010
43. Kang JMK, Joo SWJ, Son YDS, Kim HK, Ko KPK, Lee JSL, et al. Low white-matter integrity between the left thalamus and inferior frontal gyrus in patients with insomnia disorder. *J Psychiatry Neurosci.* (2018) 43:366–74. doi: 10.1503/jpn.170195

Conflict of Interest: XW was employed by GE Healthcare. SW was employed by Siemens Healthineers.

The remaining authors declare that the research was conducted in the absence of any commercial or financial relationships that could be construed as a potential conflict of interest.

frontiers | Frontiers in Psychiatry

ORIGINAL RESEARCH
published: 30 June 2022
doi: 10.3389/fpsyt.2022.863056

Improved Regional Homogeneity in Chronic Insomnia Disorder After Amygdala-Based Real-Time fMRI Neurofeedback Training

Zhonglin Li[1†], Jiao Liu[2,3†], Bairu Chen[4†], Xiaoling Wu[5†], Zhi Zou[1], Hui Gao[6], Caiyun Wang[1], Jing Zhou[7], Fei Qi[1], Miao Zhang[1], Junya He[1], Xin Qi[1], Fengshan Yan[1], Shewei Dou[1], Li Tong[6], Hongju Zhang[8], Xingmin Han[2,3] and Yongli Li[7]**

[1] Department of Radiology, Henan Provincial People's Hospital and People's Hospital of Zhengzhou University, Zhengzhou, China, [2] Department of Nuclear Medicine, First Affiliated Hospital of Zhengzhou University, Zhengzhou, China, [3] Henan Medical Key Laboratory of Molecular Imaging, Zhengzhou, China, [4] Department of Medical Imaging, Fifth Affiliated Hospital of Zhengzhou University, Zhengzhou, China, [5] Department of Nuclear Medicine, Henan Provincial People's Hospital and People's Hospital of Zhengzhou University, Zhengzhou, China, [6] Henan Key Laboratory of Imaging and Intelligent Processing, PLA Strategic Support Force Information Engineering University, Zhengzhou, China, [7] Health Management Center, Henan Provincial People's Hospital and People's Hospital of Zhengzhou University, Zhengzhou, China, [8] Department of Neurology, Henan Provincial People's Hospital and People's Hospital of Zhengzhou University, Zhengzhou, China

OPEN ACCESS

Edited by:
Karen M. von Deneen,
Xidian University, China

Reviewed by:
Liang Gong,
Chengdu Second People's Hospital, China
Xiaofen Ma,
Guangdong Second Provincial General Hospital, China

***Correspondence:**
Xingmin Han
xmhan@zzu.edu.cn
Yongli Li
shyliyongli@126.com

[†] These authors have contributed equally to this work

Specialty section:
This article was submitted to Neuroimaging and Stimulation, a section of the journal Frontiers in Psychiatry

Received: 26 January 2022
Accepted: 31 May 2022
Published: 30 June 2022

Citation:
Li Z, Liu J, Chen B, Wu X, Zou Z, Gao H, Wang C, Zhou J, Qi F, Zhang M, He J, Qi X, Yan F, Dou S, Tong L, Zhang H, Han X and Li Y (2022) Improved Regional Homogeneity in Chronic Insomnia Disorder After Amygdala-Based Real-Time fMRI Neurofeedback Training. Front. Psychiatry 13:863056. doi: 10.3389/fpsyt.2022.863056

Background: Chronic insomnia disorder (CID) is a highly prevalent sleep disorder, which influences people's daily life and is even life threatening. However, whether the resting-state regional homogeneity (ReHo) of disrupted brain regions in CID can be reshaped to normal after treatment remains unclear.

Methods: A novel intervention real-time functional magnetic resonance imaging neurofeedback (rtfMRI-NF) was used to train 28 CID patients to regulate the activity of the left amygdala for three sessions in 6 weeks. The ReHo methodology was adopted to explore its role on resting-state fMRI data, which were collected before and after training. Moreover, the relationships between changes of clinical variables and ReHo value of altered regions were determined.

Results: Results showed that the bilateral dorsal medial pre-frontal cortex, supplementary motor area (SMA), and left dorsal lateral pre-frontal cortex had decreased ReHo values, whereas the bilateral cerebellum anterior lobe (CAL) had increased ReHo values after training. Some clinical scores markedly decreased, including Pittsburgh Sleep Quality Index, Insomnia Severity Index, Beck Depression Inventory, and Hamilton Anxiety Scale (HAMA). Additionally, the ReHo values of the left CAL were positively correlated with the change in the Hamilton depression scale score, and a remarkable positive correlation was found between the ReHo values of the right SMA and the HAMA score.

Conclusion: Our study provided an objective evidence that amygdala-based rtfMRI-NF training could reshape abnormal ReHo and improve sleep in patients with CID. The improved ReHo in CID provides insights into the neurobiological mechanism for the effectiveness of this intervention. However, larger double-blinded sham-controlled trials are needed to confirm our results from this initial study.

Keywords: chronic insomnia disorder, regional homogeneity, real-time, fMRI, neurofeedback, amygdala

INTRODUCTION

Chronic insomnia disorder (CID) is a highly prevalent sleep disorder, especially with the spread of coronavirus disease 2019 around the world in recent years (1). According to reports, the prevalence of insomnia among American adults is 18.8% and that among the general population in China is 15% (2). The typical symptom of CID is difficulty in falling asleep at bedtime, frequent awakening in the middle of the night, and waking up too early in the morning (1). Long-term insomnia or low sleep quality causes imbalance in the interaction between sympathetic and parasympathetic nerves, resulting in anxiety, depression, and other negative emotions (1, 3). The neurobiological mechanism of CID remains unclear, thus affecting the development of therapeutic methods (4). Therefore, the neurobiological mechanisms should be urgently identified, and innovative therapies of CID should be studied.

Recently, resting-state functional magnetic resonance imaging (rs-fMRI) is an increasingly recognized technique to investigate functional alterations in patients with CID, and this method has unique advantages in clinical research (3, 4). Different methods have been applied to determine the disruptions of the brain activity in CID by using rs-fMRI, including seed-based functional connectivity (FC) (5), independent component analyses (ICA) (6), voxel-mirrored homotopic connectivity (VMHC) (7), amplitude of low-frequency fluctuations (ALFFs) (8), and regional homogeneity (ReHo) (2, 9, 10). However, FC is a hypothesis-driven method, and the definition and exact placement of ROI seeds can be somewhat arbitrary, thus introducing potential biases in the assessment results and impeding the discovery of unexpected regions of interest (11). For ICA, the determination of the generated components with an optimal number is relatively arbitrary, thereby greatly influencing the number of connectivity patterns that can be obtained and producing considerable variations among studies (11). In addition, VMHC focuses on exploring the differences in homotopic coordination rather than the whole brain (12). ReHo and ALFF are both data-driven methods that reflect spontaneous neuronal activity from different perspectives. However, some studies have recognized that ReHo analysis achieves better performance in depict clinical trait than ALFF (13). Therefore, ReHo analysis could be used to gain insight into the neural mechanisms underlying CID.

Resting-state regional homogeneity measures the similarity or synchronicity of the time series of nearest neighboring voxels and reflects the strength of local spontaneous neural activity in the brain (14). It has been successfully applied to reveal abnormalities in the brain function of patients with CID (2, 9, 10). Earlier, Dai et al. (9) found increased ReHo in the left fusiform gyrus and lower ReHo in the bilateral cingulate gyrus and right cerebellum anterior lobe (CAL) in patients with CID. The correlations between the clinical measurements and ReHo value of the fusiform gyrus and frontal lobe were observed (9). Wang et al. (10) discovered abnormal ReHo activities in multiple brain regions, especially in emotion-related areas in patients with CID. Significant correlations were observed between ReHo values of altered brain regions and clinical scores (10). Zhang et al. (2) found that ReHo alterations in the left inferior occipital gyrus may play an important role in the dysfunctional beliefs and attitudes about sleep in patients with CID. Therefore, ReHo is a highly effective and sensitive method for mapping disrupted neural activity to reflect the underlying neurobiological mechanism of CID. However, whether the ReHo of disrupted brain regions in patients with CID can be reshaped to normal after treatment remains unclear.

A novel intervention real-time fMRI neurofeedback (rtfMRI-NF), which has no known side effects and potential longer-term neuroplastic effects, can train people to autonomously regulate brain activity and has huge application prospect in improving cognition or curing diseases (15–20). In comparison with other neurofeedback techniques, such as EEG and non-invasive physical stimulation techniques (transcranial magnetic stimulation), rtfMRI-NF has the advantage of higher spatial resolution and better access to deep relevant brain structures (15–17). Subjects can use rtfMRI-NF to regulate the activity of local brain regions or the functional connections of multiple brain regions to improve clinical symptoms, including depression, anxiety, schizophrenia, and other diseases (18–20). Spiegelhalder et al. (3) found that rtfMRI-NF may be useful for future studies on the treatment of patients with CID. Therefore, we aimed to verify whether the abnormal local ReHo of patients with CID can be reshaped to normal by rtfMRI-NF training.

A target brain region, which is closely related to the pathogenesis of CID, was needed for rtfMRI-NF training (15–18). Multiple local and overall dysfunctions occur in patients with CID, and these dysfunctions are mainly concentrated in the amygdala and emotion and cognition-related brain areas (3, 5, 21, 22). CID is associated with increased amygdala responsiveness to negative stimuli, and its treatment may benefit from strategies that modulate its association with emotion (22). Huang et al. discovered decreased FC between the amygdala and insula, striatum, and thalamus. They also found increased FC of the amygdala with the pre-motor and sensorimotor cortex (5). The amygdala, which is positioned in the limbic system's center and plays a critical role in the formation, expression, and perception of unpleasant emotions, has been implicated in the important pathophysiology of CID (23). Previous studies supported a functional dissociation between the left and right amygdala in terms of temporal dynamics. The right amygdala is engaged in the rapid and automatic detection of emotional stimuli, whereas the left amygdala participates in more detailed and elaborate stimulus evaluation (24, 25). Moreover, many researchers have successfully used rtfMRI-NF training to help patients regulate the activity of their left amygdala through positive autobiographical memory to change brain function and clinical symptoms (16–18). As a result, targeting the activity of the left amygdala for rtfMRI-NF regulation may improve the sleep of patients with CID, thereby providing a new breakthrough point for investigating the neurological mechanism.

Taken together, amygdala-based rtfMRI-NF training could reshape resting-state local spontaneous neural activity accompanying improvement of sleep in patients with CID. To prove our hypothesis, we used rtfMRI-NF to train patients with CID to regulate the activity of the left amygdala for three sessions

in 6 weeks. The rs-fMRI data were collected before and after training. Then, the ReHo method was used to explore the effect of rtfMRI-NF training. We also investigated the relationships between the ReHo value of altered regions and the changes of clinical variables.

MATERIALS AND METHODS

Participants

The study design and patient approval for this study were granted by the Ethics Committee of the Henan Provincial People's Hospital. All patients with CID were recruited by advertisement or introduction of hospital doctors from January 2018 to December 2021. All patients signed an informed consent form and were compensated for their participation. All participants underwent a comprehensive neuropsychological and clinical assessment, including Pittsburgh Sleep Quality Index (PSQI) (26), Insomnia Severity Index (ISI) (27), Hamilton Depression Scale (HAMD) of 17 items (28), Beck Depression Inventory (BDI) (29), and Hamilton Anxiety Scale (HAMA) of 14 items (30). To exclude the potential influence of drugs, the patients were asked not to take medications or other treatment methods for insomnia from 2 weeks before the experiment to the end of training. Patients who cannot bear the torture of insomnia can quit at any time. Based on the Fifth Edition of Diagnostic and Statistical Manual of Mental Disorders diagnostic criteria (DSM-V), the inclusion criteria are as follows: (1) age of 18–70 years; (2) right-hand dominance and native Chinese speaker; (3) fatigue, irritability, cognitive decline, and other insomnia symptoms should last for at least 3 months; (4) PSQI score $\geq$8; (5) no history of psychiatric or neurological disorders (e.g., schizophrenia, stroke); (6) no any secondary sleep problems (e.g., restless leg syndrome, obstructive sleep apnea); (7) no history of alcohol and substance abuse or dependence; and (8) no brain lesions or prior substantial head trauma found by T2-weighted dark-fluid and T1-weighted MR images. Considering the concomitant relationship between CID and depression and anxiety (31, 32), this study did not limit the depression and anxiety score of patients with CID when recruiting them. In addition, an overnight polysomnography (PSG) was used to exclude participants with occult sleep disorders. The PSG was recorded using an ambulatory recording system (Compumedics Siesta, Australia). The collected PSG parameters included total sleep time (TST), sleep efficiency (SE), sleep onset latency (SOL), and number of awakenings (NOA).

Power Calculation

The sample size was calculated using the G*Power software (33). Considering that no relevant research has been published, the parameters of effect size were set at 0.5 to estimate the sample size (18). To achieve 80% power at $P = 0.05$ in the two-sided (t-test) test, a sample size of $n = 34$ participants was required. Considering a maximum possible dropout rate of 20%, 41 subjects were needed. Given that this clinical trial of fMRI-NF was conducted as a pilot study to test the feasibility, the performed power calculation was of limited value because it is based on effect sizes (18). Furthermore, fMRI-NF is still in the early phases of clinical evaluation, and it is a relatively complex and time-consuming process (18). Finally, 33 patients with CID completed all experimental procedures. However, four participants were excluded because of excessive head movements during resting-state scanning. One subject dropped out because of the pause during training.

Procedure

The experimental procedure of rtfMRI-NF training is shown in **Figure 1A**. The participants completed the experiment by visiting six times with 1 week internal. During the first visit, we gathered information on broad demographic parameters. The PSQI, ISI, HAMD, BDI, and HAMA were also provided by the participants. During the second visit, the participants completed MRI scans and familiarized themselves with the MRI scanning environment. To rule out any structural abnormalities in the brain, we collected routine axial T2-weighted dark-fluid and T1-weighted MR images. To register the template of the amygdala from the standard space to the subject space for real-time processing data during training, we collected high-resolution T1-weighted structural images. Afterward, PSG was performed overnight. During the third, fourth, and fifth visits, the participants completed the same clinical and self-report measures as the first visit and their three rtfMRI-NF training sessions. The detailed paradigm of rtfMRI-NF training is shown in the following section. During the sixth visit, the participants finished overnight PSG as in their second visit. Meanwhile, the participants finished rs-fMRI scans, and the same clinical score as in their third visit was obtained.

rtfMRI-NF Training Paradigm

The schematic of amygdala-based rtfMRI-NF loop is shown in **Figure 1B**. The participants were required to write down three or more specific autobiographical memories about themselves. Before rtfMRI-NF training, we informed the patients about the details of experimental process and the specific tasks under different stimuli. The signals of brain activity from the left amygdala region were provided as feedback to them for regulation during training. The amygdala is defined from the Talairach space with a radius of 7 mm and the coordinates (i.e., −21, −5, and −16), and its signal is displayed as temperature bars updating once per reaction time (TR) (2 s) (20, 34). The OpenNFT system was used to perform real-time online data analysis (35). Detailed information about the steps and parameter are provided in the article published by Koush et al. (35). Eight runs were carried out in each training session lasting for ∼50 min, including the functional localizer, resting-state scan, practice-training, three NF-training, transfer-training, and resting-state scan. The functional localizer run was carried out for 20 s, and the resting-state scan run was carried out for 7 min. The five remaining runs were carried out for 6 min and 50 s. In the two resting-state scan runs, we collected rs-fMRI data of the participants, who were instructed to fix on green cross, remain awake, and think of nothing in particular. The practice-training and transfer-training runs shared the same paradigms with NF training but without a feedback signal. The participants were allowed to familiarize with the rtfMRI-NF training procedure by

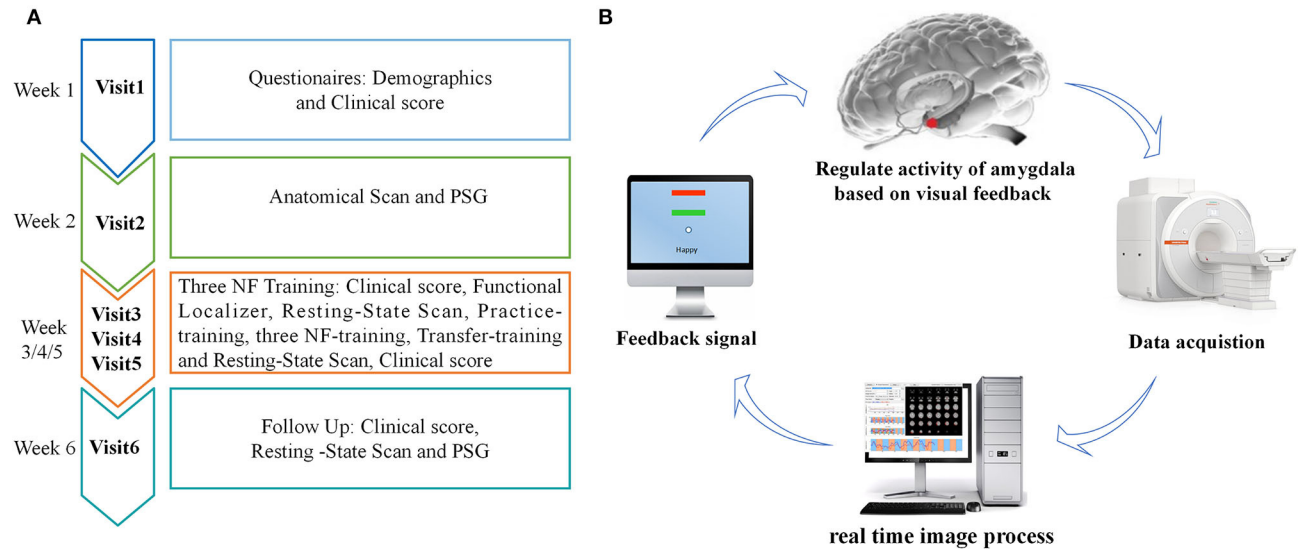

FIGURE 1 | (A) Procedure of rtfMRI-NF training experiment. The experimental protocol consisted of six visits, lasting for ∼6 weeks. During the third, fourth, and fifth visits, each rtfMRI-NF training session included eight runs, lasting for ∼50 min. **(B)** Schematic of amygdala-based rtfMRI-NF loop for patients with CID. Typically, brain images were acquired using the MR scanner online and analyzed using the OpenNFT software in real time. Then, the signal of amygdala activity was provided as feedback to patients with CID for neural self-regulation. rtfMRI-NF, real-time fMRI neurofeedback; PSG, polysomnography; CID, chronic insomnia disorder.

designing the practice-training run. To test whether participants had mastered the regulation strategy, we added a transfer training run after three NF training runs. Each NF training run consisted of alternating 30 s rest and 30 s happy blocks, with seven blocks of rest and six blocks of happy. At rest blocks, participants were asked to stare at the green cross on the screen to calm their mind. During happy blocks, the participants were instructed to increase the height of thermometer on the screen by recalling a positive autobiographical memory.

Data Acquisition

A MAGNETOM Prisma 3T MR scanner (Siemens Healthcare, Erlangen, Germany) with a 64-channel head-neck coil was used for fMRI data acquisition at the Medical Imaging Center of our hospital. Earplugs and foam pads were used to minimize scanner noise and head motion. A medical tape was fixed on participants' foreheads to help them control their movements. rs-fMRI data were acquired using an echo-planar imaging sequence with 210 volumes lasting for 420 s. The corresponding acquisition parameters were set as follows: TR: 2,000 ms, echo time (TE): 30 ms, field of view (FOV): 224 mm × 224 mm, matrix size: 112 × 112, slices: 27, slice thickness: 4 mm, gap: 1 mm, and flip angle: 90°. High-resolution T1-weighted structural images were acquired with the following parameters: TR: 2,300 ms, TE: 2.27 ms, FOV: 250 mm × 250 mm, matrix size: 256 × 256, slices: 192, slice thickness: 1 mm, and flip angle: 8°.

Data Processing

The rs-fMRI data collected in Visit 6 and the first scan of Visit 3 (**Figure 1A**) were used for analysis in this study. Data pre-processing and ReHo analysis were carried out by using the Data Processing and Analysis of Brain Imaging (DPABI, http://rfmri.org/DPABI) toolbox (36). First, we discarded the first 10 volumes of each run for signal stabilization and participant adaptation. Then, slice timing and head-motion correction were carried out. Data with maximum displacement in head rotation of larger than 2° or any directions of larger than 2 mm were excluded from further analysis. For precise spatial normalization of the fMRI data, individual high-resolution T1-anatomic images were registered to the mean fMRI data, and the resulting aligned T1-weighted images were segmented and transformed into standard Montreal Neurological Institute space by using the DARTEL toolbox. Furthermore, white matter, cerebral-spinal fluid signals, and 24-head realignment parameter were regressed out as covariates. Subsequently, regressed functional images were specially normalized to the group template by using the transfer parameter estimated by DARTEL segmentation and resampled to 3 × 3 × 3 mm^3 voxels. Finally, linear trend and temporal band-pass filtering (0.01–0.1 Hz) was applied to reduce low-frequency drift and physiological high-frequency respiratory and cardiac noise.

ReHo Calculation

Regional homogeneity maps were generated on the pre-processed rs-fMRI data as previously described (2, 9, 10). The Kendall's coefficient of concordance (KCC) was calculated to measure the similarity of the time series of a given voxel to those of its nearest 26 voxels. To reduce the influence of individual variation in KCC values, we performed ReHo map normalization by dividing the KCC of each voxel by the averaged whole-brain KCC. Finally, the ReHo maps were spatially smoothed using a Gaussian kernel with 6 mm full-width at half-maximum. A group template of 90% was generated for fMRI processing and statistics. To assess the effect of amygdala-based rtfMRI-NF training on

TABLE 1 | Changes in clinical variables before and after training in patients with chronic insomnia disorder.

Variables	Before training	After training	T/Z value	*P*-Value
PSQI	13.86 ± 3.35	11.25 ± 3.31	4.87	<0.001
ISI	17.82 ± 4.83	14.18 ± 6.14	3.46	0.002
HAMD	19.11 ± 8.01	16.86 ± 7.47	1.76	0.09
BDI	19.29 ± 10.70	15.89 ± 9.25	2.88	0.008
HAMA	19.82 ± 9.45	16 ± 12.15	2.65	0.013
TST (min)	380.11 ± 101.70	404.27 ± 81.22	1.18	0.25
SE (%)	78.75 (66.25–84.78)	78.6 (71.33–89.98)	−0.62	0.539
SOL (min)	20.5 (7.25–58.13)	12 (6.63–27.13)	−1.95	0.052
NOA	20.5 (10.25–26.75)	15 (8–26.5)	−1.49	0.137

Normally distributed data are expressed as mean ± SD, and P-values were obtained using two-tailed paired t-test. Non-normally distributed data were presented as median and interquartile range, and P-values were obtained using the Wilcoxon signed-rank test. PSQI, Pittsburgh sleep quality index; ISI, insomnia severity index; HAMD, Hamilton depression rating scale; BDI, Beck depression inventory; HAMA, Hamilton anxiety rating scale; TST, total sleep time; SE, sleep efficiency; SOL, sleep onset latency; NOA, number of awakenings.

TABLE 2 | Brain regions exhibited altered ReHo in patients with chronic insomnia disorder (after training vs. before training).

Brain regions	Whole cluster size	Cluster size	MNI co-ordinates			*t* score
			x	y	z	
Left supplementary motor area	152	43	0	21	48	−6.2269
Left dorsal lateral pre-frontal cortex		35	−15	30	45	−5.3858
Right supplementary motor area		26	3	24	48	−6.3088
Left dorsal medial pre-frontal cortex		23	0	27	48	−5.7855
Right dorsal medial pre-frontal cortex		19	3	30	45	−6.2449
Left cerebellum anterior lobe	137	62	12	−48	−15	6.8476
Right cerebellum anterior lobe		42	−12	−48	−12	4.55

Results were set at voxel-level: P < 0.001, cluster-level: P < 0.05, t = 3.29 (Gaussian random field corrected). ReHo, regional homogeneity; MNI, Montreal Neurological Institute.

the CID brain, we compared the whole-brain ReHo differences between after training and before training conditions *via* the paired *t*-test. The Gaussian random field (GRF) theory correction procedure was used for multiple comparisons.

Statistical Analysis

Demographic and Clinical Data Analysis

The data of the clinical score analyzed were collected during the sixth visit and at the beginning of the third visit. The PSG data analyzed were collected during the sixth and second visits. The distribution of clinical data was tested using the Kolmogorov-Smirnov method. Continuous variables with normal distribution were analyzed using the independent paired *t*-test and expressed as mean ± standard deviation. Otherwise, the Wilcoxon signed-rank test was used to analyze non-normally distributed data, which were expressed as median and interquartile range. All statistical analyses were performed using SPSS version 22.0 (http://www.spss.com; Chicago, IL). The threshold for statistical significance was set at $P < 0.05$, and all hypothesis tests were two-tailed.

Brain-Behavior Correlation Analysis

Based on the paired *t*-test, the altered ReHo brain regions were located. Then, the mean ReHo values of these brain regions in after training condition were extracted. After this, partial correlation was performed to examine the association between the values of ReHo and the changes in the clinical scores and indexes of PSG, including PSQI, ISI, HAMD, HAMA, BDI, TST, SE, SOL, and NOA with age, gender, and education as covariates. Statistical significance was considered at $P < 0.05$. Multiple comparison correction was performed by the false discovery rate (FDR).

RESULTS

Demographic and Clinical Data

In this article, 28 patients with CID were included for further analysis. The demographic data were as follows: 21 females; education: 13.1 ± 3.3 years; and age: 45.7 ± 13.2 years. The normal distribution of clinical characteristics data included PSQI, ISI, HAMD, HAMA, BDI, and TST. However, the SE, SOL, and NOA non-normally distributed. After rtfMRI-NF training, the PSQI, ISI, BDI, and HAMA of patients with CID showed significant differences ($P < 0.05$, **Table 1**) compared with those before training. However, HAMD, TST, SE, SOL, and NOL showed no significant differences. Detailed information of these results are shown in **Table 1**.

ReHo Analysis

In comparison with the ReHo before training condition, patients with CID showed decreased ReHo in bilateral dorsal medial pre-frontal cortex (DMPFC), supplementary motor area (SMA), and left dorsal lateral pre-frontal cortex (DLPFC) and increased ReHo in bilateral CAL. **Table 2** shows the detailed information on activation centers. The spatial distributions of altered ReHo regions are shown in **Figure 2**. The results were set at voxel-level: $P < 0.001$, cluster-level: $P < 0.05$, $t = 3.29$, GRF corrected. The distributions of z-transform ReHo values in brain regions that exhibited altered ReHo are shown in **Figure 3**.

Brain Behavior Correlation Analysis

The ReHo values of right SMA also showed significant positive correlation with the changed HAMA score ($r = 0.405$, $P = 0.045$, FDR corrected, **Figure 4A**). A remarkable positive correlation was also found in the changed HAMD score (after training minus before training) with ReHo values of the left CAL ($r = 0.46$, $P = 0.042$, FDR corrected, **Figure 4B**). The changed ISI score and ReHo values of the left CAL showed a positive correlation but did not reach a significant level ($r = 0.356$, $P =$

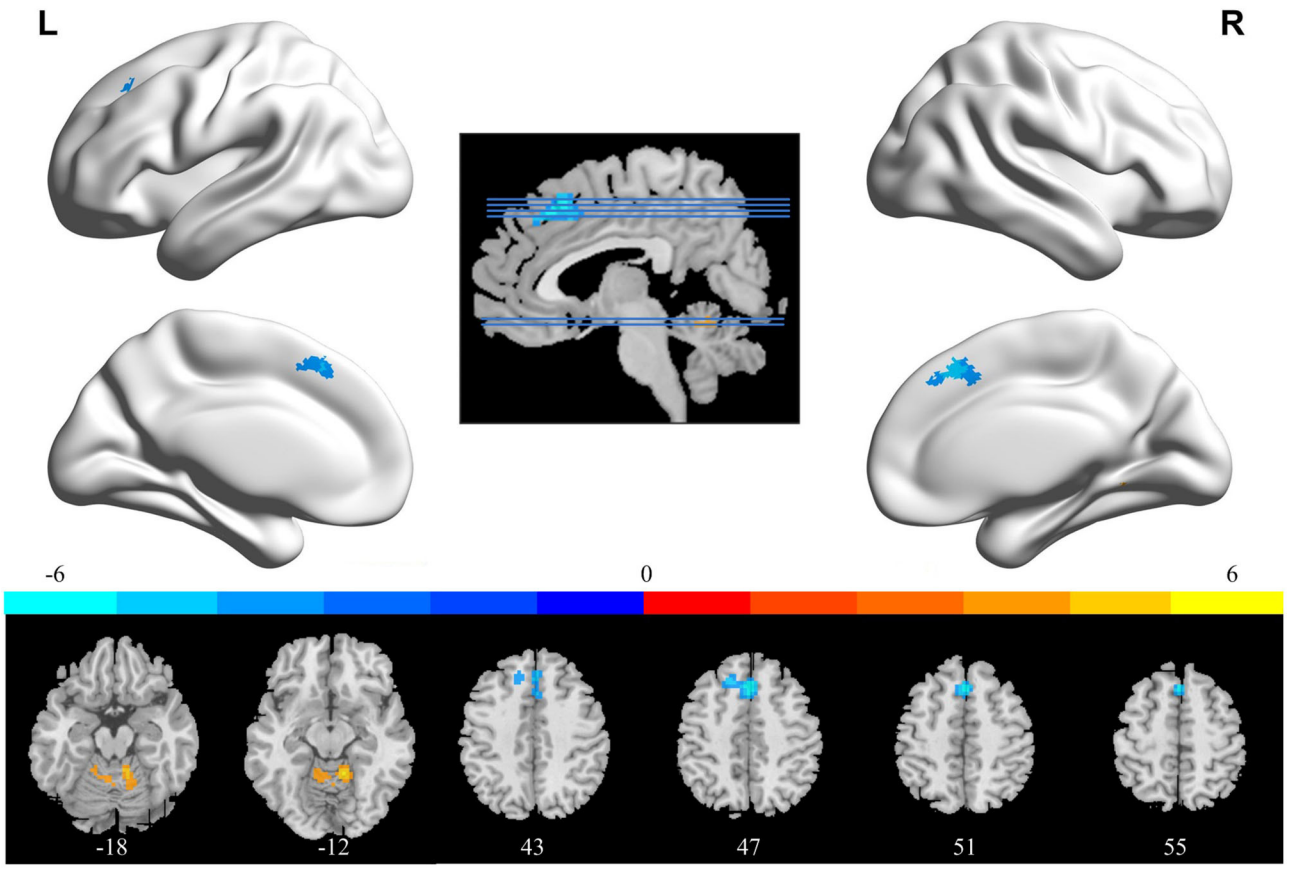

FIGURE 2 | Brain areas that exhibited altered ReHo induced by real-time fMRI neurofeedback training (after training vs. before training). Results were set at voxel-level $P < 0.001$, cluster-level $P < 0.05$, and $t = 3.29$ (Gaussian random field corrected). Warm colors indicate regions in which ReHo increased significantly, whereas cool colors indicate regions in which ReHo decreased significantly. The color bar indicates the *t*-value. The numbers at the bottom indicate the axial slices. ReHo, regional homogeneity; L, left; R, right.

0.08, **Supplementary Figure S1**). The ReHo values of the others altered brain regions did not show significant correlation with the other changed clinical scores and indexes of PSG.

DISCUSSION

In this study, based on the ReHo method, we explored whether the resting-state local spontaneous neural activity in patients with CID could be regulated by amygdala-based rtfMRI-NF training accompanying improvement of clinical symptoms. Results showed that the bilateral DMPFC, SMA, and left DLPFC had decreased ReHo values, and the bilateral CAL had increased ReHo values. Some clinical scores, including PSQI, ISI, BDI, and HAMA, were markedly decreased. Additionally, the ReHo values of the left CAL were positively correlated with the changed HAMD score. The ReHo values of the right SMA also showed remarkably positive correlation with the HAMA score. These results support our hypothesis that amygdala-based rtfMRI-NF training could reshape abnormal ReHo and improve sleep of patients with CID.

The DMPFC, as a key node of default mode network (DMN), is engaged in self-referential mental activity and emotional processing and has more connection with limbic areas such as amygdala (37–39). Koenigs et al. (40) discovered that the sleep initiation and maintenance is related to damage of the left DMPFC. Notably, the intrinsic activity in the DMPFC of the normal sleep subject is reduced during a natural sleep and shifts to a deep sleep (37). Furthermore, Yu et al. (38) reported that the patients with CID showed significantly increased global FC density in the left DMPFC. Besides, core areas of the DMN showed greater activation in patients with CID compared with healthy controls (HCs) in self-referential-related tasks (41). These results support the hypothesis of hyperarousal to explain the etiology and maintenance of CID (3, 4, 38). An increasing number of studies supports that CID may be conceptualized as a disorder associated with the overactivity of certain brain areas of the DMN (42, 43). The widespread hyperarousal of several systems (e.g., cognitive, physiological, and emotional) occurs during insomnia, which consequently prevents relaxation (42). In this study, the ReHo values of the bilateral DMPFC decreased after training. Our findings may reflect that the

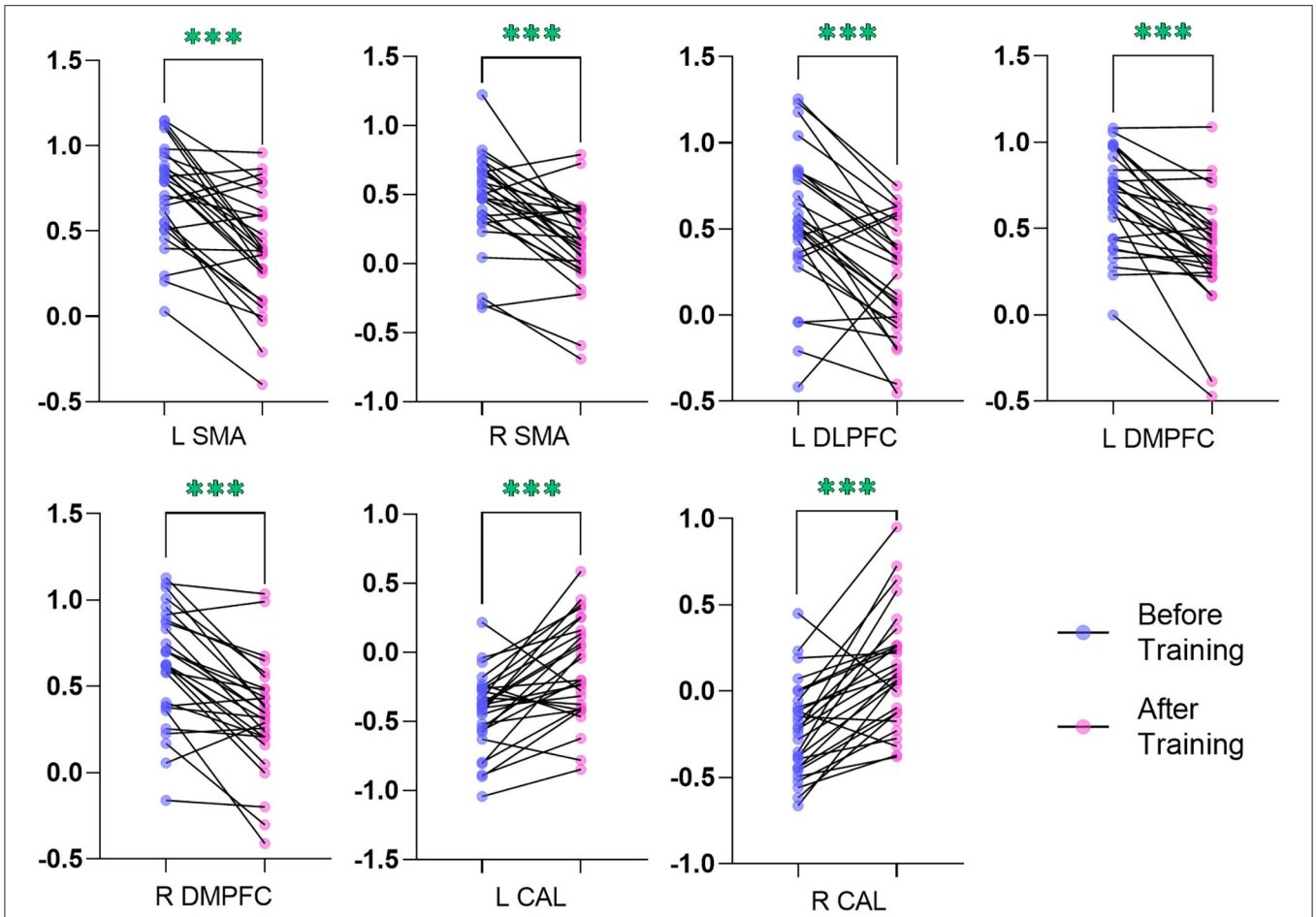

FIGURE 3 | Plot of the z-transform ReHo values in brain regions that exhibited altered ReHo. The blue dots (before training condition) and the pink dots (after training condition) indicated the mean values of ReHo in the different brain regions of all the subjects. L, left; R, right; ReHo, regional homogeneity; SMA, supplementary motor area; DLPFC, dorsal lateral pre-frontal cortex; DMPFC, dorsal medial pre-frontal cortex; CAL, cerebellum anterior lobe. ***indicates $p < .001$.

amygdala-based rtfMRI-NF training could reshape the disrupted ReHo of DMPFC.

Chronic insomnia disorder has a close relationship with depression and anxiety (44, 45). Therefore, our study aimed to improve the sleep of patients with CID by training them to regulate amygdala activity through recalling happy emotions and then improve emotions states. The DMPFC and amygdala are the key structures of cognitive-affective brain systems (46). Insomnia may disrupt reward-related brain function, a potentially important factor in the development of depressive disorder (47). Melynda et al. (47) found that DMPFC response to reward anticipation and depressive symptoms mediates the relationship between early adolescent non-restorative sleep and late adolescent depressive symptoms. Moreover, the activity of DMPFC increased in HCs during a positive emotion regulation task (46). Taken together, our results indicate that the cognitive-affective brain systems in patients with CID could be modulated through amygdala-based rtfMRI-NF training.

The DLPFC is a critical brain region of central executive network (CEN) and is involved in neurocognitive functions, including executive functions, decision-making, working memory, social cognition, and top-down emotional regulation (48, 49). The DLPFC of patients with CID exhibits structural and functional impairment, which may be lead to early rising and difficulty in falling asleep (50–53). In comparison with HCs, two studies observed decreased gray matter volume in the bilateral DLPFC of patients with CID, thus providing basis for functional abnormalities (52, 53). Huang et al. (50) discovered reduced FC strength in the right DLPFC in patients with CID. The global FC density increased in the right DLPFC (38). These results indicated an impairment of intrinsic FC network in patients with CID. In addition, patients with CID showed high FC between the DLPFC and salience network, which had a remarkable significant positive correlation with PSQI score (49). In terms of spontaneous neuronal activity, Liu et al. (54) discovered increased ALFF values in the bilateral DLPFC of patients with major depressive disorder (MDD) and high insomnia and patients with MDD and low insomnia compared with HCs. Zhang et al. (2) discovered increased ReHo values in the right DLPFC of patients with CID.

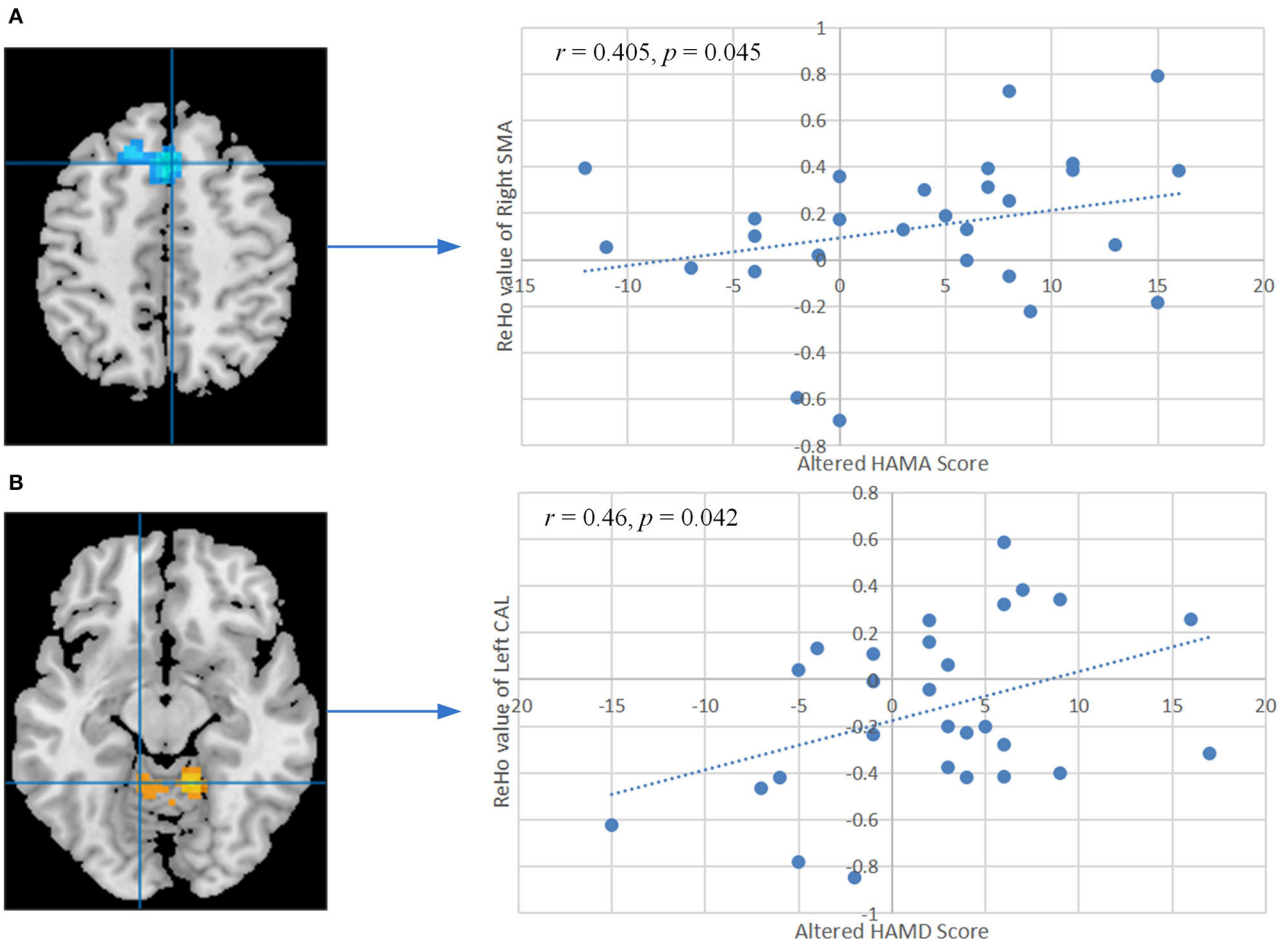

FIGURE 4 | (A) Correlation between the altered HAMA score and ReHo values of the right SMA after training. **(B)** Correlation between the altered HAMD score and ReHo values of the left CAL after training. The *P*-values were corrected by the false discovery rate. ReHo, regional homogeneity; HAMA, Hamilton Anxiety Scale; HAMD, Hamilton Depression Scale; SMA, supplementary motor area; CAL, cerebellum anterior lobe.

Notably, decreased ReHo values were found in left DLPFC after training in this research. DLPFC not only plays a major role in cognitive control but also has an intimate relationship with emotional processes (49, 55). Patients with CID also showed increased amygdala reactivity to insomnia-related stimuli and increased levels of anxiety and depression (22, 49). Thus, DPLFC controls amygdala activity in response to external sleep-related emotional stimuli. At rest, people are less responsive to the outside stimuli. However, this function was disrupted in patients with CID and the activity of DLPFC is increased to inhibit excessive emotional response. Our training enhanced the top-down executive controlling of amygdala by DLPFC. Subsequently, the activity of DLPFC was reduced at rest, thus promoting sleep. In this study, the improvement in symptoms of both depression and anxiety in patients with CID also support the influence of rtfMRI-NF training in reducing hyperarousal. Recently, several studies selected DLPFC as a brain target of non-invasive brain stimulation, including transcranial magnetic stimulation (TMS) and transcranial direct/alternating current stimulation (tDCS/tACS), for CID treatment (56–58). The results showed that it could be a good supplement to drugs in the treatment of CID (56–58). Therefore, DLPFC may also be an effective target for rtfMRI-NF training in the treatment of CID, and future studies are needed to verify this hypothesis.

The sensory-motor network (SMN), including SMA, pre-central gyrus, and post-central gyrus, plays a role in the continuous sensory process of environmental stimuli and proprioceptive information (59). FC within SMN is increased in patients with CID (5, 59–61). In comparison with HCs, Huang et al. (5) found increased FC mainly between the amygdala and pre-motor cortex, sensorimotor cortex in patients with CID. This result might reflect an adaptive response to the "internal" threat in patients with CID (5). The difficulty in falling asleep is associated with high FC between primary sensory and SMA in patients with CID (60). By using the graph theory analysis method, our previous study found increased nodal centralities of right pre-central gyrus in patients with CID (61). The node betweenness of the right pre-central gyrus was positively

correlated with the PSQI score in patients with CID (61). Wang et al. (10) discovered increased ReHo in the bilateral pre-central gyrus belonging to SMN, and this parameter is significantly correlated with SAS scores. Therefore, the SMA of patients with CID may be hyperactivity and hyperconnectivity. After amygdala-based rtfMRI-NF training, we found decreased ReHo in bilateral SMA in patients with CID. To some extent, this result is consistent with previous findings. After the CID group underwent cognitive-behavioral therapy, response to sleep-related stimuli of left SMA and FC between the left putamen and left SMA decreased (62, 63). The ReHo values of the right SMA also showed a remarkably positive correlation with the changed HAMA score, indicating an improved anxiety state to external environment in patients with CID. In HCs, those with shorter sleep duration show greater impairment of psychomotor ability than those with longer sleep duration, that is, mental movement in the brain increases before falling asleep and during sleep, resulting in light sleep or difficulty falling asleep in patients with CID (64). Patients with CID fall into a perpetual cycle of somatic hyperarousal and increased sensitivity to sensory stimulation, causing further cortical arousal and difficulty in sleep initiation and maintenance (60). Therefore, amygdala-based rtfMRI-NF training may exert its treatment effects on CID by reducing hyperarousal of the SMA to sleep-related threatening stimuli.

The cerebellum is closely related to cognitive and emotional processing and sleep (9, 65). Several neuroimaging studies have reported cerebellar changes in CID (2, 9, 10, 65). A structural neuroimaging reported that the severity of insomnia has a negative correlation with the gray matter volume of the cerebellum (65). In comparison with HC, Dai et al. (9) found that patients with CID showed decreased ReHo values in the right CAL. Recently, Zhang et al. (2) also found decreased ReHo values in left CAL in patients with CID compared with HC. Therefore, disturbed nocturnal sleep may damage the function of the cerebellum and may be associated with disturbed negative mood state in CID (2, 10). In terms of the FC network, Huang et al. (50) discovered a significant reduction in FC strength in the right CAL, which is mainly located in the bilateral basal ganglia/thalamus and bilateral superior frontal gyrus. They pointed out that the disrupted connectivity in the right CAL affects patients with CID *via* the CEN and SMN system (50). However, the diminished activity of CAL was normalized after amygdala-based rtfMRI-NF training, as well as DMPFC in the CEN system and SMA in SMN system. The ReHo values of the left CAL showed a remarkably positive correlation with the changed HAMD score and may reflect the improved emotional state of the patients with CID. CID and depression are intimately related, which may suggest an overlapping neurobiology (1). Sleep disturbance is common in patients with depression, and patients with insomnia are at high risk of developing depression (31). Gebara et al. (32) indicated that treating CID in patients with depression has a positive effect on mood. The results of this article also confirmed this conclusion. Therefore, in the future treatment of CID, the patient's depression needs to be considered at the same time. Additionally, the ReHo values in the left CAL is associated with higher changed ISI score and closely reached significance level. Although this result did not reach significance, we think that this result is meaningful for the exploratory study of rtfMRI-NF in the treatment of CID. Thus, we added it to this report. We speculated that some influencing factors were present, including rtfMRI-NF training duration, participants' cooperation, training specifications, and so on, which affected the clinical changes in ISI and CLA. Hence, this result should be interpreted properly with caution. In summary, amygdala-based rtfMRI-NF training may normalize the activity of CAL to enhance the emotion regulation ability and thus improve sleep.

Limitations and Strengths

This study has several limitations. We did not include a sham feedback group. Thus, the ReHo changes of brain after amygdala-based rtfMRI-NF training may be attributable to placebo rather than the actual therapeutic effects. Patients with CID that participate in the experiment hope to improve sleep, thereby reducing the suffering of insomnia. Their compliance is greatly reduced, and if they find that the effect is not significant, they may realize that they are in the sham feedback group. Therefore, only a real feedback group was included to ensure the training effect of patients with CID. Accordingly, in future studies, we aim to add three sham feedback sessions before three real feedback sessions. Moreover, the sample size of this study was relatively small. The rtfMRI-NF training is time-consuming and relatively complex, and the enrolled participants are required to meet PSG diagnostic criteria, thus limiting the number of enrolled patients with CID. Therefore, controlled studies with larger sample size are needed to verify our results from this initial study.

CONCLUSION

In summary, our study provided an objective evidence that amygdala-based rtfMRI-NF training could reshape abnormal ReHo and improve the sleep in patients with CID. The improved regions with abnormal ReHo are mainly located in DMN, CEN, SMA, and CAL. The improved abnormal spontaneous neural activity in CID provided insights into the neurobiological mechanism for the effectiveness of amygdala-based rtfMRI-NF training. However, double-blinded sham-controlled trials with a larger sample size are needed to confirm our results from this initial study.

DATA AVAILABILITY STATEMENT

The raw data supporting the conclusions of this article will be made available by the authors, without undue reservation.

ETHICS STATEMENT

The studies involving human participants were reviewed and approved by Ethics Committee of the Henan Provincial People's Hospital. The patients/participants provided their written informed consent to participate in this study.

AUTHOR CONTRIBUTIONS

ZL and JL conceived the study, analyzed the data, and wrote the manuscript. BC and XW performed the experiments and wrote the manuscript. ZZ, HG, CW, JZ, FY, and SD designed and

performed the experiments. FQ, MZ, JH, XQ, and HZ collected the clinical samples and performed the experiments. LT, XH, and YL conceived the study, designed the experiments, supervised the project, and wrote the manuscript. All authors contributed to the article and approved the submitted version.

FUNDING

This study was supported by the National Natural Science Foundation of China (82071884), Science and Technology Project of Henan Provincial Science and Technology Department (222102310198), Young and Middle-aged Health Science and Technology Innovative Talent Cultivation Project of Henan Provincial Leading Talents (YXKC2020004), and Henan Province Medical Science and Technology Research Project (LHGJ20200060).

SUPPLEMENTARY MATERIAL

The Supplementary Material for this article can be found online at: https://www.frontiersin.org/articles/10.3389/fpsyt.2022.863056/full#supplementary-material

REFERENCES

1. Buysse DJ, Rush AJ, Reynolds CF. Clinical management of insomnia disorder. *JAMA*. (2017) 318:1973–4. doi: 10.1001/jama.2017.15683
2. Zhang Y, Zhang Z, Wang Y, Zhu F, Liu X, Chen W, et al. Dysfunctional beliefs and attitudes about sleep are associated with regional homogeneity of left inferior occidental gyrus in primary insomnia patients: a preliminary resting state functional magnetic resonance imaging study. *Sleep Med.* (2021) 81:188–93. doi: 10.1016/j.sleep.2021.02.039
3. Spiegelhalder K, Regen W, Baglioni C, Nissen C, Riemann D, Kyle SD. Neuroimaging insights into insomnia. *Curr Neurol Neurosci Rep*. (2015) 15:1–7. doi: 10.1007/s11910-015-0527-3
4. Kay DB, Buysse DJ. Hyperarousal and beyond: new insights to the pathophysiology of insomnia disorder through functional neuroimaging studies. *Brain Sci*. (2017) 7:23. doi: 10.3390/brainsci7030023
5. Huang Z, Liang P, Jia X, Zhan S, Li N, Ding Y, et al. Abnormal amygdala connectivity in patients with primary insomnia: evidence from resting state fMRI. *Eur J Radiol.* (2012) 81:1288–95. doi: 10.1016/j.ejrad.2011.03.029
6. Marques DR, Gomes AA, Clemente V, dos Santos JM, Duarte IC, Caetano G, et al. Unbalanced resting-state networks activity in psychophysiological insomnia. *Sleep Biol Rhythms.* (2017) 15:167–77. doi: 10.1007/s41105-017-0096-8
7. Zhou F, Zhao Y, Huang M, Zeng X, Wang B, Gong H. Disrupted interhemispheric functional connectivity in chronic insomnia disorder: a resting-state fMRI study. *Neuropsychiatr Dis Treat*. (2018) 14:1229. doi: 10.2147/NDT.S162325
8. Zhou F, Huang S, Zhuang Y, Gao L, Gong H. Frequency-dependent changes in local intrinsic oscillations in chronic primary insomnia: a study of the amplitude of low-frequency fluctuations in the resting state. *Neuroimage Clin.* (2017) 15:458–65. doi: 10.1016/j.nicl.2016.05.011
9. Dai XJ, Peng DC, Gong HH, Wan AL, Nie X, Li HJ, et al. Altered intrinsic regional brain spontaneous activity and subjective sleep quality in patients with chronic primary insomnia: a resting-state fMRI study. *Neuropsychiatr Dis Treat.* (2014) 10:2163. doi: 10.2147/NDT.S69681
10. Wang T, Li S, Jiang G, Lin C, Li M, Ma X, et al. Regional homogeneity changes in patients with primary insomnia. *Eur Radiol.* (2016) 26:1292–300. doi: 10.1007/s00330-015-3960-4
11. Wei S, Su Q, Jiang M, Liu F, Yao D, Dai Y, et al. Abnormal default-mode network homogeneity and its correlations with personality in drug-naive somatization disorder at rest. *J Affect Disord.* (2016) 193:81–8. doi: 10.1016/j.jad.2015.12.052
12. He L, Chen G, Zheng R, Hu Y, Chen X, Ruan J. Heterogeneous acupuncture effects of Taixi (KI3) on functional connectivity in healthy youth and elder: a functional MRI study using regional homogeneity and large-scale functional connectivity analysis. *Neural Plast*. (2020) 2020:1–9. doi: 10.1155/2020/8884318
13. Li MG, Liu TF, Zhang TH, Chen ZY, Nie BB, Lou X, et al. Alterations of regional homogeneity in Parkinson's disease with mild cognitive impairment: a preliminary resting-state fMRI study. *Neuroradiology.* (2020) 62:327–34. doi: 10.1007/s00234-019-02333-7
14. Zang Y, Jiang T, Lu Y, He Y, Tian L. Regional homogeneity approach to fMRI data analysis. *Neuroimage.* (2004) 22:394–400. doi: 10.1016/j.neuroimage.2003.12.030
15. Weiskopf N. Real-time fMRI and its application to neurofeedback. *Neuroimage.* (2012) 62:682–92. doi: 10.1016/j.neuroimage.2011.10.009
16. Samantha JF, Sarah FD, Thushini M, Reza M. A guide to literature informed decisions in the design of real time fMRI neurofeedback studies: a systematic review. *Front Hum Neurosci.* (2020) 14:60. doi: 10.3389/fnhum.2020.00060
17. Watanabe T, Sasaki Y, Shibata K, Kawato M. Advances in fMRI real-time neurofeedback. *Trends Cogn Sci.* (2017) 21:997–1010. doi: 10.1016/j.tics.2017.09.010
18. Tursic A, Eck J, Lührs M, Linden DE, Goebel R. A systematic review of fMRI neurofeedback reporting and effects in clinical populations. *Neuroimage Clin.* (2020) 28:102496. doi: 10.1016/j.nicl.2020.102496
19. Morgenroth E, Saviola F, Gilleen J, Allen B, Lührs M, Eysenck MW, et al. Using connectivity-based real-time fMRI neurofeedback to modulate attentional and resting state networks in people with high trait anxiety. *Neuroimage Clin.* (2020) 25:102191. doi: 10.1016/j.nicl.2020.102191
20. Tsuchiyagaito A, Smith JL, El-Sabbagh N, Zotev V, Misaki M, Al Zoubi O, et al. Real-time fMRI neurofeedback amygdala training may influence kynurenine pathway metabolism in major depressive disorder. *Neuroimage Clin.* (2021) 29:102559. doi: 10.1016/j.nicl.2021.102559
21. Baglioni C, Spiegelhalder K, Lombardo C, Riemann D. Sleep and emotions: a focus on insomnia. *Sleep Med Rev.* (2010) 14:227–38. doi: 10.1016/j.smrv.2009.10.007
22. Baglioni C, Spiegelhalder K, Regen W, Feige B, Nissen C, Lombardo C, et al. Insomnia disorder is associated with increased amygdala reactivity to insomnia-related stimuli. *Sleep.* (2014) 37:1907–17. doi: 10.5665/sleep.4240
23. Pessoa L. Emotion and cognition and the amygdala: from "what is it?" to "what's to be done?" *Neuropsychologia*. (2010) 48:3416–29. doi: 10.1016/j.neuropsychologia.2010.06.038
24. Sergerie K, Chochol C, Armony JL. The role of the amygdala in emotional processing: a quantitative meta-analysis of functional neuroimaging studies. *Neurosci Biobehav Rev.* (2008) 32:811–30. doi: 10.1016/j.neubiorev.2007.12.002
25. Zotev V, Krueger F, Phillips R, Alvarez RP, Simmons WK, Bellgowan P, et al. Self-regulation of amygdala activation using real-time fMRI neurofeedback. *PloS ONE*. (2011) 6:e24522. doi: 10.1371/journal.pone.0024522
26. Buysse DJ, Reynolds III CF, Monk TH, Berman SR, Kupfer DJ. The Pittsburgh sleep quality index: a new instrument for psychiatric practice and research. *Psychiatry Res.* (1989) 28:193–213. doi: 10.1016/0165-1781(89)90047-4
27. Bastien CH, Vallières A, Morin CM. Validation of the insomnia severity index as an outcome measure for insomnia research. *Sleep Med.* (2001) 2:297–307. doi: 10.1016/S1389-9457(00)00065-4
28. Hamilton M, Guy W. Hamilton depression scale. *Group*. (1976) 1:4.
29. Beck AT, Steer RA, Carbin MG. Psychometric properties of the Beck depression inventory: twenty-five years of evaluation. *Clin Psychol Rev.* (1988) 8:77–100. doi: 10.1016/0272-7358(88)90050-5
30. Hamilton M. Hamilton anxiety scale. *Group.* (1959) 1:10–1037. doi: 10.1037/t02824-000

31. Benca RM, Peterson MJ. Insomnia and depression. *Sleep Med.* (2008) 9:S3–9. doi: 10.1016/S1389-9457(08)70010-8
32. Gebara MA, Siripong N, DiNapoli EA, Maree RD, Germain A, Reynolds CF, et al. Effect of insomnia treatments on depression: a systematic review and meta-analysis. *Depress Anxiety*. (2018) 35:717–31. doi: 10.1002/da.22776
33. Faul F, Erdfelder E, Buchner A, Lang AG. Statistical power analyses using G* power 3.1: tests for correlation and regression analyses. *Behav Res Methods*. (2009) 41:1149–60. doi: 10.3758/BRM.41.4.1149
34. Young KD, Siegle GJ, Zotev V, Phillips R, Misaki M, Yuan H, et al. Randomized clinical trial of real-time fMRI amygdala neurofeedback for major depressive disorder: effects on symptoms and autobiographical memory recall. *Am J Psychiatry*. (2017) 174:748–55. doi: 10.1176/appi.ajp.2017.16060637
35. Koush Y, Ashburner J, Prilepin E, Sladky R, Zeidman P, Bibikov S, et al. OpenNFT: an open-source Python/Matlab framework for real-time fMRI neurofeedback training based on activity, connectivity and multivariate pattern analysis. *Neuroimage.* (2017) 156:489–503. doi: 10.1016/j.neuroimage.2017.06.039
36. Yan CG, Wang XD, Zuo XN, Zang YF. DPABI: data processing & analysis for (resting-state) brain imaging. *Neuroinformatics.* (2016) 14:339–51. doi: 10.1007/s12021-016-9299-4
37. Horovitz SG, Braun AR, Carr WS, Picchioni D, Balkin TJ, Fukunaga M, et al. Decoupling of the brain's default mode network during deep sleep. *Proc Nat Acad Sci USA*. (2009) 106:11376–81. doi: 10.1073/pnas.0901435106
38. Yu S, Guo B, Shen Z, Wang Z, Kui Y, Hu Y, et al. The imbalanced anterior and posterior default mode network in the primary insomnia. *J Psychiatr Res.* (2018) 103:97–103. doi: 10.1016/j.jpsychires.2018.05.013
39. Chou KH, Kuo CY, Liang CS, Lee PL, Tsai CK, Tsai CL, et al. Shared patterns of brain functional connectivity for the comorbidity between migraine and insomnia. *Biomedicines.* (2021) 9:1420. doi: 10.3390/biomedicines9101420
40. Koenigs M, Holliday J, Solomon J, Grafman J. Left dorsomedial frontal brain damage is associated with insomnia. *J Neurosci.* (2010) 30:16041–3. doi: 10.1523/JNEUROSCI.3745-10.2010
41. Marques DR, Gomes AA, Caetano G, Castelo-Branco M. Insomnia disorder and brain's default-mode network. *Curr Neurol Neurosci Rep.* (2018) 18:1–4. doi: 10.1007/s11910-018-0861-3
42. Marques DR, Gomes AA, Clemente V, dos Santos JM, Castelo-Branco M. Default-mode network activity and its role in comprehension and management of psychophysiological insomnia: a new perspective. *New Ideas Psychol.* (2015) 36:30–7. doi: 10.1016/j.newideapsych.2014.08.001
43. Buysse DJ, Germain A, Hall M, Monk TH, Nofzinger EA. A neurobiological model of insomnia. *Drug Discov Today Dis Model.* (2011) 8:129–37. doi: 10.1016/j.ddmod.2011.07.002
44. Taylor DJ, Lichstein KL, Durrence HH, Reidel BW, Bush AJ. Epidemiology of insomnia, depression, and anxiety. *Sleep.* (2005) 28:1457–64. doi: 10.1093/sleep/28.11.1457
45. Neckelmann D, Mykletun A, Dahl AA. Chronic insomnia as a risk factor for developing anxiety and depression. *Sleep.* (2007) 30:873–80. doi: 10.1093/sleep/30.7.873
46. Li Z, Tong L, Wang L, Li Y, He W, Guan M, et al. Self-regulating positive emotion networks by feedback of multiple emotional brain states using real-time fMRI. *Exp Brain Res.* (2016) 234:3575–86. doi: 10.1007/s00221-016-4744-z
47. Casement MD, Keenan KE, Hipwell AE, Guyer AE, Forbes EE. Neural reward processing mediates the relationship between insomnia symptoms and depression in adolescence. *Sleep.* (2016) 39:439–47. doi: 10.5665/sleep.5460
48. Bagherzadeh-Azbari S, Khazaie H, Zarei M, Spiegelhalder K, Walter M, Leerssen J, et al. Neuroimaging insights into the link between depression and insomnia: a systematic review. *J Affect Disord.* (2019) 258:133–43. doi: 10.1016/j.jad.2019.07.089
49. Cheng Y, Xue T, Dong F, Hu Y, Zhou M, Li X, et al. Abnormal functional connectivity of the salience network in insomnia. *Brain Imaging Behav.* (2022) 16:930–8. doi: 10.1007/s11682-021-00567-9
50. Huang S, Zhou F, Jiang J, Huang M, Zeng X, Ding S, et al. Regional impairment of intrinsic functional connectivity strength in patients with chronic primary insomnia. *Neuropsychiatr Dis Treat.* (2017) 13:1449–62. doi: 10.2147/NDT.S137292
51. Xie D, Qin H, Dong F, Wang X, Liu C, Xue T, et al. Functional connectivity abnormalities of brain regions with structural deficits in primary insomnia patients. *Front Neurosci.* (2020) 14:566. doi: 10.3389/fnins.2020.00566
52. Joo EY, Noh HJ, Kim JS, Koo DL, Kim D, Hwang KJ, et al. Brain gray matter deficits in patients with chronic primary insomnia. *Sleep.* (2013) 36:999–1007. doi: 10.5665/sleep.2796
53. Li M, Yan J, Li S, Wang T, Wen H, Yin Y, et al. Altered gray matter volume in primary insomnia patients: a DARTEL-VBM study. *Brain Imaging Behav.* (2018) 12:1759–67. doi: 10.1007/s11682-018-9844-x
54. Liu CH, Guo J, Lu SL, Tang LR, Fan J, Wang CY, et al. Increased salience network activity in patients with insomnia complaints in major depressive disorder. *Front Psychiatry.* (2018) 9:93. doi: 10.3389/fpsyt.2018.00093
55. Cromheeke S, Mueller SC. Probing emotional influences on cognitive control: an ALE meta-analysis of cognition emotion interactions. *Brain Struct Funct.* (2014) 219:995–1008. doi: 10.1007/s00429-013-0549-z
56. Gong L, Xu R, Qin M, Liu D, Zhang B, Bi Y, et al. New potential stimulation targets for non-invasive brain stimulation treatment of chronic insomnia. *Sleep Med.* (2020) 75:380–7. doi: 10.1016/j.sleep.2020.08.021
57. Feng J, Zhang Q, Zhang C, Wen Z, Zhou X. The Effect of sequential bilateral low-frequency rTMS over dorsolateral pre-frontal cortex on serum level of BDNF and GABA in patients with primary insomnia. *Brain Behav.* (2019) 9:e01206. doi: 10.1002/brb3.1206
58. Zhou Q, Yu C, Yu H, Zhang Y, Liu Z, Hu Z, et al. The effects of repeated transcranial direct current stimulation on sleep quality and depression symptoms in patients with major depression and insomnia. *Sleep Med.* (2020) 70:17–26. doi: 10.1016/j.sleep.2020.02.003
59. Fasiello E, Gorgoni M, Scarpelli S, Alfonsi V, Strambi LF, De Gennaro L. Functional connectivity changes in insomnia disorder: a systematic review. *Sleep Med Rev.* (2022) 61:101569. doi: 10.1016/j.smrv.2021.101569
60. Killgore WD, Schwab ZJ, Kipman M, DelDonno SR, Weber M. Insomnia-related complaints correlate with functional connectivity between sensory–motor regions. *Neuroreport.* (2013) 24:233–40. doi: 10.1097/WNR.0b013e32835edbdd
61. Li Z, Chen R, Guan M, Wang E, Qian T, Zhao C, et al. Disrupted brain network topology in chronic insomnia disorder: a resting-state fMRI study. *Neuroimage Clin.* (2018) 18:178–85. doi: 10.1016/j.nicl.2018.01.012
62. Kim SJ, Lee YJ, Kim N, Kim S, Choi JW, Park J, et al. Exploration of changes in the brain response to sleep-related pictures after cognitive–behavioral therapy for psychophysiological insomnia. *Sci Rep.* (2017) 7:1–10. doi: 10.1038/s41598-017-13065-0
63. Lee YJG, Kim S, Kim N, Choi JW, Park J, Kim SJ, et al. Changes in subcortical resting-state functional connectivity in patients with psychophysiological insomnia after cognitive–behavioral therapy. *Neuroimage Clin.* (2018) 17:115–23. doi: 10.1016/j.nicl.2017.10.013
64. Tachibana N, Shinde A, Ikeda A, Akiguchi I, Kimura J, Shibasaki H. Supplementary motor area seizure resembling sleep disorder. *Sleep.* (1996) 19:811–6. doi: 10.1093/sleep/19.10.811
65. Jung KI, Park MH, Park B, Kim SY, Kim YO, Kim BN, et al. Cerebellar gray matter volume, executive function, and insomnia: gender differences in adolescents. *Sci Rep.* (2019) 9:1–9. doi: 10.1038/s41598-018-37154-w

Conflict of Interest: The authors declare that the research was conducted in the absence of any commercial or financial relationships that could be construed as a potential conflict of interest.

frontiers | Frontiers in Psychiatry

TYPE Original Research
PUBLISHED 22 August 2022
DOI 10.3389/fpsyt.2022.958994

OPEN ACCESS

EDITED BY
Ning Hua Wang,
Fourth Military Medical University, China

REVIEWED BY
Jie Yang,
Central South University, China
Xueling Zhu,
Central South University, China

*CORRESPONDENCE
Yanqing Tang
tangyanqing@cmu.edu.cn

†These authors have contributed equally to this work and share first authorship

SPECIALTY SECTION
This article was submitted to Neuroimaging and Stimulation, a section of the journal Frontiers in Psychiatry

RECEIVED 01 June 2022
ACCEPTED 29 July 2022
PUBLISHED 22 August 2022

CITATION
Deng Z, Jiang X, Liu W, Zhao W, Jia L, Sun Q, Xie Y, Zhou Y, Sun T, Wu F, Kong L and Tang Y (2022) The aberrant dynamic amplitude of low-frequency fluctuations in melancholic major depressive disorder with insomnia. *Front. Psychiatry* 13:958994. doi: 10.3389/fpsyt.2022.958994

The aberrant dynamic amplitude of low-frequency fluctuations in melancholic major depressive disorder with insomnia

Zijing Deng[1,2†], Xiaowei Jiang[1,3†], Wen Liu[1,2], Wenhui Zhao[1,2], Linna Jia[1,2], Qikun Sun[4], Yu Xie[1], Yifang Zhou[1,2], Ting Sun[1,2], Feng Wu[1,2], Lingtao Kong[1,2] and Yanqing Tang[2,5*]

[1]Brain Function Research Section, The First Affiliated Hospital of China Medical University, Shenyang, China, [2]Department of Psychiatry, The First Affiliated Hospital of China Medical University, Shenyang, China, [3]Department of Radiology, The First Affiliated Hospital of China Medical University, Shenyang, China, [4]Department of Radiation Oncology, The First Affiliated Hospital of China Medical University, Shenyang, China, [5]Department of Gerontology, The First Affiliated Hospital of China Medical University, Shenyang, China

Background: Insomnia is considered one of the manifestations of sleep disorders, and its intensity is linked to the treatment effect or suicidal thoughts. Major depressive disorder (MDD) is classified into various subtypes due to heterogeneous symptoms. Melancholic MDD has been considered one of the most common subtypes with special sleep features. However, the brain functional mechanisms in melancholic MDD with insomnia remain unclear.

Materials and methods: Melancholic MDD and healthy controls (HCs, n = 46) were recruited for the study. Patients were divided into patients with melancholic MDD with low insomnia (mMDD-LI, n = 23) and patients with melancholic MDD with high insomnia (mMDD-HI, n = 30), according to the sleep disturbance subscale of the 17-item Hamilton Depression Rating Scale. The dynamic amplitude of low-frequency fluctuation was employed to investigate the alterations of brain activity among the three groups. Then, the correlations between abnormal dALFF values of brain regions and the severity of symptoms were investigated.

Results: Lower dALFF values were found in the mMDD-HI group in the right middle temporal gyrus (MTG)/superior temporal gyrus (STG) than in the mMDD-LI (p = 0.014) and HC groups ($p < 0.001$). Melancholic MDD groups showed decreased dALFF values than HC in the right middle occipital gyri (MOG)/superior occipital gyri (SOG), the right cuneus, the bilateral lingual gyrus, and the bilateral calcarine ($p < 0.05$). Lower dALFF values than HC in the left MOG/SOG and the left cuneus in melancholic MDD groups were found, but no significant difference was found between the mMDD-LI group and HC group (p = 0.079). Positive correlations between the dALFF values in the right MTG/STG and HAMD-SD scores (the sleep disturbance subscale of the HAMD-17) in the mMDD-HI group (r = 0.41, p = 0.042) were found. In the pooled melancholic MDD, the dALFF values in the right MOG/SOG and the

right cuneus (r = 0.338, p = 0.019), the left MOG/SOG and the left cuneus (r = 0.299, p = 0.039), and the bilateral lingual gyrus and the bilateral calcarine (r = 0.288, p = 0.047) were positively correlated with adjusted HAMD scores.

Conclusion: The occipital cortex may be related to depressive symptoms in melancholic MDD. Importantly, the right MTG/STG may play a critical role in patients with melancholic MDD with more severe insomnia.

KEYWORDS

melancholic depression, resting-state, magnetic resonance imaging, the dynamic amplitude of low-frequency fluctuation, sleep disturbance, insomnia

Introduction

Major depressive disorder (MDD) is a widely distributed, heterogeneous, and disabling psychiatric disease (1, 2), characterized by different clinical manifestations, such as persistently depressed mood, anhedonia, low self-esteem, somatization, weight change, cognitive dysfunction, retardation, and sleep disturbances (1). Sleep disturbances, particularly insomnia, are prevalent and prodromal clinical characteristics in MDD (3), and 92% of patients with major depressive episodes reported substantial sleep complaints (4). Insomnia, as one of the main manifestations of sleep disturbances, is not only an important risk factor for developing depression (5, 6) but also for recurrence (7), and its severity is associated with the quality of life (8), the severity of depression (8), the therapeutic effect (9, 10), and suicidal thoughts (11, 12). In addition, the link between MDD and insomnia showed a strong bond based on substantial shared genetic liability (13, 14).

Previous research has shown a significant relationship between sleep disturbance (insomnia especially) and depression (15, 16). Furthermore, several neuroimaging studies have also found objective differences in brain regions and changes in neural activity in patients with MDD (17–21) and insomnia individuals (22–25) by using distinctive imaging approaches, such as the amplitude of low-frequency fluctuation (ALFF), functional connectivity (FC), and regional homogeneity (ReHo). These studies implied that neuroimaging characteristics can correctly reflect individual sleep disturbances and performance and could be used as diagnostic biomarkers of MDD (26). There is also some research into the underlying brain mechanisms of patients with MDD with sleep disturbances using resting-state functional MRI (rs-fMRI). Carried out using various methods of rs-fMRI, such as ALFF or FC in patients with MDD with insomnia, researchers noticed changes in the activity of some brain regions, such as the salience network, the suprachiasmatic nuclei, and the default mode network (27–29). A study using a multicenter dataset found that the combination of gray matter (GM) density and fractional ALFF can accurately predict individual total sleep disturbance scores of the 17-Item Hamilton Depression Rating Scale (HAMD-17) which includes items 4 (sleep initiation disorder), 5 (sleep maintenance disorder), and 6 (early awakening) of HAMD-17 in patients with MDD (26). According to certain findings, patients with MDD with more severe insomnia had smaller cortical surface areas in several frontoparietal cortical areas (30), and the interaction between depression and insomnia was related to reduced GM volume in the right orbitofrontal cortex (31). Besides, abnormal global FC density in the visual system was considered a biomarker in patients with MDD with insomnia (32). As a result, the underlying biological mechanisms of sleep disruption in MDD are being investigated constantly.

However, these studies mentioned above did not go deep into each subtype of MDD, and the heterogeneity of symptoms may bring inconsistent experimental results. In addition, newer imaging methods can also be used in future research.

As a heterogeneous mental disorder, dividing MDD into subcategories based on diagnostic criteria is essential for identifying underlying pathophysiological mechanisms, and this form of individualized diagnosis is required for precise MDD treatment (26). Melancholic MDD has been viewed as the most serious subtype of MDD (33) with specific clinical symptoms, such as persistent anhedonia, psychomotor disturbances, cognitive impairment, early morning awakening, excessive guilt, and anorexia (34). In addition, there are several biological indicators, such as disturbances in sleep architecture, occurring more frequently in melancholia than in other types of depression (35, 36). Studies also found that patients with melancholic MDD had a higher rate of nightmares, middle, and terminal insomnia than patients with non-melancholic MDD (37, 38). Previous research revealed that patients with melancholic MDD displayed evident sleep-electroencephalogram (EEG) changes, which involved low quantities of slow-wave sleep, disrupted sleep, a short rapid eye movement (REM) latency, and a high REM density compared to non-melancholic depression (36, 39–41). However, limited studies use imaging methods to investigate underlying neuroimaging mechanisms of melancholic MDD with insomnia.

Resting-state functional magnetic resonance imaging (rs-fMRI) is a method to measure spontaneous activity in the brain that has been generally utilized to explore functional changes in the human brain (42). There are also several studies about melancholic MDD. These studies found that the melancholic MDD had distinct fractional ALFF values in the right middle temporal gyrus (MTG)/and bilateral superior occipital gyrus (SOG) (43), lower ReHo values in the right SOG/middle occipital gyrus (MOG) (44), different network homogeneity values in the right posterior cingulate cortex (PCC)/precuneus, right angular gyrus, and the right MTG (45), decreased voxel-mirrored homotopic connectivity values in the fusiform gyrus, PCC, and SOG (46). As a promising approach to rs-fMRI, ALFF has been adopted widely because it can reflect the spontaneous neuronal activity of specific regions (47). Simultaneously, ALFF is also considered to be momentarily stationary during a typical rs-MRI session (48). However, the activity of brain areas is inherently dynamic (49). Therefore, to capture the dynamic properties of distinct brain regions' activity effectively, the dynamic sliding window method such as dALFF has been adopted in several types of research in contrast to the "static" approaches of rs-fMRI. Furthermore, a previous study demonstrated that dALFF changes are related to changes in EEG band power (50). Recently, many psychiatric illnesses have discovered a significant change in dALFF, such as MDD (51), bipolar disorder (52), Schizophrenia (53), primary insomnia (54), and generalized anxiety disorder (55). For an instance, Staner found that temporal dALFF can predict suicidal thoughts in depressed patients, while static ALFF cannot (16). Nevertheless, the dynamics of brain activity in patients with melancholic MDD with insomnia have not yet been quantified.

Therefore, our goal is to investigate the dynamic spontaneous brain activity in patients with melancholic MDD along with insomnia compared to HCs by employing the dALFF. We assume that melancholic MDD with variable degrees of insomnia may show certain particular dynamic brain functional changes and these features are associated with insomnia symptoms of melancholic MDD.

Materials and methods

Participants

In the current research, a total of 53 melancholic MDD individuals and 46 healthy controls (HCs) matched for age, gender, and education were recruited from the Shenyang Mental Health Center and The First Affiliated Hospital of China Medical University. Participants ranged in age from 18 to 40. The Medical Research Ethical Committee of the First Affiliated Hospital of China Medical University has approved the study. Before starting the study, all participants were informed of the purpose of the study and signed an informed consent form.

The diagnosis of melancholic MDD was independently performed by two seasoned psychiatrists, according to the Diagnostic and Statistical Manual of Mental Disorders, fourth edition (DSM-IV) criteria. The inclusion criteria for melancholic MDD were: (1) continuously anhedonia; (2) at least three of the symptoms as follows are required: depressive mood, feeling worse in the morning, early morning awakening, remarkable psychomotor disturbances, severe anorexia or weight loss, and excessive or inappropriate guilt. Patients were enrolled in the research while experiencing a depressive episode with a total of HAMD-17 scores $\geq$ 17 on the day of the MRI scan. These patients were excluded if diagnosed with other Axis I or Axis II disorder.

HCs with HAMD-17 scores $\leq$ 7 were recruited from the local community and they had no Axis I or Axis II disorder. Meanwhile, their first-degree relatives could not have any family history of psychiatric disorders.

The following exclusion criteria applied to all participants: history of neurological such as head injury, stroke, seizures, or transient ischemic attack; caffeine, drug, or alcohol abuse; and pregnancy.

Assessments

The depression severity was evaluated by HAMD-17 (56) and the anxiety severity was measured based on the Hamilton Anxiety Rating Scale (HAMA) (57). Insomnia symptoms were evaluated using the insomnia subscale of the HAMD-17 (HAMD-SD) (22, 26, 58), which involved items 4 (sleep initiation disorder), 5 (sleep maintenance disorder), and 6 (early awakening). The scores of the HAMD insomnia subscale and sleep diary data are widely considered to be well correlated, which has been a global measure of insomnia severity in depressive disorders (59). The adjusted HAMD scores meant the HAMD-17 scores after the omission of the sleep subscale scores (27, 32). Patients with melancholic MDD were separated into patients with melancholic MDD with low insomnia group (mMDD-LI, HAMD-SD $\leq$ 3, n = 23) and patients with melancholic MDD with high insomnia (mMDD-HI, HAMD-SD $\geq$ 4, n = 30), according to the HAMD-SD.

Image acquisition

The rs-MRI functional images were acquired by adopting a 3.0 T GE SIGNA MRI system at the Image Institute of The First Affiliated Hospital of China Medical University, Shenyang, China. The following are the parameters that were obtained using a gradient echo-planar imaging (EPI) sequence: repetition time (TR) = 2,000 ms, echo time (TE) = 40 ms, field of view (FOV) = 240 × 240 mm^2, flip angle (FA) = 90°, image matrix size = 64 × 64, slices = 35, slice thickness = 3 mm, spacing

between slices = 3 mm. Participants were required to wear earplugs and use foam pads to reduce scanner noise and head motion, and their head was fixedly positioned during scan time. The resting state meant that participants were not doing any cognitive tasks during the scan time and they were asked to keep relaxed and awake with their eyes closed while simultaneously keeping their minds blank. After completing scanning, we obtained a total of 200 volumes of images.

Image pre-processing

Images were processed by applying the Statistical Parametric Mapping 12 (SPM12)[1] and the Data Processing Assistant for Resting-State fMRI (DPABI 4.1, Advanced edition) (60) based on the custom code written in MATLAB. To maintain the stability of the initial signal, the first 10 volumes of each participant's scanned data were eliminated. Then, the remaining 190 images were adjusted for slice-timing and head motion. Participants with the translation of more than 2 mm or rotation of more than 2° of head motion in each direction were not included in the present study. The mean framewise displacement (FD) was used to measure the scrubbing-related micro-head motion of each participant. Additionally, no statistical difference existed in mean FD when comparing the three groups. After realignment, the imaging data corrected were spatially normalized into a standard EPI template in the Montreal Neurological Institute (MNI) space and resampled to a voxel size of 3 mm × 3 mm × 3 mm. The spatial smoothing of the EPI images adopted a 4 mm full width at half maximum (FWHM) Gaussian kernel. The BOLD signals were then detrended to correct a linear trend. Finally, the linear regression of the nuisance covariates was performed to remove the effects, including head motion parameters, cerebrospinal fluid signal, and white matter signal. Normalization of T1 images was also conducted, and details and results are shown in **Supplementary Table 3** and **Supplementary Figure 3**, and pre-processing part.

Dynamic amplitude of low-frequency fluctuation acquisition

The dynamic ALFF was computed using temporal dynamic analysis (TDA) toolkits in DPABI 4.1 (60) based on a sliding window analysis. The window length which was considered a crucial parameter of resting-state dynamic computation should be larger than $1/f_{min}$. The f_{min} referred to the minimum frequency of the time series. As a shorter window length is more likely to introduce misleading fluctuations in the observed dALFF, a longer window length may fail to discover the potential dALFF. Therefore, a window length of 50 TRs (100 s) was selected to compute the temporal variability of ALFF according to prior research (51, 61). We calculated the ALFF of each subject with a sliding window and obtained the ALFF values of each given voxel, the time series of which were then transformed into a frequency domain with a fast Fourier transform. The square root of the power spectrum of each voxel was computed and summed from 0.01 to 0.08 Hz. The dALFF values were obtained through computing the standard deviation (SD) of ALFF values at each voxel across the sliding window dynamics. SD is a useful and quantified indicator that is generally applied to describe the degree of change in dALFF in the research of temporal dynamic brain activity. Therefore, we used SD as dALFF for the next analysis.

Statistical analysis

The demographic features and clinical symptoms were analyzed by several statistical methods, such as one-way analysis of variance (ANOVA), two-sample *t*-test, and chi-square test, and $p < 0.05$ was set as significance. The specific use of these statistical methods is shown in **Table 1**. The relationships between the total HAMD-17 scores, adjusted HAMD scores, HAMD-SD scores, and HAMA scores were explored by Pearson's correlation in the pooled melancholic MDD groups, and the statistical significance was also set at $p < 0.05$. Images data were analyzed by two software, and two types of correction are used. Altered dynamic ALFF values across the three groups were investigated by ANOVA in DPABI 4.1 and the results were corrected with the Gaussian random field (GRF) one-tailed (62), the threshold of voxel-wise was $p < 0.001$, and the cluster-level was $p < 0.05$. The extracted dALFF values were evaluated by SPSS (Statistical Product and Service Solutions) and the one-way analysis of covariance (ANCOVA) was used to compare differences among three groups when age, gender, years of education, and FD were covariates. Significance was set at $p < 0.05$ after correcting by Bonferroni correction. The partial correlation analysis was conducted to examine the relationship between the altered dALFF values and clinical features (HAMD-SD scores, HAMA scores, and adjusted HAMD scores) in melancholic MDD groups when age, gender, medication, HAMA scores, adjusted HAMD scores, or HAMD-SD scores were used as covariates. Significance was set at $p < 0.05$ after correcting by Bonferroni correction.

Validation analysis

To verify the results of dALFF variability obtained from a sliding window length of 50 TR, we adopted using two other window lengths (30 and 70 TR).

1 www.fil.ion.ucl.ac.uk/spm/software/spm12

TABLE 1 Demographic and clinical measurement among three groups.

Measurement	mMDD-LI (n = 23)	mMDD-HI (n = 30)	HC (n = 46)	Statistical value	P-value
Age (years)	24.65 ± 5.57	26.83 ± 6.81	25.65 ± 6.08	0.832	0.442*
Gender (male/female)	8/15	6/24	20/26	4.441	0.109#
Education (years)	14.70 ± 2.42	14.73 ± 2.27	14.63 ± 1.88	0.022	0.978*
Mean FD	0.11 ± 0.54	0.93 ± 0.39	0.12 ± 0.51	2.061	0.133*
Illness duration (months)	17.39 ± 19.61	13.15 ± 18.28	NA	0.81	0.420
Number of episodes	1.13 ± 0.34	1.17 ± 0.38	NA	−0.36	0.720
HAMD-SD	2.52 ± 0.67	4.87 ± 0.82	NA	−11.18	<0.001
Adjusted HAMD	19.43 ± 2.83	20.20 ± 5.25	NA	−0.68	0.500
HAMD-17	21.96 ± 3.07	25.07 ± 5.45	NA	−2.63	0.012
HAMA	19.61 ± 7.05	24.17 ± 8.24	NA	−2.12	0.039
Medication	19 (83%)	19 (63%)	NA	0.171	0.879#
Antidepressants	19 (83%)	15 (60%)	NA	NA	NA
Benzodiazepines	13 (57%)	12 (40%)	NA	NA	NA
Medication-free	4 (17%)	11 (37%)	NA	NA	NA

Data are presented as either percentages (%) or means (standard deviations). #P-value for chi-square test, *P-value for one-way ANOVA, the rest P-value for two-sample t-tests. NA stands for not available; mMDD-LI, patients with melancholic MDD with low insomnia group; mMDD-HI, patients with melancholic MDD with high insomnia; HC, healthy control; FD, framewise displacement; HAMD-17, 17-item Hamilton Depression Rating Scale; HAMD-SD, the sleep disturbance factor of the HAMD-17 subscale; adjusted HAMD, HAMD-17 scores after the omission of the sleep subscale scores; HAMA, Hamilton Anxiety Rating Scale.

Results

Demographic characteristics and clinical symptoms

As Table 1 illustrates age, sex, years of education, and mean FD were not significantly different among the mMDD-LI, mMDD-HI, and HC groups ($p > 0.05$). And there were no significant differences in medication, duration of disease, or number of episodes between the two melancholic MDD groups ($p > 0.05$). Compared with the mMDD-LI, mMDD-HI showed higher HAMD ($p = 0.012$) and HAMA scores ($p = 0.039$). However, the adjusted HAMD scores were not statistically different between the two melancholic MDD groups ($p = 0.50$). In the pooled melancholic MDD, the HAMD-SD scores were significantly positively associated with the HAMD scores ($r = 0.452$, $p = 0.001$) and HAMA scores ($r = 0.377$, $p = 0.005$), but not with the adjusted HAMD scores ($r = 0.178$, $p = 0.203$). The HAMA scores were also positively associated with the HAMD scores ($r = 0.68$, $p < 0.001$) and the adjusted HAMD scores ($r = 0.629$, $p < 0.001$) in the pooled melancholic MDD.

Differences in dynamic amplitude of low-frequency fluctuation values among three groups

Significant group differences of dALFF were found in the right MTG/superior temporal gyrus (STG), the bilateral MOG/SOG, the bilateral cuneus, the bilateral calcarine, and the bilateral lingual gyrus ($p < 0.001$, GRF correction). The ANCOVA revealed that the mMDD-HI group displayed lower dALFF values in the right MTG/STG than the mMDD-LI group ($p = 0.014$, Bonferroni correction) and HC group ($p < 0.001$, Bonferroni correction). Meanwhile, two melancholic MDD groups showed lower dALFF values than HC in the right MOG/SOG, the right cuneus, the bilateral lingual gyrus, and the bilateral calcarine ($p < 0.05$, Bonferroni correction). The two melancholic MDD groups had lower dALFF values than HC in the left MOG/SOG and the left cuneus, although the difference between the mMDD-LI group and HC group was not statistically significant ($p = 0.079$, Bonferroni correction). Table 2 and Figure 1 illustrate these findings.

Correlations between dynamic amplitude of low-frequency fluctuation values and clinical characteristics

The partial correlation analysis revealed that the dALFF values in the right MTG/STG were positively correlated with HAMD-SD scores in the mMDD-HI group when age, gender, medication, and adjusted HAMD scores, and HAMA scores were covariates ($r = 0.41$, $p = 0.042$). In the pooled melancholic MDD, the dALFF values in the right MOG/SOG and the right cuneus were significantly positively correlated with adjusted HAMD scores ($r = 0.338$, $p = 0.019$), the dALFF values in the left MOG/SOG and the left cuneus were positively correlated with adjusted HAMD scores ($r = 0.299$, $p = 0.039$), and the dALFF values in the bilateral lingual

TABLE 2 Brain regions showing significant group differences in dALFF values.

Cluster	Hemisphere	Brain regions	Cluster size (voxels)	MINI coordinates (x, y, z)			*F*-values
1	Right	Middle temporal gyrus/superior temporal gyrus	43	48	−27	3	12.913
2	Bilateral	Calcarine/lingual gyrus	92	−6	−72	15	11.936
3	Right	Middle occipital gyrus/superior occipital gyrus/cuneus	81	21	−96	9	14.964
4	Left	Middle occipital gyrus/superior occipital gyrus/cuneus	135	−24	−87	15	12.318

MINI, Montreal Neurological Institute; dALFF, the dynamic amplitude of low-frequency fluctuation.

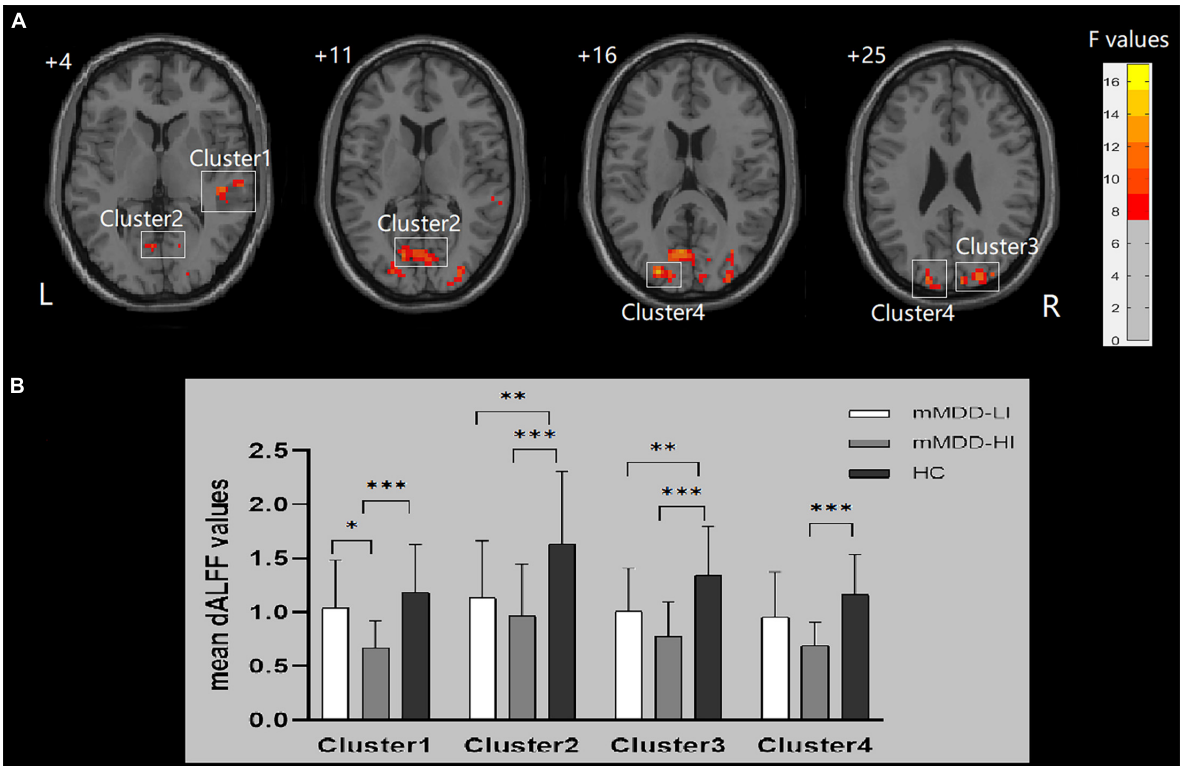

FIGURE 1
Differences in dALFF values and *post hoc* analysis of dALFF values among three groups. Cluster 1: right MTG/STG, Cluster 2: bilateral lingual gyrus/calcarine; Cluster 3: right middle occipital gyrus/superior occipital gyrus/cuneus; Cluster 4: left middle occipital gyrus/superior occipital gyrus/cuneus. **(A)** Significant difference in dALFF values among the three groups. Significant at $p < 0.001$ after GRF correction. R, right side; L, left side. **(B)** *Post hoc* analysis of dALFF values with significant variations across the three groups. ***$p < 0.001$ level, **$p < 0.01$ level, *$p < 0.05$ level, Bonferroni correction.

gyrus and the bilateral calcarine were positively correlated with adjusted HAMD scores ($r = 0.288$, $p = 0.047$) when age, gender, medication, HAMD-SD scores, HAMA scores were as covariates. The above results are shown in Tables 3, 4. No other correlation was found.

Validation results

In the present study, we validated our results by using different sliding window lengths (30 and 70 TR). Finally, the relevant results were presented in Supplementary Tables 1, 2 and Supplementary Figures 1, 2.

Discussion

In the present study, we investigated the neuroimaging features of melancholic MDD with varying degrees of insomnia by adopting the dynamic sliding window method. Our research found that the mMDD-HI group displayed significantly decreased dALFF values in the right MTG/STG than the mMDD-LI and HC groups. Furthermore, the dALFF values in the right MTG/STG were significantly positively correlated with HAMD-SD scores in the mMDD-HI group. We also found two melancholic MDD groups showed decreased dALFF values than HC in the right MOG/SOG, the right cuneus, the bilateral lingual gyrus, and the bilateral calcarine. The two melancholic

TABLE 3 The partial correlation analysis between the dALFF values and adjusted HAMD scores in the pooled melancholic MDD.

Cluster	Hemisphere	Brain regions	Cluster size (voxels)	MINI coordinates (x, y, z)			*r*	*p*
2	Bilateral	Calcarine/lingual gyri	92	−6	−72	15	0.288	0.047
3	Right	Middle occipital gyrus/superior occipital gyrus/cuneus	81	21	−96	9	0.338	0.019
4	Left	Middle occipital gyrus/superior occipital gyrus/cuneus	135	−24	−87	15	0.299	0.039

Covariates included age, gender, medication, HAMD-SD scores, and HAMA scores. MINI, Montreal Neurological Institute; dALFF, the dynamic amplitude of low-frequency fluctuation.

TABLE 4 The partial correlation analysis between the dALFF values and HAMD-SD scores in patients with melancholic MDD with high insomnia.

Cluster	Hemisphere	Brain regions	Cluster size (voxels)	MINI coordinates (x, y, z)			*r*	*p*
1	Right	Middle temporal gyrus/superior temporal gyrus	43	48	−27	3	0.41	0.042

Covariates included age, gender, medication, adjusted HAMD scores, and HAMA scores. MINI, Montreal Neurological Institute; dALFF, the dynamic amplitude of low-frequency fluctuation; HAMD-SD, the sleep disturbance factor of the HAMD-17 subscale.

MDD groups had lower dALFF values than HC in the left MOG/SOG and the left cuneus, but the difference between the mMDD-LI group and HC group was not statistically significant. Meanwhile, the dALFF values in the bilateral MOG/SOG, the bilateral cuneus, the bilateral lingual gyrus, and the bilateral calcarine were significantly positively correlated with adjusted HAMD scores in the pooled melancholic MDD. These findings suggested that the bilateral occipital cortex may be associated with the neuroimaging mechanisms of melancholic MDD depressive symptoms other than insomnia, while the temporal cortex may play an important role in more severe insomnia symptoms in patients with melancholic MDD.

In the present study, the mMDD-HI group revealed alterations of dALFF in the right temporal cortex. Meanwhile, the right temporal cortex may be associated with more severe insomnia symptoms in patients with melancholic MDD. Previous studies also speculated that functional alterations in the right MTG/STG may be a neurobiological characteristic of melancholic MDD (44, 45). Some studies found GM hypertrophies (63) and diminished ALFF in the right MTG (64) in patients with insomnia disorder. The altered fALFF brain areas of patients with insomnia were found in the right STG, which was unaffected by age and gender factors (65). This evidence suggests that the right MTG/STG may play an important role in insomnia symptoms of melancholic depression. Previous studies have proposed the hyperarousal hypothesis to explain the mechanism of insomnia, which is the result of hyperarousal in emotional or cognitive networks (66, 67). Furthermore, emotional and cognitive functions, such as emotional regulation, social cognition, and the process of memory, have been considered to be associated with the temporal lobe (55, 68), which may explain the hyperarousal hypothesis. Hence, we speculated that the abnormal dALFF values in the right temporal cortex may be one of the neuroimaging mechanisms of high insomnia symptoms in melancholic MDD.

However, there are also studies that are inconsistent with our results. They found several brain regions, such as the left inferior temporal gyrus (32), the posterior parahippocampal/hippocampal gyrus (32), frontoparietal cortical areas (30), caudate nuclei (69), and the anterior insular subregions (70), were associated with insomnia symptoms in patients with MDD. We went on to think about the reasons for these differences, which may be caused by distinct rs-fMRI methods or the heterogeneous symptoms of patients with MDD. This suggests that we need to expand the sample size, pay more attention to the heterogeneity of MDD, and adopt newer methods for analysis in future.

In the current study, we also discovered that melancholic MDD caused changes in dALFF values in the occipital cortex. Furthermore, these findings revealed that the occipital cortex may be associated with depressive characteristics. In recent years, multiple studies reported that patients with melancholic MDD manifested considerably lower values in the MOG/SOG than patients with non-melancholic MDD or HCs by applying rs-fMRI neuroimaging methods (44–46). However, there is not much literature on melancholic MDD, and we found similar results in other studies on MDD. Another research also found lower ALFF in the bilateral occipital cortex in treatment-free MDD subjects (71). The results indicate that decreased dALFF values of the calcarine in MDD are essentially consistent with findings from another study, where lower ALFF values were investigated in the left calcarine (27). Apart from functional changes, melancholic depression involves structural abnormalities, according to growing neuroimaging research evidence. Previous studies have found that patients with melancholic MDD showed asymmetrical cerebrospinal fluid (CSF) volume enlargement in the Sylvian fissure region (72, 73). The increased CSF volume may cause occipital bending, which may result in functional changes in the occipital cortex (74). These present findings are in line with the results of the previous studies. Therefore, these results revealed that alterations in the occipital cortex may be specific in melancholic MDD.

Besides, correlation analysis results show that the occipital cortex may be associated with depressive traits. The lingual

gyrus and cuneus, located in the medial occipital lobe, are necessary for both basic and advanced visual processing (75). The function of the occipital cortex is to process initial visual stimuli, consolidate information into visual working memory (76), and revolve in the consciousness of facial expressions (77), and its aberrant changes may explain working memory impairment in melancholic MDD (78). A study demonstrated functional changes in the occipital cortex when depressed adolescents are presented with sad faces, and the occipital cortex is important to the interaction of depression status, attention, and mood processing (79). In addition, the functional stability in the middle occipital gyri (MOG) was negatively linked with depressive symptoms, which could predict long-term recovery in depressive symptoms in patients with MDD (80). As a result, we hypothesized that the occipital cortex maybe plays a major role in the neuroimaging mechanisms of other depressive symptoms more than insomnia symptoms in melancholic.

In addition, we also observed that the mMDD-HI group showed lower dALFF values in all brain regions found in the current study compared to the mMDD-LI group and HC group, although certain differences did not achieve statistical significance. However, previous similar investigations using different imaging methods have yielded inconsistent results (27, 32). As a result, future studies will require a larger sample size to verify these results.

From our research, we observed several limitations. First, HAMD was adopted to evaluate the severity of insomnia, which may cause an incomplete assessment. In further studies, we could apply more objective and subjective measurements, such as Pittsburgh Insomnia Rating Scale or polysomnography, to improve the precision of the severity of insomnia assessments. Second, most patients had been on medicine before the scan and the drug-related effects cannot be excluded. In subsequent statistical analysis, we attempted to limit the impact of medication on the results by taking medication as a covariance. More medication-free patients should be enrolled in our research. Finally, our study was a cross-sectional study with a small sample size for each subgroup, and the sample size should be expanded in future, and relevant longitudinal work should be conducted.

In conclusion, the present study investigated brain functional alterations in melancholic MDD with insomnia. We found that the occipital cortex may be related to depressive symptoms in those with melancholic MDD, which further supports the findings of previous imaging studies on melancholic MDD. Moreover, the major finding of the present study revealed that the right temporal cortex was associated with more severe insomnia symptoms in melancholic MDD, which is consistent with our earlier hypothesis, and it suggested that the right temporal cortex could be a biomarker for melancholic MDD with high insomnia.

Data availability statement

The raw data supporting the conclusions of this article will be made available by the corresponding author.

Ethics statement

The studies involving human participants were reviewed and approved by the Medical Research Ethical Committee of The First Affiliated Hospital of China Medical University. The patients/participants provided their written informed consent to participate in this study. Written informed consent was obtained from the individual(s) for the publication of any potentially identifiable images or data included in this article.

Author contributions

ZD performed investigation, data processing, statistical analyses, and visualization, and wrote the original draft. XJ was responsible for conceptualization, data curation, writing of original draft, and funding acquisition. WL wrote the original draft. WZ and LJ performed investigation and data processing. QS acquired the data. YX was responsible for statistical analyses. YZ and TS validated the results. FW and LK recruited patients, confirmed the diagnosis, and acquired funding. YT was responsible for conceptualization, project administration, and funding acquisition. All authors reviewed and approved the manuscript.

Funding

This work was supported by the National Key R&D Program of China (Grants #2018YFC1311600 and 2016YFC1306900 to YT), the Liaoning Revitalization Talents Program (Grant #XLYC1808036 to YT), the Natural Science Foundation of Liaoning Province (2020-MS-176 to XJ), the National Key R&D Program "Science and Technology Winter Olympics" (2021YFF0306503 to FW), the Joint Fund of National Natural Science Foundation of China (U1808204 to FW), and the Natural Science Foundation of Liaoning Province (2019-MS-05 to FW).

Acknowledgments

We thank all participants who contributed to this research.

Conflict of interest

The authors declare that the research was conducted in the absence of any commercial or financial relationships that could be construed as a potential conflict of interest.

Publisher's note

All claims expressed in this article are solely those of the authors and do not necessarily represent those of their affiliated organizations, or those of the publisher, the editors and the reviewers. Any product that may be evaluated in this article, or claim that may be made by its manufacturer, is not guaranteed or endorsed by the publisher.

Supplementary material

The Supplementary Material for this article can be found online at: https://www.frontiersin.org/articles/10.3389/fpsyt.2022.958994/full#supplementary-material

References

1. American Psychiatric Association. *Diagnostic and Statistical Manual of Mental Disorders (DSM-5)*. Arlington, V A: American Psychiatric Association (2013).

2. Lu J, Xu X, Huang Y, Li T, Ma C, Xu G, et al. Prevalence of depressive disorders and treatment in China: a cross-sectional epidemiological study. *Lancet Psychiatry.* (2021) 8:981–90. doi: 10.1016/s2215-0366(21)00251-0

3. Perlis ML, Giles DE, Buysse DJ, Tu X, Kupfer DJ. Self-reported sleep disturbance as a prodromal symptom in recurrent depression. *J Affect Disord.* (1997) 42:209–12. doi: 10.1016/s0165-0327(96)01411-5

4. Geoffroy PA, Hoertel N, Etain B, Bellivier F, Delorme R, Limosin F, et al. Insomnia and hypersomnia in major depressive episode: Prevalence, sociodemographic characteristics and psychiatric comorbidity in a population-based study. *J Affect Disord.* (2018) 226:132–41. doi: 10.1016/j.jad.2017.09.032

5. Riemann D, Voderholzer U. Primary insomnia: a risk factor to develop depression? *J Affect Disord.* (2003) 76:255–9. doi: 10.1016/s0165-0327(02)00072-1

6. Baglioni C, Battagliese G, Feige B, Spiegelhalder K, Nissen C, Voderholzer U, et al. Insomnia as a predictor of depression: a meta-analytic evaluation of longitudinal epidemiological studies. *J Affect Disord.* (2011) 135:10–9. doi: 10.1016/j.jad.2011.01.011

7. Li SX, Lam SP, Chan JW, Yu MW, Wing YK. Residual sleep disturbances in patients remitted from major depressive disorder: a 4-year naturalistic follow-up study. *Sleep.* (2012) 35:1153–61. doi: 10.5665/sleep.2008

8. McCall WV, Reboussin BA, Cohen W. Subjective measurement of insomnia and quality of life in depressed inpatients. *J Sleep Res.* (2000) 9:43–8. doi: 10.1046/j.1365-2869.2000.00186.x

9. Jindal RD, Thase ME. Treatment of insomnia associated with clinical depression. *Sleep Med Rev.* (2004) 8:19–30. doi: 10.1016/s1087-0792(03)00025-x

10. Howland RH. Sleep interventions for the treatment of depression. *J Psychos Nurs Mental Health Serv.* (2011) 49:17–20. doi: 10.3928/02793695-20101208-01

11. Richardson JD, Thompson A, King L, Corbett B, Shnaider P, St Cyr K, et al. Insomnia, psychiatric disorders and suicidal ideation in a National Representative Sample of active Canadian Forces members. *BMC Psychiatry.* (2017) 17:211. doi: 10.1186/s12888-017-1372-5

12. Pompili M, Innamorati M, Forte A, Longo L, Mazzetta C, Erbuto D, et al. Insomnia as a predictor of high-lethality suicide attempts. *Int J Clin Pract.* (2013) 67:1311–6. doi: 10.1111/ijcp.12211

13. Baranova A, Cao H, Zhang F. Shared genetic liability and causal effects between major depressive disorder and insomnia. *Hum Mol Genet.* (2021) 31:1336–45. doi: 10.1093/hmg/ddab328

14. Melhuish Beaupre LM, Tiwari AK, Gonçalves VF, Zai CC, Marshe VS, Lewis CM, et al. Potential genetic overlap between insomnia and sleep symptoms in major depressive disorder: a polygenic risk score analysis. *Front Psychiatry.* (2021) 12:734077. doi: 10.3389/fpsyt.2021.734077

15. Riemann D, Krone LB, Wulff K, Nissen C. Sleep, insomnia, and depression. *Neuropsychopharmacology.* (2020) 45:74–89. doi: 10.1038/s41386-019-0411-y

16. Staner L. Comorbidity of insomnia and depression. *Sleep Med Rev.* (2010) 14:35–46. doi: 10.1016/j.smrv.2009.09.003

17. Yao X, Yin Z, Liu F, Wei S, Zhou Y, Jiang X, et al. Shared and distinct regional homogeneity changes in bipolar and unipolar depression. *Neurosci Lett.* (2018) 673:28–32. doi: 10.1016/j.neulet.2018.02.033

18. Sun H, Luo L, Yuan X, Zhang L, He Y, Yao S, et al. Regional homogeneity and functional connectivity patterns in major depressive disorder, cognitive vulnerability to depression and healthy subjects. *J Affect Disord.* (2018) 235:229–35. doi: 10.1016/j.jad.2018.04.061

19. Wang M, Ju Y, Lu X, Sun J, Dong Q, Liu J, et al. Longitudinal changes of amplitude of low-frequency fluctuations in MDD patients: A 6-month follow-up resting-state functional magnetic resonance imaging study. *J Affect Disord.* (2020) 276:411–7. doi: 10.1016/j.jad.2020.07.067

20. Kaiser RH, Andrews-Hanna JR, Wager TD, Pizzagalli DA. Large-Scale network dysfunction in major depressive disorder: a meta-analysis of resting-state functional connectivity. *JAMA Psychiatry.* (2015) 72:603–11. doi: 10.1001/jamapsychiatry.2015.0071

21. Wang L, Kong Q, Li K, Su Y, Zeng Y, Zhang Q, et al. Frequency-dependent changes in amplitude of low-frequency oscillations in depression: a resting-state fMRI study. *Neurosci Lett.* (2016) 614:105–11. doi: 10.1016/j.neulet.2016.01.012

22. Liu CH, Liu CZ, Zhang J, Yuan Z, Tang LR, Tie CL, et al. Reduced spontaneous neuronal activity in the insular cortex and thalamus in healthy adults with insomnia symptoms. *Brain research* (2016) 1648(Pt A):317–24. doi: 10.1016/j.brainres.2016.07.024

23. Zhu Y, Zhao X, Yin H, Zhang M. Functional connectivity density abnormalities and anxiety in primary insomnia patients. *Brain Imaging Behav.* (2021) 15:114–21. doi: 10.1007/s11682-019-00238-w

24. Zhang Y, Zhang Z, Wang Y, Zhu F, Liu X, Chen W, et al. Dysfunctional beliefs and attitudes about sleep are associated with regional homogeneity of left inferior occidental gyrus in primary insomnia patients: a preliminary resting state functional magnetic resonance imaging study. *Sleep Med.* (2021) 81:188–93. doi: 10.1016/j.sleep.2021.02.039

25. Ran Q, Chen J, Li C, Wen L, Yue F, Shu T, et al. Abnormal amplitude of low-frequency fluctuations associated with rapid-eye movement in chronic primary insomnia patients. *Oncotarget.* (2017) 8:84877–88. doi: 10.18632/oncotarget.17921

26. Shi Y, Zhang L, He C, Yin Y, Song R, Chen S, et al. Sleep disturbance-related neuroimaging features as potential biomarkers for the diagnosis of major depressive disorder: a multicenter study based on machine learning. *J Affect Disord.* (2021) 295:148–55. doi: 10.1016/j.jad.2021.08.027

27. Liu CH, Guo J, Lu SL, Tang LR, Fan J, Wang CY, et al. Increased Salience Network Activity in Patients With Insomnia Complaints in Major Depressive Disorder. *Front Psychiatry.* (2018) 9:93. doi: 10.3389/fpsyt.2018.00093

28. McKinnon AC, Hickie IB, Scott J, Duffy SL, Norrie L, Terpening Z, et al. Current sleep disturbance in older people with a lifetime history of depression is associated with increased connectivity in the Default Mode Network. *J Affect Disord.* (2018) 229:85–94. doi: 10.1016/j.jad.2017.12.052

29. Gong L, Yu SY, Xu RH, Liu D, Dai XJ, Wang ZY, et al. The abnormal reward network associated with insomnia severity and depression in chronic insomnia disorder. *Brain Imaging Behav.* (2021) 15:1033–42. doi: 10.1007/s11682-020-00310-w

30. Leerssen J, Blanken TF, Pozzi E, Jahanshad N, Aftanas L, Andreassen OA, et al. Brain structural correlates of insomnia severity in 1053 individuals with major depressive disorder: results from the ENIGMA MDD Working Group. *Transl Psychiatry.* (2020) 10:425. doi: 10.1038/s41398-020-01109-5

31. Yu S, Shen Z, Lai R, Feng F, Guo B, Wang Z, et al. The orbitofrontal cortex gray matter is associated with the interaction between insomnia and depression. *Front Psychiatry.* (2018) 9:651. doi: 10.3389/fpsyt.2018.00651

32. Gong L, Xu R, Liu D, Zhang C, Huang Q, Zhang B, et al. Abnormal functional connectivity density in patients with major depressive disorder with comorbid insomnia. *J Affect Disord.* (2020) 266:417–23. doi: 10.1016/j.jad.2020.01.088

33. Cui X, Guo W, Wang Y, Yang TX, Yang XH, Wang Y, et al. Aberrant default mode network homogeneity in patients with first-episode treatment-naive melancholic depression. *Int J Psychophysiol.* (2017) 112:46–51. doi: 10.1016/j.ijpsycho.2016.12.005

34. Parker G, Fink M, Shorter E, Taylor MA, Akiskal H, Berrios G, et al. Issues for DSM-5: whither melancholia? The case for its classification as a distinct mood disorder. *Am J Psychiatry.* (2010) 167:745–7. doi: 10.1176/appi.ajp.2010.09101525

35. Armitage R. Sleep and circadian rhythms in mood disorders. *Acta Psychiatr Scand.* (2007) 115:104–15. doi: 10.1111/j.1600-0447.2007.00968.x

36. Antonijevic I. HPA axis and sleep: identifying subtypes of major depression. *Stress Int J Biol Stress.* (2008) 11:15–27. doi: 10.1080/10253890701378967

37. Agargun MY, Besiroglu L, Cilli AS, Gulec M, Aydin A, Incl R, et al. Nightmares, suicide attempts, and melancholic features in patients with unipolar major depression. *J Affect Disord.* (2007) 98:267–70. doi: 10.1016/j.jad.2006.08.005

38. Besiroglu L, Agargun MY, Inci R. Nightmares and terminal insomnia in depressed patients with and without melancholic features. *Psychiatry Res.* (2005) 133:285–7. doi: 10.1016/j.psychres.2004.12.001

39. Wichniak A, Wierzbicka A, Jernajczyk W. Sleep as a biomarker for depression. *Int Rev Psychiatry (Abingdon, England).* (2013) 25:632–45. doi: 10.3109/09540261.2013.812067

40. Harald B, Gordon P. Meta-review of depressive subtyping models. *J Affect Disord.* (2012) 139:126–40. doi: 10.1016/j.jad.2011.07.015

41. Bruun CF, Arnbjerg CJ, Kessing LV. Electroencephalographic parameters differentiating melancholic depression, non-melancholic depression, and healthy controls. a systematic review. *Front Psychiatry.* (2021) 12:648713. doi: 10.3389/fpsyt.2021.648713

42. Biswal B, Yetkin FZ, Haughton VM, Hyde JS. Functional connectivity in the motor cortex of resting human brain using echo-planar MRI. *Mag Reson Med.* (1995) 34:537–41. doi: 10.1002/mrm.1910340409

43. Zhang Y, Cui X, Ou Y, Liu F, Li H, Chen J, et al. Differentiating melancholic and non-melancholic major depressive disorder using fractional amplitude of low-frequency fluctuations. *Front Psychiatry.* (2021) 12:763770. doi: 10.3389/fpsyt.2021.763770

44. Yan M, He Y, Cui X, Liu F, Li H, Huang R, et al. Disrupted regional homogeneity in melancholic and non-melancholic major depressive disorder at rest. *Front Psychiatry.* (2021) 12:618805. doi: 10.3389/fpsyt.2021.618805

45. Yan M, Cui X, Liu F, Li H, Huang R, Tang Y, et al. Abnormal default-mode network homogeneity in melancholic and nonmelancholic major depressive disorder at rest. *Neural Plasticity.* (2021) 2021:6653309. doi: 10.1155/2021/6653309

46. Shan X, Cui X, Liu F, Li H, Huang R, Tang Y, et al. Shared and distinct homotopic connectivity changes in melancholic and non-melancholic depression. *J Affect Disord.* (2021) 287:268–75. doi: 10.1016/j.jad.2021.03.038

47. Tian S, Zhu R, Chattun MR, Wang H, Chen Z, Zhang S, et al. Temporal dynamics alterations of spontaneous neuronal activity in anterior cingulate cortex predict suicidal risk in bipolar II patients. *Brain Imag Behav.* (2021) 15:2481–91. doi: 10.1007/s11682-020-00448-7

48. Zhang L, Zhang R, Han S, Womer FY, Wei Y, Duan J, et al. Three major psychiatric disorders share specific dynamic alterations of intrinsic brain activity. *Schizophr Res.* (2021) 243:322–9. doi: 10.1016/j.schres.2021.06.014

49. Calhoun VD, Miller R, Pearlson G, Adalı T. The chronnectome: time-varying connectivity networks as the next frontier in fMRI data discovery. *Neuron.* (2014) 84:262–74. doi: 10.1016/j.neuron.2014.10.015

50. Liao W, Zhang Z, Mantini D, Xu Q, Ji GJ, Zhang H, et al. Dynamical intrinsic functional architecture of the brain during absence seizures. *Brain Struct Funct.* (2014) 219:2001–15. doi: 10.1007/s00429-013-0619-2

51. Zheng R, Chen Y, Jiang Y, Wen M, Zhou B, Li S, et al. Dynamic altered amplitude of low-frequency fluctuations in patients with major depressive disorder. *Front Psychiatry.* (2021) 12:683610. doi: 10.3389/fpsyt.2021.683610

52. Liang Y, Jiang X, Zhu W, Shen Y, Xue F, Li Y, et al. Disturbances of dynamic function in patients with bipolar disorder i and its relationship with executive-function deficit. *Front Psychiatry.* (2020) 11:537981. doi: 10.3389/fpsyt.2020.537981

53. Li Q, Cao X, Liu S, Li Z, Wang Y, Cheng L, et al. Dynamic alterations of amplitude of low-frequency fluctuations in patients with drug-naïve first-episode early onset schizophrenia. *Front Neurosci.* (2020) 14:901. doi: 10.3389/fnins.2020.00901

54. van den Noort M, Bosch P, Yeo S, Lim S. Emotional memory processing: which comes first - depression or poor sleep? *Sleep Med.* (2016) 22:100. doi: 10.1016/j.sleep.2015.07.029

55. Beauregard M, Paquette V, Lévesque J. Dysfunction in the neural circuitry of emotional self-regulation in major depressive disorder. *Neuroreport.* (2006) 17:843–6. doi: 10.1097/01.wnr.0000220132.32091.9f

56. Hamilton M. A rating scale for depression. *J Neurol Neurosurg Psychiatry.* (1960) 23:56–62. doi: 10.1136/jnnp.23.1.56

57. Hamilton M. The assessment of anxiety states by rating. *Br J Med Psychol.* (1959) 32:50–5. doi: 10.1111/j.2044-8341.1959.tb00467.x

58. Park SC, Kim JM, Jun TY, Lee MS, Kim JB, Jeong SH, et al. Prevalence and clinical correlates of insomnia in depressive disorders: the crescend study. *Psychiatry Invest.* (2013) 10:373–81. doi: 10.4306/pi.2013.10.4.373

59. Manber R, Blasey C, Arnow B, Markowitz JC, Thase ME, Rush AJ, et al. Assessing insomnia severity in depression: comparison of depression rating scales and sleep diaries. *J Psychiatr Res.* (2005) 39:481–8. doi: 10.1016/j.jpsychires.2004.12.003

60. Yan CG, Wang XD, Zuo XN, Zang YFDPABI. Data processing & analysis for (resting-state) brain imaging. *Neuroinformatics.* (2016) 14:339–51. doi: 10.1007/s12021-016-9299-4

61. Li J, Duan X, Cui Q, Chen H, Liao W. More than just statics: temporal dynamics of intrinsic brain activity predicts the suicidal ideation in depressed patients. *Psychol Med.* (2019) 49:852–60. doi: 10.1017/s0033291718001502

62. Chen X, Lu B, Yan CG. Reproducibility of R-fMRI metrics on the impact of different strategies for multiple comparison correction and sample sizes. *Hum Brain Mapp.* (2018) 39:300–18. doi: 10.1002/hbm.23843

63. Li S, Wang BA, Li C, Feng Y, Li M, Wang T, et al. Progressive gray matter hypertrophy with severity stages of insomnia disorder and its relevance for mood symptoms. *Eur Radiol.* (2021) 31:6312–22. doi: 10.1007/s00330-021-07701-7

64. Wu Y, Zhuang Y, Qi J. Explore structural and functional brain changes in insomnia disorder: A PRISMA-compliant whole brain ALE meta-analysis for multimodal MRI. *Medicine.* (2020) 99:e19151. doi: 10.1097/md.0000000000019151

65. Wang YK, Shi XH, Wang YY, Zhang X, Liu HY, Wang XT, et al. Evaluation of the age-related and gender-related differences in patients with primary insomnia by fractional amplitude of low-frequency fluctuation: a resting-state functional magnetic resonance imaging study. *Medicine.* (2020) 99:e18786. doi: 10.1097/md.0000000000018786

66. Riemann D, Spiegelhalder K, Feige B, Voderholzer U, Berger M, Perlis M, et al. The hyperarousal model of insomnia: a review of the concept and its evidence. *Sleep Med Rev.* (2010) 14:19–31. doi: 10.1016/j.smrv.2009.04.002

67. Levenson JC, Kay DB, Buysse DJ. The pathophysiology of insomnia. *Chest.* (2015) 147:1179–92. doi: 10.1378/chest.14-1617

68. Gallagher HL, Frith CD. Functional imaging of 'theory of mind'. *Trends Cogn Sci.* (2003) 7:77–83. doi: 10.1016/s1364-6613(02)00025-6

69. Blank TS, Meyer BM, Wieser MK, Rabl U, Schögl P, Pezawas L. Brain morphometry and connectivity differs between adolescent- and adult-onset major depressive disorder. *Depress Anxiety.* (2022) 39:387–96. doi: 10.1002/da.23254

70. Wu H, Zheng Y, Zhan Q, Dong J, Peng H, Zhai J, et al. Covariation between spontaneous neural activity in the insula and affective temperaments is related to sleep disturbance in individuals with major depressive disorder. *Psychol Med.* (2021) 51:731–40. doi: 10.1017/s0033291719003647

71. Liu J, Ren L, Womer FY, Wang J, Fan G, Jiang W, et al. Alterations in amplitude of low frequency fluctuation in treatment-naïve major depressive disorder measured with resting-state fMRI. *Hum Brain Mapp.* (2014) 35:4979–88. doi: 10.1002/hbm.22526

72. Via E, Cardoner N, Pujol J, Martínez-Zalacaín I, Hernández-Ribas R, Urretavizacaya M, et al. Cerebrospinal fluid space alterations in melancholic depression. *PLoS One.* (2012) 7:e38299. doi: 10.1371/journal.pone.0038299

73. Greenberg DL, Payne ME, MacFall JR, Steffens DC, Krishnan RR. Hippocampal volumes and depression subtypes. *Psychiatry Res.* (2008) 163:126–32. doi: 10.1016/j.pscychresns.2007.12.009

74. Maller JJ, Thomson RH, Rosenfeld JV, Anderson R, Daskalakis ZJ, Fitzgerald PB. Occipital bending in depression. *Brain J Neurol.* (2014) 137(Pt 6):1830–7. doi: 10.1093/brain/awu072

75. Palejwala AH, Dadario NB, Young IM, O'Connor K, Briggs RG, Conner AK, et al. Anatomy and white matter connections of the lingual gyrus and cuneus. *World Neurosurg.* (2021) 151:e426–37. doi: 10.1016/j.wneu.2021.04.050

76. Garrett A, Kelly R, Gomez R, Keller J, Schatzberg AF, Reiss AL. Aberrant brain activation during a working memory task in psychotic major depression. *Am J Psychiatry.* (2011) 168:173–82. doi: 10.1176/appi.ajp.2010.09121718

77. Tao H, Guo S, Ge T, Kendrick KM, Xue Z, Liu Z, et al. Depression uncouples brain hate circuit. *Mol Psychiatry.* (2013) 18:101–11. doi: 10.1038/mp.2011.127

78. Makovski T, Lavidor M. Stimulating occipital cortex enhances visual working memory consolidation. *Behav Brain Res.* (2014) 275:84–7. doi: 10.1016/j.bbr.2014.09.004

79. Colich NL, Foland-Ross LC, Eggleston C, Singh MK, Gotlib IH. Neural aspects of inhibition following emotional primes in depressed adolescents. *J Clin child Adolesc Psychol.* (2016) 45:21–30. doi: 10.1080/15374416.2014.982281

80. Li X, Zhang Y, Meng C, Zhang C, Zhao W, Zhu DM, et al. Functional stability predicts depressive and cognitive improvement in major depressive disorder: a longitudinal functional MRI study. *Prog Neuro-psychopharmacol Biol Psychiatry.* (2021) 111:110396. doi: 10.1016/j.pnpbp.2021.110396

frontiers | Frontiers in Psychiatry

TYPE Original Research
PUBLISHED 29 September 2022
DOI 10.3389/fpsyt.2022.926292

OPEN ACCESS

EDITED BY
Yuanqiang Zhu,
Fourth Military Medical University, China

REVIEWED BY
Cong Zhou,
Jining Medical University, China
Wei Deng,
Affiliated Mental Health Center and Hangzhou Seventh People's Hospital, China
Chun Wang,
Nanjing Brain Hospital Affiliated to Nanjing Medical University, China

*CORRESPONDENCE
Zhongchun Liu
zcliu6@whu.edu.cn
Gaohua Wang
wgh6402@163.com
Yujun Gao
2021103020031@whu.edu.cn

†These authors have contributed equally to this work

SPECIALTY SECTION
This article was submitted to Neuroimaging and Stimulation, a section of the journal Frontiers in Psychiatry

RECEIVED 22 April 2022
ACCEPTED 28 July 2022
PUBLISHED 29 September 2022

CITATION
Guo X, Wang W, Kang L, Shu C, Bai H, Tu N, Bu L, Gao Y, Wang G and Liu Z (2022) Abnormal degree centrality in first-episode medication-free adolescent depression at rest: A functional magnetic resonance imaging study and support vector machine analysis.
Front. Psychiatry 13:926292.
doi: 10.3389/fpsyt.2022.926292

Abnormal degree centrality in first-episode medication-free adolescent depression at rest: A functional magnetic resonance imaging study and support vector machine analysis

Xin Guo[1,2], Wei Wang[1], Lijun Kang[1], Chang Shu[1], Hanpin Bai[1], Ning Tu[3], Lihong Bu[3], Yujun Gao[1*†], Gaohua Wang[1*†] and Zhongchun Liu[1*†]

[1]Department of Psychiatry, Renmin Hospital of Wuhan University, Wuhan, Hubei, China, [2]Department of Psychosis Studies, Institute of Psychiatry, Psychology and Neuroscience, King's College of London, London, United Kingdom, [3]PET/CT/MRI and Molecular Imaging Center, Renmin Hospital of Wuhan University, Wuhan, Hubei, China

Background: Depression in adolescents is more heterogeneous and less often diagnosed than depression in adults. At present, reliable approaches to differentiating between adolescents who are and are not affected by depression are lacking. This study was designed to assess voxel-level whole-brain functional connectivity changes associated with adolescent depression in an effort to define an imaging-based biomarker associated with this condition.

Materials and methods: In total, 71 adolescents affected by major depressive disorder (MDD) and 71 age-, sex-, and education level-matched healthy controls were subjected to resting-state functional magnetic resonance imaging (rs-fMRI) based analyses of brain voxel-wise degree centrality (DC), with a support vector machine (SVM) being used for pattern classification analyses.

Results: DC patterns derived from 16-min rs-fMRI analyses were able to effectively differentiate between adolescent MDD patients and healthy controls with 95.1% accuracy (136/143), and with respective sensitivity and specificity values of 92.1% (70/76) and 98.5% (66/67) based upon DC abnormalities detected in the right cerebellum. Specifically, increased DC was evident in the bilateral insula and left lingual area of MDD patients, together with reductions in the DC values in the right cerebellum and bilateral superior parietal lobe. DC values were not significantly correlated with disease severity or duration in these patients following correction for multiple comparisons.

Conclusion: These results suggest that whole-brain network centrality abnormalities may be present in many brain regions in adolescent depression

patients. Accordingly, these DC maps may hold value as candidate neuroimaging biomarkers capable of differentiating between adolescents who are and are not affected by MDD, although further validation of these results will be critical.

KEYWORDS

adolescent depression, resting state, functional magenetic resonance imaging, degree centrality, support vector machine (SVM)

Introduction

Major depressive disorder (MDD) is a highly prevalent yet deleterious psychiatric illness that can impair the psychological and social functioning of affected patients, reducing the overall quality of life and imposing a major burden on individuals suffering from this disease (1). First-episode MDD most often manifests between the middle of adolescents and the mid-40s, with an estimated 40% of first episodes occurring before the age of 20 (2). According to one recent meta-analysis, approximately 17.2% of children and adolescents between the ages of 6 and 15 in China have reported symptoms consistent with depression (3). Depression that occurs during adolescence, which is defined as 10–19 years of age by the World Health Organization (WHO), is more likely to be overlooked than depression in adults such that publically available statistics fail to accurately reflect the true burden of this illness (4, 5). In addition to cultural concerns pertaining to stigma and loss of privacy (6), the low rates of detection for adolescent depression are also driven by its highly heterogeneous presentation, which can manifest in the form of reactive moods, aggressive behaviors, and irritability with comorbid reductions in academic performance, eating disorders, anxiety, and other behavioral issues (7). As such, precisely detecting and diagnosing depression remains very challenging in this age group. Patterned symptom identification is an intrinsic component of MDD diagnosis under the Diagnostic and Statistical Manual of Mental Disorders (DSM) and International Classification of Diseases (ICD) diagnostic symptoms, yet these symptoms are not reliably associated with adolescent depression, and are also observed in the context of a range of other physical and mental ailments (8). Moreover, while the diagnosis of patients based on clinical descriptions has been shown to exhibit validity, it is associated with relatively poor specificity, contributing to the potential for diagnostic uncertainty, which can make appropriate clinical decision-making more challenging. There is thus an urgent need to gain further insight into the mechanistic basis for adolescent depression and to define robust and reliable means of detecting this condition.

Several recent neuroimaging studies have shown that young adults with MDD exhibit a range of neural functional connectivity analyses as compared to healthy control (HC) individuals. In a systematic review of functional brain imaging studies focused on young MDD patients published recently, these patients were found to exhibit changes in emotional processing, affective cognition, cognitive control, reward processing, and resting-state functional connectivity. While relatively few differences were observed when comparing younger adolescents and older youths, a comparison of youths with adult MDD patients revealed significant differences in the affective cognition and cognitive control domains (9). A meta-analysis of functional neuroimaging findings from young MDD patients revealed abnormal activation in several executive functions and affective processing tasks relative to HC individuals (10). These results suggest that differences in brain connectivity may offer a more objective opportunity to diagnose adolescents suffering from MDD.

Degree centrality (DC) is an index that measures whole-brain connectivity based on a global description of the characteristics of a particular region of the grain through analyses of functional connectivity between that region and the brain as a whole based on graph theory measures. DC analyses have recently been employed as a means of defining the core architectural conformation of brain networks, with higher and lower levels of DC in particular brain areas corresponding to increased and decreased global connectivity, respectively (11). Here, voxel-wise DC values were used to explore neuroimaging abnormalities in adolescents affected by depression. This approach offers great promise given that DC has been successfully used to examine whole-brain changes associated with conditions such as MDD (12–14), schizophrenia (15, 16), autism spectrum disorder (ASD) (17), and bipolar disorder (BPD) (12, 18, 19), providing a highly sensitive, specific, and reproducible biomarker that is physiologically meaningful. While DC holds great promise as a means of comprehensively analyzing brain networks in MDD patients, studies defining adolescent depression-specific changes in DC are lacking. Accordingly, the main goal of this study was to define specific neuroimaging biomarkers of MDD in adolescents.

Machine learning techniques offer a key advantage when analyzing large-scale, complex datasets. Support vector machine (SVM) machine learning methods, which were developed using

statistical learning theory, have been successfully used to aid in the diagnosis and prediction of therapeutic responses or prognostic outcomes (20) for conditions such as ASD (21), BPD (22, 23), MDD (12, 24), and schizophrenia (25–27) using both structural and functional neuroimaging data. SVM techniques are the most commonly employed machine learning methods in the context of brain imaging classification and depression given that they exhibit a robust theoretical foundation and can flexibly respond to high-dimensional data (28). SVM approaches are also ideally suited to small sample sizes and the recognition of non-linear, high-dimensional patterns (29).

Here, a kernel SVM was employed to detect voxel-wise DC changes when comparing 71 unmedicated adolescent first-episode MDD patients to 72 age-, gender-, and educational level-matched HCs, with the goal of developing a stronger understanding of the mechanisms governing MDD and providing a new approach to effectively diagnosing this condition.

Materials and methods

Participants

Ethical oversight

The Renmin Hospital of Wuhan University (Wuhan, China) ethics committee approved this study, which was consistent with the Declaration of Helsinki (Version 2002). All participants and their legal guardians provided written informed consent after receiving a full study description.

Recruitment and assessment

Patients participating in this study were recruited through the Center of Prevention and Management of Depression in Hubei Province, Renmin Hospital of Wuhan University through advertising and word-of-mouth interactions with past and current patients and volunteers. Data collection ran from May 4, 2018 through December 30, 2018. In total, 71 adolescents diagnosed with MDD as per the DSM-IV were recruited for this study, with diagnoses having been confirmed *via* the Structured Clinical Interview for DSM-IV Axis I disorders (SCID) by two board-certified psychiatrists. To be eligible for participation, patients had to meet the following criteria: (1) 14–18 years of age; (2) a history of MDD illness < 12 months; (3) no history of depression-related medication or electroconvulsive therapy; (4) no diagnoses of other mental health conditions as per the DSM-IV diagnostic criteria; (5) no instances of head trauma that resulted in the loss of consciousness; (6) no current or prior somatic illnesses with the potential to impact brain morphology; (7) no history of substance abuse; and (8) right-handed. Patients were excluded if: (1) they exhibited any serious physical or neurological conditions, somatic disease, brain morphological abnormalities, or a history of drug or alcohol abuse; (2) were ineligible for MRI due to the surgical placement of metal or electronic materials; (3) have utilized any medications within the last five medication-specific half-lives. The 17-item Hamilton Rating Scale for Depression (HRSD) (30) tool was used to gauge MDD severity. This instrument was administered by two board-certified psychiatrists, with patients exhibiting an HRSD score ≥ 17 being eligible for inclusion. Of the 71 patients included in this study, 22 exhibited anxiety-related features, 12 exhibited psychotic symptoms congruent with emotion, 6 exhibited psychotic symptoms not congruent with emotion, 14 had a history of suicidal thoughts, and 11 had a history of self-harm.

Healthy control recruitment

In total, 72 HCs that were age-, sex-, ethnicity-, education level-, and handedness-matched were recruited at random from the local community based on the national population register. The healthy status of HCs was confirmed through the use of the Structured Clinical Interview for DSM-IV Axis I disorders-Research version-Non-Patient Edition (SCID-I/NP).

Magnetic resonance imaging acquisition and postprocessing

Image acquisition

All resting-state fMRI (rs-fMRI) scans were performed with a 3.0T General Electric scanner at the PET center of Renmin Hospital of Wuhan University using previously described methods (31). Briefly, participants were directed to lie in the supine position with their eyes closed while remaining awake and motionless. An echoplanar imaging (EPI) sequence was then conducted with the following settings: repetition time/echo time (TR/TE) 2000/30 ms, 32 slices, 64*64 matrix, 90° flip angle, 24 cm field of view, 3.0 mm slice thickness, no gap, and axial scanning 212 times for 16 min.

Data postprocessing

The Data Processing Assistant for rs-fMRI (DPARSF) (32) advanced edition based on SPM8 implemented in the MATLAB platform was used for all rs-fMRI data analyses. After discarding the first 5 imaging time points for each participant, those individuals exhibiting a maximal displacement > 2 mm in any direction (x, y, or z axis) or $> 2°$ of maximal rotation were excluded following correction for head motion and slice timing. After spatial normalization to the MNI space and 3*3*3 mm^3 resampling, images were smoothed using an 8 mm full width at half-maximum Gaussian kernel, subjected to bandpass filtration (0.01–0.1°Hz), and linearly detrended. Spurious covariates were additionally removed such as ventricular ROI signal, signal from a region centered in the white matter, and six head motion parameters obtained through rigid body correction.

Degree centrality calculations

Data processing assistant for rs-fMRI (DPARSF) was used for all DC calculations. As reported previously (33), Pearson's correlation coefficients between a given voxel and all other voxels were used to establish a voxel-wise correlation matrix. Potential spurious connectivity was eliminated from this matrix through binarization for each correlation at an $r > 0.25$ threshold, thereby generating individual-level DC maps (34, 35) (Please see more details in **Supplementary material**). These maps were then normalized to Z-score maps *via* Fisher's r-to-z transformation, and standard deviation within the whole gray matter mask (36), followed by spatial smoothing with a 6 mm full-width at half-maximum Gaussian kernel.

Statistical analyses

SPSS was used for all statistical testing. Continuous and categorical data were compared between MDD and HC individuals *via* independent two-sample *t*-tests and chi-squared tests, with $P < 0.05$ as the threshold of significance. Individual whole-brain DC maps were subject to voxel-by-voxel ANCOVAs to detect group differences, with results being subject to GRF correction at the voxel level ($P < 0.01$), as GRF correction is better suited to this study than the false discovery rate (FDR; traditional approach with less smoothness) voxel-level familywise error (few; relatively conversive), and AlphaSim (less stringent) approaches (37, 38).

Correlation analysis

Pearson's correlations and multiple factors regression analysis were used to explore correlations between the severity of MDD and DC values in the six abnormal brain regions identified above and the demographic and clinical characteristics of patients included in this study.

Classification analysis

An SVM approach conducted with the LIBSVM package in MATLAB was utilized to examine the ability of DC values in six abnormal regions of the brain (left lingual gyrus, left insula and right insula, right cerebellum, right superior parietal lobule, and left superior parietal lobule) to differentiate between MDD patients and HCs. The radial basis function (RBF) was selected as the kernel function, while a grid of parameters was evaluated with LIBSVM, and the optimal parameters including C (penalty coefficient) and g (gamma) were chosen. The accuracy values for all parameter settings were established, and the maximal cross-validation accuracy of these parameters was evaluated (Please see a more detailed description of the SVM method in **Supplementary material**).

Results

Participant characteristics

No significant differences in age, gender, or education level were evident when comparing MDD and HC participant groups (**Table 1**), while MDD patients exhibited higher HRSD-17 total scores relative to HCs, as expected.

Group difference in degree centrality

Figure 1 summarizes significant differences in DC values between the adolescent MDD and HC groups. Relative to HC individuals, those with MDD present with higher DC in the left lingual gyrus, left insula, and right insula, as well as with decreased DC in the right cerebellum, right superior parietal lobule, and left superior parietal lobule (**Table 2**).

Correlation between degree centrality and HRSD-17 total scores

A matrix-based correlation approach and multiple factors regression analysis were used to explore relationships between DC values in the six abnormal brain regions identified above and the demographic and clinical characteristics of patients included in this study, but no significant correlations were detected between DC values and the severity of MDD symptoms (Please see **Figure 1**, **Tables 1**, **2** in **Supplementary material**).

TABLE 1 Demographic and clinical variables.

Demographic variables	Depression (70) A	Health control (71)
Age (mean/SD, year)	15.1 ± 1.9	16.5 ± 1.9
Sex n(%)		
Male	44 (62)	44 (61)
Female	27 (38)	28 (39)
Education n(%)		
High school or lower	65 (88.7)	63 (87.5)
Undergraduate	6 (11.3)	9 (12.5)
HRSD-17 total score (mean/SD)	22.9 (4.3)	8.7 (5.8)
Illness duration (mean/SD, month)	6.3 (3.6)	

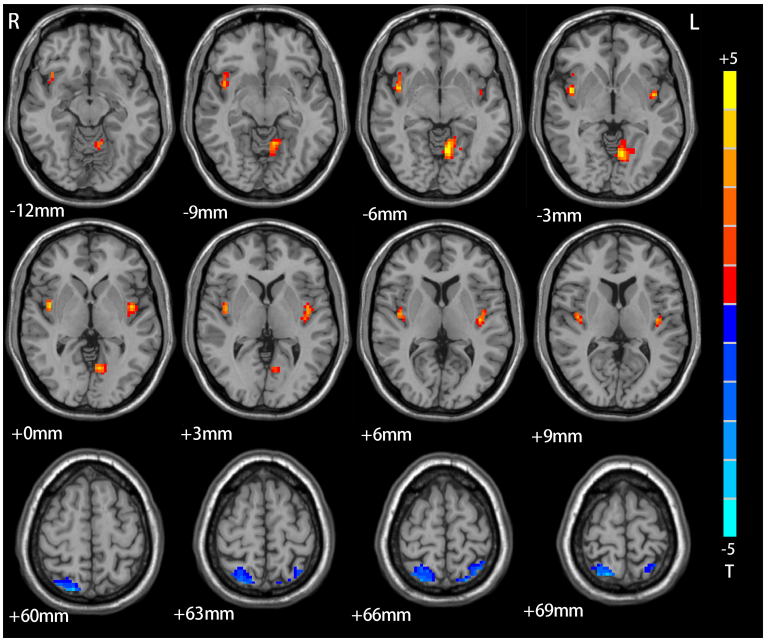

FIGURE 1
The difference between adolescents depression patients and HCs. Red means increase of DC value, blue means decrease of DC value.

TABLE 2 Significant resting-state degree centrality difference across groups.

Clusterlocation adolescent depression vs. HC	Peak MNI coordinate			Number of voxels	*T*-value
	x	*y*	*z*		
Right cerebellum	30	−30	−39	199	−11.4
Left lingual	−9	−66	−3	105	9.5
Right insula	45	0	−3	74	9.2
Left insula	−42	−3	0	64	8.9
Right superior parietal	15	−63	72	157	−10.9
Left superior parietal	−18	−51	78	78	−9.8

DC, degree centrality; MNI, Montreal Neurological Institute.

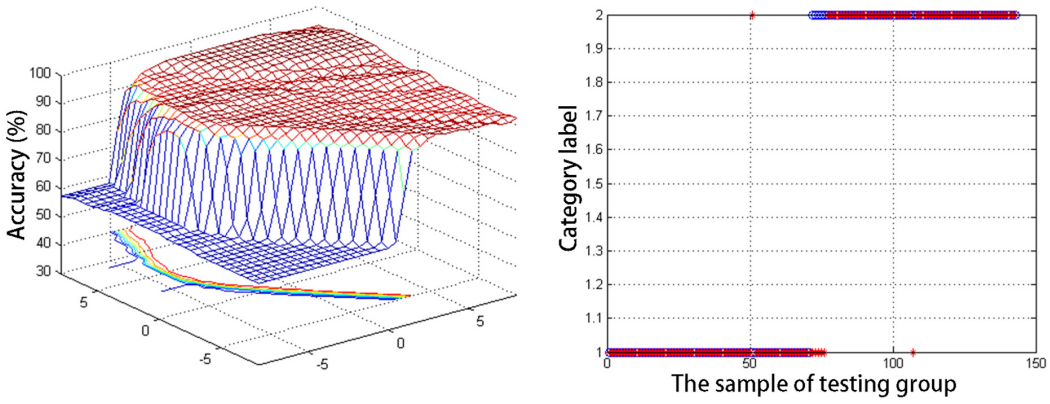

FIGURE 2
The general information of support vector machine results for discriminating adolescent depression patients and HCs.

Support vector machine results

Figure 2 summarizes the general SVM results when differentiating between MDD patients and HCs. Overall, abnormal DC values in the right cerebellum were found to offer the greatest utility when discriminating between these two participant groups, with respective accuracy, sensitivity, and specificity values of 95.1, 92.1, and 98.5%.

Discussion

Here, DC values were explored as a promising neuroimaging biomarker capable of differentiating between adolescent MDD patients and healthy individuals. This approach revealed that DC maps for the right cerebellum were able to reliably discriminate between these two participant groups with respective accuracy, sensitivity, and specificity values of 95.1, 92.1, and 98.5%. Moreover, changes in DC values in the lingual area, insula, and superior parietal gyrus were evident when comparing adolescent MDD patients and HCs. However, no correlations were observed between abnormal DC values and clinical findings in patients.

The accuracy value detected herein when using DC values to differentiate between MDD and HC individuals (95.1%) is similar to the 94% value published in a recent report employing DC maps to differentiate between healthy adults and MDD patients (12), and both values are much higher than those for other previously reported neuroimaging modalities, which generally range from 26 to 81% (39–41). These results underscore the value of DC maps as tools capable of accurately extracting abnormal connectivity findings specific to a given illness, although follow-up validation of these results remains to be completed. Depression is regarded as an affective disorder that can impact individuals of all ages, but the rate of diagnosis among younger individuals has been rising in recent years (3). Sub-clinical depressive symptom incidence is also a common finding in healthy adolescent individuals (42), highlighting the value of using DC maps to differentiate between potentially at-risk adolescents who may be suffering from sub-clinical depression and healthy peers.

Here, reductions in DC values were observed in both the right cerebellum and bilateral superior parietal regions in adolescents with MDD relative to HC individuals. In addition to serving as the motor domain, the cerebellum is important for many cognitive and affective functions (43). Cerebellar lesions, accordingly, can result in affective and/or cognitive symptoms that are collectively referred to as cerebellar cognitive affective syndrome, which results in characteristically impaired linguistic and executive function with concomitant apathy, depressed mood, or abnormal social cognition (44). The observed loss of cerebellar DC in this study is consistent with recent evidence from analyses of both first-episode treatment-naïve adolescent MDD patients and unmedicated adults with this disease (45). Specifically, other studies have reported an increase in the connectivity of the left cerebellum in depressed adolescents considered suicidal, whereas non-suicidal adolescent MDD patients exhibited decreased connectivity in the lower left cerebellum, potentially owing to differences in sample subgrouping in these studies. The results of the present analysis are consistent with prior data regarding the important role that the cerebellum plays in the pathogenesis of MDD (46–49), highlighting the possibility of defining novel neuroimaging-based biomarkers for this condition.

The superior parietal lobule (SPL) is an important mediator of diverse perceptive, cognitive, and motor-associated processes such as spatial cognition, attention, working memory, visual perception, and visually guided visuomotor functions (50, 51). The ENIGMA-MDD working group performed a meta-analysis which revealed that relative to HCs, depressed adolescents exhibited significant reductions in the surface area of the left (213 cases, 294 controls) and right (213 cases, 293 controls) superior parietal cortex (52). Depressed children and adolescents who were naïve to psychotropic medication treatment also exhibited a thinner SPL than that observed in matched HC individuals (53). Here, lower DC in the bilateral SPL was observed in adolescent MDD patients, in line with prior evidence from adult MDD patients (54, 55). In one prior fMRI-based study employing attentional tasks, medication-naive first-episode adolescent MDD patients performed more poorly in an attention-focused testing battery, and exhibited lower levels of parietal lobe activation in regions related to tasks being performed for both attentional switching (Switch task) and error detection (Stop task) (54). Prior work also suggests that medication-naïve adolescent MDD patients exhibit changes in brain function compared to those in adults with MDD. Changes in SPL function may thus represent an early pathogenic abnormality associated with the onset of MDD, although more work will be necessary to test this possibility.

This study further revealed that increases in DC values were evident in the lingual gyrus in adolescents with MDD. Lingual gyrus activation has previously been reported to be evident in the context of tasks requiring memorization and the maintenance of human faces in the working memory (55), and it also serves as a structural component of the visual cortex that is critical for word identification and recognition (56). It is also potentially functionally linked with the amygdala, and may thus play a role in emotional processing (57). The ENIGMA-MDD group meta-analysis reported the left lingual gyrus surface area to be significantly reduced in adolescents with depression (58). While this meta-analysis incorporated medicated patients and failed to correct for total surface area, lingual gray matter density was found to predict patient

responses to antidepressant treatment. Another recent meta-analysis of the neurological activity of youths and adults diagnosed with MDD in the context of emotional processing indicated that lingual gyrus activity levels were higher in youths with depression as compared to adults (13). Accordingly, the finding herein that the DC of the left lingual gyrus was increased in adolescent MDD patients may be consistent with intrinsic functional alterations in this area in adolescents with depression.

Here, increases in bilateral insular DC values were detected in MDD patients relative to HCs. The insula serves as a site of fronto-limbic network integration owing to its anatomical connections to associated brain regions (59). Both adolescent and adult MDD patients consistently exhibit abnormal fronto-limbic network activity, with a bias toward negative stimuli and increased attention to and processing of emotional information (60–62). In line with the present results, prior rs-fMRI studies have found adolescents with MDD to exhibit increases in the activity and functional connectivity of the insula (63–65). Studies have also reported hypoactivation of the dorsal anterior insula in executive function tasks and hypoactivation of the posterior insula in positive valence tasks in neuroimaging studies (10). Insular structural alterations have also been reported in adolescents with MDD in the meta-analysis published by the ENIGMA-MDD group (44). These results suggest that insular dysfunction may represent a mechanism underlying the pathophysiological basis for MDD in adolescents. Notably, reductions in insular functional connectivity have been reported in adolescents with depression suffering from comorbid anxiety disorder, ADHD, and post-traumatic stress disorder (66, 67), consistent with the multidisciplinary function that the insula plays in a range of psychiatric conditions (66–68). However, additional studies with appropriate patient subgroups will be needed to test these possibilities.

There are multiple limitations to this analysis. For one, the lack of any observed correlation between DC values and MDD symptoms may be impacted by a range of factors including the timing of DC changes, cognitive impairment, and emotional/somatic disease-related burden. As the present study relied on rs-fMRI data in the absence of any emotion- or cognition-related tasks, additional follow-up studies exploring DC abnormalities in these contexts are warranted for adolescents with MDD. This study also included a relatively small number of patients, potentially contributing to this lack of any observed correlation. Moreover, accurately subgrouping MDD patients based on their comorbidities (such as anxiety, attention deficit-hyperactivity disorder, or stress-associated disorders) or clinical findings may have an impact on these results, highlighting a need for more detailed subgroup-based analyses (69–72). It is also important to take into consideration that some adolescents with BPD are initially misdiagnosed with MDD, and the delay between the initial onset of affective symptoms and the diagnosis of BPD can be up to 10 years (73). As such, further follow-up validation of these results will be critical. This study also specifically focused on patients with an illness duration of < 12 months to ensure that patients were able to accurately recall depressive episodes. However, this inclusion criterion has the potential to have biased these results. Lastly, while the HDRS has been used as a gold standard tool to rate the severity of MDD in adolescents, there have been questions raised in recent years regarding its internal reliability, its discriminant and convergent validity, and its utility when assessing adolescent patients. As such, the establishment of diagnostic tools more closely tailored to the symptoms of adolescent MDD may be of value in future research.

In summary, the present results suggest that adolescent MDD is associated with DC abnormalities in several brain regions associated with sensorimotor activity, emotional processing, and cognitive impairment. These DC values may ultimately offer good utility as a neuroimaging biomarker for the early detection and monitoring of MDD in this patient population.

Data availability statement

The raw data supporting the conclusions of this article will be made available by the authors, without undue reservation.

Ethics statement

The studies involving human participants were reviewed and approved by Renmin Hospital of Wuhan University (Wuhan, China). Written informed consent to participate in this study was provided by the participants' legal guardian/next of kin.

Author contributions

All authors listed have made a substantial, direct, and intellectual contribution to the work, and approved it for publication.

Funding

This work was supported by the National Key R&D Program of China (grant number: 2018YFC1314600) and

the National Natural Science Foundation of China (grant number: 81771472).

Acknowledgments

We thank all participants of this study. We are also grateful to ZL and all other authors for their great efforts in this study.

Conflict of interest

The authors declare that the research was conducted in the absence of any commercial or financial relationships that could be construed as a potential conflict of interest.

Publisher's note

Supplementary material

The Supplementary Material for this article can be found online at: https://www.frontiersin.org/articles/10.3389/fpsyt.2022.926292/full#supplementary-material

References

1. Mokdad AH, Forouzanfar MH, Daoud F, Mokdad AA, El BC, Moradi-Lakeh M, et al. Global burden of diseases, injuries, and risk factors for young people's health during 1990-2013: a systematic analysis for the global burden of disease study 2013. *Lancet.* (2016) 387:2383–401. doi: 10.1016/S0140-6736(16)00648-6

2. Moffitt TE, Caspi A, Taylor A, Kokaua J, Milne BJ, Polanczyk G, et al. How common are common mental disorders? Evidence that lifetime prevalence rates are doubled by prospective versus retrospective ascertainment. *Psychol Med.* (2010) 40:899–909. doi: 10.1017/S0033291709991036

3. Xu DD, Rao WW, Cao XL, Wen SY, An FR, Che WI, et al. Prevalence of depressive symptoms in primary school students in China: a systematic review and meta-analysis. *J Affect Disord.* (2020) 268:20–7. doi: 10.1016/j.jad.2020.02.034

4. Johnco C, Rapee RM. Depression literacy and stigma influence how parents perceive and respond to adolescent depressive symptoms. *J Affect Disord.* (2018) 241:599–607. doi: 10.1016/j.jad.2018.08.062

5. Leaf PJ, Alegria M, Cohen P, Goodman SH, Horwitz SM, Hoven CW, et al. Mental health service use in the community and schools: results from the four-community MECA study. Methods for the epidemiology of child and adolescent mental disorders study. *J Am Acad Child Adolesc Psychiatry.* (1996) 35:889–97. doi: 10.1097/00004583-199607000-00014

6. Kong LZ, Lai JB, Hu SH. China initiates depression screening in children and adolescents. *Lancet Psychiatry.* (2022) 9:107–8. doi: 10.1016/S2215-0366(21)00479-X

7. Thapar A, Collishaw S, Pine DS, Thapar AK. Depression in adolescence. *Lancet.* (2012) 379:1056–67. doi: 10.1016/S0140-6736(11)60871-4

8. Malhi GS, Mann JJ. Depression. *Lancet.* (2018) 392:2299–312. doi: 10.1016/S0140-6736(18)31948-2

9. Kerestes R, Davey CG, Stephanou K, Whittle S, Harrison BJ. Functional brain imaging studies of youth depression: a systematic review. *Neuroimage Clin.* (2014) 4:209–31. doi: 10.1016/j.nicl.2013.11.009

10. Miller CH, Hamilton JP, Sacchet MD, Gotlib IH. Meta-analysis of functional neuroimaging of major depressive disorder in youth. *JAMA Psychiatry.* (2015) 72:1045–53. doi: 10.1001/jamapsychiatry.2015.1376

11. Zuo XN, Ehmke R, Mennes M, Imperati D, Castellanos FX, Sporns O, et al. Network centrality in the human functional connectome. *Cereb Cortex.* (2012) 22:1862–75. doi: 10.1093/cercor/bhr269

12. Li M, Das T, Deng W, Wang Q, Li Y, Zhao L, et al. Clinical utility of a short resting-state MRI scan in differentiating bipolar from unipolar depression. *Acta Psychiatr Scand.* (2017) 136:288–99. doi: 10.1111/acps.12752

13. Li X, Wang J. Abnormal neural activities in adults and youths with major depressive disorder during emotional processing: a meta-analysis. *Brain Imaging Behav.* (2021) 15:1134–54. doi: 10.1007/s11682-020-00299-2

14. Gao C, Wenhua L, Liu Y, Ruan X, Chen X, Liu L, et al. Decreased subcortical and increased cortical degree centrality in a nonclinical college student sample with subclinical depressive symptoms: a resting-state fMRI study. *Front Hum Neurosci.* (2016) 10:617. doi: 10.3389/fnhum.2016.00617

15. Wang Y, Jiang Y, Su W, Xu L, Wei Y, Tang Y, et al. Temporal dynamics in degree centrality of brain functional connectome in first-episode schizophrenia with different short-term treatment responses: a longitudinal study. *Neuropsychiatr Dis Treat.* (2021) 17:1505–16. doi: 10.2147/NDT.S305117

16. Zhou M, Zhuo L, Ji R, Gao Y, Yao H, Feng R, et al. Alterations in functional network centrality in first-episode drug-naive adolescent-onset schizophrenia. *Brain Imaging Behav.* (2022) 16:316–23. doi: 10.1007/s11682-021-00505-9

17. Wan B, Wang Z, Jung M, Lu Y, He H, Chen Q, et al. Effects of the co-occurrence of anxiety and attention-deficit/hyperactivity disorder on intrinsic functional network centrality among children with autism spectrum disorder. *Autism Res.* (2019) 12:1057–68. doi: 10.1002/aur.2120

18. Deng W, Zhang B, Zou W, Zhang X, Cheng X, Guan L, et al. Abnormal degree centrality associated with cognitive dysfunctions in early bipolar disorder. *Front Psychiatry.* (2019) 10:140. doi: 10.3389/fpsyt.2019.00140

19. Zhou Q, Womer FY, Kong L, Wu F, Jiang X, Zhou Y, et al. Trait-related cortical-subcortical dissociation in bipolar disorder: analysis of network degree centrality. *J Clin Psychiatry.* (2017) 78:584–91. doi: 10.4088/JCP.15m10091

20. Orru G, Pettersson-Yeo W, Marquand AF, Sartori G, Mechelli A. Using support vector machine to identify imaging biomarkers of neurological and psychiatric disease: a critical review. *Neurosci Biobehav Rev.* (2012) 36:1140–52. doi: 10.1016/j.neubiorev.2012.01.004

21. Yassin W, Nakatani H, Zhu Y, Kojima M, Owada K, Kuwabara H, et al. Machine-learning classification using neuroimaging data in schizophrenia, autism, ultra-high risk and first-episode psychosis. *Transl Psychiatry.* (2020) 10:278. doi: 10.1038/s41398-020-00965-5

22. Fung G, Deng Y, Zhao Q, Li Z, Qu M, Li K, et al. Distinguishing bipolar and major depressive disorders by brain structural morphometry: a pilot study. *BMC Psychiatry.* (2015) 15:298. doi: 10.1186/s12888-015-0685-5

23. Sawalha J, Cao L, Chen J, Selvitella A, Liu Y, Yang C, et al. Individualized identification of first-episode bipolar disorder using machine learning and cognitive tests. *J Affect Disord.* (2021) 282:662–8. doi: 10.1016/j.jad.2020.12.046

24. Zandvakili A, Philip NS, Jones SR, Tyrka AR, Greenberg BD, Carpenter LL. Use of machine learning in predicting clinical response to transcranial magnetic stimulation in comorbid posttraumatic stress disorder and major depression: a resting state electroencephalography study. *J Affect Disord.* (2019) 252:47–54. doi: 10.1016/j.jad.2019.03.077

25. Schnack HG, Nieuwenhuis M, van Haren NE, Abramovic L, Scheewe TW, Brouwer RM, et al. Can structural MRI aid in clinical classification? A machine learning study in two independent samples of patients with schizophrenia, bipolar disorder and healthy subjects. *Neuroimage.* (2014) 84:299–306. doi: 10.1016/j.neuroimage.2013.08.053

26. Bak N, Ebdrup BH, Oranje B, Fagerlund B, Jensen MH, During SW, et al. Two subgroups of antipsychotic-naive, first-episode schizophrenia patients identified with a Gaussian mixture model on cognition and electrophysiology. *Transl Psychiatry.* (2017) 7:e1087. doi: 10.1038/tp.2017.59

27. Li A, Zalesky A, Yue W, Howes O, Yan H, Liu Y, et al. A neuroimaging biomarker for striatal dysfunction in schizophrenia. *Nat Med.* (2020) 26:558–65. doi: 10.1038/s41591-020-0793-8

28. Gao S, Calhoun VD, Sui J. Machine learning in major depression: from classification to treatment outcome prediction. *CNS Neurosci Ther.* (2018) 24:1037–52. doi: 10.1111/cns.13048

29. Tong HA. Note on support vector machines with polynomial kernels. *Neural Comput.* (2016) 28:71–88. doi: 10.1162/NECO_a_00794

30. Zimmerman M, Martinez JH, Young D, Chelminski I, Dalrymple K. Severity classification on the Hamilton depression rating scale. *J Affect Disord.* (2013) 150:384–8. doi: 10.1016/j.jad.2013.04.028

31. Wang W, Kang L, Zhang N, Guo X, Wang P, Zong X, et al. The interaction effects of suicidal ideation and childhood abuse on brain structure and function in major depressive disorder patients. *Neural Plast.* (2021) 2021:7088856. doi: 10.1155/2021/7088856

32. Chao-Gan Y, Yu-Feng Z. DPARSF: a MATLAB toolbox for "pipeline" data analysis of resting-state fMRI. *Front Syst Neurosci.* (2010) 4:13. doi: 10.3389/fnsys.2010.00013

33. Gao Y, Xiong Z, Wang X, Ren H, Liu R, Bai B, et al. Abnormal degree centrality as a potential imaging biomarker for right temporal lobe epilepsy: a resting-state functional magnetic resonance imaging study and support vector machine analysis. *Neuroscience.* (2022) 487:198–206. doi: 10.1016/j.neuroscience.2022.02.004

34. Palaniyappan L, Liddle PF. Diagnostic discontinuity in psychosis: a combined study of cortical gyrification and functional connectivity. *Schizophr Bull.* (2014) 40:675–84. doi: 10.1093/schbul/sbt050

35. Buckner RL, Sepulcre J, Talukdar T, Krienen FM, Liu H, Hedden T, et al. Cortical hubs revealed by intrinsic functional connectivity: mapping, assessment of stability, and relation to Alzheimer's disease. *J Neurosci.* (2009) 29:1860–73. doi: 10.1523/JNEUROSCI.5062-08.2009

36. Takeuchi H, Taki Y, Nouchi R, Sekiguchi A, Hashizume H, Sassa Y, et al. Degree centrality and fractional amplitude of low-frequency oscillations associated with Stroop interference. *Neuroimage.* (2015) 119:197–209. doi: 10.1016/j.neuroimage.2015.06.058

37. Han H, Glenn AL. Evaluating methods of correcting for multiple comparisons implemented in SPM12 in social neuroscience fMRI studies: an example from moral psychology. *Soc Neurosci.* (2018) 13:257–67. doi: 10.1080/17470919.2017.1324521

38. Chen X, Lu B, Yan CG. Reproducibility of R-fMRI metrics on the impact of different strategies for multiple comparison correction and sample sizes. *Hum Brain Mapp.* (2018) 39:300–18. doi: 10.1002/hbm.23843

39. Sankar A, Zhang T, Gaonkar B, Doshi J, Erus G, Costafreda SG, et al. Diagnostic potential of structural neuroimaging for depression from a multi-ethnic community sample. *BJPsych Open.* (2016) 2:247–54. doi: 10.1192/bjpo.bp.115.002493

40. Yang J, Zhang M, Ahn H, Zhang Q, Jin TB, Li I, et al. Development and evaluation of a multimodal marker of major depressive disorder. *Hum Brain Mapp.* (2018) 39:4420–39. doi: 10.1002/hbm.24282

41. Koutsouleris N, Meisenzahl EM, Borgwardt S, Riecher-Rossler A, Frodl T, Kambeitz J, et al. Individualized differential diagnosis of schizophrenia and mood disorders using neuroanatomical biomarkers. *Brain.* (2015) 138:2059–73. doi: 10.1093/brain/awv111

42. Bertha EA, Balazs J. Subthreshold depression in adolescence: a systematic review. *Eur Child Adolesc Psychiatry.* (2013) 22:589–603. doi: 10.1007/s00787-013-0411-0

43. Depping MS, Schmitgen MM, Kubera KM, Wolf RC. Cerebellar contributions to major depression. *Front Psychiatry.* (2018) 9:634. doi: 10.3389/fpsyt.2018.00634

44. Schmahmann JD, Weilburg JB, Sherman JC. The neuropsychiatry of the cerebellum – insights from the clinic. *Cerebellum.* (2007) 6:254–67. doi: 10.1080/14734220701490995

45. Hoche F, Guell X, Vangel MG, Sherman JC, Schmahmann JD. The cerebellar cognitive affective/Schmahmann syndrome scale. *Brain.* (2018) 141:248–70. doi: 10.1093/brain/awx317

46. Pan F, Xu Y, Zhou W, Chen J, Wei N, Lu S, et al. Disrupted intrinsic functional connectivity of the cognitive control network underlies disease severity and executive dysfunction in first-episode, treatment-naive adolescent depression. *J Affect Disord.* (2020) 264:455–63. doi: 10.1016/j.jad.2019.11.076

47. Zeng M, Yu M, Qi G, Zhang S, Ma J, Hu Q, et al. Concurrent alterations of white matter microstructure and functional activities in medication-free major depressive disorder. *Brain Imaging Behav.* (2021) 15:2159–67. doi: 10.1007/s11682-020-00411-6

48. Li J, Gong H, Xu H, Ding Q, He N, Huang Y, et al. Abnormal voxel-wise degree centrality in patients with late-life depression: a resting-state functional magnetic resonance imaging study. *Front Psychiatry.* (2019) 10:1024. doi: 10.3389/fpsyt.2019.01024

49. Zhang S, Chen JM, Kuang L, Cao J, Zhang H, Ai M, et al. Association between abnormal default mode network activity and suicidality in depressed adolescents. *BMC Psychiatry.* (2016) 16:337. doi: 10.1186/s12888-016-1047-7

50. Wang J, Yang Y, Fan L, Xu J, Li C, Liu Y, et al. Convergent functional architecture of the superior parietal lobule unraveled with multimodal neuroimaging approaches. *Hum Brain Mapp.* (2015) 36:238–57. doi: 10.1002/hbm.22626

51. Vialatte A, Yeshurun Y, Khan AZ, Rosenholtz R, Pisella L. Superior parietal lobule: a role in relative localization of multiple different elements. *Cereb Cortex.* (2021) 31:658–71. doi: 10.1093/cercor/bhaa250

52. Schmaal L, Hibar DP, Samann PG, Hall GB, Baune BT, Jahanshad N, et al. Cortical abnormalities in adults and adolescents with major depression based on brain scans from 20 cohorts worldwide in the ENIGMA major depressive disorder working group. *Mol Psychiatry.* (2017) 22:900–9. doi: 10.1038/mp.2016.60

53. Fallucca E, MacMaster FP, Haddad J, Easter P, Dick R, May G, et al. Distinguishing between major depressive disorder and obsessive-compulsive disorder in children by measuring regional cortical thickness. *Arch Gen Psychiatry.* (2011) 68:527–33. doi: 10.1001/archgenpsychiatry.2011.36

54. Luo Q, Chen J, Li Y, Wu Z, Lin X, Yao J, et al. Altered regional brain activity and functional connectivity patterns in major depressive disorder: a function of childhood trauma or diagnosis? *J Psychiatr Res.* (2022) 147:237–47. doi: 10.1016/j.jpsychires.2022.01.038

55. Schilbach L, Hoffstaedter F, Muller V, Cieslik EC, Goya-Maldonado R, Trost S, et al. Transdiagnostic commonalities and differences in resting state functional connectivity of the default mode network in schizophrenia and major depression. *Neuroimage Clin.* (2016) 10:326–35. doi: 10.1016/j.nicl.2015.11.021

56. Halari R, Simic M, Pariante CM, Papadopoulos A, Cleare A, Brammer M, et al. Reduced activation in lateral prefrontal cortex and anterior cingulate during attention and cognitive control functions in medication-naive adolescents with depression compared to controls. *J Child Psychol Psychiatry.* (2009) 50:307–16. doi: 10.1111/j.1469-7610.2008.01972.x

57. Sulpizio V, Committeri G, Lambrey S, Berthoz A, Galati G. Selective role of lingual/parahippocampal gyrus and retrosplenial complex in spatial memory across viewpoint changes relative to the environmental reference frame. *Behav Brain Res.* (2013) 242:62–75. doi: 10.1016/j.bbr.2012.12.031

58. Mangun GR, Buonocore MH, Girelli M, Jha AP. ERP and fMRI measures of visual spatial selective attention. *Hum Brain Mapp.* (1998) 6:383–9.

59. Isenberg N, Silbersweig D, Engelien A, Emmerich S, Malavade K, Beattie B, et al. Linguistic threat activates the human amygdala. *Proc Natl Acad Sci U.S.A.* (1999) 96:10456–9. doi: 10.1073/pnas.96.18.10456

60. Jung J, Kang J, Won E, Nam K, Lee MS, Tae WS, et al. Impact of lingual gyrus volume on antidepressant response and neurocognitive functions in major depressive disorder: a voxel-based morphometry study. *J Affect Disord.* (2014) 169:179–87. doi: 10.1016/j.jad.2014.08.018

61. Sliz D, Hayley S. Major depressive disorder and alterations in insular cortical activity: a review of current functional magnetic imaging research. *Front Hum Neurosci.* (2012) 6:323. doi: 10.3389/fnhum.2012.00323

62. Shen X, MacSweeney N, Chan S, Barbu MC, Adams MJ, Lawrie SM, et al. Brain structural associations with depression in a large early adolescent sample (the ABCD study(R)). *EClinicalMedicine.* (2021) 42:101204. doi: 10.1016/j.eclinm.2021.101204

63. Tang S, Lu L, Zhang L, Hu X, Bu X, Li H, et al. Abnormal amygdala resting-state functional connectivity in adults and adolescents with major depressive disorder: a comparative meta-analysis. *EBiomedicine.* (2018) 36:436–45. doi: 10.1016/j.ebiom.2018.09.010

64. Monkul ES, Hatch JP, Nicoletti MA, Spence S, Brambilla P, Lacerda AL, et al. Fronto-limbic brain structures in suicidal and non-suicidal female patients with major depressive disorder. *Mol Psychiatry.* (2007) 12:360–6. doi: 10.1038/sj.mp.4001919

65. Jin C, Gao C, Chen C, Ma S, Netra R, Wang Y, et al. A preliminary study of the dysregulation of the resting networks in first-episode medication-naive adolescent depression. *Neurosci Lett.* (2011) 503:105–9. doi: 10.1016/j.neulet.2011.08.017

66. Connolly CG, Wu J, Ho TC, Hoeft F, Wolkowitz O, Eisendrath S, et al. Resting-state functional connectivity of subgenual anterior cingulate cortex in

depressed adolescents. *Biol Psychiatry.* (2013) 74:898–907. doi: 10.1016/j.biopsych.2013.05.036

67. Henje BE, Connolly CG, Ho TC, LeWinn KZ, Mobayed N, Han L, et al. Altered insular activation and increased insular functional connectivity during sad and happy face processing in adolescent major depressive disorder. *J Affect Disord.* (2015) 178:215–23. doi: 10.1016/j.jad.2015.03.012

68. Jiao Q, Ding J, Lu G, Su L, Zhang Z, Wang Z, et al. Increased activity imbalance in fronto-subcortical circuits in adolescents with major depression. *PLoS One.* (2011) 6:e25159. doi: 10.1371/journal.pone.0025159

69. Cullen KR, Gee DG, Klimes-Dougan B, Gabbay V, Hulvershorn L, Mueller BA, et al. A preliminary study of functional connectivity in comorbid adolescent depression. *Neurosci Lett.* (2009) 460:227–31. doi: 10.1016/j.neulet.2009.05.022

70. Harricharan S, Nicholson AA, Thome J, Densmore M, McKinnon MC, Theberge J, et al. PTSD and its dissociative subtype through the lens of the insula: anterior and posterior insula resting-state functional connectivity and its predictive validity using machine learning. *Psychophysiology.* (2020) 57:e13472.

71. Vetter NC, Buse J, Backhausen LL, Rubia K, Smolka MN, Roessner V. Anterior insula hyperactivation in ADHD when faced with distracting negative stimuli. *Hum Brain Mapp.* (2018) 39:2972–86. doi: 10.1002/hbm.24053

72. Alvarez, RP, Kirlic N, Misaki M, Bodurka J, Rhudy JL, Paulus MP, et al. Increased anterior insula activity in anxious individuals is linked to diminished perceived control. *Transl Psychiatry.* (2015) 5:e591. doi: 10.1038/tp.2015.84

73. Berk M, Dodd S, Callaly P, Berk L, Fitzgerald P, de Castella AR, et al. History of illness prior to a diagnosis of bipolar disorder or schizoaffective disorder. *J Affect Disord.* (2007) 103:181–6. doi: 10.1016/j.jad.2007.01.027

frontiers | Frontiers in Psychiatry

TYPE Original Research
PUBLISHED 13 October 2022
DOI 10.3389/fpsyt.2022.1036997

OPEN ACCESS

EDITED BY
Yuanqiang Zhu,
Fourth Military Medical University, China

REVIEWED BY
Ruiwang Huang,
South China Normal University, China
Qunxi Dong,
Beijing Institute of Technology, China

*CORRESPONDENCE
Shumei Li
shumeili0412@gmail.com

SPECIALTY SECTION
This article was submitted to Neuroimaging and Stimulation, a section of the journal Frontiers in Psychiatry

RECEIVED 05 September 2022
ACCEPTED 22 September 2022
PUBLISHED 13 October 2022

CITATION
Jiang G, Feng Y, Li M, Wen H, Wang T, Shen Y, Chen Z and Li S (2022) Distinct alterations of functional connectivity of the basal forebrain subregions in insomnia disorder.
Front. Psychiatry 13:1036997.
doi: 10.3389/fpsyt.2022.1036997

Distinct alterations of functional connectivity of the basal forebrain subregions in insomnia disorder

Guihua Jiang[1], Ying Feng[2], Meng Li[1], Hua Wen[1], Tianyue Wang[1], Yanan Shen[3], Ziwei Chen[4] and Shumei Li[1]*

[1]Department of Medical Imaging, Guangdong Second Provincial General Hospital, Guangzhou, China, [2]Department of Radiology, Affiliated Hospital of Chengdu University, Chengdu, China, [3]The First School of Clinical Medicine, Guangdong Medical University, Zhanjiang, China, [4]Department of Medical Imaging, Guangdong Second Provincial General Hospital, Jinan University, Guangzhou, China

Background: Cholinergic basal forebrain (BF) plays an important role in sleep-wake regulation and is implicated in cortical arousal and activation. However, less is known currently regarding the abnormal BF-related neuronal circuit in human patients with insomnia disorder (ID). In this study, we aimed to explore alterations of functional connectivity (FC) in subregions of the BF and the relationships between FC alterations and sleep and mood measures in ID.

Materials and methods: One hundred and two ID patients and ninety-six healthy controls (HC) were included in this study. Each subject underwent both resting-state fMRI and high-resolution anatomical scanning. All participants completed the sleep and mood questionnaires in ID patients. Voxel-based resting-state FC in each BF subregion (Ch_123 and Ch_4) were computed. For the voxel-wise FC differences between groups, a two-sample *t*-test was performed on the individual maps in a voxel-by-voxel manner. To examine linear relationships with sleep and mood measures, Pearson correlations were calculated between FC alterations and sleep and mood measures, respectively.

Results: The ID group showed significantly decreased FC between the medial superior frontal gyrus and Ch_123 compared to HC. However, increased FC between the midbrain and Ch_4 was found in ID based on the voxel-wise analysis. The correlation analysis only revealed that the altered FC between the midbrain with Ch_4 was significantly negatively correlated with the self-rating anxiety scale.

Conclusion: Our findings of decreased FC between Ch_123 and medial superior frontal gyrus and increased FC between midbrain and Ch4 suggest distinct roles of subregions of BF underlying the neurobiology of ID.

KEYWORDS

functional connectivity, insomnia disorder, anxiety, basal forebrain, resting-state fMRI

Introduction

Insomnia Disorder (ID) is predominantly characterized by difficulties in initiating sleep, remaining sleep or early morning awakenings for at least three times per week over at least 3 months. Patients with ID are generally accompanied by impaired daytime function, mood disruption and cognitive impairments (1–3). Moreover, it increases the risk of accidents and impacts negatively the quality of life, and social productivity (4, 5). ID is a common sleep-wake disorder and is often considered to be related to central nervous system hyperarousal and increased cortical activation (6, 7). Previous animal studies have suggested that the cholinergic basal forebrain (BF) plays an important role in sleep-wake regulation and is implicated in cortical arousal and activation (8, 9). Moreover, the cholinergic BF is reported to be active during both wakefulness and rapid eye movement (REM) sleep but silent during non-REM (NREM) sleep (10), and the activation of cholinergic neurons enhances arousal, attention, and memory (11–16). Optogenetic activation of cholinergic BF causes animals to transition from slow wave sleep to wake (17). These previous animal findings suggest that BF might play a key role in understanding the underlying neuronal circuit for ID.

Most previous human studies that explored the role of BF in the sleep-wake cycle or ID are based on invasive positron emission tomography (PET) imaging techniques. Using H2(15)O-PET to evaluate the dynamic changes in cerebral blood flow (CBF) throughout the sleep-wake cycle in 37 normal male volunteers, one study found that BF showed profound deactivations during slow-wave sleep and reactivations during REM sleep (18). Nofzinger et al. reported insomnia patients showed a smaller decline in relative global cerebral glucose metabolism from waking to sleep states in BF compared to healthy controls (7). Moreover, the same research group further found that depressed patients with severe insomnia symptoms showed increased activation in the BF from waking to the REM sleep state (19). More importantly, Kajimura et al., found that CBF in the BF was lower during non-REM sleep when subjects were given triazolam (a short-acting benzodiazepine) than when they were given a placebo based on the H2(15)O-PET imaging (20). The finding suggests that the hypnotic effect of the benzodiazepines may be mediated mainly by the deactivation of the BF system. Therefore, these previous PET studies have shown that BF is involved in the sleep-wake cycle and is closely related to sleep disorders. However, it is not well established regarding the underlying neuronal mechanism of BF in ID as revealed by non-invasive fMRI techniques.

Resting-state fMRI (rs-fMRI) is a useful non-invasive imaging technique to measure spontaneous neural activity and is crucial for uncovering the intrinsic brain functional architecture. Functional connectivity (FC) analyses, using rs-fMRI to measure synchronous low-frequency brain activity fluctuations, have attracted increasing attention in the study of intrinsic neuronal properties of the brain in ID (21–24). However, non-invasive investigation of BF function has proven challenging due to difficulty in localizing with fMRI. A cytoarchitectonic atlas of the BF generated using post-mortem brains (25) has partially improved these issues. Currently, there is only premilitary evidence regarding the intrinsic FC alterations of BF in ID (26). The BF is important in the production of acetylcholine and is distributed widely to the cortical and limbic structures. Mesulam et al., identified four overlapping magnocellular groups within the basal forebrain BF and described four cholinergic cell groups Ch1–Ch_4 (27). More recently, Fritz et al., found that BF is functionally organized into two subregions that largely follow anatomically defined boundaries of the medial septum and diagonal band of Broca (MS/DB, Ch1-3) and nucleus basalis of Meynert (NBM, Ch_4) using the FC of BF based on rs-fMRI technique (28). Therefore, given that the BF is a heterogeneous structure with different subregions, we focused on exploring the distinct FC alterations of BF subregions in ID in this study.

To this end, we used voxel-based FC of BF subregions to investigate intrinsic spontaneous neuronal activity alterations in a large sample of ID patients (n = 102) and HCs (n = 96) who completed sleep and mood relate questionnaires. Additionally, we further explored the associations of sleep and mood measures with FC alterations. We hypothesized that Ch_123 and Ch_4 showed distinct patterns of FC alterations in patients with ID compared to HC. In addition, the altered FC of BF subregions correlated with sleep or mood-related symptoms in ID.

Materials and methods

Participants

The current study was approved by the ethics committee of Guangdong Second Provincial General Hospital. Written informed consent was obtained from each participant. The patients with ID were recruited in the Department of Neurology at Guangdong Second Provincial General Hospital. The diagnostic criteria for patients with ID were determined by an experienced neurologist, based on the criteria of the Diagnostic and Statistical Manual of Mental Disorders, version 5 (DSM-V). The specific criteria for each patient with ID are as follows: (i) self-complaint of difficulty in falling asleep, staying asleep, or waking up and being unable to fall back to sleep; (ii) symptoms occurring at least three times a week for at least 3 months; (iii) sleep problems occurred despite adequate opportunities to sleep; and (iv) no other sleep disorders (e.g., obstructive sleep apnea, sleep-related movement disorders), mental disorders, substance use, serious organ diseases. Moreover, the patients were free of any psychoactive medication for at least 2 weeks before and during the study.

All participants completed the Pittsburgh Sleep Quality Index (PSQI), the insomnia severity index (ISI), the self-rating depression scale (SDS), and the self-rating anxiety scale (SAS) to evaluate the sleep quality and mood status of ID patients. We excluded four subjects from further examination due to their depression scores (SDS > 73) or severe anxiety scores (SAS > 69). After these tests, each patient underwent rs-fMRI and structural MRI scanning. Three patients were excluded since T2-weighted fluid-attenuated inversion-recovery MR images for these patients showed abnormal hyperintense signals. Finally, 102 patients with ID were included in the study.

We also included 96 HC participants from the local community *via* advertisements. Sleep and mood questionnaires were also completed for all participants in the HC group. The inclusion criteria for participants in HC were as follows: (i) good sleep quality and an ISI score < 7; (ii) no psychiatric or neurologic diseases; (iii) no brain lesions or prior substantial head trauma, verified by conventional T1- or T2-weighted fluid-attenuated inversion-recovery MR imaging. None of the participants in the HC group was excluded from further analysis.

MRI data acquisition

MRI data acquisition for each subject was performed on a 3.0-T MRI scanner (Ingenia; Philips, Best, Netherlands) at the Department of Medical Imaging at Guangdong Second Provincial General Hospital. Each subject underwent both the rs-fMRI and high-resolution anatomical data scanning. The rs-FMRI data were acquired using an echo-planar imaging (EPI) sequence with the following sequence parameters: TR/TE = 2000 ms/30 ms, flip angle: 90°, field of view = 224 × 224 mm^2, resolution = 64 × 64 matrix, number of slices = 33, slice thickness = 3.5 mm with a 0.7 mm gap, a total of 240 volumes, and an acquisition time of approximately 8 min. To determine the cooperation of the participant during the MRI scanning, each subject was asked whether they fell asleep and opened their eyes during scanning after MRI scanning. We rescanned the subject to obtain new rs-MRI data if a participant could not follow the instruction.

The high-resolution anatomical images were acquired using the following parameters: TR/TE: 8 ms/4 ms; flip angle: 8°; 256 × 256 matrix, field of view: 256 × 256 mm^2; voxel size: 1 × 1 × 1 mm^3; and 185 sagittal sections without gaps, covering the whole brain.

Resting-state-fMRI data preprocessing

The rs-fMRI datasets were pre-processed based on Data Processing and Analysis for Brain Imaging (DPARSF) toolbox, version 4.3.[1] The first 10 EPI volumes for each participant were discarded for transient signal changes before magnetization reached a steady state. The head motion of all participants in the present study meets the criteria of translation < 1 mm or rotation < 1 degree in any direction as well as volume-to-volume mean frame-wise displacement (FD) < 2.0 m (29). There were no significant differences in the maximum ($p > 0.05$) or mean framewise displacement ($p > 0.05$) of head motion

1 http://rfmri.org/DPARSF

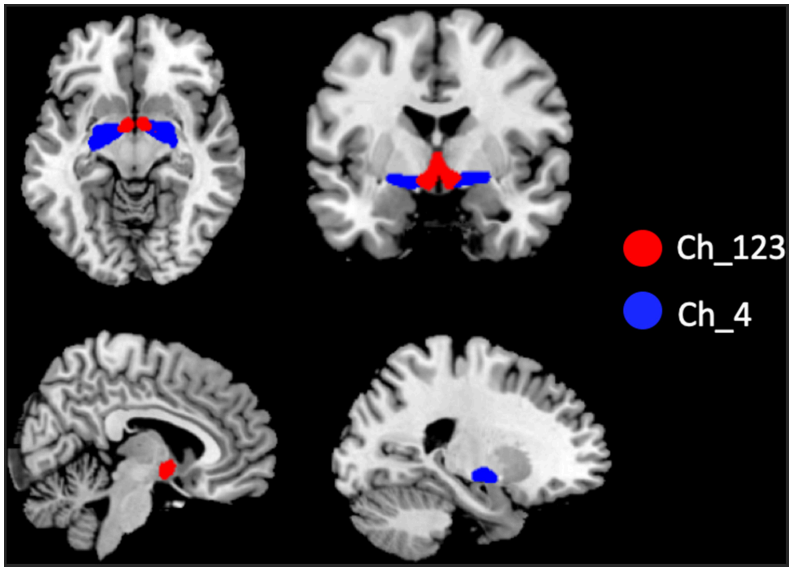

FIGURE 1
Illustration of the locations of basal forebrain (BF) subregions. The red color represents Ch_123; the blue color represents Ch_4.

profiles between the two groups. Individual T1 structural images were segmented and the DARTEL toolbox was used to create a study-specific template for accurate normalization. The functional images were co-registered to the structural images and normalized into standard MNI space. To reduce the effects of confounding factors on the BOLD signal in gray matter, the signal of white matter, cerebrospinal fluid signals, as well as the Friston 24 parameters of head motion (30), were then regressed out from the time course of each voxel. Global signal regression was not regressed in the current study considering that it is a controversial preprocessing option in rs-fMRI analyses (31, 32) and BF is proven to regulate the global signal (33). Finally, temporal band-pass filtering (0.01–0.1 Hz) was adopted.

Voxel-based functional connectivity analysis of basal forebrain subregions

The two BF subregions, Ch_4 and Ch_123 covering both left and right hemispheres (**Figure 1**), were generated from the BF probabilistic maps in the SPM Anatomy toolbox (25, 34). The reasons we chose to use the BF probabilistic maps are as follows. First, the probabilistic cytoarchitectonic map of BF has been widely used in previous studies (35–38); Second, a recent study revealed that BF is functionally organized into two subdivisions that largely follow anatomically defined boundaries of Ch_123 and Ch_4 (28). The two seed regions were resampled to MNI space, in correspondence with the normalized rs-fMRI data. FC analysis of the two seed regions was conducted in a voxel-wise manner. For each seed region, voxel-wise FC maps were calculated by correlating voxel-wise the mean time series across a certain BF subnucleus with all time series across the brain. To assure the normality of FC correlation coefficient maps, the correlation coefficients were converted to *z*-values using Fisher's transformation. Finally, the obtained z-maps were smoothed with a 6-mm full width at half maximum (FWHM) isotropic Gaussian kernel. The flow chart of the seed-based FC analysis was shown in **Figure 2**.

TABLE 1 Demographic and clinical characteristics between insomnia disorder (ID) and healthy controls groups.

Characteristic	ID (n = 102)	HC (n = 96)	Statistics	P-value
Age (years)	44.66 ± 15.42 (21–65 years)	44.26 ± 12.62 (24–65 years)	0.20	0.84
Gender (F/M)	76/26	64/32	1.47	0.23
Education (years)	13.32 ± 3.12	14.03 ± 3.85	−1.43	0.16
BMI (kg/m^2)	21.69 ± 3.09	21.87 ± 2.51	−0.43	0.67
FD (mm)	0.10 ± 0.09	0.09 ± 0.04	0.830	0.13
PSQI	12.73 ± 3.57	2.67 ± 0.29	28.38	<0.001
ISI	15.62 ± 5.76	2.79 ± 1.00	21.52	<0.001
SAS	49.21 ± 11.28	33.46 ± 2.69	13.32	<0.001
SDS	52.91 ± 12.00	33.16 ± 1.52	16.00	<0.001

ID, insomnia disorder; HC, healthy control; PSQI, Pittsburgh Sleep Quality Index; ISI, insomnia severity index; SAS, self-rating anxiety scale; SDS, self-rating depression scale. Age range of the two groups is given in the brackets.

TABLE 2 Brain region showing decreased functional connectivity with Ch_123 in insomnia disorder.

Brain region	Voxels	MNI			T-value
		x	y	z	
Frontal_Sup_Medial_R	60	6	24	60	4.340

R, right; MNI, Montreal Neurological Institute.

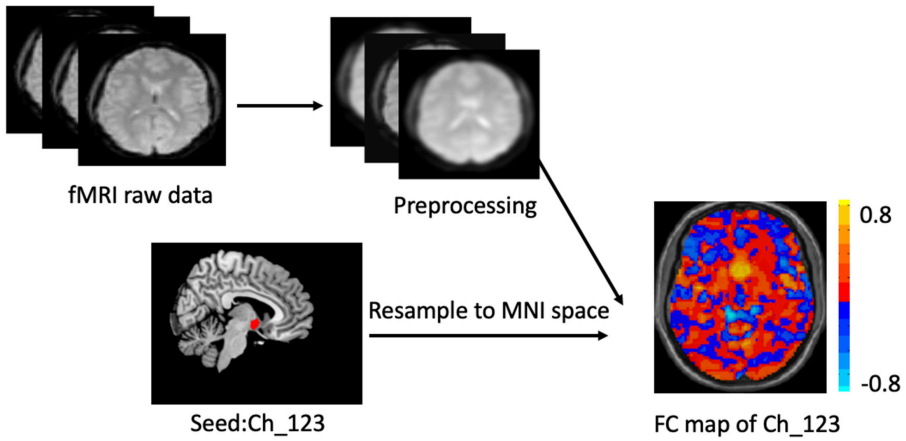

FIGURE 2
Flow chart of the seed_based functional analysis. Illustration of Ch-123 based functional connectivity (FC). Warms color in the FC map represents voxels with positive correlation with Ch_123, while cold colors represent voxels with negative correlation with Ch_123.

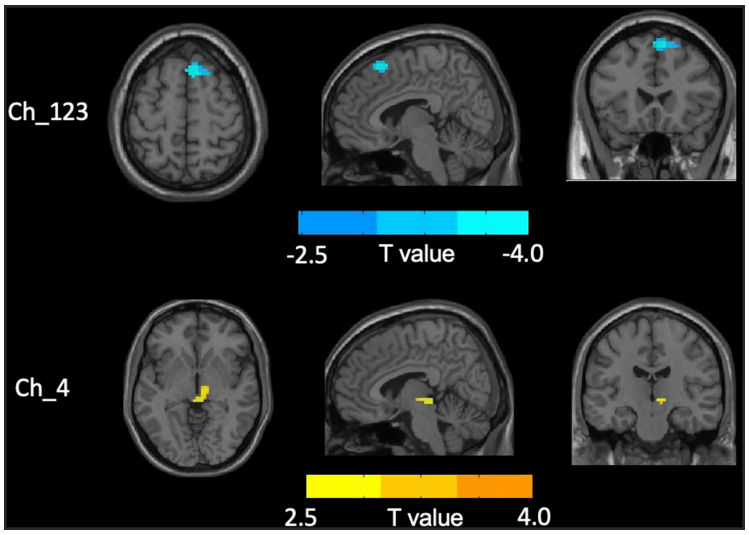

FIGURE 3
Distinct functional connectivity (FC) alterations of basal forebrain (BF) subregions in insomnia disorder (ID) compared to healthy control (HC). The figure represents decreased FC between medial superior frontal gyrus and Ch_123 as well as increased Ch4-midbrain FC in ID group compared to HC. The color bar represents the height of suprathreshold *t*-values.

Statistical analysis

A two-sample *t*-test was used to compare demographic data and neuropsychological tests between the HC and ID groups. The chi-squared test was used to examine sex distribution. For the voxel-wise FC differences between groups, a two-sample *t*-test was performed on the individual maps in a voxel-by-voxel manner. We used two cluster-forming thresholds to determine the significant results in this study. One is the stringent analysis using $p < 0.05$, Gaussian random field (GRF) corrected at the cluster level, based on a voxel-level threshold $p < 0.001$. The other one is a more liberal analysis using $p < 0.05$, GRF corrected at the cluster level, based on a voxel-level threshold $p < 0.01$. Pearson correlations were calculated between mean FC values in clusters showing significant group differences between ID and HC and sleep or mood-related measures, respectively.

Results

Demographic and neuropsychological characteristics

The demographic and neuropsychological characteristics of the HC and ID groups are shown in Table 1. There were no significant group differences in age, gender, education level, and BMI (all $p > 0.05$). As expected, the scores in all the sleep measures (PSQI, ISI), and mood measures (SAS, SDS) in the ID group are significantly higher than those in the HC group.

Distinct functional connectivity alterations of basal forebrain subregions

No significant differences in any of the FC of subregions of BF were shown between ID and HC using the stringent statistical threshold. Under the liberal threshold, voxel-wise Ch_4-FC analysis revealed ID group showed significantly decreased FC between medial superior frontal gyrus and Ch_123 compared to HC (Table 2 and Figure 3). However, increased FC between midbrain and Ch4 was found in ID compared to HC based on the voxel-wise analysis (Table 3 and Figure 3).

Relationships between alterations of basal forebrain subregions and clinical variables

The correlation analysis only revealed that the altered FC between the midbrain with Ch_4 was significantly negatively correlated with the SAS (Figure 4).

TABLE 3 Brain region showing increased functional connectivity with Ch_4 in insomnia disorder.

Brain region	Voxels	MNI			*T*-value
		x	y	z	
Midbrain_R	31	3	−27	−3	4.02

R, right; MNI, Montreal Neurological Institute.

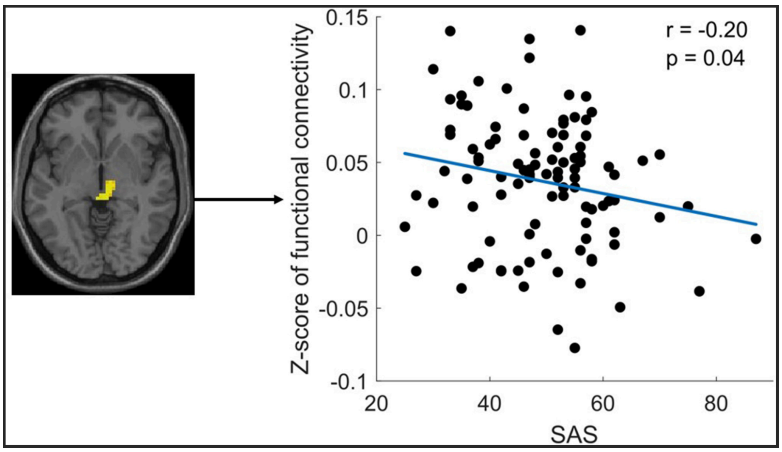

FIGURE 4
Significant correlation between functional connectivity (FC) of Ch4-midbrain and self-rating anxiety scale (SAS). The figure shows the significant negative correlation between the z-scores of the FC between Ch4-midbrain and anxiety score. The mean Z-Score of the FC was extracted from the significant cluster of the midbrain.

Discussion

In the current study, we used rs-fMRI datasets with voxel-based FC analysis to investigate FC alterations of BF subregions in ID. Our findings showed distinctly alterations of FC in the subregions of basal forebrain in ID, characterized by reduced FC between medial superior frontal gyrus and Ch_123 as well as increased FC between midbrain and Ch_4. In addition, the altered FC between the midbrain and Ch_4 correlated negatively with the SAS in ID. This study provided *in vivo* evidence for distinct alterations of FC of BF subregions in ID based on large sample size and may have important implications for understanding the neural mechanisms underlying symptoms and cognitive impairments in ID.

Our result showed reduced FC between medial superior frontal gyrus and Ch_123 in ID compared to HC. The medial superior frontal gyrus, especially the right side, has been considered to be a site of convergence of the dorsal and ventral attention networks (39). Moreover, it is also implicated in working memory, movement, and cognitive control (40, 41). Previous rs-fMRI studies have revealed the abnormal functional activity of the superior frontal gyrus from the regional level in ID, as measured by local connectivity metrics like Regional Homogeneity (ReHo) and Amplitude of Low-Frequency Fluctuations (ALFF) (42, 43). In addition, the global FC alterations of superior frontal gyrus were also reported by previous studies in ID, as measured by the seed-based FC and independent component analysis (ICA) (22, 23). Moreover, one structural neuroimaging study found a reduced gray matter volume of the parietal cortex in insomnia disorder compared to healthy controls (44). A decrease in cortical thickness in the bilateral parietal cortex has also been reported after 23 h of acute sleep deprivation (45). The BF has widespread cholinergic projections and is considered as a major neuromodulatory hub for brain regions supporting cognition, including attention, memory, and spatial navigation (6, 46–48). A recent human study using the rs-fMRI technique reported that there is specific connectivity between the Ch_123 and medial frontal gyrus in healthy young adults using the rs-fMRI technique (6). ID patients are normally characterized by deficits in working memory tasks (49) and several attentional processes (1). Therefore, the reduced FC between the Ch_123 and medial superior frontal gyrus may be the underlying neuronal circuit for cognitive impairments in ID.

Increased FC between midbrain and Ch_4 in ID compared to HC was found in this study. The enhanced FC between Ch_4 and midbrain suggests an elevated neuronal synchronization between the two regions. *Via* the monosynaptic anterograde tracing system, Zheng et al. found that cholinergic neurons in the NBM mainly projected to the midbrain and isocortex (50). The midbrain is a component of the ascending reticular activating system (ARAS), which plays a key role in arousal and sleep (51–53). Nofzinger et al. found that glucose metabolism in wake-promoting ARAS was increased in insomnia patients and ARAS hypermetabolism heightens emotional activities and produces an arousal state and insomnia (7). Furthermore, increased ALFF in the midbrain was reported in the insomnia patients compared to healthy controls (54). Therefore, the increased FC between the NBM-midbrain in our study may provide further evidence to support the theory of hyperarousal underlying the neurobiology of insomnia patients. Furthermore, the current study's correlation analysis showed a significant negative correlation between the NBM-midbrain connectivity and the SAS score. This correlation result was supported by recent studies, which have reported that the midbrain has been

critically implicated in anxiety-like behaviors (55, 56). The negative correlation in the current study may indicate that the increased NBM-midbrain connectivity reflects a compensatory mechanism to combat the anxiety problem in the ID patient.

There are several limitations in the current study. First, we only conducted the limited sleep-related variables using the sleep-related scales, the objective and comprehensive polysomnography was not employed. This could possibly explain the missing relationship between the altered FC of BF with the sleep-related variables. Further studies are needed to elucidate this research question. Second, cognitive tests were not included in this study. It's better to use a battery of cognitive tests to comprehensively understand the specific correlation between the altered FC of BF and the cognitive functions of ID. Finally, the current study was cross-sectional, precluding inferences about the longitudinal alterations of the altered FC of BF over time.

In summary, our study based on a large sample size provides an important addition to previous literature, namely, by providing evidence for decreased FC between Ch_123 and medial superior frontal gyrus as well as increased Ch_4-midbrain FC in ID. The FC alterations of the BF subregions may reflect the abnormal and specific BF subregion neurotransmitter projections in ID. The distinct FC alterations of subregions of BF may indicate different roles of subregions of BF underlying the neurobiology of ID.

Data availability statement

The raw data supporting the conclusions of this article will be made available by the authors, without undue reservation.

Ethics statement

The studies involving human participants were reviewed and approved by Ethics Committee of Guangdong Second People's Hospital. The patients/participants provided their written informed consent to participate in this study.

Author contributions

GJ and SL contributed to the design of the study. YF, ML, and HW contributed to the data acquisitions. SL and YF contributed to the data analysis. GJ, SL, YF, ML, TW, and HW contributed to the interpretation of the results. All authors contributed to the manuscript preparation and revision and approved the final version of the manuscript.

Funding

This study was funded by the National Natural Science Foundation of China (Grant Nos. 81901731 and U1903120) and the Science and Technology Planning Project of Guangdong (202002030234).

Conflict of interest

The authors declare that the research was conducted in the absence of any commercial or financial relationships that could be construed as a potential conflict of interest.

Publisher's note

All claims expressed in this article are solely those of the authors and do not necessarily represent those of their affiliated organizations, or those of the publisher, the editors and the reviewers. Any product that may be evaluated in this article, or claim that may be made by its manufacturer, is not guaranteed or endorsed by the publisher.

References

1. Fortier-Brochu E, Beaulieu-Bonneau S, Ivers H, Morin CM. Insomnia and daytime cognitive performance: A meta-analysis. *Sleep Med Rev.* (2012) 16:83–94. doi: 10.1016/j.smrv.2011.03.008

2. Riemann D, Berger M, Voderholzer U. Sleep and depression–results from psychobiological studies: An overview. *Biol Psychol.* (2001) 57:67–103. doi: 10.1016/s0301-0511(01)00090-4

3. Taylor DJ, Lichstein KL, Durrence HH, Reidel BW, Bush AJ. Epidemiology of insomnia, depression, and anxiety. *Sleep.* (2005) 28:1457–64. doi: 10.1093/sleep/28.11.1457

4. Léger D, Bayon V. Societal costs of insomnia. *Sleep Med Rev.* (2010) 14:379–89. doi: 10.1016/j.smrv.2010.01.003

5. Roth T. Insomnia: Definition, prevalence, etiology, and consequences. *J Clin Sleep Med.* (2007) 3:S7–10.

6. Markello RD, Spreng RN, Luh W-M, Anderson AK, de Rosa E. Segregation of the human basal forebrain using resting state functional MRI. *Neuroimage.* (2018) 173:287–97. doi: 10.1016/j.neuroimage.2018.02.042

7. Nofzinger EA, Buysse DJ, Germain A, Price JC, Miewald JM, Kupfer DJ. Functional neuroimaging evidence for hyperarousal in insomnia. *Am J Psychiatry.* (2004) 161:2126–8. doi: 10.1176/appi.ajp.161.11.2126

8. Szymusiak R. Magnocellular nuclei of the basal forebrain: Substrates of sleep and arousal regulation. *Sleep.* (1995) 18:478–500. doi: 10.1093/sleep/18.6.478

9. Xu M, Chung S, Zhang S, Zhong P, Ma C, Chang W-C, et al. Basal forebrain circuit for sleep-wake control. *Nat Neurosci.* (2015) 18:1641–7. doi: 10.1038/nn.4143

10. Lee MG, Hassani OK, Alonso A, Jones BE. Cholinergic basal forebrain neurons burst with theta during waking and paradoxical sleep. *J Neurosci.* (2005) 25:4365–9. doi: 10.1523/JNEUROSCI.0178-05.2005

11. Jones BE. The organization of central cholinergic systems and their functional importance in sleep-waking states. *Prog Brain Res.* (1993) 98:61–71. doi: 10.1016/s0079-6123(08)62381-x

12. Everitt BJ, Robbins TW. Central cholinergic systems and cognition. *Annu Rev Psychol.* (1997) 48:649–84. doi: 10.1146/annurev.psych.48.1.649

13. Sarter M, Hasselmo ME, Bruno JP, Givens B. Unraveling the attentional functions of cortical cholinergic inputs: Interactions between signal-driven and cognitive modulation of signal detection. *Brain Res Brain Res Rev.* (2005) 48:98–111. doi: 10.1016/j.brainresrev.2004.08.006

14. Pinto L, Goard MJ, Estandian D, Xu M, Kwan AC, Lee S-H, et al. Fast modulation of visual perception by basal forebrain cholinergic neurons. *Nat Neurosci.* (2013) 16:1857–63. doi: 10.1038/nn.3552

15. Fu Y, Tucciarone JM, Espinosa JS, Sheng N, Darcy DP, Nicoll RA, et al. A cortical circuit for gain control by behavioral state. *Cell.* (2014) 156:1139–52. doi: 10.1016/j.cell.2014.01.050

16. Eggermann E, Kremer Y, Crochet S, Petersen CCH. Cholinergic signals in mouse barrel cortex during active whisker sensing. *Cell Rep.* (2014) 9:1654–60. doi: 10.1016/j.celrep.2014.11.005

17. Irmak SO, de Lecea L. Basal forebrain cholinergic modulation of sleep transitions. *Sleep.* (2014) 37:1941–51. doi: 10.5665/sleep.4246

18. Braun AR, Balkin TJ, Wesenten NJ, Carson RE, Varga M, Baldwin P, et al. Regional cerebral blood flow throughout the sleep-wake cycle. An H2(15)O PET study. *Brain.* (1997) 120 (Pt 7):1173–97. doi: 10.1093/brain/120.7.1173

19. Nofzinger EA, Buysse DJ, Germain A, Carter C, Luna B, Price JC, et al. Increased activation of anterior paralimbic and executive cortex from waking to rapid eye movement sleep in depression. *Arch Gen Psychiatry.* (2004) 61:695–702. doi: 10.1001/archpsyc.61.7.695

20. Kajimura N, Nishikawa M, Uchiyama M, Kato M, Watanabe T, Nakajima T, et al. Deactivation by benzodiazepine of the basal forebrain and amygdala in normal humans during sleep: A placebo-controlled [15O]H2O PET study. *Am J Psychiatry.* (2004) 161:748–51. doi: 10.1176/appi.ajp.161.4.748

21. Huang Z, Liang P, Jia X, Zhan S, Li N, Ding Y, et al. Abnormal amygdala connectivity in patients with primary insomnia: Evidence from resting state fMRI. *Eur J Radiol.* (2012) 81:1288–95. doi: 10.1016/j.ejrad.2011.03.029

22. Li Y, Wang E, Zhang H, Dou S, Liu L, Tong L, et al. Functional connectivity changes between parietal and prefrontal cortices in primary insomnia patients: Evidence from resting-state fMRI. *Eur J Med Res.* (2014) 19:32. doi: 10.1186/2047-783X-19-32

23. Li S, Tian J, Li M, Wang T, Lin C, Yin Y, et al. Altered resting state connectivity in right side frontoparietal network in primary insomnia patients. *Eur Radiol.* (2018) 28:664–72. doi: 10.1007/s00330-017-5012-8

24. Wang T, Yan J, Li S, Zhan W, Ma X, Xia L, et al. Increased insular connectivity with emotional regions in primary insomnia patients: A resting-state fMRI study. *Eur Radiol.* (2017) 27:3703–9. doi: 10.1007/s00330-016-4680-0

25. Zaborszky L, Hoemke L, Mohlberg H, Schleicher A, Amunts K, Zilles K. Stereotaxic probabilistic maps of the magnocellular cell groups in human basal forebrain. *Neuroimage.* (2008) 42:1127–41. doi: 10.1016/j.neuroimage.2008.05.055

26. Ma X, Fu S, Yin Y, Wu Y, Wang T, Xu G, et al. Aberrant functional connectivity of basal forebrain subregions with cholinergic system in short-term and chronic insomnia disorder. *J Affect Disord.* (2021) 278:481–7. doi: 10.1016/j.jad.2020.09.103

27. Mesulam MM, Mufson EJ, Levey AI, Wainer BH. Cholinergic innervation of cortex by the basal forebrain: Cytochemistry and cortical connections of the septal area, diagonal band nuclei, nucleus basalis (substantia innominata), and hypothalamus in the rhesus monkey. *J Comp Neurol.* (1983) 214:170–97. doi: 10.1002/cne.902140206

28. Fritz H-CJ, Ray N, Dyrba M, Sorg C, Teipel S, Grothe MJ. The corticotopic organization of the human basal forebrain as revealed by regionally selective functional connectivity profiles. *Hum Brain Mapp.* (2019) 40:868–78. doi: 10.1002/hbm.24417

29. Power JD, Schlaggar BL, Petersen SE. Recent progress and outstanding issues in motion correction in resting state fMRI. *Neuroimage.* (2015) 105:536–51. doi: 10.1016/j.neuroimage.2014.10.044

30. Friston KJ, Williams S, Howard R, Frackowiak RS, Turner R. Movement-related effects in fMRI time-series. *Magn Reson Med.* (1996) 35:346–55. doi: 10.1002/mrm.1910350312

31. Murphy K, Fox MD. Towards a consensus regarding global signal regression for resting state functional connectivity MRI. *Neuroimage.* (2017) 154:169–73. doi: 10.1016/j.neuroimage.2016.11.052

32. Hayasaka S. Functional connectivity networks with and without global signal correction. *Front Hum Neurosci.* (2013) 7:880. doi: 10.3389/fnhum.2013.00880

33. Turchi J, Chang C, Ye FQ, Russ BE, Yu DK, Cortes CR, et al. The basal forebrain regulates global resting-state fMRI fluctuations. *Neuron.* (2018) 97:940.e–52.e. doi: 10.1016/j.neuron.2018.01.032

34. Eickhoff SB, Paus T, Caspers S, Grosbras M-H, Evans AC, Zilles K, et al. Assignment of functional activations to probabilistic cytoarchitectonic areas revisited. *Neuroimage.* (2007) 36:511–21. doi: 10.1016/j.neuroimage.2007.03.060

35. Záborszky L, Gombkoto P, Varsanyi P, Gielow MR, Poe G, Role LW, et al. Specific basal forebrain-cortical cholinergic circuits coordinate cognitive operations. *J Neurosci.* (2018) 38:9446–58. doi: 10.1523/JNEUROSCI.1676-18.2018

36. Kline RL, Zhang S, Farr OM, Hu S, Zaborszky L, Samanez-Larkin GR, et al. The effects of methylphenidate on resting-state functional connectivity of the basal nucleus of meynert, locus coeruleus, and ventral tegmental area in healthy adults. *Front Hum Neurosci.* (2016) 10:149. doi: 10.3389/fnhum.2016.00149

37. Li CR, Ide JS, Zhang S, Hu S, Chao HH, Zaborszky L. Resting state functional connectivity of the basal nucleus of Meynert in humans: In comparison to the ventral striatum and the effects of age. *Neuroimage.* (2014) 97:321–32. doi: 10.1016/j.neuroimage.2014.04.019

38. Zhang C, Wu C, Zhang H, Dou W, Li W, Sami MU, et al. Disrupted resting-state functional connectivity of the nucleus basalis of meynert in Parkinson's disease with mild cognitive impairment. *Neuroscience.* (2020) 442:228–36. doi: 10.1016/j.neuroscience.2020.07.008

39. Japee S, Holiday K, Satyshur MD, Mukai I, Ungerleider LG. A role of right middle frontal gyrus in reorienting of attention: A case study. *Front Syst Neurosci.* (2015) 9:23. doi: 10.3389/fnsys.2015.00023

40. du Boisgueheneuc F, Levy R, Volle E, Seassau M, Duffau H, Kinkingnehun S, et al. Functions of the left superior frontal gyrus in humans: A lesion study. *Brain.* (2006) 129:3315–28. doi: 10.1093/brain/awl244

41. Zhang S, Ide JS, Li CR. Resting-state functional connectivity of the medial superior frontal cortex. *Cereb Cortex.* (2012) 22:99–111. doi: 10.1093/cercor/bhr088

42. Pang R, Guo R, Wu X, Hu F, Liu M, Zhang L, et al. Altered Regional Homogeneity in Chronic Insomnia Disorder with or without Cognitive Impairment. *AJNR Am J Neuroradiol.* (2018) 39:742–7. doi: 10.3174/ajnr.A5587

43. Li C, Ma X, Dong M, Yin Y, Hua K, Li M, et al. Abnormal spontaneous regional brain activity in primary insomnia: A resting-state functional magnetic resonance imaging study. *Neuropsychiatr Dis Treat.* (2016) 12:1371–8. doi: 10.2147/NDT.S109633

44. Altena E, Vrenken H, van der Werf YD, van den Heuvel OA, van Someren EJW. Reduced orbitofrontal and parietal gray matter in chronic insomnia: A voxel-based morphometric study. *Biol Psychiatry.* (2010) 67:182–5. doi: 10.1016/j.biopsych.2009.08.003

45. Elvsåshagen T, Zak N, Norbom LB, Pedersen PØ, Quraishi SH, Bjørnerud A, et al. Evidence for cortical structural plasticity in humans after a day of waking and sleep deprivation. *Neuroimage.* (2017) 156:214–23. doi: 10.1016/j.neuroimage.2017.05.027

46. Ballinger EC, Ananth M, Talmage DA, Role LW. Basal forebrain cholinergic circuits and signaling in cognition and cognitive decline. *Neuron.* (2016) 91:1199–218. doi: 10.1016/j.neuron.2016.09.006

47. Bell PT, Shine JM. Subcortical contributions to large-scale network communication. *Neurosci Biobehav Rev.* (2016) 71:313–22. doi: 10.1016/j.neubiorev.2016.08.036

48. Gritton HJ, Howe WM, Mallory CS, Hetrick VL, Berke JD, Sarter M. Cortical cholinergic signaling controls the detection of cues. *Proc Natl Acad Sci U.S.A.* (2016) 113:E1089–97. doi: 10.1073/pnas.1516134113

49. Drummond SPA, Walker M, Almklov E, Campos M, Anderson DE, Straus LD. Neural correlates of working memory performance in primary insomnia. *Sleep.* (2013) 36:1307–16. doi: 10.5665/sleep.2952

50. Zheng Y, Tao S, Liu Y, Liu J, Sun L, Zheng Y, et al. Basal forebrain-dorsal hippocampus cholinergic circuit regulates olfactory associative learning. *Int J Mol Sci.* (2022) 23:8472. doi: 10.3390/ijms23158472

51. Torterolo P, Vanini G. New concepts in relation to generating and maintaining arousal. *Rev Neurol.* (2010) 50:747–58.

52. Jones BE. Arousal and sleep circuits. *Neuropsychopharmacology.* (2020) 45:6–20. doi: 10.1038/s41386-019-0444-2

53. Takata Y, Oishi Y, Zhou X-Z, Hasegawa E, Takahashi K, Cherasse Y, et al. Sleep and wakefulness are controlled by ventral medial midbrain/pons GABAergic neurons in mice. *J Neurosci.* (2018) 38:10080–92. doi: 10.1523/JNEUROSCI.0598-18.2018

54. Ran Q, Chen J, Li C, Wen L, Yue F, Shu T, et al. Abnormal amplitude of low-frequency fluctuations associated with rapid-eye movement in chronic primary insomnia patients. *Oncotarget.* (2017) 8:84877–88. doi: 10.18632/oncotarget.17921

55. Tian G, Hui M, Macchia D, Derdeyn P, Rogers A, Hubbard E, et al. An extended amygdala-midbrain circuit controlling cocaine withdrawal-induced anxiety and reinstatement. *Cell Rep.* (2022) 39:110775. doi: 10.1016/j.celrep.2022.110775

56. Morel C, Montgomery SE, Li L, Durand-de Cuttoli R, Teichman EM, Juarez B, et al. Midbrain projection to the basolateral amygdala encodes anxiety-like but not depression-like behaviors. *Nat Commun.* (2022) 13:1532. doi: 10.1038/s41467-022-29155-1

frontiers | Frontiers in Psychiatry

TYPE Original Research
PUBLISHED 22 November 2022
DOI 10.3389/fpsyt.2022.1050403

OPEN ACCESS

EDITED BY
Yuanqiang Zhu,
Fourth Military Medical University, China

REVIEWED BY
Chao Li,
The First Affiliated Hospital of China Medical University, China
Yujun Wang,
Zhejiang Chinese Medical University, China

*CORRESPONDENCE
Guihua Jiang
jgh2023@outlook.com

†These authors have contributed equally to this work

SPECIALTY SECTION
This article was submitted to Neuroimaging, a section of the journal Frontiers in Psychiatry

RECEIVED 21 September 2022
ACCEPTED 31 October 2022
PUBLISHED 22 November 2022

CITATION
Chen Z, Feng Y, Li S, Hua K, Fu S, Chen F, Chen H, Pan L, Wu C and Jiang G (2022) Altered functional connectivity strength in chronic insomnia associated with gut microbiota composition and sleep efficiency.
Front. Psychiatry 13:1050403.
doi: 10.3389/fpsyt.2022.1050403

Altered functional connectivity strength in chronic insomnia associated with gut microbiota composition and sleep efficiency

Ziwei Chen[1,2†], Ying Feng[3†], Shumei Li[2], Kelei Hua[2], Shishun Fu[2], Feng Chen[2], Huiyu Chen[2,4], Liping Pan[1], Caojun Wu[2,4] and Guihua Jiang[2,1*]

[1]Jinan University, Guangzhou, China, [2]Department of Medical Imaging, Guangdong Second Provincial General Hospital, Guangzhou, China, [3]Department of Radiology, Affiliated Hospital of Chengdu University, Chengdu, China, [4]The Second School of Clinical Medicine, Southern Medical University, Guangzhou, China

Background: There is limited evidence on the link between gut microbiota (GM) and resting-state brain activity in patients with chronic insomnia (CI). This study aimed to explore the alterations in brain functional connectivity strength (FCS) in CI and the potential associations among altered FCS, GM composition, and neuropsychological performance indicators.

Materials and methods: Thirty CI patients and 34 age- and gender-matched healthy controls (HCs) were recruited. Each participant underwent resting-state functional magnetic resonance imaging (rs-fMRI) for the evaluation of brain FCS and was administered sleep-, mood-, and cognitive-related questionnaires for the evaluation of neuropsychological performance. Stool samples of CI patients were collected and subjected to 16S rDNA amplicon sequencing to assess the relative abundance (RA) of GM. Redundancy analysis or canonical correspondence analysis (RDA or CCA, respectively) was used to investigate the relationships between GM composition and neuropsychological performance indicators. Spearman correlation was further performed to analyze the associations among alterations in FCS, GM composition, and neuropsychological performance indicators.

Results: The CI group showed a reduction in FCS in the left superior parietal gyrus (SPG) compared to the HC group. The correlation analysis showed that the FCS in the left SPG was correlated with sleep efficiency and some specific bacterial genera. The results of CCA and RDA showed that 38.21% (RDA) and 24.62% (CCA) of the GM composition variation could be interpreted by neuropsychological performance indicators. Furthermore, we found complex relationships between Alloprevotella, specific members of the family Lachnospiraceae, Faecalicoccus, and the FCS alteration, and neuropsychological performance indicators.

Conclusion: The brain FCS alteration of patients with CI was related to their GM composition and neuropsychological performance indicators, and there was also an association to some extent between the latter two, suggesting a specific interaction pattern among the three aspects: brain FCS alteration, GM composition, and neuropsychological performance indicators.

KEYWORDS

chronic insomnia, gut microbiota, resting-state fMRI, functional connectivity strength, brain function

Introduction

Chronic insomnia (CI), a frequent condition in adults, is the most common sleep disorder in the human population. CI exhibits diverse manifestations, including difficulties in initiating or maintaining sleep and obtaining refreshing sleep, as well as a hyperarousal state (1, 2). Persistent insomnia disorder has been associated with chronic conditions like hypertension (3) but also with cancer (4, 5). In addition, CI can impair social, cognitive, and behavioral functioning, resulting in a high risk of suicide (6, 7) and fatal traffic accidents (8). Therefore, CI significantly impacts human physical and mental health and impairs social development, and thus has become a major public health issue worldwide (9). However, the neural mechanisms of CI have not been fully elucidated.

The potential link between sleep disorders and gut microbiota (GM) has drawn considerable interest in recent years (10–13). Studies have found that the microbial diversity and relative abundance (RA) of specific GM differed significantly between insomnia patients and healthy individuals (11, 12). Li et al. further showed that Faecalibacterium and Blautia can be used as iconic bacteria to distinguish patients with CI and healthy controls (HCs), whereas the combination of Lachnospira and Bacteroides was most helpful for identifying patients with acute insomnia (13). A study found that sleep quality and the severity of insomnia were the main factors that drove the variation in microbiome community structure in patients with major depressive disorder (14). Another study found RA changes in some members of the microbiota following two nights of partial sleep deprivation (15). Using redundancy analysis (RDA), Liu et al. found that the GM profile at the phylum level was highly correlated with clinical sleep parameters, including polysomnography (PSG) parameters, total sleep time, sleep efficiency, and sleep latency (10), which indicated that GM composition alterations could be explained by clinical sleep parameters. The findings of the above studies suggest that the GM is closely related to insomnia disorder. Some specific flora may be potential prognostic markers of insomnia symptoms or even subtypes. The microbiota-gut-brain axis (MGBA) is a well-known bidirectional communication system that has shown great potential in exploring the neural mechanisms of CI. The GM dysbiosis regulates brain physiology, cognition, and behavior *via* various pathways, including metabolic, endocrine, and immune signaling pathways (16–19). Bacterial metabolites, such as short-chain fatty acids (SCFAs), bioactive compounds, or neuroactive metabolites, can affect neuronal architecture and function (20). However, research on whether the GM has an impact on insomnia through the MGBA is still in its infancy, and further studies are needed.

Resting-state functional magnetic resonance imaging (rs-fMRI) is an effective means of studying the MGBA in humans and is currently an essential technique for studying the underlying neural mechanisms of insomnia (21). Rs-fMRI can be used to observe the link between the GM and brain function and perhaps even explain how the GM affects resting-state brain activity (22). Rs-fMRI has been applied in several studies investigating the potential brain-gut interaction mechanisms in healthy individuals (23, 24) and those with neuropsychiatric disorders (25–27), including schizophrenia and amnestic mild cognitive impairment. Rs-fMRI offers a unique perspective for studying MGBA communication pathways in insomnia. Functional connectivity strength (FCS), a graph theory-based data-driven method calculated by degree centrality (DC), can quantify the strength of network nodes with high connectivity to neighboring brain regions and thus identify communication hubs in the human brain (28–30). The FCS method based on rs-fMRI can be used to directly compute global brain connectivity and visualize important architectural topology abnormalities in the brain functional connectome at the voxel level, thus reflecting the functional interactions of the brain in the resting state (31). Previous studies based on this method showed that the brain areas with increased FCS or DC in insomnia patients were mainly located in the right superior parietal lobe, insula, cerebellum posterior lobe, precuneus, and left middle frontal gyrus. In contrast, reduced FCS or DC values were mainly located in the bilateral frontal lobe, temporal lobe, right inferior parietal gyrus, insula, right occipital lobe, and right cerebellum anterior lobe (29, 32–35). With great potential in the study of GM-brain function interaction pathways in insomnia patients, the FCS method, which is accurate and highly reproducible, could compensate for the shortcomings of traditional functional

connectivity analyses (33, 36). However, to our knowledge, no investigation has combined an evaluation of brain FCS and the intestinal flora to explore brain-gut communication mechanisms in CI patients.

This study aimed to investigate the interconnections among the three aspects of brain function, the GM, and neuropsychological performance indicators in patients with CI. We hypothesized that altered brain function in patients with CI is related to GM composition and that both are related to neuropsychological changes. To test this hypothesis, in addition to recruiting CI patients and HCs for evaluating neuropsychological performance and studying intergroup brain functional alterations based on the FCS method of rs-fMRI, we collected stool samples from the CI group to analyze the GM composition in CI patients and its potential association with brain FCS alteration and neuropsychological performance indicators. An in-depth understanding of the relationship among the altered brain function, microbiota, and neuropsychological performance of patients with CI may be used to screen for new GM-neuroimaging markers for the study of neural mechanisms of CI and to explore potential future intervention targets.

Materials and methods

Participants

Informed consent was obtained from each participant according to the principles of the Declaration of Helsinki. Ethical approval was obtained from the Ethics Committee of Guangdong Second Provincial General Hospital. All our tests were completed on the day of the patient's first visit. The stools were collected on the morning of the visit and the neuropsychological assessments were performed prior to the MRI scans. The flow chart of our whole study was shown in **Figure 1**.

The inclusion criteria for patients with CI were as follows: diagnosis of CI based on the criteria in the Diagnostic and Statistical Manual of Mental Disorders, version 5 (DSM-V); free of other sleep disorders; and no history of receiving cognitive behavioral therapy or medication. The diagnosis of CI was confirmed by two psychiatrists with >15 years of clinical experience. A third opinion was sought to reach a consensus diagnosis when disagreement happened. HCs were recruited through local advertisements with the following inclusion criteria: (a) good sleep quality without difficulty falling or maintaining asleep; and (b) no history of psychiatric or neurological disorders. In addition, participants were excluded if the following criteria were met: (a) T1-weighted and T2-weighted fluid-attenuated inversion-recovery (T2-FLAIR) weighted sequences identifying organic brain disease or a history of head trauma; (b) a history of transient ischemic attack or stroke; (c) the presence of other systematic diseases, including severe respiratory, cardiovascular, renal, liver, or endocrine diseases; (d) pregnancy, lactation, or menstruation in females; (e) a history of smoking or drug/alcohol abuse; (f) the use of any psychotropic drug or medication that could affect sleep; (g) a diagnosis of irritable bowel syndrome; (h) diarrhea while participating in the study or the use of antibiotics, probiotics, and prebiotics before sample collection; and (i) rotating shift work or crossing more than one-time zone within 2 weeks before the study. According to the strict inclusion/exclusion criteria, we excluded three patients due to the lack of access to fresh fecal samples collection. Two patients were excluded after MRI scanning due to the presence of abnormal hyperintense signals on T2-FLAIR images. One healthy individual was excluded because of falling asleep during scanning. Finally, 30 patients with CI and 34 HCs were included. The two groups were matched by age, sex, and education. All participants were right-handed and aged 18–60 years.

Before the MRI scans, neuropsychological tests were administered by trained psychiatrists to all participants to evaluate their sleep quality, emotional state, and general cognitive level. These tests included: the Pittsburgh Sleep Quality Index (PSQI) and Insomnia Severity Index (ISI) for the evaluation of sleep; the Self-Rating Depression Scale (SDS), Self-Rating Anxiety Scale (SAS), and Hamilton Anxiety Scale (HAMA) for the evaluation of emotional state; and the Montreal Cognitive Assessment (MoCA), Digit Symbol Test, and Digit Symbol Substitution Test (DSST) for the evaluation of the general cognitive level. In addition, information on sleep efficiency (the percentage of time asleep while in bed at night) and total sleep time was collected using answers to individual questions within the PSQI. The above evaluation of neuropsychological performance was carried out in total by two trained psychiatrists in a face-to-face, one-to-one approach.

Collection of fecal samples and gut microbiota analysis

Fresh fecal samples were collected from CI patients into sterile fecal boxes and stored immediately in −80°C freezers to avoid air oxidation and urine contamination during transport. The subsequent 16SrDNA high-throughput sequencing was performed on the MiSeq platform. First, DNA was extracted from fecal samples using a QIAamp DNA Mini Kit (QIAGEN, Hilden, Germany). After quality control, the amplification of the 16S rDNA variable region, library construction, sequencing, and subsequent data analyses were performed. Then QIIME2 software[1] was used to filter out the low-quality reads and obtain the remaining high-quality clean data. FLASH (37) (Fast Length

1 https://qiime2.org/

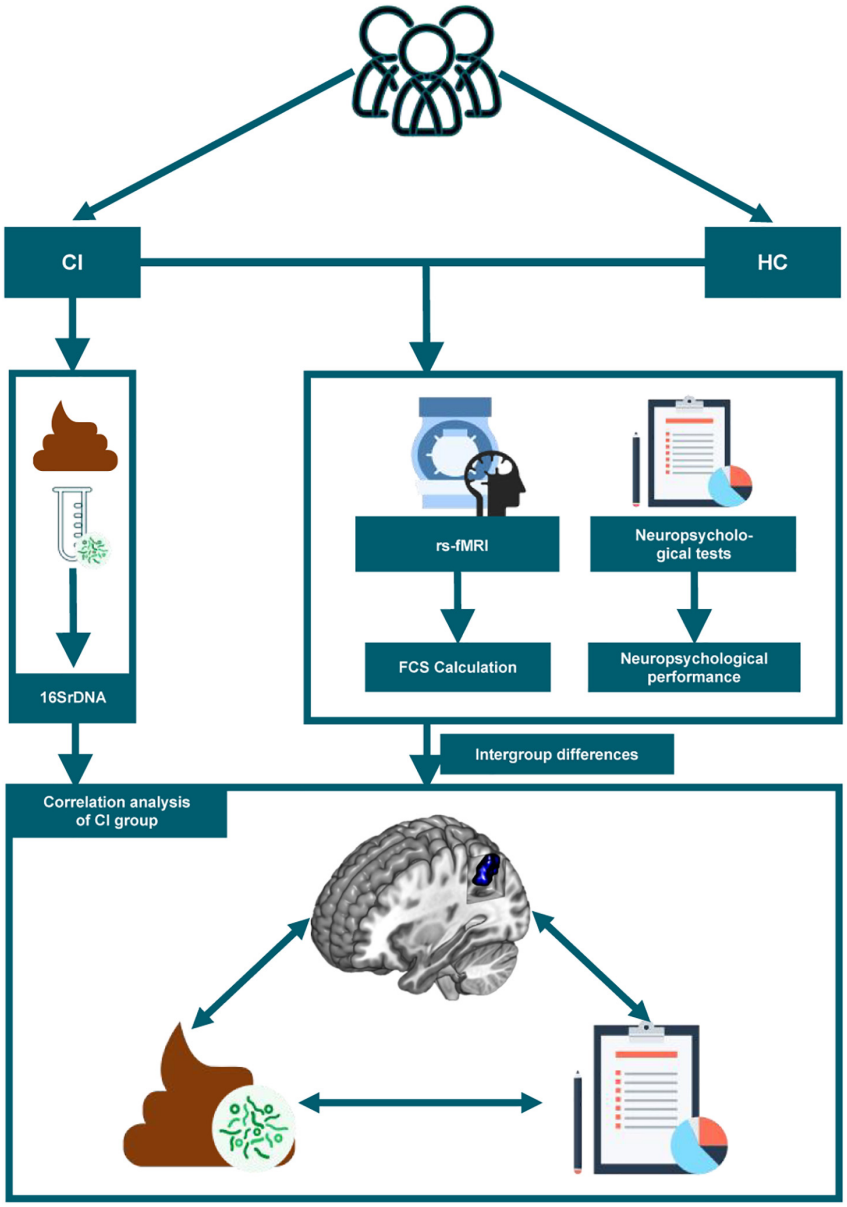

FIGURE 1
The study flow chart is depicted. CI, chronic insomnia; HC, healthy controls; rs-fMRI, resting-state functional magnetic resonance imaging; FCS, functional connectivity strength.

Adjustment of Short, FLASH, v1.2.11) software was used to assemble paired-end reads for obtaining high-quality sequences. After that, chimeras were removed using the UCHIME (38) algorithm based on VSEARCH.

Operational taxonomic units (OTUs) were clustered by UPARSE software at 97% similarity in the next step. The OTU representative sequence was compared with the template sequence from the Ribosomal Database Project (RDP) (39) for species annotation using a confidence threshold of 0.8. After OTU classifications, stacked bar figures were generated from the phylum- and genus -level RA, to visually display the GM composition of CI patients.

fMRI data acquisition, preprocessing, and functional connectivity strength calculation

fMRI data acquisition

All participants were scanned on a Philips 3.0 T MRI scanner. Image acquisition was performed by two trained

radiographers. Participants laid supine with their head fixed by foam pads and body fixed by straps. Noise-canceling earplugs were provided to minimize scanning noise. During scanning, participants were asked to remain quiet and to avoid thinking about anything particular. The radiographers communicated with the participants through a microphone to be sensitive to any discomfort that the subjects might have during the examination. Communication only takes place when necessary. Finally, self-reports were collected after scanning to assess patient cooperation. In the presence of a poor degree of patient cooperation, we rescanned the participant again to obtain new rs-fMRI datasets for further analysis.

Imaging parameters for high-resolution anatomical imaging were as follows: TR/TE: 7.6/3.6 ms; 256 × 256 matrix; FOV: 256 × 256 mm^2; flip angle: 8°; and 185 axial slices with no gap. Rs-fMRI data were obtained *via* gradient-recalled echo-planar imaging (EPI) with the following parameters: TR/TE: 2,000/30 ms; 64 × 61 matrix; FOV: 224 × 224 mm^2; flip angle: 90°; and 33 slices obtained using an interleaved slice acquisition sequence with a 1.0 mm gap. The scanning time for each participant was approximately 8 min with 240 time points. T1-WI and T2-FLAIR images were used to detect organic brain disease or a history of head trauma.

Data preprocessing and functional connectivity strength calculation

Data preprocessing was performed in MATLAB by DPABI_V4.3 software.[2] First, initial functional images were excluded to allow magnetic field stabilization and the participants' acclimation to the scanner environment. Then, time layer correction and motion correction were conducted. Data with head movement displacement > 1.5 mm or rotation angle > 1.5° were excluded. The remaining functional images were spatially normalized into a standard EPI template from the Montreal Neurological Institute (MNI) and resampled to 3 mm isotropic voxels. Next, the resampled images were smoothed by a 4 mm full-width half-maximum Gaussian kernel and detrended to remove the linear signal drift. After this, nuisance covariates were removed by regression. All image data were filtered with a bandpass filter on a frequency range of 0.01–0.08 to remove the effects of noise.

For preprocessed rs-fMRI data, FCS values were computed by the DPARSF.[3] First, for each participant, the Pearson correlation of time series between each pair of voxels was calculated to construct the brain functional connectivity matrix. Then, Pearson correlation coefficients were corrected by Fisher's r-to-z transformation to make the data meet the normal distribution.

For each voxel, FCS was computed as the summed weights of its connections with the remaining voxels of the brain (40). The correlation threshold for the FCS calculation was set at 0.25 (41, 42) to eliminate the influence of noise.

Statistical analysis

Statistical analyses for demographic data of the participants were processed with R software (R Studio software, version 4.1.2) and SPSS 25.0 (SPSS Inc., Chicago, IL, United States). The Shapiro–Wilk test was applied to test whether the data satisfied a normal distribution. Continuous variables are presented as the mean value ± standard deviation (if normally distributed), and comparisons of the two groups were carried out with independent sample *t*-test. The Mann–Whitney *U* test was used to compare groups when the data for continuous variables were not normally distributed. The comparison of sex between groups was performed with a χ^2 test.

To explore the voxel-based FCS differences between CI patients and HCs, two independent sample *t*-tests with age, gender, education, and head movement as covariates were performed in DPABI software. Two-tailed Gaussian random field theory (GRF) was used to correct for multiple comparisons (voxel level $p < 0.005$, cluster level $p < 0.05$). At last, the mean FCS value of brain regions with significant differences was extracted for subsequent analysis. Then, we used Spearman rank correlation for the correlation analysis between FCS alterations and neuropsychological performances in CI patients. The clinical indicators of neuropsychological performance included in the correlation analysis were those with significant group differences and sleep parameters related to the altered brain FCS in the CI group.

To further demonstrate whether neuropsychological performance indicators related to CI could explain the GM composition, in addition to creating stacked bar charts of the microbiota composition, we performed RDA or CCA for the RAs in patients with CI. The clinical indicators for neuropsychological performance included in the RDA and CCA analysis were as described above. Constrained ordination technique and detrended correspondence analysis (DCA) were used to determine the chosen method. The results of DCA and the specific selection principles of RDA or CCA are provided in the **Supplementary Table 1**. Then, the correlation between the RAs of GM and, neuropsychological performance indicators, and the RAs of GM and abnormal FCS were analyzed by Spearman's rank correlation, respectively. *P*-values were corrected for multiple inferences using the Benjamini-Hochberg false discovery rate (FDR) procedure (43). Finally, the heatmaps (the absolute value of $r > 0.3$, significance level $p < 0.05$) were plotted by R software to visualize the results.

2 http://rfmri.org/dpabi

3 http://rfmri.org/dparsf

Results

Demographic and clinical characteristics

The analysis of the general data of participants showed no significant differences (all $p > 0.05$) in age, gender, or years of education between groups. Sleep assessments (PSQI and ISI), mood assessments (SAS, SDS, and HAMA), and total MoCA scores representing cognition were significantly different between the CI and HC groups ($p < 0.05$). Table 1 shows the general characteristics of the participants.

Relationships between brain functional connectivity strength alteration and neuropsychological performance indicators

The FCS value of the left superior parietal gyrus (SPG) was significantly reduced in the CI group compared with the HC group (Figure 2 and Table 2). The correlation analysis showed that the FCS value of the left SPG was negatively correlated with sleep efficiency ($r = -0.430$, $p = 0.018$), while no significant correlations were found between the FCS value of the left SPG and other clinical indicators for neuropsychological performance (Figure 3).

Gut microbiota composition of chronic insomnia patients

The RAs of intestinal bacteria at the phylum and genus levels are shown in Figure 4. Firmicutes and Bacteroidetes were the dominant bacterial phyla in the CI group, accounting for 46.50 and 40.78%, respectively. At the genus level, the predominant genera in CI patients were Bacteroides, Prevotella 9, Faecalibacterium, and Blautia. RAs at other levels in CI patients are shown in the Supplementary Figure 1.

Gut microbiota composition was highly correlated with neuropsychological performance indicators in the chronic insomnia group

We found 38.21% (RDA) and 24.62% (CCA) of the variance could be interpreted by seven environmental factors, in other words, neuropsychological performance indicators, including sleep efficiency, PSQI, ISI, SAS, SDS, HAMA, and MoCA scores (Figure 5).

Associations between gut microbiota, regional functional connectivity strength alteration, and neuropsychological performance indicators

As shown in Figure 5, we found that the GM composition at phylum level and genus level were both partially microbially significantly correlated with the neuropsychological performance indicators. The RA of GM in CI patients at the phylum level showed no significant correlation with reduced FCS in the left SPG (Figure 6A); however, significant correlations were found at the genus level (Figure 6B). At the genus level, Alloprevotella ($r = -0.366$, $p = 0.047$), Intestinibacter ($r = -0.486$, $p = 0.007$), Lachnospiraceae_UCG-003 ($r = -0.416$, $p = 0.022$), Gordonibacter ($r = 0.362$, $p = 0.049$), Faecalicoccus ($r = -0.371$, $p = 0.043$), and Selenomonas_3 ($r = -0.363$, $p = 0.049$) were significantly correlated with the reduced FCS value of the left SPG. After FDR adjustment (q-value < 0.05), Intestinibacter (q-value = 0.048), Lachnospiraceae_UCG-003 (q-value = 0.048), and Faecalicoccus (q-value = 0.049) were still significantly correlated. At the same time, Alloprevotella, Gordonibacter, and Selenomonas_3 showed a trend for a significant correlation (q-value = 0.050) with the reduced FCS value of the left SPG. In the dominant florae, we found a negative correlation between Blautia and MoCa score (see Supplementary Table 2). In addition, we also found significant correlations between other specific non-dominant genera and some indicators of neuropsychological performance as well as altered FCS value.

Among the aforementioned taxa, three taxa, namely, Alloprevotella, specific members of family Lachnospiraceae, and Faecalicoccus, were also significantly associated with neuropsychological performance indicators: Alloprevotella ($r = 0.445$, $p = 0.014$), Faecalicoccus ($r = 0.361$, $p = 0.050$), and Lachnospiraceae_UCG-010 ($r = 0.3795$, $p = 0.039$) were positively correlated with sleep efficiency, and Lachnospiraceae_FCS020_group ($r = -0.4078$, $p = 0.025$) and Lachnospiraceae_ ND3007_group ($r = -0.4038$, $p = 0.027$) were negatively correlated with the SAS score. The correlation coefficients and FDR-corrected p-values for the significant results of the correlation analysis between each bacterium at the phylum and genus levels and neuropsychological performance indicators are shown in Supplementary Table 2.

Discussion

In the present study, we used the FSC method based on rs-fMRI to measure abnormal brain functional connectivity at the voxel level. The CI group showed lower FCS in the left SPG than the HC group. The decreased FCS

TABLE 1 Demographics and clinical characteristics of CI patients and HCs.

Characteristic	CIs ($N = 30$)	HCs ($N = 34$)	Statistics	*P*-value
Age (y)	39.50 (26.50∼49.75)	35.00 (29.00∼48.50)	527.00[c]	0.82
Gender (F/M)	7/23	5/29	1.00[b]	0.57
Education (y)	15.50 (12.00∼16.00)	16.00 (15.25∼16.00)	412.50[c]	0.13
PSQI (score)	12.40 ± 2.98	4.35 ± 1.89	12.71[a]	<0.01*
ISI (score)	16.50 ± 5.35	4.14 ± 1.28	12.34[a]	<0.01*
SAS (score)	50.47 ± 9.31	40.32 ± 8.31	4.57.00[a]	<0.01*
SDS (score)	54.00 (48.00∼61.00)	41.00 (38.00∼43.00)	877.00[c]	<0.01*
HAMA (score)	18.50 ± 7.91	2.53 ± 1.05	10.98	<0.01*
MoCA (score)	25.00 (23.00∼27.00)	28.00 (26.25∼29.00)	274.50[c]	0.01*
DSST (*n*)	45.50 (37.00∼63.75)	57.00 (48.00∼64)	392.50[c]	0.12
DST (*n*)	13.83 ± 2.61	13.65 ± 1.82	0.33[a]	0.75
Sleep efficiency (%)	72.57 ± 15.75	/	/	/
Total sleep time (h)	6.00 (5.00∼6.00)	/	/	/

[a]Independent two sample *t*-test; [b]χ^2 test; [c]Mann–Whitney *U* test; *$p < 0.05$.
CIs, chronic insomnia patients; HCs, healthy controls; PSQI, Pittsburgh Sleep Quality Index; ISI, Insomnia Severity Index; SAS, Self-Rating Anxiety Scale; SDS, Self-Rating Depression Scale; HAMA, Hamilton Anxiety Scale; MoCA, Montreal Cognitive Assessment; DSST, Digit Symbol Substitution Test; DST, Digit Span Test; y, year; h, hour; min, minute; s, second.

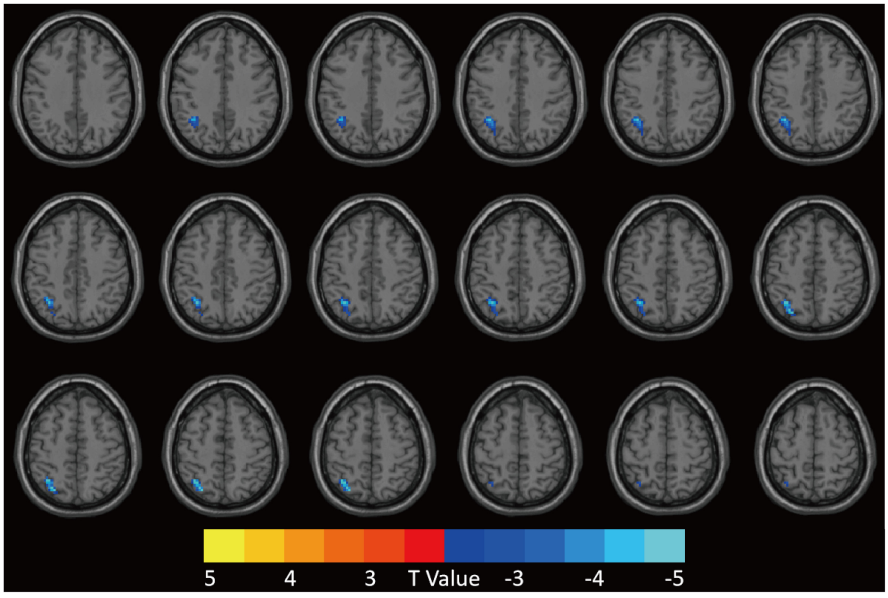

FIGURE 2
Patients with CI showed decreased FCS value in the left SPG compared to HCs. GRF was used for multiple comparisons, setting the height threshold at $p < 0.005$ and the clustering threshold at $p < 0.05$. CI, chronic insomnia; FCS, functional connectivity strength; SPG, superior parietal gyrus; HCs, healthy controls; GRF, Gaussian random fields.

TABLE 2 Brain regions with abnormal FCS in CI group compared with HCs.

Brain area	Cluster size	Peak MNI coordinate			Peak *t*-value	*P*-value
		x	y	z		
Parietal_Sup_L	109	−30	−66	51	−4.1618	<0.05

FCS, functional connectivity strength; CI, chronic insomnia; HCs, healthy controls; Sup, superior; L, left; MNI, Montreal Neurological Institute.

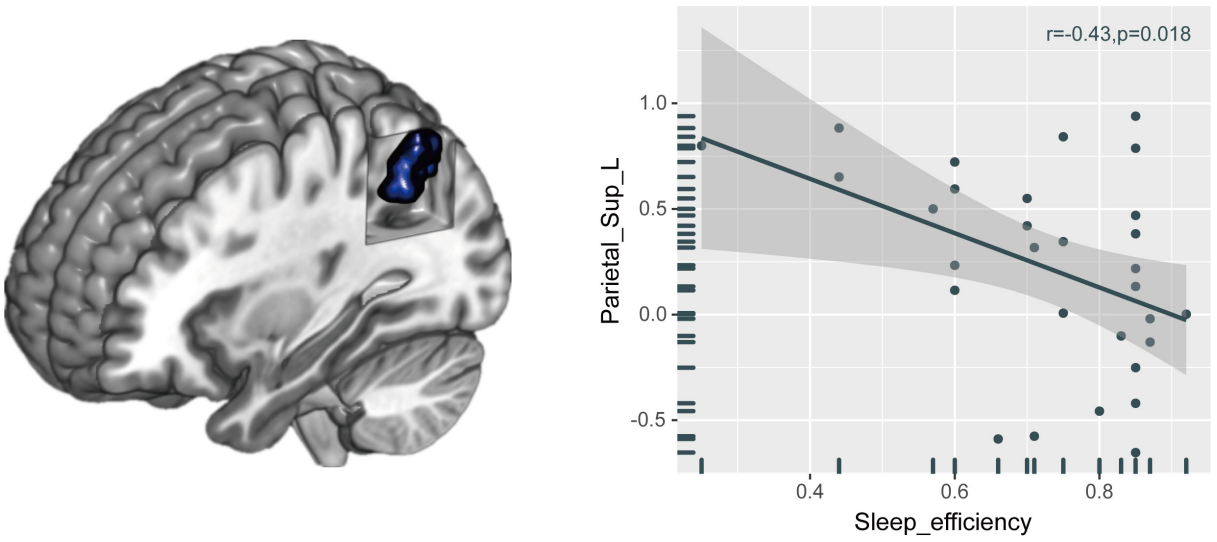

FIGURE 3
Relationships between brain FCS alteration and neuropsychological performances in patients with CI. The FCS value of the left SPG was negatively correlated with sleep efficiency. FCS, functional connectivity strength; CI, chronic insomnia; SPG, superior parietal gyrus.

in the left SPG was significantly correlated with sleep efficiency and specific intestinal microbiota. Specifically, the composition of Intestinibacter, Lachnospiraceae_UCG-003, and Faecalicoccus were significantly correlated with the FCS alteration in the left SPG. It is worth noting that after FDR adjustment, there were still complex relationships between Alloprevotella and specific members of the family Lachnospiraceae, Faecalicoccus and the FCS alteration and neuropsychological performance indicators. These findings together suggested a complex association among three aspects: altered regional FCS, neuropsychological performance indicators, and specific intestinal microbiota. This research is the first, as far as we are aware, to evaluate the relationship between the SPG and the GM profile. Our findings may provide new neuroimaging evidence for MGBA interaction mechanisms in CI.

Functional connectivity strength alteration in the left superior parietal gyrus in chronic insomnia patients

In our study, the FCS value of the left SPG was significantly reduced in the CI group. In patients with primary insomnia, the presence of weakened connectivity between the right SPG and the superior frontal gyrus and other brain regions (44) and between the bilateral superior parietal lobule and superior frontal gyrus (45) was confirmed, supporting our finding of reduced FCS value in the SPG. Previous studies have shown that altered SPG function is complexly correlated with sleep quality and cognitive changes, including mood, memory, and attention (46–50). After sleep restriction, the functional connectivity variability of the SPG and thalamus was reduced and was significantly correlated with insomnia severity (51). This finding is consistent with the significant negative correlation between the reduced FCS values in the left SPG and sleep efficiency in our study. In a recent study, Li et al. (32) found increased DC values in the right post-central gyrus, rolandic operculum, insula, and SPG in CI patients using real-time fMRI neurofeedback. An interventional study by Huang et al. (52) also found that applying 1 Hz low-frequency repetitive transcranial magnetic stimulation of the parietal cortex was practical for the improvement of anxiety and insomnia symptoms in patients with generalized anxiety disorder and insomnia. The findings of the studies mentioned above longitudinally corroborated the relationship between the parietal cortex and insomnia, suggesting that the potential mechanism of the involvement of the SPG in insomnia may be due to the impaired ability of CI patients to regulate top-down attention and several memory processes. While significant differences in DSST or DST assessments between insomnia patients and HCs were not always found in previous studies (53, 54), it is not surprising that our study did not show differences in memory and attention assessments between groups. The differences in sample sizes could contribute to the discordant results. However, taken together, the FCS changes in the CI group and their correlation with sleep efficiency in our study were supported, suggesting that the SPG is somehow involved in sleep regulation and that its functional alteration may be an important neurobiological change in CI patients.

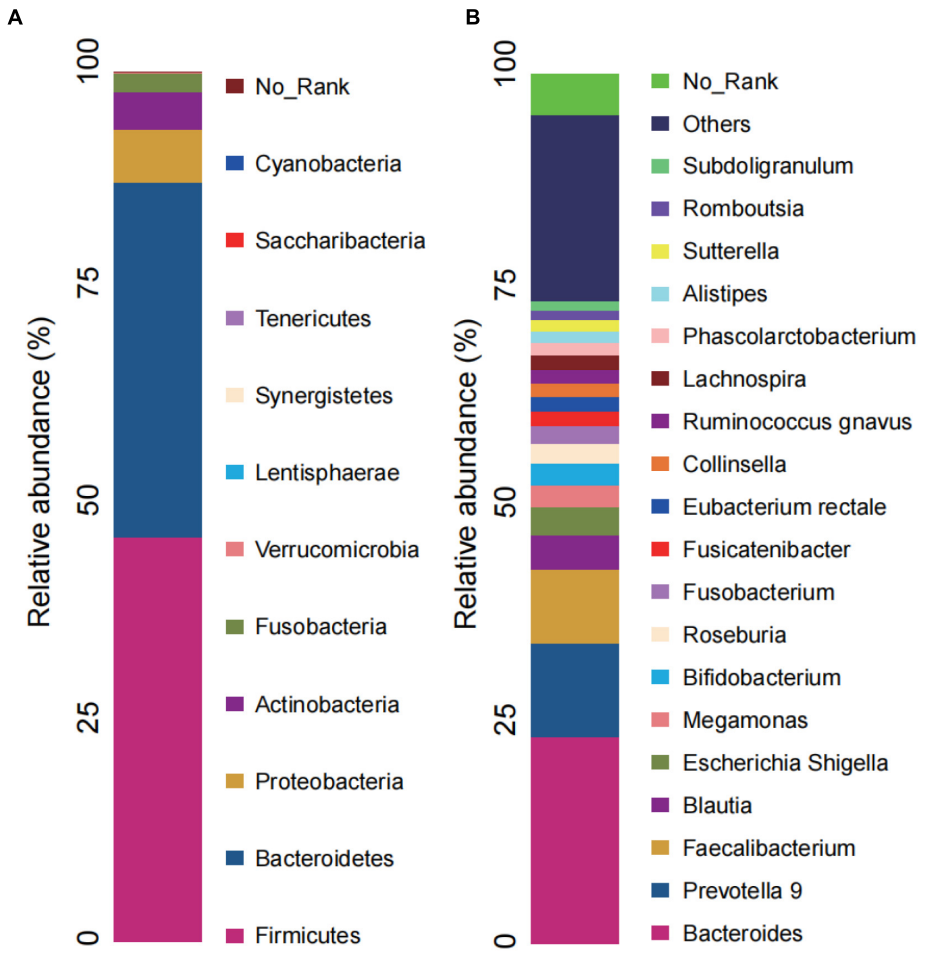

FIGURE 4
Microbial composition in CI. **(A)** Relative abundance bar charts of GM in the CI group at the phylum level. **(B)** Relative abundance bar charts of GM in the CI group at the genus level. GM, gut microbiota; CI, chronic insomnia.

Associations among the gut microbiota, altered functional connectivity strength, and neuropsychological performance indicators

In the present study, Firmicutes and Bacteroidetes were the dominant phyla in the CI group, as supported in other literature (12). The predominant genera in CI patients were Bacteroides, Prevotella 9, Faecalibacterium, and Blautia. The genera above have also been shown to be significantly different between HCs and CI patients (11–13). Therefore, although GM data from the HC group were not collected to assess differences between baseline in our study, the CI group may have dominant bacteria that differ from those of the HC group.

The results of the subsequent CCA and RDA implied that the GM profile was highly correlated with the neuropsychological performance indicators of CI patients, suggesting that neuropsychological performance indicators could explain the GM composition (10). Our study showed results that were similar to those of a previous study (10), and the results of the genus-level CCA provided additional support for the correlation of flora with neuropsychological performance indicators. Follow-up Spearman correlation analysis results showed complicated relationships between the reduced value FCS value of the left SPG and genus-level bacteria. Although the exact mechanism is unknown, to the best of our knowledge, significant correlations between Intestinibacter, Lachnospiraceae_UCG-003, and Faecalicoccus bacteria and left SPG function in CI patients have never been reported before. Interestingly, among the bacteria associated with FCS changes in the SPG, Alloprevotella, specific members of the Lachnospiraceae family, and Faecalicoccus were also correlated with mood assessment or sleep assessment scores after strict FDR correction. This finding indicates that mood and sleep alterations in CI patients may be related to supraparietal gyrus

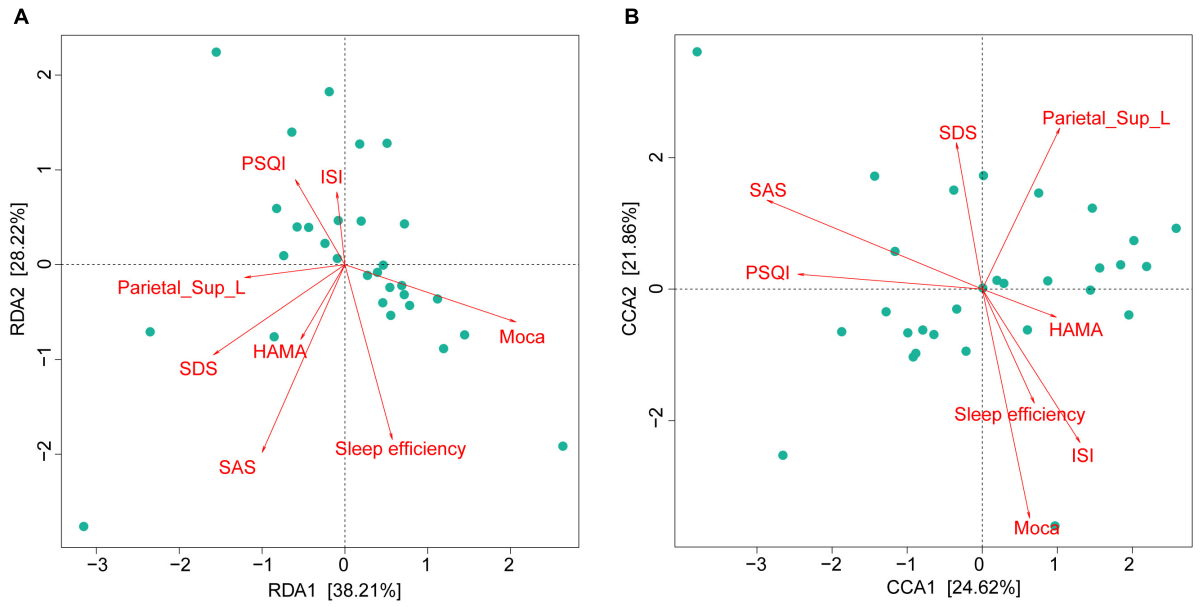

FIGURE 5
Gut microbiota composition strongly associated with neuropsychological performances in CI patients. RDA (at the phylum level) and CCA (at the genus level) demonstrated that 38.21% **(A)** and 24.62% **(B)** of the variance could be interpreted by seven environmental factors (in other words: neuropsychological performances). CI, chronic insomnia; RDA, redundancy analysis; CCA, canonical correspondence analysis.

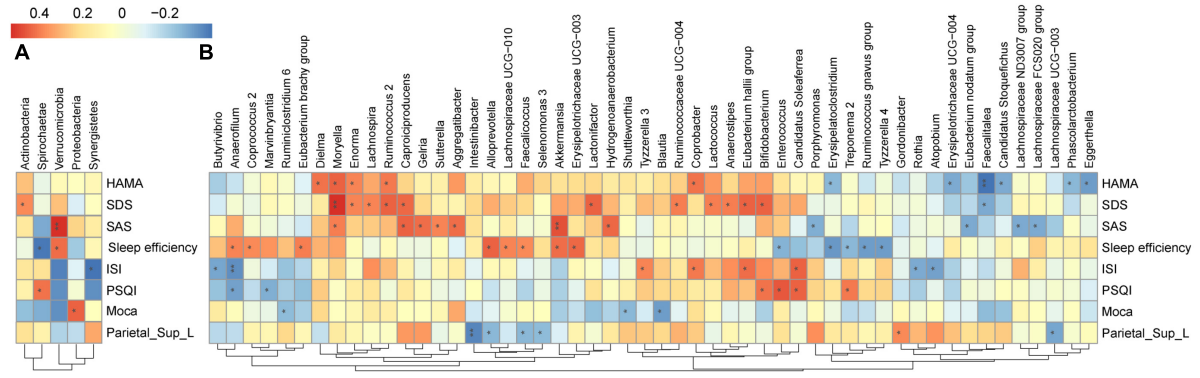

FIGURE 6
Heatmap of the associations between GM and altered brain FCS and neuropsychological performances in CI patients. Heat maps at the phylum level **(A)** and genus level **(B)** demonstrate the correlation coefficients between these variables. Blue, negative correlation; red, positive correlation. *$p < 0.05$, **$p < 0.01$. GM, gut microbiota; FCS, functional connectivity strength; CI, chronic insomnia.

function, and GM composition also might be involved in sleep regulation in some way.

Intestinibacter was found to be correlated with the reduced FCS of the left SPG in CI patients. The latest study found that Intestinibacter was significantly correlated with sleep phenotypes, including chronotype and sleep duration, in different brain aging patterns (55), and another study also found that Intestinibacter was directly related to sleep quality independent of depression severity (14). However, no previous studies have explored the relationship between Intestinibacter and changes in brain function in patients with CI, while our study found an association between Intestinibacter and left SPG function in CI patients. In summary, the present study found that the RA of Intestinibacter was strongly associated with the FCS in the left SPG and that this association was independent of neuropsychological performance, suggesting that Intestinibacter might somehow be involved in the neural mechanisms of altered brain function in insomnia.

Alloprevotella and Lachnospiraceae were also found to be associated with functional alterations of the left SPG in CI patients. Alloprevotella and Lachnospiraceae are closely associated with the production of SCFAs (e.g., significant

positive correlation with metabolic changes in butyrate) (56, 57) and amino acid metabolism (56). SCFAs can penetrate the blood-brain barrier, increase neurogenesis, and improve neuronal homeostasis and function (58). SCFAs are thought to have a wide range of effects on neural and behavioral processes (58) and may mediate the relationship between gut bacteria and the neural mechanisms of sleep (59, 60). For example, butyrate, according to the neurochemical basis of the hypersomnia-hyperarousal theory (61), is a source of sleep- and wakefulness-related signals. Increasing butyrate by using GABA-rich fermented milk or other means can increase non-rapid eye movement sleep and affect sleep duration and sleep onset latency in mice (62). Therefore, we hypothesized that Alloprevotella and Lachnospiraceae bacteria could affect brain function in CI patients by modulating SCFA production. In addition, our study found that some members of the Lachnospiraceae family were significantly associated with both mood assessment and sleep assessment scores in the CI group. Several previous studies have also implied the interaction of specific Lachnospiraceae family members with sleep deprivation, sleep fragmentation, and insomnia severity (11, 63–65). The abovementioned findings suggest that Alloprevotella and Lachnospiraceae may be involved in the MGBA through SCFA metabolism, affecting insomnia performance and mood changes.

The results of the correlation analysis also showed a correlation between FCS changes in the SPG and the genera Faecalicoccus/Faecalitalea, which are all members of the family Erysipelotrichaceae. Several studies have shown that Erysipelotrichaceae is associated with not only sleep (15, 66) but also organismal metabolism, such as lipid metabolism, in humans and rodents (67–69). Sleep loss (including sleep restriction, sleep deprivation, and sleep disruption) triggers GM-related abnormalities in organismal metabolism (64, 70), for example, sleep deprivation may be an important step in oxidative stress and adenosine triphosphate depletion (71), which Erysipelotrichaceae is associated with (72). There have also been studies showing that Erysipelotrichaceae can influence neurological inflammation. Autoimmune encephalomyelitis enhances the response of T helper 17 cells in the gut (73, 74). In addition, the RA of Erysipelotrichaceae has been associated with impaired cognitive function due to other diseases (75) like spatial memory performance before and after treatment in patients with phenylketonuria (73). The aforementioned studies provided support for those of our study, in which the genus Faecalicoccus of the family Erysipelotrichaceae was positively correlated with sleep efficiency and the genus Faecalitalea was negatively correlated with SDS. On the basis of these results combined with the results of our study, we speculate that Erysipelotrichaceae family members communicate with the parietal gyrus through the endocrine metabolic and inflammatory stress pathways of the MGBA, which may be the underlying neurobiological basis for altered cognitive functions such as mood changes in CI patients.

Thus, the complex relationships that exist among GM, including Alloprevotella, Lachnospiraceae, and Faecalicoccus; FCS changes in the left SPG; and neuropsychological performance indicators in CI patients may represent a way in which the GM communicates with local brain regions through SCFA metabolism and inflammatory stress pathways and further affects patients' neuropsychological performance.

Limitations

Nevertheless, there are several limitations of our work. First, this was a cross-sectional study. Therefore, a longitudinal study is needed to determine whether therapeutic interventions affect stool microbiota structure in CI patients or, conversely, whether specific interventions such as microbiota transplantation or probiotic therapies can improve the brain function and symptoms of insomnia patients. Second, we were unable to control for all possible confounders that may affect GM composition. The participants included in this study were all local residents with relatively consistent dietary habits who were advised by the researchers to eat lightly and avoid a stimulating diet before the experiment. The inclusion and exclusion criteria were closely followed to minimize the effects on the composition of the GM. In addition, 16SrDNA amplicon sequencing was used in this study. Although the results of metagenomic sequencing may be more comprehensive, 16SrDNA amplicon sequencing can ensure the credibility of the results at a lower cost and is widely used in similar types of research. Moreover, we did not evaluate the baseline difference in GM composition between the groups, as performed in other studies (10, 13). However, to avoid important omissions, we performed RDA and CCA to analyze the correlation between environmental factors (neuropsychological performance indicators) and the microbial community (GM composition), as reported in the previous literature. We also performed a correlation analysis of FCS value in the abnormal brain region and the GM profile in CI patients to explore in detail the potential relationship among brain function changes, GM composition, and neuropsychological performance in CI. Finally, the FCS method calculated by degree centrality was used to explore the abnormal brain areas in CI patients without combining this method with brain structural methods based on 3D-T1WI, DTI, etc. However, our team has explored brain structural alterations and the mechanism of CI in the past (53, 76, 77). In the future, we will further explore the complex mechanism of the interaction between brain functional and structural alterations and the GM in CI patients to screen for more accurate imaging biomarkers for MGBA interaction mechanisms.

Conclusion

In conclusion, we found a complex association between specific GM composition, FCS abnormalities (left SPG), and neuropsychological performance indicators in patients with CI. Notably, to the best of our knowledge, this research showed a link between left SPG functional alterations and specific GM profile in patients with CI, which has not previously been reported. Alloprevotella, several members of the Lachnospiraceae family, and Faecalicoccus were significantly correlated or trended toward correlating with altered SPG function and neuropsychological performance indicators. These findings have substantial implications for screening new GM-neuroimaging markers for the study of neural mechanisms of CI and exploring potential future intervention targets for its treatment.

Data availability statement

The original contributions presented in the study are publicly available. This data can be found here: https://www.ncbi.nlm.nih.gov/bioproject/PRJNA882369. Further inquiries can be directed to jgh2023@outlook.com.

Ethics statement

The studies involving human participants were reviewed and approved by Ethics Committee of the Guangdong Second Provincial General Hospital. The patients/participants provided their written informed consent to participate in this study. Written informed consent was obtained from the individual(s) for the publication of any potentially identifiable images or data included in this article.

Author contributions

GJ and YF designed the study. ZC and YF coordinated subject enrollment and data collection. ZC performed the analysis, interpreted the data, and wrote the first draft of the manuscript. ZC, KH, SF, and FC assisted in the several procedures of fMRI data preprocessing and FCS calculation. YF, SL, and GJ contributed to the final revision of the manuscript. GJ took full responsibility for this study, including the study design and the decision to publish the manuscript. All authors contributed to the article and approved the submitted version.

Funding

This work was supported by grants from the National Natural Science Foundation of China (Grant Nos. 81901731, U1903120, 81771807, and 81901729).

Acknowledgments

We thank all participants.

Conflict of interest

The authors declare that the research was conducted in the absence of any commercial or financial relationships that could be construed as a potential conflict of interest.

Publisher's note

Supplementary material

The Supplementary Material for this article can be found online at: https://www.frontiersin.org/articles/10.3389/fpsyt.2022.1050403/full#supplementary-material

References

1. American Psychiatric Association [APA]. *Diagnostic and Statistical Manual of Mental Disorders [Internet]*. 5th ed. Washington, DC: American Psychiatric Association (2013).

2. Chung KF, Yeung WF, Ho FYY, Yung KP, Yu YM, Kwok CW. Cross-cultural and comparative epidemiology of insomnia: the diagnostic and statistical manual (DSM), international classification of diseases (ICD) and international classification of sleep disorders (ICSD). *Sleep Med.* (2015) 16:477–82. doi: 10.1016/j.sleep.2014.10.018

3. Sofi F, Cesari F, Casini A, Macchi C, Abbate R, Gensini GF. Insomnia and risk of cardiovascular disease: a meta-analysis. *Eur J Prev Cardiol.* (2014) 21:57–64.

4. Hwang Y, Knobf MT. Sleep health in young women with breast cancer: a narrative review. *Support Care Cancer.* (2022) 30:6419–28.

5. Palagini L, Miniati M, Massa L, Folesani F, Marazziti D, Grassi L, et al. Insomnia and circadian sleep disorders in ovarian cancer: evaluation and management of underestimated modifiable factors potentially contributing to morbidity. *J Sleep Res.* (2022) 31:e13510. doi: 10.1111/jsr.13510

6. Tucker RP, Cramer RJ, Langhinrichsen-Rohling J, Rodriguez-Cue R, Rasmussen S, Oakey-Frost N, et al. Insomnia and suicide risk: a multi-study replication and extension among military and high-risk college student samples. *Sleep Med.* (2021) 85:94–104. doi: 10.1016/j.sleep.2021.06.032

7. Giora E, Galbiati A, Marelli S, Zucconi M, Ferini-Strambi L. Impaired visual processing in patients with insomnia disorder revealed by a dissociation in visual search. *J Sleep Res.* (2017) 26:338–44. doi: 10.1111/jsr.12487

8. Léger D, Massuel MA, Metlaine A. SISYPHE study group. professional correlates of insomnia. *Sleep*. (2006) 29:171–8.

9. Morin CM, Jarrin DC, Ivers H, Mérette C, LeBlanc M, Savard J. Incidence, persistence, and remission rates of insomnia over 5 years. *Jama Netw Open.* (2020) 3:e2018782.

10. Liu B, Lin W, Chen S, Xiang T, Yang Y, Yin Y, et al. Gut microbiota as a subjective measurement for auxiliary diagnosis of insomnia disorder. *Front Microbiol.* (2019) 10:1770. doi: 10.3389/fmicb.2019.01770

11. Masyutina AA, Gumenyuk LN, Fatovenko Y, Sorokina LE, Bayramova SS, Alekseenko A, et al. Changes in gut microbiota composition and their associations with cortisol, melatonin and interleukin 6 in patients with chronic insomnia. *BRSMU.* (2021) 2021:18–24.

12. Zhou J, Wu X, Li Z, Zou Z, Dou S, Li G, et al. Alterations in gut microbiota are correlated with serum metabolites in patients with insomnia disorder. *Front Cell Infect Microbiol.* (2022) 12:722662. doi: 10.3389/fcimb.2022.722662

13. Li Y, Zhang B, Zhou Y, Wang D, Liu X, Li L, et al. Gut microbiota changes and their relationship with inflammation in patients with acute and chronic insomnia. *Nat Sci Sleep.* (2020) 12:895–905.

14. Zhang Q, Yun Y, An H, Zhao W, Ma T, Wang Z, et al. Gut microbiome composition associated with major depressive disorder and sleep quality. *Front Psychiatry.* (2021) 12:645045. doi: 10.3389/fpsyt.2021.645045

15. Benedict C, Vogel H, Jonas W, Woting A, Blaut M, Schuermann A, et al. Gut microbiota and glucometabolic alterations in response to recurrent partial sleep deprivation in normal-weight young individuals. *Mol Metab.* (2016) 5:1175–86. doi: 10.1016/j.molmet.2016.10.003

16. Heijtz RD, Wang S, Anuar F, Qian Y, Björkholm B, Samuelsson A, et al. Normal gut microbiota modulates brain development and behavior. *Proc Natl Acad Sci USA.* (2011) 108:3047–52.

17. Mayer EA, Knight R, Mazmanian SK, Cryan JF, Tillisch K. Gut microbes and the brain: paradigm shift in neuroscience. *J Neurosci.* (2014) 34:15490–6.

18. Smith PA. The tantalizing links between gut microbes and the brain. *Nature.* (2015) 526:312–4. doi: 10.1038/526312a

19. Jenkins T, Nguyen J, Polglaze K, Bertrand P. Influence of tryptophan and serotonin on mood and cognition with a possible role of the gut-brain axis. *Nutrients.* (2016) 8:56. doi: 10.3390/nu8010056

20. Cryan JF, O'Riordan KJ, Cowan CSM, Sandhu KV, Bastiaanssen TFS, Boehme M, et al. The microbiota-gut-brain axis. *Physiol Rev.* (2019) 99:1877–2013. doi: 10.17116/jnevro202212210157

21. Fasiello E, Gorgoni M, Scarpelli S, Alfonsi V, Strambi LF, De Gennaro L. Functional connectivity changes in insomnia disorder: a systematic review. *Sleep Med Rev.* (2022) 61:101569. doi: 10.1016/j.smrv.2021.101569

22. Montoro RA, Singh AP, Yu JPJ. Structural and functional neuroimaging of the effects of the gut microbiome. *Eur Radiol.* (2022) 32:3683–92.

23. Kohn N, Szopinska-Tokov J, Arenas AL, Beckmann CF, Arias-Vasquez A, Aarts E. Multivariate associative patterns between the gut microbiota and large-scale brain network connectivity. *Gut Microbes.* (2021) 13:2006586. doi: 10.1080/19490976.2021.2006586

24. Zhu J, Wang C, Qian Y, Cai H, Zhang S, Zhang C, et al. Multimodal neuroimaging fusion biomarkers mediate the association between gut microbiota and cognition. *Prog Neuro-Psychopharmacol Biol Psychiatry.* (2022) 113:110468. doi: 10.1016/j.pnpbp.2021.110468

25. Li S, Song J, Ke P, Kong L, Lei B, Zhou J, et al. The gut microbiome is associated with brain structure and function in schizophrenia. *Sci Rep.* (2021) 11:9743.

26. De Santis S, Moratal D, Canals S. Radiomicrobiomics: advancing along the gut-brain axis through big data analysis. *Neuroscience.* (2019) 403:145–9. doi: 10.1016/j.neuroscience.2017.11.055

27. Liu P, Jia XZ, Chen Y, Yu Y, Zhang K, Lin YJ, et al. Gut microbiota interacts with intrinsic brain activity of patients with amnestic mild cognitive impairment. *CNS Neurosci Ther.* (2021) 27:163–73. doi: 10.1111/cns.13451

28. Yan CQ, Huo JW, Wang X, Zhou P, Zhang YN, Li J. Different degree centrality changes in the brain after acupuncture on contralateral or ipsilateral acupoint in patients with chronic shoulder pain: a resting-state fmri study. *Neural Plast.* (2020) 2020:1–11.

29. Yan CQ, Wang X, Huo JW, Zhou P, Li JL, Wang ZY, et al. Abnormal global brain functional connectivity in primary insomnia patients: a resting-state functional mri study. *Front Neurol.* (2018) 9:856. doi: 10.3389/fneur.2018.00856

30. Tomasi D, Shokri-Kojori E, Volkow ND. High-resolution functional connectivity density: hub locations, sensitivity, specificity, reproducibility, and reliability. *Cereb Cortex.* (2016) 26:3249–59. doi: 10.1093/cercor/bhv171

31. Zuo XN, Ehmke R, Mennes M, Imperati D, Castellanos FX, Sporns O, et al. Network centrality in the human functional connectome. *Cereb Cortex.* (2012) 22:1862–75.

32. Li X, Li Z, Zou Z, Wu X, Gao H, Wang C, et al. Real-time fmri neurofeedback training changes brain degree centrality and improves sleep in chronic insomnia disorder: a resting-state fmri study. *Front Mol Neurosci.* (2022) 15:825286. doi: 10.3389/fnmol.2022.825286

33. Liu X, Zheng J, Liu BX, Dai XJ. Altered connection properties of important network hubs may be neural risk factors for individuals with primary insomnia. *Sci Rep.* (2018) 8:5891. doi: 10.1038/s41598-018-23699-3

34. Huang S, Zhou F, Jiang J, Huang M, Zeng X, Ding S, et al. Regional impairment of intrinsic functional connectivity strength in patients with chronic primary insomnia. *Neuropsych Dis Treat.* (2017) 13:1449–62. doi: 10.2147/NDT.S137292

35. Li C, Mai Y, Dong M, Yin Y, Hua K, Fu S, et al. Multivariate pattern classification of primary insomnia using three types of functional connectivity features. *Front Neurol.* (2019) 10:1037. doi: 10.3389/fneur.2019.01037

36. Zuo XN, Xing XX. Test-retest reliabilities of resting-state fmri measurements in human brain functional connectomics: a systems neuroscience perspective. *Neurosci Biobehav Rev.* (2014) 45:100–18. doi: 10.1016/j.neubiorev.2014.05.009

37. Magoc T, Salzberg SL. Flash: fast length adjustment of short reads to improve genome assemblies. *Bioinformatics.* (2011) 27:2957–63. doi: 10.1093/bioinformatics/btr507

38. Edgar RC, Haas BJ, Clemente JC, Quince C, Knight R. Uchime improves sensitivity and speed of chimera detection. *Bioinformatics.* (2011) 27:2194–200. doi: 10.1093/bioinformatics/btr381

39. Wang Q, Garrity GM, Tiedje JM, Cole JR. Naïve bayesian classifier for rapid assignment of rRNA sequences into the new bacterial taxonomy. *Appl Environ Microb.* (2007) 73:5261–7. doi: 10.1128/AEM.00062-07

40. Bu X, Hu X, Zhang L, Li B, Zhou M, Lu L, et al. Investigating the predictive value of different resting-state functional mri parameters in obsessive-compulsive disorder. *Transl Psychiatry.* (2019) 9:17. doi: 10.1038/s41398-018-0362-9

41. Zhou FQ, Tan YM, Wu L, Zhuang Y, He LC, Gong HH. Intrinsic functional plasticity of the sensory-motor network in patients with cervical spondylotic myelopathy. *Sci Rep.* (2015) 5:9975.

42. Li W, Xie K, Ngetich RK, Zhang J, Jin Z, Li L. Inferior frontal gyrus-based resting-state functional connectivity and medium dispositional use of reappraisal strategy. *Front Neurosci.* (2021) 15:681859. doi: 10.3389/fnins.2021.681859

43. Benjamini Y, Hochberg Y. Controlling the false discovery rate - a practical and powerful approach to multiple testing. *J R Stat Soc B.* (1995) 57:289–300.

44. Li S, Tian J, Li M, Wang T, Lin C, Yin Y, et al. Altered resting state connectivity in right side frontoparietal network in primary insomnia patients. *Eur Radiol.* (2018) 28:664–72. doi: 10.1007/s00330-017-5012-8

45. Li Y, Wang E, Zhang H, Dou S, Liu L, Tong L, et al. Functional connectivity changes between parietal and prefrontal cortices in primary insomnia patients: evidence from resting-state fmri. *Eur J Med Res.* (2014) 19:32. doi: 10.1186/2047-783X-19-32

46. Fischer M, Moscovitch M, Alain C. A systematic review and meta-analysis of memory-guided attention: frontal and parietal activation suggests involvement of fronto-parietal networks. *Wiley Interdiscip Rev Cogn Sci.* (2021) 12:e1546. doi: 10.1002/wcs.1546

47. Koenigs M, Barbey AK, Postle BR, Grafman J. Superior parietal cortex is critical for the manipulation of information in working memory. *J Neurosci.* (2009) 29:14980–6.

48. Rohr CS, Vinette SA, Parsons KAL, Cho IYK, Dimond D, Benischek A, et al. Functional connectivity of the dorsal attention network predicts selective attention in 4-7 year-old girls. *Cereb Cortex.* (2017) 27:4350–60. doi: 10.1093/cercor/bhw236

49. Wolpert DM, Goodbody SJ, Husain M. Maintaining internal representations: the role of the human superior parietal lobe. *Nat Neurosci.* (1998) 1:529–33. doi: 10.1038/2245

50. Zimmermann J, Ross B, Moscovitch M, Alain C. Neural dynamics supporting auditory long-term memory effects on target detection. *Neuroimage.* (2020) 218:116979.

51. Long Z, Zhao J, Chen D, Lei X. Age-related abnormalities of thalamic shape and dynamic functional connectivity after three hours of sleep restriction. *PeerJ.* (2021) 9:e10751. doi: 10.7717/peerj.10751

52. Huang Z, Li Y, Bianchi MT, Zhan S, Jiang F, Li N, et al. Repetitive transcranial magnetic stimulation of the right parietal cortex for comorbid generalized anxiety disorder and insomnia: a randomized, double-blind, sham-controlled pilot study. *Brain Stimul.* (2018) 11:1103–9. doi: 10.1016/j.brs.2018.05.016

53. Li S, Wang BA, Li C, Feng Y, Li M, Wang T, et al. Progressive gray matter hypertrophy with severity stages of insomnia disorder and its relevance for mood symptoms. *Eur Radiol.* (2021) 31:6312–22. doi: 10.1007/s00330-021-07701-7

54. Joo EY, Noh HJ, Kim JS, Koo DL, Kim D, Hwang KJ, et al. Brain gray matter deficits in patients with chronic primary insomnia. *Sleep.* (2013) 36:999–1007. doi: 10.5665/sleep.2796

55. Zhang H, Liu L, Cheng S, Jia Y, Wen Y, Yang X, et al. Assessing the joint effects of brain aging and gut microbiota on the risks of psychiatric disorders. *Brain Imaging Behav.* (2022) 16:1504–15. doi: 10.1007/s11682-022-00630-z

56. Chen H, Zhang F, Zhang J, Zhang X, Guo Y, Yao Q. A holistic view of berberine inhibiting intestinal carcinogenesis in conventional mice based on microbiome-metabolomics analysis. *Front Immunol.* (2020) 11:588079. doi: 10.3389/fimmu.2020.588079

57. Meehan CJ, Beiko RG. A phylogenomic view of ecological specialization in the lachnospiraceae, a family of digestive tract-associated bacteria. *Genome Biol Evol.* (2014) 6:703–13. doi: 10.1093/gbe/evu050

58. Magzal F, Even C, Haimov I, Agmon M, Asraf K, Shochat T, et al. Associations between fecal short-chain fatty acids and sleep continuity in older adults with insomnia symptoms. *Sci Rep*. (2021) 11:4052.

59. Szentirmai É, Millican NS, Massie AR, Kapás L. Butyrate, a metabolite of intestinal bacteria, enhances sleep. *Sci Rep.* (2019) 9:7035. doi: 10.1038/s41598-019-43502-1

60. Heath ALM, Haszard JJ, Galland BC, Lawley B, Rehrer NJ, Drummond LN, et al. Association between the faecal short-chain fatty acid propionate and infant sleep. *Eur J Clin Nutr.* (2020) 74:1362–5. doi: 10.1038/s41430-019-0556-0

61. Plante DT, Jensen JE, Schoerning L, Winkelman JW. Reduced gamma-aminobutyric acid in occipital and anterior cingulate cortices in primary insomnia: a link to major depressive disorder? *Neuropsychopharmacology.* (2012) 37:1548–57. doi: 10.1038/npp.2012.4

62. Yu L, Han X, Cen S, Duan H, Feng S, Xue Y, et al. Beneficial effect of GABA-rich fermented milk on insomnia involving regulation of gut microbiota. *Microbiol Res.* (2020) 233:126409. doi: 10.1016/j.micres.2020.126409

63. El Aidy S, Bolsius YG, Raven F, Havekes R. A brief period of sleep deprivation leads to subtle changes in mouse gut microbiota. *J Sleep Res.* (2020) 29:e12920. doi: 10.1111/jsr.12920

64. Poroyko VA, Carreras A, Khalyfa A, Khalyfa AA, Leone V, Peris E, et al. Chronic sleep disruption alters gut microbiota, induces systemic and adipose tissue inflammation and insulin resistance in mice. *Sci Rep.* (2016) 6:35405. doi: 10.1038/srep35405

65. Tang Q, Xiong J, Wang J, Cao Z, Liao S, Xiao Y, et al. Queen bee larva consumption improves sleep disorder and regulates gut microbiota in mice with pcpa-induced insomnia. *Food Biosci.* (2021) 43:101256.

66. Carmen Collado M, Katila MK, Vuorela NM, Saarenpaa-Heikkila O, Salminen S, Isolauri E. Dysbiosis in snoring children: an interlink to comorbidities? *J Pediatr Gastr Nutr.* (2019) 68:272–7. doi: 10.1097/MPG.0000000000002161

67. Zhang C, Zhang M, Wang S, Han R, Cao Y, Hua W, et al. Interactions between gut microbiota, host genetics and diet relevant to development of metabolic syndromes in mice. *ISME J.* (2010) 4:232–41.

68. Spencer MD, Hamp TJ, Reid RW, Fischer LM, Zeisel SH, Fodor AA. Association between composition of the human gastrointestinal microbiome and development of fatty liver with choline deficiency. *Gastroenterology.* (2011) 140:976–86. doi: 10.1053/j.gastro.2010.11.049

69. Martínez I, Perdicaro DJ, Brown AW, Hammons S, Carden TJ, Carr TP, et al. Diet-induced alterations of host cholesterol metabolism are likely to affect the gut microbiota composition in hamsters. *Appl Environ Microb.* (2013) 79:516–24. doi: 10.1128/AEM.03046-12

70. Park YS, Kim SH, Park JW, Kho Y, Seok PR, Shin JH, et al. Melatonin in the colon modulates intestinal microbiota in response to stress and sleep deprivation. *Intest Res.* (2020) 18:325–36. doi: 10.5217/ir.2019.00093

71. Trivedi MS, Holger D, Bui AT, Craddock TJA, Tartar JL. Short-term sleep deprivation leads to decreased systemic redox metabolites and altered epigenetic status. *PLoS One.* (2017) 12:e0181978. doi: 10.1371/journal.pone.0181978

72. Cedernaes J, Schiöth HB, Benedict C. Determinants of shortened, disrupted, and mistimed sleep and associated metabolic health consequences in healthy humans. *Diabetes.* (2015) 64:1073–80. doi: 10.2337/db14-1475

73. van der Goot E, Vink SN, van Vliet D, van Spronsen FJ, Falcao Salles J, van der Zee EA. Gut-microbiome composition in response to phenylketonuria depends on dietary phenylalanine in BTBR pah(enu2) mice. *Front Nutr.* (2022) 8:735366. doi: 10.3389/fnut.2021.735366

74. Miyauchi E, Kim SW, Suda W, Kawasumi M, Onawa S, Taguchi-Atarashi N, et al. Gut microorganisms act together to exacerbate inflammation in spinal cords. *Nature.* (2020) 585:102–6. doi: 10.1038/s41586-020-2634-9

75. Sanguinetti E, Collado MC, Marrachelli VG, Monleon D, Selma-Royo M, Pardo-Tendero MM, et al. Microbiome-metabolome signatures in mice genetically prone to develop dementia, fed a normal or fatty diet. *Sci Rep.* (2018) 8:4907.

76. Li S, Tian J, Bauer A, Huang R, Wen H, Li M, et al. Reduced integrity of right lateralized white matter in patients with primary insomnia: a diffusion-tensor imaging study. *Radiology.* (2016) 280:520–8. doi: 10.1148/radiol.2016152038

77. Wu Y, Zhou Z, Fu S, Zeng S, Ma X, Fang J, et al. Abnormal rich club organization of structural network as a neuroimaging feature in relation with the severity of primary insomnia. *Front Psychiatry.* (2020) 11:308. doi: 10.3389/fpsyt.2020.00308

frontiers | Frontiers in Psychiatry

TYPE Original Research
PUBLISHED 05 May 2023
DOI 10.3389/fpsyt.2023.1058721

OPEN ACCESS

EDITED BY
Stefan Borgwardt,
University of Lübeck, Germany

REVIEWED BY
Axel Steiger,
Ludwig Maximilian University of Munich, Germany
Taous Meriem Laleg,
King Abdullah University of Science and Technology, Saudi Arabia

*CORRESPONDENCE
Changwei W. Wu
✉ sleepbrain@tmu.edu.tw
Chi-Wen Cristina Huang
✉ Cth.mail05@gmail.com

RECEIVED 30 September 2022
ACCEPTED 18 April 2023
PUBLISHED 05 May 2023

CITATION
Hsu A-L, Li M-K, Kung Y-C, Wang ZJ, Lee H-C, Li C-W, Huang C-WC and Wu CW (2023) Temporal consistency of neurovascular components on awakening: preliminary evidence from electroencephalography, cerebrovascular reactivity, and functional magnetic resonance imaging.
Front. Psychiatry 14:1058721.
doi: 10.3389/fpsyt.2023.1058721

Temporal consistency of neurovascular components on awakening: preliminary evidence from electroencephalography, cerebrovascular reactivity, and functional magnetic resonance imaging

Ai-Ling Hsu[1,2], Ming-Kang Li[1], Yi-Chia Kung[3], Zhitong John Wang[4], Hsin-Chien Lee[5,6], Chia-Wei Li[7], Chi-Wen Cristina Huang[7]* and Changwei W. Wu[4,6,8]*

[1]Bachelor Program in Artificial Intelligence, Chang Gung University, Taoyuan, Taiwan, [2]Department of Psychiatry, Chang Gung Memorial Hospital at Linkou, Taoyuan, Taiwan, [3]Department of Radiology, Tri-Service General Hospital, Taipei, Taiwan, [4]Graduate Institute of Mind, Brain and Consciousness, Taipei Medical University, Taipei, Taiwan, [5]Department of Psychiatry, School of Medicine, College of Medicine, Taipei Medical University, Taipei, Taiwan, [6]Research Center of Sleep Medicine, Taipei Medical University Hospital, Taipei, Taiwan, [7]Department of Radiology, Wan Fang Hospital, Taipei Medical University, Taipei, Taiwan, [8]Brain and Consciousness Research Center, Taipei Medical University-Shuang Ho Hospital, New Taipei, Taiwan

Sleep inertia (SI) is a time period during the transition from sleep to wakefulness wherein individuals perceive low vigilance with cognitive impairments; SI is generally identified by longer reaction times (RTs) in attention tasks immediately after awakening followed by a gradual RT reduction along with waking time. The sluggish recovery of vigilance in SI involves a dynamic process of brain functions, as evidenced in recent functional magnetic resonance imaging (fMRI) studies in within-network and between-network connectivity. However, these fMRI findings were generally based on the presumption of unchanged neurovascular coupling (NVC) before and after sleep, which remains an uncertain factor to be investigated. Therefore, we recruited 12 young participants to perform a psychomotor vigilance task (PVT) and a breath-hold task of cerebrovascular reactivity (CVR) before sleep and thrice after awakening (A1, A2, and A3, with 20min intervals in between) using simultaneous electroencephalography (EEG)-fMRI recordings. If the NVC were to hold in SI, we hypothesized that time-varying consistencies could be found between the fMRI response and EEG beta power, but not in neuron-irrelevant CVR. Results showed that the reduced accuracy and increased RT in the PVT upon awakening was consistent with the temporal patterns of the PVT-induced fMRI responses (thalamus, insula, and primary motor cortex) and the EEG beta power (Pz and CP1). The neuron-irrelevant CVR did not show the same time-varying pattern among the brain regions associated with PVT. Our findings imply that the temporal dynamics of fMRI indices upon awakening are dominated by neural activities. This is the first study to explore the temporal consistencies of neurovascular components on awakening, and the discovery provides a neurophysiological basis for further neuroimaging studies regarding SI.

KEYWORDS

sleep, sleep inertia, simultaneous EEG-fMRI, psychomotor vigilance task, cerebrovascular reactivity, neurovascular coupling, EEG power

Introduction

Every morning, upon opening our eyes in bed, we experience a certain period of time perceiving hypovigilance, cognitive impairments, and disoriented behavior; this phenomenon is termed as "sleep inertia" (SI). The difficulty of returning to vigilance may occur every day because the transition from sleep to wakefulness is never an on/off quick switch but is rather a sluggish dynamic process. A typical demonstration of hypovigilance in SI is through repeated observations of the slow, as compared to their presleep conditions, reaction time (RT) soon after awakening [usually using a psychomotor vigilance task (PVT) or auditory RT task] (1, 2). In general, the postsleep cognitive deficit recovers gradually as time passes until we feel rejuvenated with full control following a long sleep. SI can last roughly a few to thirty minutes (2–4), and such short-term hypovigilance period can be further lengthened among the participants with prior sleep deprivation, patients with obstructive sleep apnea, or those with narcolepsy (5, 6). In other words, the SI period involves a time-varying transition that alters an individual's mental status from a sleeping unconscious state to an alert conscious state, depending on their neurophysiological conditions. The underlying brain-rebooting procedure of regaining cognitive performances, or even the consciousness, has attracted a series of neuroscience studies on SI. Previous studies have shown that immediately upon awakening, the sleep-like electroencephalography (EEG) features are prominent in SI, such as the persistent theta power (associated with deep sleep) and decreased beta (β) power (associated with wakefulness) (7, 8). EEG analyses have also presented an anterior-to-posterior spatial mismatch with prominent delta/theta power in the parieto-occipital lobe, indicating the carryover effect of sleep neurophysiology during SI. Nevertheless, the EEG studies are limited to delineating the spatial information of brain reorganizations in the post-awakening period.

For spatially localizing brain functionality in SI, Balkin et al., using $H_2{}^{15}O$ positron emission tomography, studied the rapid recovery of cerebral blood flow (CBF) in the thalamus and a gradual CBF recovery in the anterior cortical regions (9), indicating post-awakening hemodynamic re-establishment. Based on similar hemodynamic perspectives, recent studies using functional magnetic resonance imaging (fMRI), in conjunction with EEG or polysomnography, have presented asynchronous brain-network reorganizations during SI. Our group first demonstrated that the functional connectivity pattern of the sensorimotor network (SMN) in the SI period after nocturnal sleep seemed disconnected, as if it remained disrupted in non-rapid eye movement (NREM) sleep, whereas the default-mode network (DMN) showed an intact connectivity pattern with quick recovery (10, 11). Probing the nap inertia after partial sleep deprivation, Vallat et al. demonstrated a distinction in between-network recovery between the participants awakened from deep sleep (NREM sleep stage 3, N3) and those awakened from light sleep (NREM sleep stage 2, N2) (12). On the basis of simultaneous EEG-fMRI recordings, Chen et al. showed that the strong correlation between the EEG vigilance index and fMRI frontoparietal network activity before sleep disappeared within the 5 min SI period after a 2 h nocturnal sleep (13). These neuroimaging studies indeed paved the way for new strategies to probe brain functional reorganization upon awakening from various neurophysiological angles (CBF, within-network connectivity, between-network connectivity, and EEG-fMRI associations).

After reading the slow recovery of brain functionality in the SI period, we found two obstacles impeded linking of these novel SI neuroimaging findings to the transient cognitive impairments. First, all the fMRI findings were based on the functional hyperemia or blood oxygenation level dependent (BOLD) principle (14, 15), which is an indirect measure of neural activities, and the spontaneous activities in the resting-state fMRI are also observed under the same BOLD assumptions. Considering the fMRI findings as the evidence of underlying neural activity can only be trusted when confirmed through neurovascular coupling (NVC) (16). However, our previous investigations revealed inconsistent dynamic changes between EEG (surrogate of neuron-related local field potential, LFP) and fMRI (neuron-related hemodynamic outcome based on BOLD principle) across NREM sleep stages, implying the neurovascular coupling during sleep may not be as static as that during the wakefulness (17). Thus, whether the assumption of static NVC holds in SI remains an open question. Second, the neuroimaging findings to date regarding SI have all been based on the brain connectivity in a "resting state" instead of involving cognitive engagements, which means that these findings cannot intuitively reflect cognitive performances in the SI period. Therefore, we aimed to solve these two difficulties regarding further SI investigations on brain reorganizations in this study.

Theoretically, NVC was affected by many microscopic factors such as adenosine, nitric oxide, lactate, etc. (18, 19); however, the quantification of these microscopic factors in the human brain is an arduous task. To evaluate the NVC assumption in SI from the neuroimaging perspective, we turned to evaluate the macroscopic brain signals from multi-modal neuroimaging methods through independent measures of EEG and BOLD-fMRI response. Meanwhile, we attempted to use the breath-hold task for inducing hypercapnia, termed as cerebrovascular reactivity (CVR, surrogate of pure hemodynamic response irrelevant to neural activity), immediately upon awakening from sleep (20, 21). Here the breath-hold CVR is regarded as an approach to probe the hemodynamic response function (HRF) irrelevant to the neural activities along the SI period. We hypothesize that the CVR pattern would remain the same across multiple measures between presleep and SI periods, indicating an unchanged NVC. Regarding cognitive associations, we had participants perform a modified PVT in order to measure vigilance in the SI period after nocturnal sleep, leveraging the technical advances of simultaneous EEG-fMRI recordings. Figure 1 delineates the concept of neurophysiology and experimental design in this study.

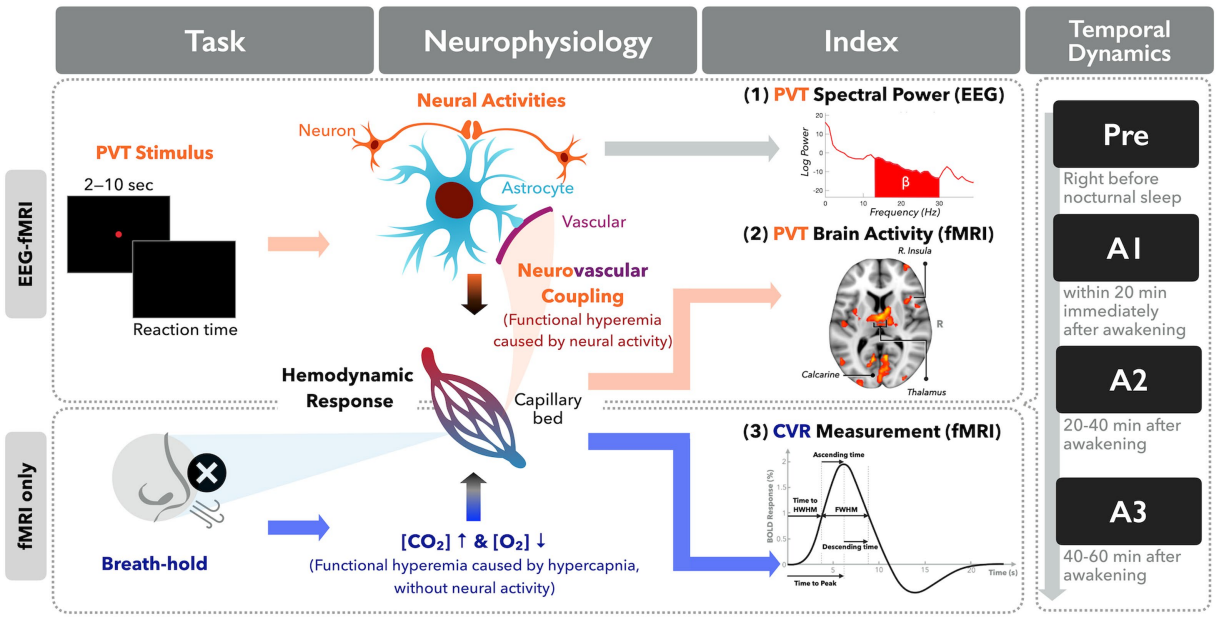

FIGURE 1
Diagram illustration of the neurophysiological concept underlying neuroimaging indices in this study.

Materials and methods

Study participants

Fifteen adults aged between 20 and 40 years participated in this study and maintained consistent sleep–wake patterns for at least 3 days preceding the MRI scan. Their wake-sleep rhythms were monitored through wrist actigraphy (SOMNOwatchTM plus, SOMNOmedics GmbH, Randersacker, Germany). All participants self-reported to have ability to undergo EEG-fMRI scanning without history of neurological, or psychiatric diseases. Neither alcohol nor caffeinated products were allowed on the scanning day. The Pittsburgh Sleep Quality Index (PSQI) was administered to all participants to assess their sleep quality and disturbances over a 1-month period. All study procedures were approved by the Research Ethics Committee of National Taiwan University (Approval No. 201512ES054). Informed consent was obtained from all participants included in the study.

Experimental design

The participants were instructed to lie supine in the MRI scanner. Following a 5 min anatomical scan, participants were required to perform four 20 min experimental sessions during SI. Considering that the duration of SI has been reported to be 15 to 30 min upon awakening (4, 5), the four sessions were designed to include one presleep (Pre) session as the baseline, and three post-awake (A1, A2, and A3) sessions. Specifically, the presleep session was set to 20 min before the averaged bedtime over the past week, and the first post-awake session was conducted after the maximum duration of 180 min of sleep. Each 20 min experimental session consisted of a 5 min resting state (RS), 6 min PVT, and 4 min CVR scan. The RS fMRI data were designed for other purposes beyond the scope of this work; thus, they are not reported here.

We designed a PVT task with a total of 72 trials in the current study to assess alertness during SI (22, 23). Participants were asked to passively view the visual stimuli and respond with a mouse click as soon as they saw a target. Each target was presented as a red solid circle with a 1 s duration, followed by a white cross fixation with a random time interval of 1 s to 7 s. Regarding the CVR scan at the end of each session, participants were asked to perform breath-hold (BH) tasks based on the instruction presented by visual stimuli to assess their CVR (24). The BH paradigm comprises an initial 6 s natural breathing period, followed by three blocks of alternations between 15 s BH and 45 s natural breathing, ending with a block of 15 s BH and 39 s natural breathing (25). A respiration monitoring device was utilized to confirm the participant's compliance during the CVR scan. Cushions were provided to minimize head motion.

Simultaneous EEG-fMRI recording

The simultaneous EEG-fMRI recordings were conducted for the four 20 min sessions. According to the international 10–20 system, the EEG data were recorded by a 32-channel MRI-compatible system, including two electrooculography (EOG) channels, two electromyography (EMG) channels, and one electrocardiogram (ECG) channel (Brain Products GmbH, Gilching, Germany). For the details setting of EEG recording, please refer to a previous study by Tsai et al. (11). Briefly, the impedances of the reference (FCz) and ground (AFz) channels were kept below 5 kΩ, yet those of other channels were kept below 15 kΩ. The EEG signals were synchronized with the MR trigger and recorded using BrainVision Recorder software (Brain Products) with settings of 5 kHz sampling rate and 0.1 μV voltage resolution. In addition, online filtering was applied with an analog band-pass filter

(0.0159–250 Hz) and a 60 Hz notch filter. In addition, we carried out a three-end synchronization among MRI, EEG recording and task stimulation computers using the Brain Products Trigger Box and the software of E-Prime Extensions for Brain Products. The MR images were acquired by a 3T Tim Trio scanner (Siemens, Erlangen, Germany) with a 12-channel head coil, including a high-resolution T_1-weighted anatomical images obtained using a 3D-MPRAGE sequence (TR/TE/TI = 1900 msec/2.28 msec/900 msec; flip angle = 9°; 176 slices with voxel size of $1 \times 1 \times 1\,mm^3$), and functional scans using a T_2*-weighted gradient-echo echo-planar imaging sequence (TR/TE = 2000 msec/30 msec; flip angle = 77°; 32 slices with 4 mm thickness and no gap; in-plane resolution = $3.44 \times 3.44\ mm^2$). A total of 150, 180, 120 volumes were acquired for RS, PVT, and CVR scans, respectively.

EEG analysis and sleep staging

Recorded EEG data was preprocessed offline using Brain Vision Analyzer 2.1 (Brain Products) and EEGLAB v13.6.5b (26). Analyzer with the average artifact subtraction method was used to remove artifacts induced by MR gradient and ballistocardiogram. In gradient-induced artifact removal, EEG data was up-sampled to 50k Hz. EEG data was then down-sample to 250 Hz to remove ballistocardiogram artifact. Subsequently, EEGLAB was used for the further four preprocess steps, including (1) bandpass filtering the EEG frequencies between 0.1 and 50 Hz, (2) rejecting noisy epochs (single TR per epoch) with the criterion 5 times of standard deviation above the mean of each channel (27), (3) re-referencing each EEG channel to the average over all EEG channels, and (4) utilizing temporal independent component analysis (ICA) to eliminate ICs with the characteristics similar to ECG, EMG, EOG channels. For the sleep staging, technicians scored EEG preprocessed data based on the American Academy of Sleep Medicine criteria (28), which used six EEG channels (F3, F4, C3, C4, O1, O2), two EOG channels, and two EMG channels for every time window with 30 s. After preprocessing, EEG data were epoched 250 milliseconds prior to PVT stimuli onset and 1750 milliseconds after. Power spectral density (PSD) was calculated using the psd_multitaper function in MNE-python (29), and then averaged across all epochs for each participant. The averaged PSD was further decomposed into four canonical frequency bands (delta: 0.5–4.5 Hz, theta: 4.5–7.5 Hz, alpha: 7.5–11.5 Hz, beta: 11.5–30 Hz) to assess the relative power across sessions.

fMRI analysis and behavior indices

The PVT fMRI data were preprocessed using an in-house script based on AFNI (version number: 18.0.25) (30) through motion correction, slice-timing, alignment to the T_1-weighted anatomical image, spatial smoothing with a 6 mm full width at half maximum (FWHM) Gaussian kernel, and spatial normalization into the standard Montreal Neurologic Institute (MNI) space. The first-level analysis was performed using the general linear model with 9 regressors, including one for onset timing of the corresponding 1 s stimuli convolved with the canonical hemodynamic response function, six for motion parameters, the other two for baseline intensity and linear trend. Next, only beta estimates in the presleep session were analyzed with second-level analysis using *3dttest++* to identify the brain regions that were significantly activated across participants. Regarding correction for multiple comparisons, the significant activations were corrected using the AFNI *3dClustSim* method with autocorrelation function (corrected $p < 0.05$), wherein the parameter setting was a combination of an uncorrected threshold of $p < 0.0005$ and an individual cluster size of 46 contiguous voxels. Among significant clusters activated in the presleep session, the three regions of interest (ROIs) that most related to the PVT task were further selected for the ROI analysis. Along with PVT experiments, behavioral indices were measured in terms of accuracy and mean response time (RT). Only hit trials, in which participants responded within 0.95 s, were used to calculate the latter two indices.

The CVR data were preprocessed using IClinfMRI (31) with the default setting and normalized into the MNI space using SPM12 (6685) (The Wellcome Centre for Human Neuroimaging, UCL, London, United Kingdom). Magnitudes of each preprocessed data were then normalized to their voxel-wise baseline signal to yield percent signal change. To estimate the temporal characteristics of CVR upon awakening, the CVR response function was averaged across four blocks from the BH onset (0 s) to the 54th seconds within ROIs selected based on presleep PVT activations. Subsequently, each averaged CVR response function was nonlinearly fitted with a canonical dual-gamma function using Matlab's *lsqcurvefit* function (The MathWorks, Inc., Natick, MA, United States). Accordingly, the fitted curves were used to estimate temporal characteristics, including time-to-half width half maximum of the peak, ascending time, time to peak, FWHM of the peak, and descending time (see Supplementary Figure S1).

Statistical analysis

A nonparametric repeated-measure Friedman test and false discovery rate (FDR)-corrected *post hoc* test were performed using Python (SciPy version 1.9.1) to determine significant differences across four sessions in behavior, EEG, PVT, and CVR indices. The significance level was set as $p < 0.05$.

Results

A total of 15 participants aged between 20 and 31 years (eight females; mean age = 24.9 ± 4.0 years; all obtaining at least a high school degree) completed the EEG-fMRI recording, and three participants had incomplete PVT data. Accordingly, all participants were used in the neuron-irrelevant CVR analysis, but only 12 participants were used for the PVT-induced fMRI and behavior analysis. Supplementary Table S1 shows the demographic and sleep characteristics of each participant. All participants reported at least 20% sleepiness, with their average being 64.3 ± 19.53%. The average PSQI was 4.40 ± 2.77, and total sleep time was 24.97 ± 43.96 min. However, three participants out of twelve, who self-reported being able to sleep inside the scanner with zero total sleep time according to sleep scoring, were further excluded in the EEG analysis.

Compared to an accuracy of 0.97 ± 0.08 in the PVT task before sleep, nonsignificant reduced postsleep accuracies of 0.95 ± 0.16, 0.94 ± 0.14, and 0.95 ± 0.11 were found for A1, A2, and A3, respectively (Supplementary Figure S2). By contrast, nonsignificant increased RTs

in the postsleep sessions (358 ± 66, 363 ± 70, and 356 ± 57 milliseconds for A1, A2, and A3, respectively) were observed; for comparison, the presleep RT was 338 ± 49 milliseconds.

Figure 2A depicts the significant recruitment of brain regions engaged in PVT tasks during the presleep session (corrected $p < 0.05$). The brain regions included the supplementary motor area, anterior/middle cingulate cortex, left primary motor cortex, right superior frontal gyrus, right insula, right superior parietal gyrus, bilateral supramarginal, gyrus and bilateral thalamus. For the ROI analysis, Figure 2B demonstrates that the regional BOLD response (average β values) significantly decreased in the postsleep sessions (FDR-corrected *post hoc* $^*p < 0.05$ and $^{**}p < 0.01$) compared to the presleep session for the bilateral thalamus, left primary motor cortex, and right insula. In addition to the PVT-induced fMRI results, a significant difference was evident in the relative β power measured by the EEG at electrodes of Pz and CP1 (Figure 3). The group means of relative β power in Pz were 0.26 ± 0.12, 0.23 ± 0.06, 0.23 ± 0.10, and 0.18 ± 0.05 for the Pre, A1, A2, and A3 sessions, respectively; those in CP1 were 0.28 ± 0.18, 0.24 ± 0.14, 0.27 ± 0.20, and 0.17 ± 0.04 for the four sessions, respectively. Specifically, in comparing with the presleep session at Pz, the relative β power in A3 was significantly decreased. At both Pz and CP1, the relative β power in A3 was significantly smaller than that in A1.

Regarding the neuron-irrelevant CVR, Table 1 lists the CVR temporal indices across sessions for the three selected ROIs. The Friedman test found that the FWHM within the bilateral thalamus was significant across sessions. The *post hoc* test with FDR correction showed that the FWHM was significantly narrower in A3 than in the presleep session ($p = 0.03$). However, there were nonsignificant *post hoc* differences in the CVR indices within both the left primary motor cortex and right insula across sessions.

Discussion

This is the first attempt using the EEG-fMRI fusion technique to study the neuro-vascular variations during sleep inertia. Because of the difficulty of NVC quantification, we bypassed the complex neurophysiological mechanisms within NVC and targeted on observing the time-varying consistency of separate NVC

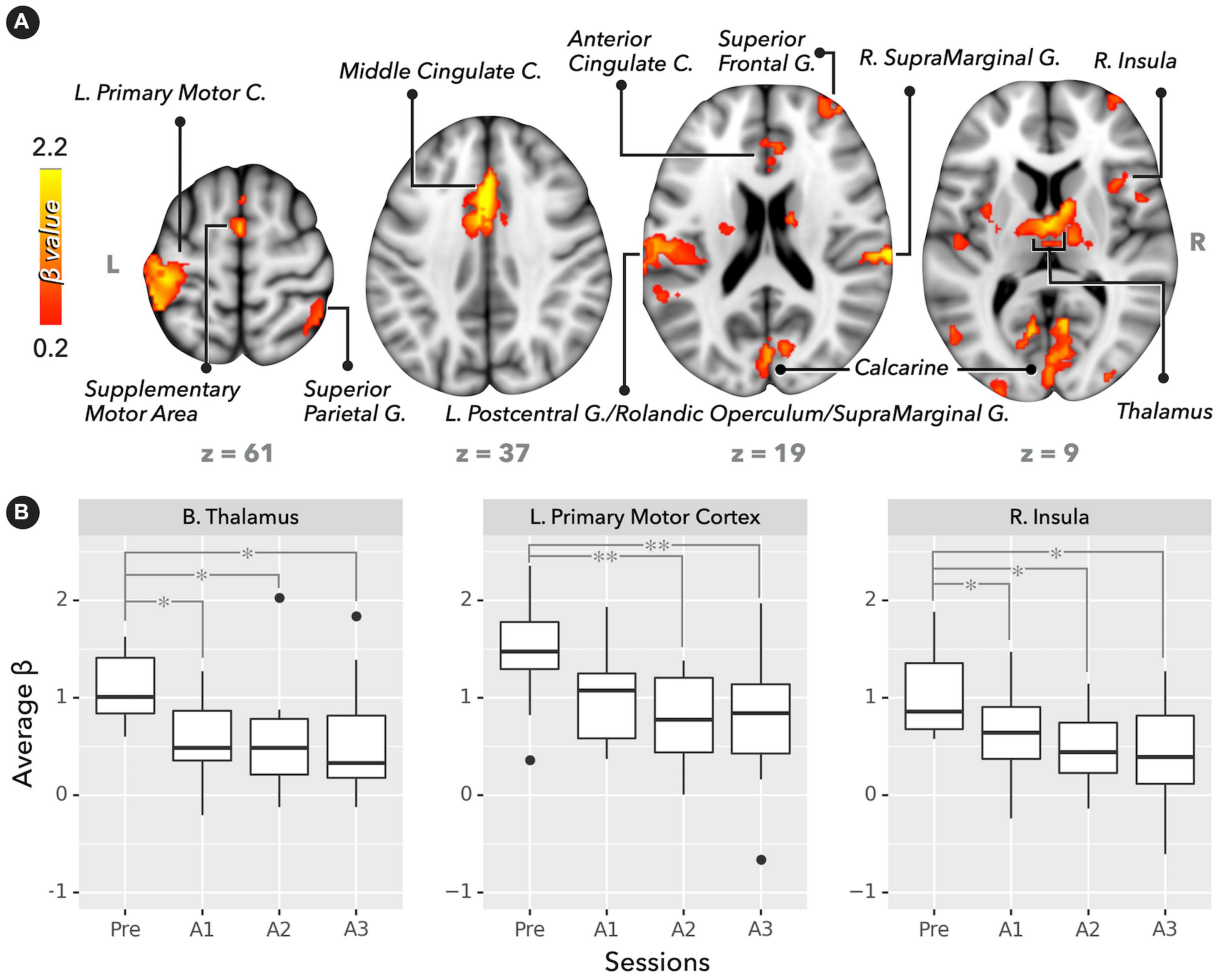

FIGURE 2
Brain activation map and regional BOLD response (average β values) in PVT (n=12). **(A)** Significant activation map in the presleep session (corrected p<0.05). **(B)** BOLD responses for bilateral thalamus, left primary motor cortex, and right insula. Compared with the presleep session, BOLD responses significantly decreased after sleep (FDR-corrected *post hoc* $^*p$<0.05 and $^{**}p$<0.01).

10.3389/fpsyt.2023.1058721

components during the sleep inertia period. The separate NVC components include EEG signals (neuron-related local field potential, LFP), CVR (neuron-irrelevant hemodynamic response function) and BOLD response (neuron-related HRF) along the awakening time. We hypothesize that if the NVC stays intact during sleep inertia, EEG β power and BOLD response would show a consistency among temporal dynamics, but the neuron-irrelevant CVR would remain time-invariant across different time points on awakening. Our results confirmed this hypothesis because both EEG β power and BOLD response showed significant reductions upon awakening, as compared with the presleep condition. For the CVR, we fitted multiple temporal characteristics to the hemodynamic responses irrelevant to the neural activity under the BH task and found that the induced HRF did not show prominent changes before and after sleep, even though the baseline CBF varied during the SI period (9). In fact, although the thalamus exhibited a shorter FWHM upon awakening in the *post hoc* test, the overall CVR temporal patterns remained untouched without presleep/postsleep differences in the BOLD fMRI response and EEG β power. Thereby, the temporal patterns of EEG, CVR and fMRI preliminarily indicated that the BOLD responses upon awakening were contributed from neural activities, implying that the static NVC presumption still holds upon awakening after sleep.

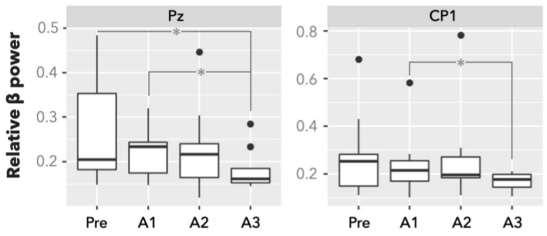

FIGURE 3
Relative β power of EEG electrodes of Pz and CP1 in PVT (n=9). There is a significant difference between presleep and the third 20-min sessions after sleep (A3) in Pz. Compared with the first session after sleep (A1), the power at the A3 session significantly decreased in both Pz and CP1. Significance was determined by FDR-corrected *post hoc* *p<0.05.

In lack of task engagements, prior SI-based neuroimaging studies could not approach NVC on awakening. Here we conducted PVT experiments in the SI period using simultaneous EEG-fMRI recordings, which was carried out through a three-end synchronization among MRI, EEG recording and task stimulation computers. This is the first attempt to conduct the task-based fMRI upon awakening, linking cognitive performance with the fMRI brain mapping in the SI period. Furthermore, we measured multiple neuroimaging indices (EEG, CVR, and fMRI) to approach NVC through observing their temporal consistency (as shown in Figure 1). Unlike calibrated methods using mathematical modeling (18), this act of observing temporal consistency is imperative in this study because during SI, both neural activity and BOLD response were all varying along with time without a fixed reference for calibration (12, 13). Thus, we bypassed the neurophysiological modeling and turned to measure the macroscopic neuroimaging indices with task engagements repeatedly for estimating the both ends of neurovascular components, according to previous literature (17, 32). However, using this strategy we only provided preliminary evidence of static NVC on awakening with limited sample size. Further investigations with microscopic

TABLE 1 Temporal characteristics of breath-hold CVR estimated from fitted HRF within region of interests.

	Pre	A1	A2	A3	Friedman test
Left primary motor cortex					
Time to HWHM	29.39 ± 6.27	26.31 ± 1.94	25.71 ± 1.86	25.83 ± 1.84	χ^2 = 3.96, p = 0.27
Ascending time	3.46 ± 1.46	4.89 ± 2.14	6.15 ± 6.00	4.45 ± 1.94	χ^2 = 9.00, p = 0.03*
Time to peak	32.84 ± 5.50	31.19 ± 3.27	31.86 ± 5.72	30.28 ± 1.98	χ^2 = 0.04, p = 1.00
Descending time	4.82 ± 2.96	6.31 ± 4.50	7.11 ± 6.07	4.97 ± 1.92	χ^2 = 1.64, p = 0.65
FWHM	8.28 ± 3.97	11.2 ± 5.52	13.26 ± 7.75	9.42 ± 2.51	χ^2 = 5.64, p = 0.13
Bilateral thalamus					
Time to HWHM	25.42 ± 1.83	25.77 ± 1.81	25.83 ± 1.37	26.05 ± 1.51	χ^2 = 2.60, p = 0.46
Ascending time	5.09 ± 1.27	4.69 ± 1.76	4.34 ± 0.85	4.17 ± 1.36	χ^2 = 8.68, p = 0.03*
Time to peak	30.51 ± 1.99	30.46 ± 2.00	30.17 ± 1.91	30.22 ± 1.95	χ^2 = 0.26, p = 0.97
Descending time	6.53 ± 1.99	6.03 ± 3.12	6.86 ± 5.03	4.85 ± 1.80	χ^2 = 7.51, p = 0.06
FWHM	11.62 ± 2.58	10.72 ± 3.94	11.21 ± 5.74	9.02 ± 2.72*	χ^2 = 9.00, p = 0.03*
Right insula					
Time to HWHM	22.3 ± 1.47	23.05 ± 1.23	22.47 ± 2.26	23.31 ± 1.67	χ^2 = 2.25, p = 0.52
Ascending time	6.38 ± 2.04	5.32 ± 1.38	5.51 ± 2.56	4.9 ± 1.10	χ^2 = 3.56, p = 0.31
Time to peak	28.68 ± 1.75	28.37 ± 1.14	27.97 ± 1.4	28.21 ± 1.45	χ^2 = 8.84, p = 0.03*
Descending time	8.09 ± 2.05	6.98 ± 1.78	8.1 ± 3.89	6.85 ± 2.72	χ^2 = 5.48, p = 0.14
FWHM	14.47 ± 3.64	12.3 ± 2.39	13.61 ± 6.34	11.75 ± 3.37	χ^2 = 5.56, p = 0.14

Time unit is second. Data is summarized as mean ± standard deviation. Pre, presleep session; A1/A2/A3, the first/second/third 20-min session after sleep; FWHM, full width half maximum of the peak; HWHM, half width half maximum of the peak. The statistical significance between Pre and A3 of p < 0.05 with FDR *post hoc* tests is marked as *.

NVC-related factors are warranted to validate the static NVC assumption in the period of sleep inertia.

Neurovascular coupling before sleep and after awakening

Previous fMRI investigations have all been based on the presumption of NVC and the BOLD principle (33). However, recent studies have suggested that the presumption might not be as valid as our prior expectation, even in the normal human participants without neuropathology. For example, Czisch et al. observed different patterns of fMRI activity between wakefulness (positive activity) and sleep stages (negative response) in response to the same acoustic stimuli (task) (34), and our recent studies demonstrated the temporal inconsistency between EEG and fMRI indices (power and connectivity) across sleep-wake conditions (resting) (17). Both studies highlighted the possibility of an altered neurovascular relationship in nocturnal sleep. The neurovascular relationship on awakening has not yet been explored. To understand how the brain recovers its functionality and consciousness after sleep, a critical next step is to determine whether the NVC assumption holds true during the SI period. To examine NVC through the resting-state analysis is not an easy task due to the lack of prominent targets in terms of both neural activity and the followed BOLD responses. Therefore, we utilized the PVT to probe vigilance upon awakening, which is a commonly adopted approach in the SI literature. At the current stage, the neuroimaging field lacks a quantitative index for NVC; thus, we adopted a qualitative examination method for NVC, observing the between-session consistency in the combined neurovascular responses (fMRI BOLD responses), vascular components (CVR temporal characteristics), and neural components (EEG β power). For the vascular component, we regarded the BH-induced CVR time curves as a surrogate for BOLD response without neural activity, and we carefully checked the CVR temporal characteristics through data fitting. The results indicated that the thalamus might be the only brain region with prominent changes in CVR temporal characteristics, especially for FWHM in thalamus. However, the cross-sessional patterns of FWHM were unlike those of the EEG β power or fMRI brain activity; the postsleep variation in FWHM was not prominent in other brain regions. Therefore, we could approximately conclude that the CVR function did not vary before and after sleep during the SI period. For the neural component of PVT, we found that the relative β power presented differently between the presleep session and A3 (Pz), as well as between A1 and A3 (Pz and CP1). As the EEG β power is generally regarded as an index of vigilance (8, 12, 35), we can infer that immediately after awakening, the nonsignificantly enhanced β power reflected the slight elevation in vigilance of the participants, but it decreased along the waking time, reaching a trough at A3. By contrast, upon awakening, the relative delta power increased with marginal significance in O2 ($\chi^2 = 9.1$, with *post hoc* FDR-corrected $p = 0.078$ for Pre–A3, A1–A2 and A2–A3), and FC5 ($\chi^2 = 8.3$, with *post hoc* tests of $p > 0.195$, FDR-corrected), indicating the extended sleepiness even after awakening. The findings of presleep/postsleep differences resembled the cross-session results of fMRI BOLD responses, which supports the idea of static NVC upon awakening.

Sleep inertia under insufficient sleep

The multiple repeated-measure design after awakening is a common setting in previous SI-based studies (7, 9, 12). We originally expected that the RTs and brain activities would gradually recover close to the presleep condition along with time; however, our findings only identified the difference between presleep and postsleep, without differences between A1 and A3, for all indices of RT, fMRI activity, and EEG power. The unusual cross-session pattern after awakening might be an indication of extended sleepiness in the 1 h awakening period from a maximum 3 h sleep inside the MRI scanner (reflected by low β power and high delta power). One reason for this outcome may be the irregular waking time (approximate 3–4 a.m.) relative to the participants' normal sleep-wake rhythm; the induced partial sleep deprivation might have led to an enhancement of the SI severity (5). The constrained body position inside the MRI scanner might be another influential factor for participants, as they cannot move during the 1 h scan after awakening, which may have induced sleepiness after a certain period of time. Third, the current results included the average EEG/fMRI/RT scores in sleep ($n = 12$), yet three of them did not show objective sleep signatures in sleep scoring. If we present the datasets only with objective sleep scoring ($n = 9$, see Supplementary Figure S3), the cross-session SI pattern is slightly evident in the fMRI effect size, which confirms the necessity of collecting the datasets with objective sleep scorings for SI investigations.

Limitation

The major limitation of this study was the insufficient sample size to apply the parametric statistical tests. Originally, we collected 32 participants in the protocol; however, due to certain technical obstacles (e.g., loss of synchronization markers, unable to record PVT-RTs, and disruptive motion in sleep), the number of participants completing the CVR with simultaneous EEG-fMRI recordings was only 15, and that completing both the PVT and CVR was 12. After excluding those who did not present objective sleep signatures, the number decreased to nine. Due to the limited sample size, we only provided a preliminary glimpse on the NVC upon awakening for future neuroimaging investigations, and we could not classify the data into groups of different sleep stages that participants were awakened from, which is a necessary step for future studies. Finally, neurons at different brain locations may recover at different speeds in SI (11), or with different NVC (36). However, we only focused on the PVT-related brain regions (thalamus, insula, and motor cortex) in this study based on the task engagements. Future studies are warranted to continue surveying functional reorganization at different brain regions immediately after sleep.

Conclusion

Sleep inertia is the period that involves cognitive impairments immediately after awakening from sleep. Previous papers have discussed hypovigilance in task engagement, but recent neuroimaging studies regarding SI have focused on the brain connectivity in the resting state.

This mismatch as well as the presumption of static NVC before and after sleep are two major concerns in this field. Therefore, we firstly addressed brain activity in response to task performances within 1 h of awakening. Furthermore, we preliminarily probed the appropriateness of assuming the static NVC in presleep and postsleep conditions, which may facilitate the neuroimaging studies of SI in the future.

Data availability statement

The original contributions presented in the study are included in the article/Supplementary material, further inquiries can be directed to the corresponding authors.

Ethics statement

The studies involving human participants were reviewed and approved by the Research Ethics Committee of National Taiwan University (Approval No. 201512ES054). The patients/participants provided their written informed consent to participate in this study.

Author contributions

C-WH, H-CL, and CW initiated the concept and experimental design. A-LH, M-KL, and CW wrote the manuscript. CW, Y-CK, and A-LH designed the study. M-KL, Y-CK, and C-WL collected the data. A-LH, M-KL, and ZW analyzed the data. All authors contributed to the article and approved the submitted version.

Funding

This study was supported by the funding from the Taiwan National Science and Technology Council (105-2628-B-038-013-MY3, 108-2410-H-038-007, and 111-2222-E-182-001-MY3), Taiwan Ministry of Education (DP2-110-21121-01-N-06-01), and Taipei Medical University-Wanfang Hospital (110TMU-WFH-17). This manuscript was edited by Wallace Academic Editing.

Conflict of interest

The authors declare that the research was conducted in the absence of any commercial or financial relationships that could be construed as a potential conflict of interest.

Publisher's note

All claims expressed in this article are solely those of the authors and do not necessarily represent those of their affiliated organizations, or those of the publisher, the editors and the reviewers. Any product that may be evaluated in this article, or claim that may be made by its manufacturer, is not guaranteed or endorsed by the publisher.

Supplementary material

The Supplementary material for this article can be found online at: https://www.frontiersin.org/articles/10.3389/fpsyt.2023.1058721/full#supplementary-material

References

1. Hilditch CJ, Centofanti SA, Dorrian J, Banks S. A 30-minute, but not a 10-minute nighttime nap is associated with sleep inertia. *Sleep*. (2016) 39:675–85. doi: 10.5665/sleep.5550

2. Ikeda H, Hayashi M. The effect of self-awakening from nocturnal sleep on sleep inertia. *Biol Psychol*. (2010) 83:15–9. doi: 10.1016/j.biopsycho.2009.09.008

3. Hofer-Tinguely G, Achermann P, Landolt H-P, Regel SJ, Rétey JV, Dürr R, et al. Sleep inertia: performance changes after sleep, rest and active waking. *Brain Res Cogn Brain Res*. (2005) 22:323–31. doi: 10.1016/j.cogbrainres.2004.09.013

4. Hilditch CJ, McHill AW. Sleep inertia: current insights. *Nat Sci Sleep*. (2019) 11:155–65. doi: 10.2147/nss.s188911

5. Tassi P, Muzet A. Sleep inertia. *Sleep Med Rev*. (2000) 4:341–53. doi: 10.1053/smrv.2000.0098

6. Trotti LM. Waking up is the hardest thing I do all day: sleep inertia and sleep drunkenness. *Sleep Med Rev*. (2017) 35:76–84. doi: 10.1016/j.smrv.2016.08.005

7. Marzano C, Ferrara M, Moroni F, Gennaro LD. Electroencephalographic sleep inertia of the awakening brain. *Neuroscience*. (2011) 176:308–17. doi: 10.1016/j.neuroscience.2010.12.014

8. Ferrara M, Curcio G, Fratello F, Moroni F, Marzano C, Pellicciari MC, et al. The electroencephalographic substratum of the awakening. *Behav Brain Res*. (2006) 167:237–44. doi: 10.1016/j.bbr.2005.09.012

9. Balkin TJ, Braun AR, Wesensten NJ, Jeffries K, Varga M, Baldwin P, et al. The process of awakening: a PET study of regional brain activity patterns mediating the re-establishment of alertness and consciousness. *Brain*. (2002) 125:2308–19. doi: 10.1093/brain/awf228

10. Wu CW, Liu PY, Tsai PJ, Wu YC, Hung CS, Tsai Y-C, et al. Variations in connectivity in the sensorimotor and default-mode networks during the first nocturnal sleep cycle. *Brain Connect*. (2012) 2:177–90. doi: 10.1089/brain.2012.0075

11. Tsai PJ, Chen SCJ, Hsu CY, Wu CW, Wu YC, Hung CS, et al. Local awakening: regional reorganizations of brain oscillations after sleep. *NeuroImage*. (2014) 102:894–903. doi: 10.1016/j.neuroimage.2014.07.032

12. Vallat R, Meunier D, Nicolas A, Ruby P. Hard to wake up? The cerebral correlates of sleep inertia assessed using combined behavioral, EEG and fMRI measures. *NeuroImage*. (2019) 184:266–78. doi: 10.1016/j.neuroimage.2018.09.033

13. Chen X, Hsu C-F, Xu D, Yu J, Lei X. Loss of frontal regulator of vigilance during sleep inertia: a simultaneous EEG-fMRI study. *Hum Brain Mapp*. (2020) 41:4288–98. doi: 10.1002/hbm.25125

14. Mulert C, Lemieux L. Principles of multimodal functional imaging and data integration In: C Mulert and L Lemieux, editors. *EEG-fMRI: Physiological basis, technique, and applications*. Berlin: Springer Science & Business Media (2009). 3–17.

15. Blamire AM, Ogawa S, Ugurbil K, Rothman D, McCarthy G, Ellermann JM, et al. Dynamic mapping of the human visual cortex by high-speed magnetic resonance imaging. *Proc Natl Acad Sci U S A*. (1992) 89:11069–73. doi: 10.1073/pnas.89.22.11069

16. Iannetti GD, Wise RG. BOLD functional MRI in disease and pharmacological studies: room for improvement? *Magn Reson Imaging*. (2007) 25:978–88. doi: 10.1016/j.mri.2007.03.018

17. Wu CW, Tsai PJ, Chen SCJ, Li CW, Hsu A-L, Wu HY, et al. Indication of dynamic neurovascular coupling from inconsistency between EEG and fMRI indices across sleep–wake states. *Sleep Biol Rhythms*. (2019) 17:423–31. doi: 10.1007/s41105-019-00232-1

18. Huneau C, Benali H, Chabriat H. Investigating human neurovascular coupling using functional neuroimaging: a critical review of dynamic models. *Front Neurosci*. (2015) 9:467. doi: 10.3389/fnins.2015.00467

19. Riera JJ, Sumiyoshi A. Brain oscillations: ideal scenery to understand the neurovascular coupling. *Curr Opin Neurol*. (2010) 23:374–81. doi: 10.1097/wco.0b013e32833b769f

20. Hsu Y-Y, Kuan W-C, Lim K-E, Liu H-L. Breathhold-regulated blood oxygenation level-dependent (BOLD) MRI of human brain at 3 tesla. *J Magn Reson Imaging*. (2010) 31:78–84. doi: 10.1002/jmri.22015

21. Kastrup A, Krüger G, Neumann-Haefelin T, Moseley ME. Assessment of cerebrovascular reactivity with functional magnetic resonance imaging: comparison of

CO_2 and breath holding. *Magn Reson Imaging*. (2001) 19:13–20. doi: 10.1016/S0730-725X(01)00227-2

22. Burke TM, Scheer FAJL, Ronda JM, Czeisler CA, Wright KP. Sleep inertia, sleep homeostatic and circadian influences on higher-order cognitive functions. *J Sleep Res*. (2015) 24:364–71. doi: 10.1111/jsr.12291

23. Santhi N, Groeger JA, Archer SN, Gimenez M, Schlangen LJM, Dijk D-J. Morning sleep inertia in alertness and performance: effect of cognitive domain and white light conditions. *PLoS One*. (2013) 8:e79688. doi: 10.1371/journal.pone.0079688

24. Urback AL, MacIntosh BJ, Goldstein BI. Cerebrovascular reactivity measured by functional magnetic resonance imaging during breath-hold challenge: a systematic review. *Neurosci Biobehav Rev*. (2017) 79:27–47. doi: 10.1016/j.neubiorev.2017.05.003

25. Magon S, Basso G, Farace P, Ricciardi GK, Beltramello A, Sbarbati A. Reproducibility of BOLD signal change induced by breath holding. *NeuroImage*. (2009) 45:702–12. doi: 10.1016/j.neuroimage.2008.12.059

26. Delorme A, Makeig S. EEGLAB: an open source toolbox for analysis of single-trial EEG dynamics including independent component analysis. *J Neurosci Methods*. (2004) 134:9–21. doi: 10.1016/j.jneumeth.2003.10.009

27. Delorme A, Sejnowski T, Makeig S. Enhanced detection of artifacts in EEG data using higher-order statistics and independent component analysis. *NeuroImage*. (2007) 34:1443–9. doi: 10.1016/j.neuroimage.2006.11.004

28. Ibert C, Ancoli-Israel S, Chesson AL, Quan SF. The AASM manual for the scoring of sleep and associated events. Westchester Il. American Academy of Sleep Medicine (2007)

29. Gramfort A, Luessi M, Larson E, Engemann DA, Strohmeier D, Brodbeck C, et al. MNE software for processing MEG and EEG data. *NeuroImage*. (2014) 86:446–60. doi: 10.1016/j.neuroimage.2013.10.027

30. Cox RW. AFNI: software for analysis and visualization of functional magnetic resonance neuroimages. *Comput Biomed Res*. (1996) 29:162–73. doi: 10.1006/cbmr.1996.0014

31. Hsu A-L, Hou P, Johnson JM, Wu CW, Noll KR, Prabhu SS, et al. IClinfMRI software for integrating functional MRI techniques in presurgical mapping and clinical studies. *Front Neuroinform*. (2018) 12:839–14. doi: 10.3389/fninf.2018.00011

32. Huneau C, Houot M, Joutel A, Béranger B, Giroux C, Benali H, et al. Altered dynamics of neurovascular coupling in CADASIL. *Ann Clin Transl Neurol*. (2018) 5:788–802. doi: 10.1002/acn3.574

33. Ogawa S, Lee TM, Kay AR, Tank DW. Brain magnetic resonance imaging with contrast dependent on blood oxygenation. *Proc Natl Acad Sci*. (1990) 87:9868–72. doi: 10.1073/pnas.87.24.9868

34. Czisch M, Wetter TC, Kaufmann C, Pollmächer T, Holsboer F, Auer DP. Altered processing of acoustic stimuli during sleep: reduced auditory activation and visual deactivation detected by a combined fMRI/EEG study. *NeuroImage*. (2002) 16:251–8. doi: 10.1006/nimg.2002.1071

35. Liu X, Yanagawa T, Leopold DA, Chang C, Ishida H, Fujii N, et al. Arousal transitions in sleep, wakefulness, and anesthesia are characterized by an orderly sequence of cortical events. *NeuroImage*. (2015) 116:222–31. doi: 10.1016/j.neuroimage.2015.04.003

36. Devonshire IM, Papadakis NG, Port M, Berwick J, Kennerley AJ, Mayhew JEW, et al. Neurovascular coupling is brain region-dependent. *NeuroImage*. (2012) 59:1997–2006. doi: 10.1016/j.neuroimage.2011.09.050

frontiers | Frontiers in Psychiatry

TYPE Original Research
PUBLISHED 07 June 2023
DOI 10.3389/fpsyt.2023.1055459

OPEN ACCESS

EDITED BY
Izabela Guimaraes Barbosa,
Federal University of Minas Gerais, Brazil

REVIEWED BY
Siyuan Fan,
Peking Union Medical College Hospital (CAMS), China
Takashi Kanbayashi,
University of Tsukuba, Japan

*CORRESPONDENCE
Miriam Gerstenberg
✉ miriam.gerstenberg@pukzh.ch

RECEIVED 27 September 2022
ACCEPTED 19 May 2023
PUBLISHED 07 June 2023

CITATION
Dimitriades ME, Markovic A, Gefferie SR, Buckley A, Driver DI, Rapoport JL, Nosadini M, Rostasy K, Sartori S, Suppiej A, Kurth S, Franscini M, Walitza S, Huber R, Tarokh L, Bölsterli BK and Gerstenberg M (2023) Sleep spindles across youth affected by schizophrenia or anti-*N*-methyl-D-aspartate-receptor encephalitis. *Front. Psychiatry* 14:1055459. doi: 10.3389/fpsyt.2023.1055459

Sleep spindles across youth affected by schizophrenia or anti-*N*-methyl-D-aspartate-receptor encephalitis

Maria E. Dimitriades[1,2], Andjela Markovic[3,4,5], Silvano R. Gefferie[6,7], Ashura Buckley[8], David I. Driver[9], Judith L. Rapoport[9], Margherita Nosadini[10,11], Kevin Rostasy[12], Stefano Sartori[10,11], Agnese Suppiej[13], Salome Kurth[5], Maurizia Franscini[14], Susanne Walitza[14,15,16], Reto Huber[1,2,14,15], Leila Tarokh[4,17], Bigna K. Bölsterli[1,2,18,19] and Miriam Gerstenberg[2,14]*

[1]Child Development Center, University Children's Hospital Zurich, Zurich, Switzerland, [2]Children's Research Center, University Children's Hospital Zurich, Zurich, Switzerland, [3]Department of Pulmonology, University Hospital Zurich, Zurich, Switzerland, [4]University Hospital of Child and Adolescent Psychiatry and Psychotherapy, University of Bern, Bern, Switzerland, [5]Department of Psychology, University of Fribourg, Fribourg, Switzerland, [6]Stichting Epilepsie Instellingen Nederland, Heemstede, Netherlands, [7]Department of Neurology, Leiden University Medical Center, Leiden, Netherlands, [8]Pediatrics and Neurodevelopmental Neuroscience, National Institute of Mental Health, Bethesda, MD, United States, [9]Child Psychiatry Branch, National Institute of Mental Health, Bethesda, MD, United States, [10]Paediatric Neurology and Neurophysiology Unit, Department of Women's and Children's Health, University Hospital of Padova, Padova, Italy, [11]Neuroimmunology Group, Paediatric Research Institute Città della Speranza, Padova, Italy, [12]Department of Pediatric Neurology, Children's Hospital Datteln, Witten/Herdecke University, Datteln, Germany, [13]Department of Medical Sciences, Pediatric Section, University of Ferrara, Ferrara, Italy, [14]Department of Child and Adolescent Psychiatry and Psychotherapy, Psychiatric University Hospital Zurich, University of Zurich, Zurich, Switzerland, [15]Neuroscience Center Zurich, University of Zurich and Swiss Federal Institute of Technology Zurich, Zurich, Switzerland, [16]Zurich Center for Integrative Human Physiology, University of Zurich, Zurich, Switzerland, [17]Translational Research Center, University Hospital of Psychiatry and Psychotherapy, University of Bern, Bern, Switzerland, [18]Department of Pediatric Neurology, University Children's Hospital Zurich, Zurich, Switzerland, [19]Department of Pediatric Neurology, Children's Hospital of Eastern Switzerland, St. Gallen, Switzerland

Background: Sleep disturbances are intertwined with the progression and pathophysiology of psychotic symptoms in schizophrenia. Reductions in sleep spindles, a major electrophysiological oscillation during non-rapid eye movement sleep, have been identified in patients with schizophrenia as a potential biomarker representing the impaired integrity of the thalamocortical network. Altered glutamatergic neurotransmission within this network via a hypofunction of the *N*-methyl-D-aspartate receptor (NMDAR) is one of the hypotheses at the heart of schizophrenia. This pathomechanism and the symptomatology are shared by anti-NMDAR encephalitis (NMDARE), where antibodies specific to the NMDAR induce a reduction of functional NMDAR. However, sleep spindle parameters have yet to be investigated in NMDARE and a comparison of these rare patients with young individuals with schizophrenia and healthy controls (HC) is lacking. This study aims to assess and compare sleep spindles across young patients affected by Childhood-Onset Schizophrenia (COS), Early-Onset Schizophrenia, (EOS), or NMDARE and HC. Further, the potential relationship between sleep spindle parameters in COS and EOS and the duration of the disease is examined.

Methods: Sleep EEG data of patients with COS (N = 17), EOS (N = 11), NMDARE (N = 8) aged 7–21 years old, and age- and sex-matched HC (N = 36) were assessed in 17 (COS, EOS) or 5 (NMDARE) electrodes. Sleep spindle parameters (sleep spindle density, maximum amplitude, and sigma power) were analyzed.

Results: Central sleep spindle density, maximum amplitude, and sigma power were reduced when comparing all patients with psychosis to all HC. Between patient group comparisons showed no differences in central spindle density but lower central maximum amplitude and sigma power in patients with COS compared to patients with EOS or NMDARE. Assessing the topography of spindle density, it was significantly reduced over 15/17 electrodes in COS, 3/17 in EOS, and 0/5 in NMDARE compared to HC. In the pooled sample of COS and EOS, a longer duration of illness was associated with lower central sigma power.

Conclusions: Patients with COS demonstrated more pronounced impairments of sleep spindles compared to patients with EOS and NMDARE. In this sample, there is no strong evidence that changes in NMDAR activity are related to spindle deficits.

KEYWORDS

psychosis, schizophrenia, anti-NMDAR encephalitis, sleep EEG, sleep spindles, thalamocortical network

1. Introduction

Once thought to be merely a phenotype of psychosis, sleep dysfunction is now considered to be intricately intertwined in the pathophysiology of disorders along the psychosis spectrum (1–4). Schizophrenia (SZ) is one of several conditions that falls within the psychosis spectrum and is characterized by psychotic symptoms, marking a disconnection from reality, and considerable changes in affective state, perception, and cognition. Disturbed sleep often precedes the onset of SZ and predicts relapses in remitted patients (5–7). Thus, increased research efforts are made to study sleep quality, structure, and electroencephalographic characteristics in order to identify specific parameters potentially contributing to or resulting from the emergence of the disorder. Specifically sleep spindles, a sleep electroencephalogram (EEG) characteristic, caught much attention as a potential endophenotype as well as a target for novel therapeutic approaches (8). Sleep spindles are major oscillations occurring in the sigma frequency range (12–15 Hz) and are most prominent during stage 2 of Non-Rapid Eye Movement (NREM) sleep (3). The reduction of sleep spindle density (SSD; number per minute) in patients affected by SZ when compared to healthy controls (HC) has been the most consistent finding across studies and diverse patient populations with varying age, medication status, or chronicity of the disorder (3, 8–10). This finding is most pronounced in central regions of the cortex in the fast frequency range of spindles (13–15 Hz) (3, 9, 11). Reductions in sleep spindle maximum amplitude (SSMA) and sigma power (SP) are also frequently reported, but tend to be less consistently reduced across studies. This may be in part due to differences in electrode density montages, detection methods, and chronicity of the disorder (1, 3, 9–11).

Sleep spindles are generated by inhibitory GABAergic (gamma-aminobutyric acid) neurons in the thalamic reticular nucleus (12). Thalamic reticular nucleus neurons inhibit excitatory, glutamatergic neurons that propagate signals from the thalamus to the cortex. Cortical projection neurons further communicate with thalamic reticular nucleus neurons via the activation of specific receptors, including the glutamate-specific ionotrophic receptor, the *N*-methyl-D-aspartate receptor (NMDAR) (13, 14). This NMDAR-mediated glutamatergic feedback loop is necessary to modulate and maintain sleep spindles (15, 16). The NMDAR is also highly implicated in the emergence of SZ. According to the glutamate hypothesis, glutamatergic activity is disrupted in patients with SZ due to a hypofunction of the NMDAR (17, 18). This provokes a cascade of altered neurotransmission that affects brain development and results in the diverse symptomatology of SZ, including cognitive deficits. Sleep spindles play a role in sleep-dependent memory consolidation, and the decrease in sleep spindles in schizophrenia has been hypothesized to contribute to the cognitive deficits that are integral to the disorder (8, 19). It is currently unclear if the hypofunction of the NMDAR is also a key element contributing to the detected sleep spindle reduction in SZ.

A rare form of autoimmune encephalitis, anti-NMDAR encephalitis (NMDARE), is induced by autoantibodies that target the NMDAR leading to a functional deficit (20). The symptomatology of NMDARE and SZ also greatly overlap, often presenting with sleep and cognitive disturbances and culminating with a range of psychotic symptoms (21, 22). This has encouraged research in the context of the glutamate hypothesis of SZ (23–28). Although a previous study found that SSD and SP were only reduced in patients with SZ when comparing them to other patients with mental health disorders who presented with psychosis, sleep spindles have yet to be compared to patient populations with somatic illnesses who present with psychosis (29). The shared phenotype and key pathomechanistic element make SZ and NMDARE very promising to study in concert. Further insight may be gained into the role of the NMDAR within the thalamocortical network and the detectable sleep spindle phenotype of both disorders.

Highly dynamic phases of brain development could potentially influence the relationship between sleep and psychosis spectrum disorders. During childhood and adolescence, individuals undergo drastic brain maturation that affects sleep structure and characteristics (25). Additionally, these periods introduce vulnerabilities in the developing cortex which may coincide with the onset of mental health disorders (30, 31). SZ rarely

emerges during these young, malleable periods, being classified as Childhood-Onset (COS) if the onset age precedes the age of 13 and Early-Onset Schizophrenia (EOS) if the onset age occurs between age 13 and 18. Previous studies indicate that these populations have reductions in SSD (32, 33), although the two have never been directly compared. In COS, a longer duration of illness was associated with lower SSMA and SP and a recent meta-analysis in adults with SZ points to an association of a longer duration of illness with SSD deficits (33, 34). Combining data from young patients with SZ will allow to further assess the relationship between the duration of illness and sleep spindle parameters.

Pooling sleep data from young patients affected by COS, EOS, and NMDARE, this study aims to assess sleep spindle parameters (SSD, SSMA, SP) between the patient groups and to compare them to age- and sex-matched HC. Due to evidence demonstrating reduced sleep spindles in SZ and the overlapping phenotype and pathomechanism of SZ and NMDARE, it is hypothesized that the pooled patient group will have reduced sleep spindle parameters when compared to HC. Between-patient group comparisons will be performed to elucidate the contribution of each patient population to this presumed finding. Further, to analyze potential regional differences across the cortex, topographical distribution of spindle parameters will be compared between each patient group and matched HC. Lastly, the impact of the duration of illness on spindle alterations will be assessed in an exploratory correlation analysis in young patients with SZ.

2. Materials and methods

2.1. Participants

Sleep data from three patient groups were gathered for the purpose of this study. Screening procedures and characteristics of patient groups have previously been published (22, 32, 33). All-night EEG, demographic, and clinical data from individuals with COS (N = 17, 16.0 ± 3.6 years, 70.6% female), EOS (N = 11, 16.4 ± 1.4 years, 36.4% female), NMDARE (N = 8, 13.3 ± 4.5 years, 75.0% female), and 36 age- and sex-matched HC were pooled in this project. Patients with SZ (COS, EOS) were either recruited at the National Institute of Mental Health in the United States (COS) or at the Department of Child and Adolescent Psychiatry of the Psychiatric University Hospital Zurich in Switzerland (EOS). The diagnosis for patients with COS was assessed by DSM-III-R or DSM-IV criteria and confirmed by two child psychiatrists after an in-patient stay where medication was discontinued (35, 36). For patients with EOS, mental disorders were assessed by the Mini International Neuropsychiatric Interview for Children and Adolescents (MINI-Kid), and criteria for EOS were further verified according to the DSM-IV (37). Age of onset, duration of illness, and antipsychotic medication measured as chlorpromazine equivalent were provided for each patient with SZ. IQ scores were available from 12 patients with COS and eight with EOS. One individual with EOS declined further use of non-genetic personal health data and was excluded in this study.

In the NMDARE group, three individuals had two EEG recordings available. Sleep structure and spindle parameters were calculated individually for each of these EEG and averaged to have one value for each participant. Patient data for this group was provided by three clinics, specifically the Department of Neuropediatrics, University Children's Hospital Zurich (Switzerland) (N = 4; EEG = 6); the Pediatric Neurology and Neurophysiology Unit in Padua (Italy) (N = 2; EEG = 3); the Department of Pediatric Neurology, Children's Hospital in Datteln, University Witten/Herdecke (Germany) (N = 2; EEG = 2). Clinically suspected diagnosis of NMDARE was confirmed by detection of ANMDAR antibodies in serum and/or cerebrospinal fluid.

The three patient groups had different age and sex characteristics (Table 1). Thirty-six HC were used in total; 17 were age- and sex-matched to the COS group (HC-C), accordingly 11 were matched to the EOS group (HC-E), and eight to the NMDARE group (HC-N). HC were recruited at the University Children's Hospital Zurich and underwent a screening process, excluding individuals with a history of mental health disorders and who took psychotropic medication. Written informed consent was obtained from all participants and/or their legal guardian. This research project was approved by swissethics (BASEC 2021-00215). All study procedures were performed according to the Declaration of Helsinki.

2.2. EEG recordings

All-night polysomnography recordings from patients with COS were measured using a 21-channel 10-20 system [TWin or Nihon Kohden; sampling rate (SR): 200 Hz]. EEG data from patients with EOS and HC were recorded using a 128-channel system (Electrical Geodesic Sensory Net; SR: 500 Hz). Nineteen electrodes were shared between patients with SZ and associated HC: two prefrontal (Fp1, Fp2), three frontal (F3, Fz, F4), three central (C3, C4, Cz; Cz available as a recording electrode following re-referencing), six temporal (F7, F8, T3, T4, T5, T6), three parietal (P3, Pz, P4), and two occipital (O1, O2). The patients with NMDARE had heterogeneous EEG recording protocols: (a) Zurich, 21-channel 10-20 system (NeurofileXP EE; SR: 256 Hz), (b) Padua, 8-10 channels (Galileo NT Software; SR: 256 Hz), and (c) Datteln, 11 channels (Neurofax EEG-9210 System; SR: 200 Hz). Seven electrodes were shared across the EEG montages for all three groups (COS, EOS and NMDARE): two prefrontal (Fp1, Fp2), two temporal (T3, T4), two occipital (O1, O2), and one central (Cz).

Epoch-specific sleep staging and artifact rejection were available from previous analyses (22, 32, 33). Sleep stages were scored based on standard criteria by a sleep expert and either validated by a second sleep expert (COS, EOS, HC) or by one rater only to reduce inter-rater variability (NMDARE) (38). Standard sleep stages were assigned to each epoch, composed of 20-s (EOS, HC, NMDARE) or 30-s (COS) time windows. Specific epochs were excluded on a channel to channel basis from the analyses if high levels of artifacts were found. A semi-automatic procedure was used to detect artifacts based on power thresholds in the muscle frequency band (20–40 Hz) and slow-wave frequency band (0.8–4.6 Hz, COS; 0.75–4.5 Hz, EOS, NMDARE) (39, 40). Channels with artifacts in <97% (COS, EOS, HC) or 95% (NMDARE) of their epochs were considered for subsequent analyses.

TABLE 1 Demographic and clinical characteristics.

Parameter	Patient group(s) (*N*)	Mean (SD)	HC: Mean (SD)	*p*-value	Direction (adjusted *p*-value)
Age (years)	COS (17)	16.00 (3.64)	16.41 (4.01)	0.89	
	EOS (11)	16.38 (1.43)	16.48 (1.71)	0.95	
	NMDARE (8)	13.29 (4.52)	13.65 (4.48)	0.80	
	COS, EOS, NMDARE			0.19	
Sex, female (*n*)	COS (17)	12 (70.59)	12 (70.59)	1.00	
	EOS (11)	4 (36.36)	4 (36.36)	1.00	
	NMDARE (8)	6 (75.00)	6 (75.00)	1.00	
	COS, EOS, NMDARE			0.14	
Age of onset (years)	COS (17)	9.27 (1.79)	NaN (NaN)	NaN	
	EOS (11)	15.33 (1.45)	NaN (NaN)	NaN	
	NMDARE (8)	12.03 (3.46)	NaN (NaN)	NaN	
	COS, EOS, NMDARE			**<0.0001**	COS < EOS (**<0.0001**)
Duration of illness (months)	COS (17)	80.75 (43.51)	NaN (NaN)	NaN	
	EOS (11)	12.56 (11.01)	NaN (NaN)	NaN	
	NMDARE	NaN (NaN)	NaN (NaN)	NaN	
	COS, EOS			**<0.0001**	
Chlorpromazine equivalent (mg)	COS (17)	667.65 (372.05)	NaN (NaN)	NaN	
	EOS (11)	172.50 (158.43)	NaN (NaN)	NaN	
	NMDARE	NaN (NaN)	NaN (NaN)	NaN	
	COS, EOS			**<0.001**	
IQ	COS (12)	78.00 (19.21)	NaN (NaN)	NaN	
	EOS (8)	95.13 (26.44)	NaN (NaN)	NaN	
	NMDARE	NaN (NaN)	NaN (NaN)	NaN	
	COS, EOS			0.13	

COS, childhood-onset schizophrenia; EOS, early-onset schizophrenia; NMDARE, anti-*N*-methyl-D-aspartate receptor encephalitis; SD, standard deviation; NaN, not a number, data missing. HC were 1:1 matched to each patient. When comparing the three patient groups with Kruskal Wallis Tests, any significant difference is reported represented by the adjusted *p*-value and direction of the difference. When comparing only the COS and EOS groups, Mann-Whitney *U*-tests were used. The bold values imply statistical significance.

2.3. EEG data analyses

EEG data were analyzed in MATLAB 2017b. Data were low-pass filtered (−6 dB cut-off = 40.5 Hz; Finite Impulse Response (FIR) filter), down-sampled to 125 Hz, and high-pass filtered (−6 dB cut-off = 0.38 Hz, Kaiser Window FIR filter). Electrodes were re-referenced to the mean of the occipital channels (O1, O2). The occipital channels were chosen as they are shared by all participants. Further, all other possible channel locations shared by all EEG montages (frontal, central, temporal) have previously shown disturbances in spindles in SZ (8, 32, 41–46).

Sleep spindles were analyzed during the first hour of artifact-free NREM Stage 2 and 3 for each participant. This is considered the most robust part of sleep, with little or no fragmentation. Sleep spindles were automatically detected based on an established amplitude-threshold algorithm (10). EEG signal was band-pass filtered (−6 dB cut-offs: 12.01 and 16.97 Hz, Chebyshev Type II filter) and the average signal amplitude was calculated for each channel. As signal amplitude varies for each electrode, a threshold was set relative to the average signal amplitude for each channel. Therefore, sleep spindles were detected if fluctuations in amplitude for a given channel surpassed an upper threshold of five times the average signal amplitude. The upper threshold value was determined based on previous studies examining young adults and was confirmed as the best representation of spindle detection after visual inspection (47, 48). The beginning and end of each spindle were defined as the instances where the signal surrounding the peak amplitude dipped below a lower threshold of two times the average signal. The lower duration threshold of a spindle was determined to be 0.3 s (49).

Sleep spindle density (SSD), maximum amplitude (SSMA), and sigma power (SP) were investigated in this project. SSD refers to the number of spindles per minute (13.75–14.75 Hz). SSMA refers to the largest amplitude value (positive or negative; μV) of a given spindle and was calculated for every spindle within the frequency range of interest and averaged together. Spectral analysis of EEG signals were performed for each epoch (Fast Fourier transform, 4-s Hanning window, overlapping by 2-s), resulting in a 0.25 Hz frequency resolution. Sigma power (13.75–14.75 Hz; μV^2) was calculated for each epoch.

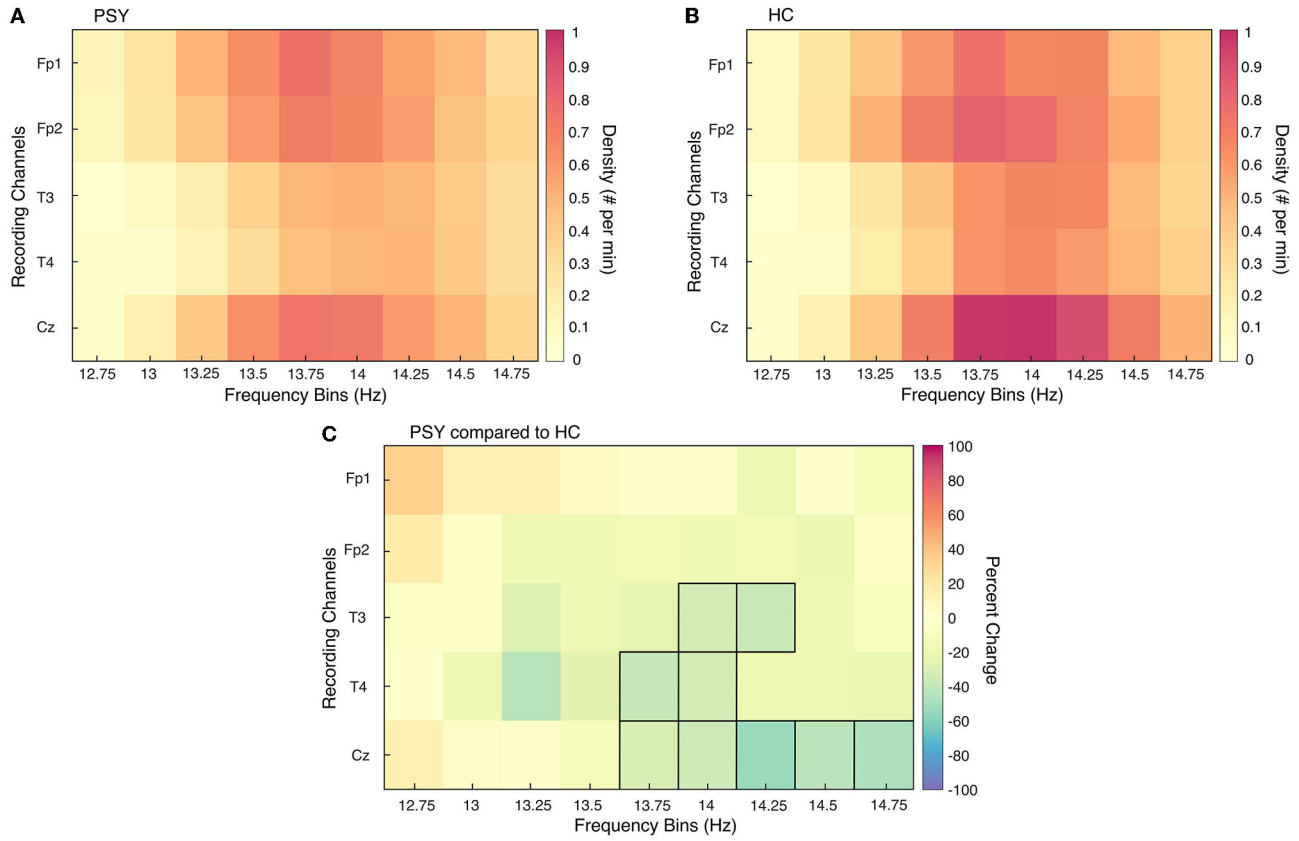

FIGURE 1
Sleep spindle density differences between PSY and HC for all channels and frequency bins. Sleep spindle density (SSD) is presented for each recording channel for all relevant frequency bins of interest for the collective patient group [PSY; **(A)**] and collective healthy control group [HC; **(B)**]. In **(C)**, the percent change in SSD is directly compared between the two groups; an increase in graph **(C)** represents an increase in SSD in PSY compared to HC. Frequency bin-channel combinations that were significantly different from unpaired *t*-tests between the two groups are outlined in black.

2.4. Statistical analyses

Sleep structure parameters and demographic and clinical characteristics were compared between patient groups and their associated HC (HC-C, HC-E, HC-N) using non-parametric Mann-Whitney *U*-tests. The same variables were compared between patient groups using non-parametric Kruskal Wallis tests. Multiple comparisons and determining the direction of interaction terms was carried out with Tukey-Kramer *post-hoc* tests for pairwise comparisons. Significant differences were considered with a p-value < 0.05. Sleep structure parameter values were calculated for either (1) the first hour of artifact-free NREM Stage 2 and 3 for each participant (the same time frame used in the sleep spindle analysis), or (2) the longest sleep recording period for each participant. The comparison of sleep structure considers the five recording electrodes shared by all groups. It was not possible to calculate sleep latency or efficiency for the NMDARE group as the time when lights were turned off was not documented.

In order to isolate the frequency band and area of interest, the a priori hypothesis regarding SSD in psychosis was investigated. This hypothesis claims that central SSD in the fast spindle frequency range is reduced in patients with psychosis compared to HC. Unpaired *t*-tests assessed SSD differences between the collective patient group (PSY; $N = 36$) and the entire HC sample ($N = 36$). A test was conducted for each recording electrode shared by all participants (Fp1, Fp2, T3, T4, Cz) at each frequency bin of interest (12–15 Hz, discretized into 0.25 steps). Values from the 12–12.5 and 15 Hz frequency bins were excluded from this analysis as the filter attenuated <20% of the signal amplitude or there were low levels of spindles, respectively. Multiple comparisons were corrected for with Benjamini and Hochberg False Discovery Rate statistical approach. Furthermore, the subsequent spindle analyses focused on values pertaining to the 13.75–14.75 Hz frequency band in the central electrode (Figure 1).

In addition to SSD, SSMA and SP were compared between the PSY and HC groups with unpaired *t*-tests. Differences in spindle parameters between the three patient groups were analyzed with one-way analysis of the variance (ANOVA); Tukey-Kramer *post-hoc* tests were applied subsequently. These two analyses were performed using spindle values specific to the central electrode (Cz). Due to large amounts of artifacts in the central electrode of two patients with NMDARE, they and their age- and sex-matched HC were not included in two above mentioned analyses. Topographical analyses of sleep spindles between each patient group and associated HC were performed with electrode-wise Student's unpaired *t*-tests; multiple comparisons were corrected for with Benjamini and Hochberg False Discovery Rate statistical approach. The comparison considers 17 electrodes for the COS and

TABLE 2 Sleep structure parameters for the longest sleep recording period.

Parameter	Patient group(s) (*N*)	Mean (SD)	HC: Mean (SD)	*p*-value	Direction (adjusted *p*-value)
Sleep latency (min)	COS (17)	36.91 (26.13)	15.47 (7.53)	**0.018**	
	EOS (11)	25.24 (17.24)	17.79 (9.22)	0.38	
	NMDARE	NaN	16.04 (7.95)	NaN	
	COS, EOS, NMDARE			NaN	
Total sleep time (min)	COS (17)	536.38 (168.66)	438.94 (50.74)	**<0.001**	
	EOS (11)	437.85 (123.67)	405.91 (80.39)	0.17	
	NMDARE (8)	557.10 (102.90)	450.58 (43.03)	**0.021**	
	COS, EOS, NMDARE			**0.026**	EOS < COS (**0.04**)
Sleep efficiency (%)	COS (17)	88.23 (17.46)	90.65 (7.51)	1.00	
	EOS (11)	87.91 (11.58)	89.39 (7.702)	1.00	
	NMDARE	NaN	89.68 (5.47)	NaN	
	COS, EOS, NMDARE			NaN	
WASO (min)	COS (17)	28.56 (79.74)	29.51 (33.75)	**0.0079**	
	EOS (11)	27.58 (21.89)	32.58 (31.71)	0.72	
	NMDARE (8)	84.79 (71.31)	38.25 (29.64)	0.20	
	COS, EOS, NMDARE			**0.0024**	COS < NMDARE (**0.0019**)
Sleep stage N1 (%)	COS (17)	3.63 (2.74)	6.54 (5.083)	**0.021**	
	EOS (11)	6.71 (3.93)	6.88 (5.51)	0.84	
	NMDARE (8)	19.04 (25.16)	4.13 (3.02)	0.11	
	COS, EOS, NMDARE			**0.028**	Inconclusive
Sleep stage N2 (%)	COS (17)	49.48 (21.61)	51.50 (6.65)	0.86	
	EOS (11)	48.06 (10.24)	53.04 (3.80)	0.36	
	NMDARE (8)	40.78 (14.88)	47.38 (8.00)	0.51	
	COS, EOS, NMDARE			0.45	
Sleep stage N3 (%)	COS (17)	29.70 (24.46)	23.77 (7.51)	0.95	
	EOS (11)	26.07 (13.01)	22.29 (6.26)	0.89	
	NMDARE (8)	21.8 (9.25)	30.82 (8.32)	**0.083**	
	COS, EOS, NMDARE			0.91	
REM sleep (%)	COS (17)	17.19 (10.73)	18.19 (5.19)	0.78	
	EOS (11)	19.16 (7.69)	17.78 (3.46)	0.29	
	NMDARE (8)	18.38 (9.50)	17.67 (3.27)	0.33	
	COS, EOS, NMDARE			0.66	

COS, childhood-onset schizophrenia; EOS, early-onset schizophrenia; NMDARE, anti-*N*-methyl-D-aspartate receptor encephalitis; WASO, wake after sleep onset; SD, standard deviation; NaN, not a number, data missing. HC were 1:1 matched to each patient. When comparing the three patient groups with Kruskal Wallis Tests, any significant difference is reported represented by the adjusted *p*-value and direction of the difference. The bold values imply statistical significance.

EOS groups and five electrodes for the NMDARE group. Normal distribution of the data was visualized with quantile-quantile plots and objectively confirmed with Shapiro-Wilk tests.

Furthermore, to assess potential relationships between sleep spindle parameters and illness duration, partial Pearson correlation analysis were performed controlling for age and chlorpromazine equivalent. This analysis was conducted in patients with SZ (COS, EOS). As only patients with SZ were included in this analysis, the value of sleep spindle parameters were taken from the mean of all available central electrodes (C3, Cz, C4).

3. Results

3.1. Demographic and clinical characteristics and sleep parameters

3.1.1. Demographic and clinical characteristics

No significant difference was found for age and sex between patient groups and associated HC and inter-patient groups (see Table 1). The COS group had a significantly longer duration of illness and a lower age of disease onset when compared to the EOS

10.3389/fpsyt.2023.1055459

TABLE 3 Sleep structure parameters for the first hour of artifact-free NREM stage 2 and 3 sleep.

Parameter	Patient group(s) (*N*)	Mean (SD)	HC: Mean (SD)	*p*-value	Direction (adjusted *p*-value)
Absolute length of first hour (min)	COS (17)	70.68 (26.35)	81.12 (38.98)	**0.0071**	
	EOS (11)	74.91 (17.80)	67.49 (2.96)	0.77	
	NMDARE (8)	123 (62.76)	68.25 (5.97)	**0.027**	
	COS, EOS, NMDARE			**0.0028**	COS < NMDARE (**0.0031**)
WASO (%)	COS (17)	0.14 (0.30)	5.01 (11.85)	**0.0019**	
	EOS (11)	5.90 (11.33)	1.43 (2.42)	0.50	
	NMDARE (8)	16.81 (15.73)	2.04 (3.77)	**0.015**	
	COS, EOS, NMDARE			**<0.001**	COS < EOS (**0.045**)
					COS < NMDARE (**<0.001**)
Sleep stage N1 (%)	COS (17)	0.35 (0.70)	4.39 (6.61)	**<0.001**	
	EOS (11)	4.20 (4.78)	2.23 (2.53)	0.45	
	NMDARE (8)	10.62 (15.82)	2.06 (4.21)	**0.063**	
	COS, EOS, NMDARE			**<0.001**	COS < EOS (**0.013**)
					COS < NMDARE (**<0.001**)
Sleep stage N2 (%)	COS (17)	39.04 (27.78)	29.67 (7.05)	0.84	
	EOS (11)	27.13 (8.78)	39.58 (14.74)	0.057	
	NMDARE (8)	27.02 (17.80)	24.97 (24.60)	0.51	
	COS, EOS, NMDARE			0.65	
Sleep stage N3 (%)	COS (17)	57.47 (31.60)	58.49 (21.91)	0.65	
	EOS (11)	62.26 (20.51)	56.45 (15.38)	0.43	
	NMDARE (8)	39.11 (22.01)	70.92 (29.80)	0.051	
	COS, EOS, NMDARE			0.18	
REM sleep (%)	COS (17)	2.95 (8.83)	2.44 (4.64)	0.49	
	EOS (11)	0.50 (1.24)	0.31 (0.78)	0.96	
	NMDARE (8)	6.43 (4.15)	0 (0)	**0.007**	
	COS, EOS, NMDARE			**0.0062**	COS < NMDARE (**0.012**)
					EOS < NMDARE (**0.011**)

COS, childhood-onset schizophrenia; EOS, early-onset schizophrenia; NMDARE, anti-*N*-methyl-D-aspartate receptor encephalitis; WASO, wake after sleep onset; SD, standard deviation. HC were 1:1 matched to each patient. When comparing the three patient groups with Kruskal Wallis Tests, any significant difference is reported represented by the adjusted *p*-value and direction of the difference. The bold values imply statistical significance.

group. Additionally, the COS group had significantly higher levels of medication, measured in chlorpromazine equivalent, than the EOS group. No significant differences were found in IQ between the COS and EOS groups.

3.1.2. Sleep parameters

Differences in sleep structure and quality for the entire night are reported in Table 2. Patients with COS took longer to fall asleep and spent more time asleep compared to HC-C. After initial sleep onset, they spent less time awake during the entire night. Sleep characteristics were comparable between the patients with EOS and HC-E. Patients with NMDARE slept for significantly longer than HC-N. Differences in sleep parameters were also detected when comparing patient groups. Patients with EOS slept for a shorter amount of time than those with COS. Patients with COS spent less time awake during the entire night following initial sleep onset than those with NMDARE. A statistical difference in percent of all-night time spent in NREM sleep stage 1 was found in the omnibus test, yet no significant differences between the means of each group (COS, EOS, NMDARE) were detected when assessing with *post-hoc* multiple comparisons.

Sleep parameters were also calculated for the time frame used in the sleep spindle analysis (Table 3). This refers to the amount of time it took to isolate 60 minu of artifact-free NREM stage 2 and 3 sleep from each participant. This amount of time was shorter for patients with COS compared to HC-C. Patients with COS also spent less time awake following initial descent into sleep and time in NREM sleep stage 1 during the first hour. The amount of time needed to isolate 60 min of artifact-free sleep in the NMDARE group was significantly longer as when compared to HC-N. Additionally, they spent more time awake and in REM sleep

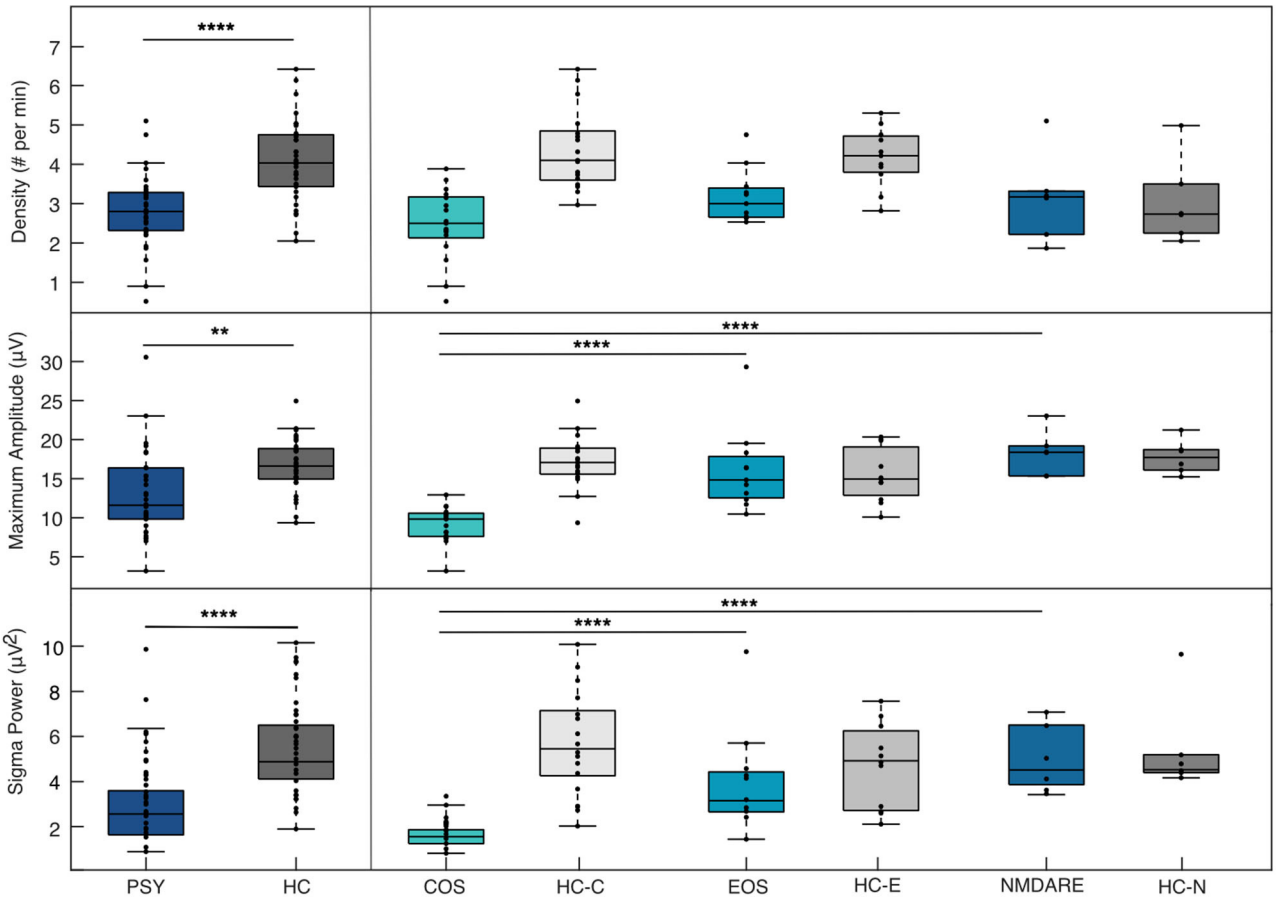

FIGURE 2
Sleep spindle parameter differences between PSY and HC & patient groups. Differences in sleep spindle parameters between the collective patient groups (PSY) and collective healthy control group (HC) are show in the left panel and between individual patient groups composing the PSY group [Childhood-Onset Schizophrenia (COS), Early-Onset Schizophrenia (EOS), anti-N-methyl-D-aspartate receptor encephalitis (NMDARE)] in the right panel. Note that significant differences between individual patient groups and associated HC are not presented here. All spindle values here are taken from the central electrode from the frequency band of 13.75–14.75 Hz. The * denotes a significant difference between the groups according to *p*-values (<0.05 implies significance). ** = $p \leq 0.01$; **** = $p \leq 0.0001$.

during the first hour compared to HC-N. When comparing patient groups, it was found that the absolute length of the first hour was less in COS when compared to NMDARE. Additionally, the COS group spent less time awake and in NREM sleep stage 1 compared to the EOS and NMDARE group. Finally, both the COS and EOS groups spent less time than the NMDARE group in REM sleep.

3.2. Sleep spindle parameters

3.2.1. Sleep spindle differences between PSY and HC and patient groups

Based on results from the unpaired *t*-test, sleep spindle parameter values from the frequency range of 13.75–14.5 Hz pertaining to the Cz electrode were used to compare the PSY and HC groups and the three patient groups. Results assessing SSD, SSMA, and SP differences between the PSY and HC groups are presented in the left column of Figure 2. For all parameters, the PSY group showed significant reductions in spindle characteristics when compared to the HC group [SSD: $t(66) = -5.24$, $p < 0.00001$; SSMA: $t(66) = -3.43$, $p = 0.0011$; SP: $t(66) = -4.20$, $p < 0.0001$].

ANOVA conducted comparing the three groups and SSD, SSMA, and SP are presented in the right column of Figure 2. No differences in SSD were found between the three groups [$F(2, 31) = 2.59$, $p = 0.091$]. For SSMA and SP, the COS group was significantly reduced compared to the EOS [SSMA: $p < 0.0001$, 95% C.I. = $(-10.58, -3.49)$; SP: $p < 0.001$, 95% C.I. = $(-4.03, -1.06)$] and the NMDARE groups [SSMA: $p < 0.0001$, 95% C.I. = $(-13.49, -4.79)$; SP: $p < 0.001$, 95% C.I. = $(-4.94, -1.29)$]. No significant differences in SSMA [$F(2, 31) = 19.19$, $p = 0.51$] and SP [$F(2, 31) = 13.4$, $p = 0.75$] were found between the EOS and NMDARE groups.

3.2.2. Topographical distribution of sleep spindles between patient groups and associated HC

Topographical comparisons of sleep spindle parameters between patient groups and associated HC are presented in Figure 3. As previously reported (33), the COS group shows global significant decreases in all sleep spindle parameters compared to

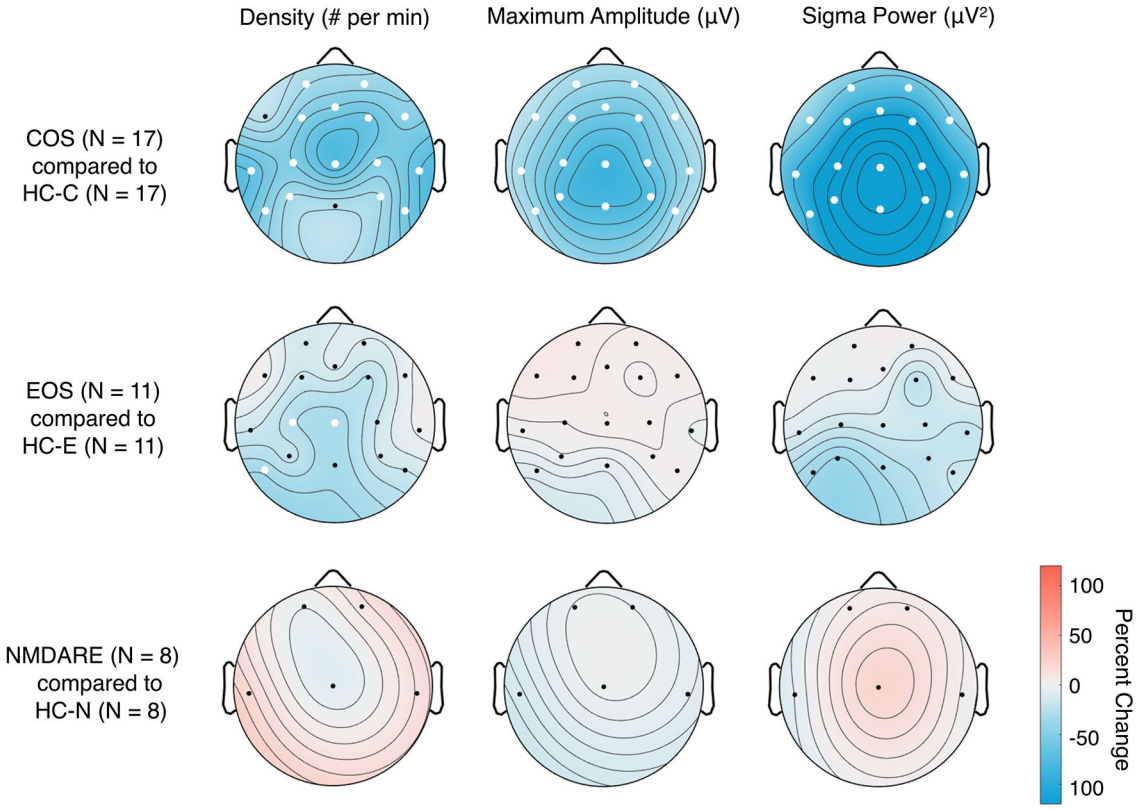

FIGURE 3
Topographical distribution of sleep spindle parameters in patient groups compared to associated HC. Two-tailed Student's unpaired *t*-tests with standard alpha-values at 0.05 were used; significant differences between the groups in individual electrodes are designated by white dots. The colors represent the percent change of the given sleep spindle parameter when comparing the patient group [Childhood-Onset Schizophrenia (COS), Early-Onset Schizophrenia (EOS), and anti-*N*-methyl-D-aspartate receptor encephalitis (NMDARE)] to the associated healthy control groups (HC-C, HC-E, and HC-N, associated with COS, EOS and NMDARE, respectively) group; e.g., a percent increase represents values that are higher in the patient group compared to HC and a percent decrease represents values that are lower in the patient group compared to HC.

HC-C. As expected, the EOS group shows significant reductions in SSD in the central region and left, posterior temporal region compared to HC-E (32). Sleep spindles for the NMDARE group were statistically comparable to the HC-N group.

3.3. Association between sleep spindles and duration of the disorder

For all patients with SZ, SP derived from the mean of central electrodes (C3, Cz, C4) was found to be significantly negatively correlated with the duration of illness ($r = -0.41$, $p = 0.035$). Duration of illness was not significantly associated with SSD ($r = -0.11$, $p = 0.603$). There was a trend for a negative correlation between duration of illness and SSMA ($r = -0.37$, $p = 0.061$). All sleep spindle parameters and duration of illness are presented in Figure 4.

4. Discussion

The main finding of this study is that all sleep spindle parameters (SSD, SSMA, SP) were reduced in the pooled sample of patients affected by SZ or NMDARE compared to matched HC. SSD was statistically comparable between the three patient groups, however patients with NMDARE showed no significant alterations in sleep spindle parameters when compared to HC-N. Young patients affected by SZ showed reductions in SSD compared to HC; the COS group also exhibited reductions in SSMA and SP. Further, in patients with SZ, reduced SP was associated with a longer duration of illness.

4.1. Sleep spindle parameters in patients with SZ

Consistent with previous literature, reduced SSD was found in patients with SZ compared to HC (9, 29, 32, 33). Topographical analysis of SSD indicated widespread reductions in patients with COS, whereas deficits in patients with EOS were restricted to primarily central electrodes. No significant differences were found in SSD measured from the central electrode between the COS and EOS groups. Patients with COS also showed global reductions in SSMA and SP, whereas no changes in these spindle parameters were found in the EOS group when comparing to HC. The COS and EOS groups differ by definition in the age of disease onset, and in this study the COS group also had a longer duration of

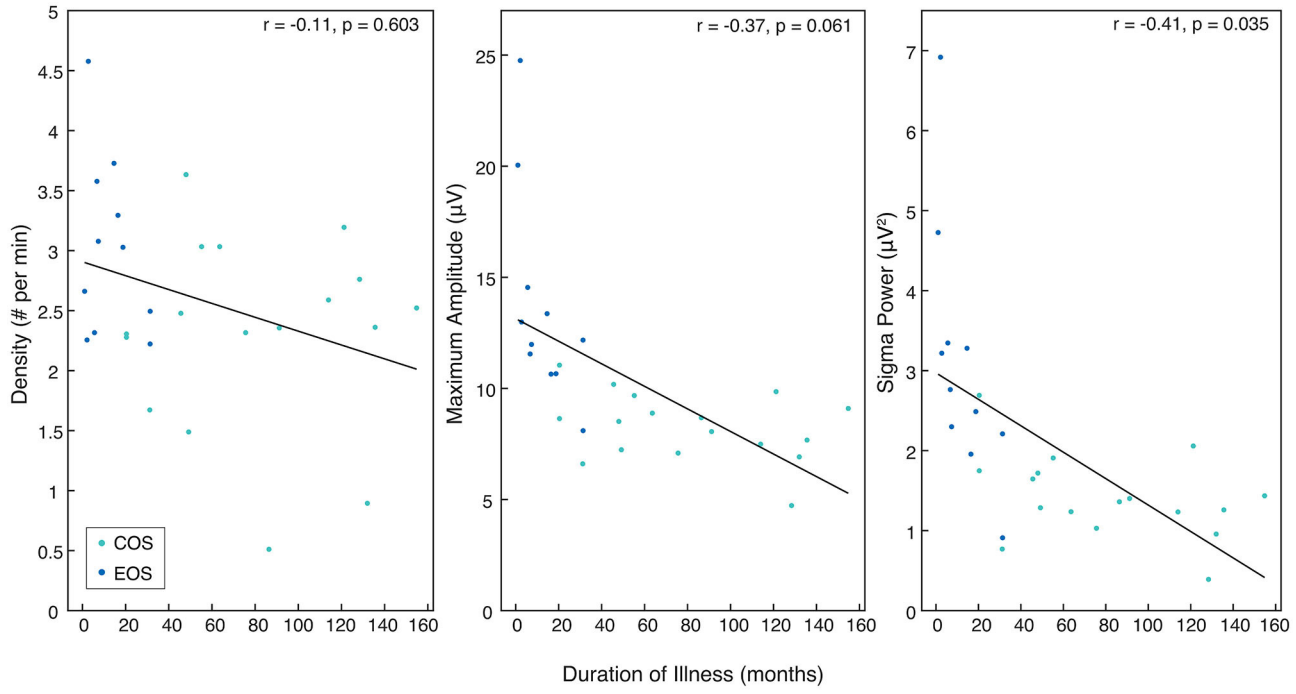

FIGURE 4
The relationship between sleep spindle parameters in patients with SZ and duration of illness. Rho and *p*-values are presented for each sleep spindle parameter when compared to duration of illness in months. All values come from the mean of the central electrodes (C3, C4, Cz) and pertain to either the Childhood-Onset Schizophrenia (COS) group (light blue) or the Early-Onset Schizophrenia (EOS) group (dark blue).

illness and higher chlorpromazine equivalent than the EOS group. The longer duration of illness is explained by the fact that sleep data from patients with EOS were recorded promptly following disease onset, whereas data from patients with COS were recorded during follow-up assessments years after the initial emergence of the disorder. This is further illustrated by the fact that the mean age at the time of the sleep assessment did not differ between the groups. Thus, in terms of duration of illness, patients with EOS rather resemble adult samples with early course psychosis or first episode SZ whereas young patients with COS may rather be compared to patients with a chronic course of SZ. Considered in this light, the findings are in line with previous literature, namely the vast reduction of SSD in COS corresponds to global reduced SSD in adults with chronic SZ (10, 50). Likewise, the local reduction of SSD in patients with EOS compared to HC-E is consistent with findings in adult patients experiencing their first episode of psychosis (51). Additionally, SSMA and SP reductions in patients with COS are similar to findings from adult samples with chronic SZ (11). When comparing adult patients with chronic SZ to HC, the effect size of the reduction was highest for SSD, followed by SP, and then SSMA. In contrast, in adult first episode psychosis or early course SZ patients there was no significant reduction in SSMA, similar to the results regarding the EOS group (29, 51). Many factors influence spindle characteristics, including genes (52), illness duration (34, 43), and severity of symptomatology (42). Given the current sample size and heterogeneity in our population, we were unable to individually examine the impact of these parameters on spindle characteristics, however, this may be a fruitful future avenue.

The potential impact of the duration of illness in the COS and EOS groups was further explored, resulting in a significant relationship between reduced SP and longer duration of illness. Although individual studies have reported no association between sleep spindle activity and duration of illness or chlorpromazine equivalent in their samples (10, 53), a recent meta-analysis including eight studies demonstrated that across all individuals, the longer the illness lasted, the lower the SSD (34). Specifically for every year of illness, SSD decreased by 0.2 spindles per minute. In conclusion, it is assumed that in this sample, as in previous single studies with similar numbers of patients, the correlation analysis of SSD with duration of illness may have been underpowered. Additionally, while age-specific aspects of sleep spindles may be accounted for by age- and sex-matching when comparing patients and HC, directly comparing the patient sample may be confounded by developmental aspects of sleep spindles across the whole age-range (14, 54).

4.2. Sleep spindle parameters in young patients with NMDARE

Central SSD was reduced in the collective patient group compared to HC and no significant differences were found between the patient groups. This suggests that all patient groups contribute to the low, central SSD. However, no significant differences in any of the sleep spindle parameters were found when comparing NMDARE to HC-N. This finding may at least in part be due to

the sample size and inter-individual variability making any definite conclusions challenging. Nonetheless, strong and global deficits in sleep spindles as found in patients with COS might have been detected irrespective of these limitations.

The exact molecular mechanism and pathways of neurotransmission underlying spindle deficits in patients with SZ is unclear. It has been suggested that a reduced binding or expression of the glutamatergic NMDAR within the thalamo-cortical system may be the key element contributing to early reductions in SSD (51). Further, postmortem studies found reductions of the NMDAR in the thalamus and in the cortex of patients with SZ (55). On the other hand, based on the premise that the spindle-pacemaker relies on GABAergic neurons, it has been hypothesized that GABA deficits may trigger the reduction in SSD whereas a hypofunction of the NMDAR within the thalamo-cortical feedback loop may rather impact the maintenance and modulation of sleep spindles and their coordination with other oscillations (53). Accordingly, the administration of eszopiclone, a GABA agonist targeting the thalamic reticular nucleus, in patients affected by SZ results in increased SSD (56). Additionally, an *in vitro* model showed that a blockade of the NMDAR shortened the spindle-like oscillation, but only the combined blockade of the NMDAR and GABA receptor repressed the spindle-like oscillation (13). Thus, the findings suggesting that patients with NMDARE do not have large spindle deficits rather support previous literature and the hypothesis that NMDAR-mediated hypofunction alone does not account for pronounced deficits in SSD. Specifically, the explicit antibody-mediated reduction of functional NMDAR in NMDARE may not entirely mimic the far less clear beginning and timing of abnormalities on the NMDAR during development and its impact on GABAergic activity and thalamocortical integrity in SZ (57, 58). Although speculative, it is possible that further research in NMDARE with increased sample size, age range, and density of electrodes may uncover more subtle reductions of SSD, perhaps making it similar to early stages of SZ such as the patient group with EOS.

4.3. Limitations and outlook

The results of the present study should be interpreted within the confines of several limitations. The rarity of NMDARE and Childhood- and Early-Onset SZ make the data of the included individuals very valuable, but the low sample size renders the statistical analyses less robust and age- and sex-matching between the patient groups challenging. Additionally, sleep disorders in the NMDARE group of patients were not assessed systematically. Thus, it remains difficult to discern and weigh the impact of the sleep spindle parameter findings, as well as the relationship with duration of illness. Further, analysis of the sleep structure showed group-specific differences that may be due to different medication and recording settings. However, sleep spindles predominantly appear in sleep stage N2, which was comparable between all groups.

Assessing sleep spindles and their coordination with other oscillations, specifically slow waves, in longitudinal studies may be essential to further discern the pathomechanism of SZ and to identify targets for novel interventions to treat this debilitating disorder. Likewise, sleep studies in larger samples of patients with NMDARE or with pharmacological models mimicking the NMDAR hypofunction may further elucidate similarities and dissimilarities of underlying signaling and thalamo-cortical impairments.

Data availability statement

The original contributions presented in the study are included in the article/supplementary material, further inquiries can be directed to the corresponding author.

Ethics statement

The studies involving human participants were reviewed and approved by Ethics Committee of the Canton of Zurich and Bern, Switzerland, BASEC 2021-00215. Written informed consent to participate in this study was provided by the participants' legal guardian/next of kin.

Author contributions

AM, SG, MN, KR, SS, AS, SK, BB, and MG previously collected, provided, and/or analyzed patient data. BB and MG contributed to the conception of the project and the study design. MG additionally contributed to the writing process. MD contributed to the project design, data analysis, and writing process. MG, BB, LT, and RH closely supervised the project. All authors reviewed and approved the article for submission.

Funding

This work was supported by the Frutiger Foundation (to MG), Swiss National Science Foundation 320030_153387 (to RH), PCEFP1-181279 (to SK), and 32003B_184943 (to LT), radiz—Rare Disease Initiative Zurich (to SG), Interfaculty Research Cooperation: Decoding Sleep (to LT), the Anna Müller Grocholski foundation (to BB), and the EMDO foundation (to BB and MG). This research was also supported in part by the Intramural Research Program of the National Institute of Mental Health (Annual Report Number ZIAMH002581, ClinicalTrials.gov identifier NCT00001198, protocol ID 84-M-0050). Additionally, MN and SS were supported by the project DOR2008453/20, University of Padova (systematic literature review and evidence-based international consensus recommendations for the treatment of pediatric anti-NMDAR encephalitis, MN).

Acknowledgments

We would like to thank the young participants who volunteered their time and/or data for the project, as well as their

families for supporting their participation. We would also like to thank the whole of RH's lab for their crucial advice and support.

Conflict of interest

In the past five years, SW has received royalties from Thieme Hogrefe, Kohlhammer, Springer, and Beltz, and her work was supported by the Swiss National Science Foundation (SNF), diff. EU FP7s, Bfarm Germany, ZInEP, Hartmann Müller, Olga Mayenfisch, Gertrud Thalmann, Vontobel, Unicentia, and Erika Schwarz Funds.

The remaining authors declare that the research was conducted in the absence of any commercial or financial relationships that could be construed as a potential conflict of interest.

Publisher's note

All claims expressed in this article are solely those of the authors and do not necessarily represent those of their affiliated organizations, or those of the publisher, the editors and the reviewers. Any product that may be evaluated in this article, or claim that may be made by its manufacturer, is not guaranteed or endorsed by the publisher.

References

1. Kaskie RE, Graziano B, Ferrarelli F. Schizophrenia and sleep disorders: links, risks, and management challenges. *Nat Sci Sleep*. (2017) 9:227–33. doi: 10.2147/NSS.S121076

2. Winsky-Sommerer R, de Oliveira P, Loomis S, Wafford K, Dijk DJ, Gilmour G. Disturbances of sleep quality, timing and structure and their relationship with other neuropsychiatric symptoms in Alzheimer's disease and schizophrenia: Insights from studies in patient populations and animal models. *Neurosci Biobehav Rev*. (2018) 97:112–37. doi: 10.1016/j.neubiorev.2018.09.027

3. Zhang Y, Quiñones GM, Ferrarelli F. Sleep spindle and slow wave abnormalities in schizophrenia and other psychotic disorders: Recent findings and future directions. *Schizophr Res*. (2020) 221:29–36. doi: 10.1016/j.schres.2019.11.002

4. Vukadinovic Z. Sleep abnormalities in schizophrenia may suggest impaired trans-thalamic cortico-cortical communication: towards a dynamic model of the illness. *Eur J Neurosci*. (2011) 34:1031–9. doi: 10.1111/j.1460-9568.2011.07822.x

5. Benson KL. Sleep in schizophrenia: impairments, correlates, and treatment. *Psychiatr Clin North Am*. (2006) 29:1033–45. doi: 10.1016/j.psc.2006.08.002

6. Lunsford-Avery JR, LeBourgeois MK, Gupta T, Mittal VA. Actigraphic-measured sleep disturbance predicts increased positive symptoms in adolescents at ultra high-risk for psychosis: a longitudinal study. *Schizophr Res*. (2015) 164:15–20. doi: 10.1016/j.schres.2015.03.013

7. Ruhrmann S, Schultze-Lutter F, Salokangas RK, Heinimaa M, Linszen D, Dingemans P, et al. Prediction of psychosis in adolescents and young adults at high risk: results from the prospective European prediction of psychosis study. *Arch Gen Psychiatry*. (2010) 67:241–51. doi: 10.1001/archgenpsychiatry.2009.206

8. Manoach DS, Pan JQ, Purcell SM, Stickgold R. Reduced sleep spindles in schizophrenia: a treatable endophenotype that links risk genes to impaired cognition? *Biol Psychiatry*. (2015) 80:1–10. doi: 10.1016/j.biopsych.2015.10.003

9. D'Agostino A, Castelnovo A, Cavallotti S. Sleep endophenotypes of schizophrenia: slow waves and sleep spindles in unaffected first-degree relatives. *npj Schizophr*. (2018) 4:2. doi: 10.1038/s41537-018-0045-9

10. Ferrarelli F, Huber R, Peterson MJ, Massimini M, Murphy M, Riedner BA, et al. Reduced sleep spindle activity in schizophrenia patients. *Am J Psychiatry*. (2007) 164:483–92. doi: 10.1176/ajp.2007.164.3.483

11. Castelnovo A, Graziano B, Ferrarelli F. D'Agostino A. Sleep spindles and slow waves in schizophrenia and related disorders: main findings, challenges and future perspectives. *Eur J Neurosci*. (2018) 48:2738–58. doi: 10.1111/ejn.13815

12. Steriade M, Domich L, Oakson G, Deschenes M. The deafferented reticular thalamic nucleus generates spindle rhythmicity. *J Neurophysiol*. (1987) 57:260–73. doi: 10.1152/jn.1987.57.1.260

13. Jacobsen RB, Ulrich D, Huguenard JR. GABA(B) and NMDA receptors contribute to spindle-like oscillations in rat thalamus *in vitro*. *J Neurophysiol*. (2001) 86:1365–75. doi: 10.1152/jn.2001.86.3.1365

14. Fernandez L, Lüthi A. Sleep spindles: mechanisms and functions. *Physiol Rev*. (2020) 100:805–68. doi: 10.1152/physrev.00042.2018

15. Astori S, Wimmer RD, Lüthi A. Manipulating sleep spindles - expanding views on sleep, memory, and disease. *Trends Neurosci*. (2013) 6:738–48. doi: 10.1016/j.tins.2013.10.001

16. Manoach DS, Stickgold R. Abnormal sleep spindles, memory consolidation, and schizophrenia. *Annu Rev Clin Psychol*. (2019) 15:451–79. doi: 10.1146/annurev-clinpsy-050718-095754

17. Coyle JT. NMDA receptor and schizophrenia: a brief history. *Schizophr Bull*. (2012) 38:920–6. doi: 10.1093/schbul/sbs076

18. Kayser MS, Dalmau J. Anti-NMDA receptor encephalitis, autoimmunity, and psychosis. *Schizophr Res*. (2016) 176:36–40. doi: 10.1016/j.schres.2014.10.007

19. Manoach DS, Mylonas D, Baxter B. Targeting sleep oscillations to improve memory in schizophrenia. *Schizophr Res*. (2020) 221:63–70. doi: 10.1016/j.schres.2020.01.010

20. Dalmau J, Gleichman AJ, Hughes EG, Rossi JE, Peng X, Lai M, et al. Anti-NMDA-receptor encephalitis: case series and analysis of the effects of antibodies. *Neurology*. (2008) 7:1091–8. doi: 10.1016/S1474-4422(08)70224-2

21. Steullet P, Cabungcal JH, Monin A, Dwir D, O'Donnell P, Cuenod M, et al. Redox dysregulation, neuroinflammation, and NMDA receptor hypofunction: A "central hub" in schizophrenia pathophysiology? *Schizophr Res*. (2016) 176:41–51. doi: 10.1016/j.schres.2014.06.021

22. Gefferie SR, Maric A, Critelli H, Gueden S, Kurlemann G, Kurth S, et al. Altered EEG markers of synaptic plasticity in a human model of NMDA receptor deficiency: anti-NMDA receptor encephalitis. *NeuroImage*. (2021) 239:118281. doi: 10.1016/j.neuroimage.2021.118281

23. Lee G, Zhou Y. NMDAR hypofunction animal models of schizophrenia. Front Mol Neurosci. (2019) 12:185. doi: 10.3389/fnmol.2019.00185

24. Marsman A, Van Den Heuvel MP, Klomp DW, Kahn RS, Luijten PR, Hulshoff Pol HE. Glutamate in schizophrenia: a focused review and meta-analysis of 1H-MRS studies. *Schizophr Bull*. (2013) 39:120–9. doi: 10.1093/schbul/sbr069

25. Uhlhaas PJ, Singer W. The development of neural synchrony and large-scale cortical networks during adolescence: relevance for the pathophysiology of schizophrenia and neurodevelopmental hypothesis. *Schizophr Bull*. (2011) 37:514–23. doi: 10.1093/schbul/sbr034

26. Moghaddam B, Javitt D. From revolution to evolution: the glutamate hypothesis of schizophrenia and its implication for treatment. *Neuropsychopharmacol*. (2012) 37:4–15. doi: 10.1038/npp.2011.181

27. McCutcheon RA, Krystal JH, Howes OD. Dopamine and glutamate in schizophrenia: biology, symptoms and treatment. *World Psychiatry*. (2020) 19:15–33. doi: 10.1002/wps.20693

28. Florance NR, Davis RL, Lam C, Szperka C, Zhou L, Ahmad S, et al. Anti-N-methyl-D-aspartate receptor (NMDAR) encephalitis in children and adolescents. *Ann Neurol*. (2009) 66:11–8. doi: 10.1002/ana.21756

29. Manoach DS, Demanuele C, Wamsley EJ, Vangel M, Montrose DM, Miewald J, et al. Sleep spindle deficits in antipsychotic-naïve early course schizophrenia and in non-psychotic first-degree relatives. *Front Hum Neurosci*. (2014) 8:762. doi: 10.3389/fnhum.2014.00762

30. Paus T, Keshavan M, Giedd JN. Why do many psychiatric disorders emerge during adolescence? *Nat Rev Neurosci*. (2008) 9:947–57. doi: 10.1038/nrn2513

31. Shaw P, Kabani NJ, Lerch JP, Eckstrand K, Lenroot R, Gogtay N, et al. Neurodevelopmental trajectories of the human cerebral cortex. *J Neurosci*. (2008) 28:3586–94. doi: 10.1523/JNEUROSCI.5309-07.2008

32. Gerstenberg M, Furrer M, Tesler N, Franscini M, Walitza S, Huber R. Reduced sleep spindle density in adolescent patients with early-onset schizophrenia compared to major depressive disorder and healthy controls. *Schizophr Res*. (2020) 221:20–8. doi: 10.1016/j.schres.2019.11.060

33. Markovic A, Buckley A, Driver DI, Dillard-Broadnax D, Gochman PA, Hoedlmoser K, et al. Sleep spindle activity in childhood onset schizophrenia: diminished and associated with clinical symptoms. *Schizophr Res*. (2020) 223:327–36. doi: 10.1016/j.schres.2020.08.022

34. Lai M, Hegde R, Kelly S, Bannai D, Lizano P, Stickgold R, et al. Investigating sleep spindle density and schizophrenia: a meta-analysis. *Psychiatry Res.* (2022) 307:114265. doi: 10.1016/j.psychres.2021.114265

35. American Psychiatric Association. *Diagnostic and Statistical Manual of Mental Disorders (3rd ed., revised)* (1987).

36. American Psychiatric Association. *Diagnostic and Statistical Manual of Mental Disorders (4th ed.)* (1994).

37. Sheehan DV, Sheehan KH, Shytle RD, Janavs J, Bannon Y, Rogers JE, et al. Reliability and validity of the Mini International Neuropsychiatric Interview for Children and Adolescents (MINI-KID). *J Clin Psychiatry*. (2010) 71:313–26. doi: 10.4088/JCP.09m05305whi

38. Iber C, Ancoli-Israel SAC. The AASM manual for the scoring of sleep and associated events: rules, terminology and technical specifications. *Am Acad Sleep Med.* (2007).

39. Huber R, Deboer T, Tobler I. Sleep deprivation in prion protein deficient mice and control mice: genotype dependent regional rebound. *Neuroreport*. (2002) 13:1–4. doi: 10.1097/00001756-200201210-00005

40. Buckelmüller J, Landolt HP, Stassen HH, Achermann P. Trait-like individual differences in the human sleep electroencephalogram. *Neuroscience.* (2006) 138:351–6. doi: 10.1016/j.neuroscience.2005.11.005

41. Cox R, Schapiro AC, Manoach DS, Stickgold R. Individual differences in frequency and topography of slow and fast sleep spindles. *Front Hum Neurosci*. (2017) 11:241–51. doi: 10.3389/fnhum.2017.00433

42. Ferrarelli F, Peterson MJ, Sarasso S, Riedner BA, Murphy MJ, Benca RM, et al. Thalamic dysfunction in schizophrenia suggested by whole-night deficits in slow and fast spindles. *Am J Psychiatry*. (2010) 167:1339–48. doi: 10.1176/appi.ajp.2010.09121731

43. Markovic A, Buckley A, Driver DI, Dillard-Broadnax D, Gochman PA, Hoedlmoser K, et al. Sleep neurophysiology in childhood onset schizophrenia. *J Sleep Res.* (2020) 30:e13039. doi: 10.1111/jsr.13039

44. Yao D, Qin Y, Hu S. Which reference should we use for EEG and ERP practice? *Brain Topogr*. (2019) 32:530–49. doi: 10.1007/s10548-019-00707-x

45. Leuchs L. Choosing your reference - and why it matters. *Brain Prod. Solut Neurohysiol Res.* (2019). Available online at: https://pressrelease.brainproducts.com/referencing/

46. Vukadinovic Z. Sleep spindle reductions in schizophrenia and its implications for the development of cortical body map. *Schizophr Res*. (2015) 168:589–90. doi: 10.1016/j.schres.2015.08.012

47. Lustenberger C, Wehrle F, Tüshaus L, Achermann P, Huber R. The multidimensional aspects of sleep spindles and their relationship to word-pair memory consolidation. *Sleep*. (2015) 38:1093–103. doi: 10.5665/sleep.4820

48. Dijk DJ, EEG. slow waves and sleep spindles: windows on the sleeping brain. *Behav Brain Res*. (1995) 69:109–16. doi: 10.1016/0166-4328(95)00007-G

49. Warby SC, Wendt SL, Welinder P, Munk EG, Carrillo O, Sorensen HB, et al. Sleep-spindle detection: crowdsourcing and evaluating performance of experts, non-experts and automated methods. *Nat Methods*. (2014) 11:385–92. doi: 10.1038/nmeth.2855

50. Manoach DS, Thakkar KN, Stroynowski E, Ely A, McKinley SK, Wamsley E, et al. Reduced overnight consolidation of procedural learning in chronic medicated schizophrenia is related to specific sleep stages. *J Psychiatr Res*. (2010) 44:112–20. doi: 10.1016/j.jpsychires.2009.06.011

51. Kaskie RE, Gill KM, Ferrarelli F. Reduced frontal slow wave density during sleep in first-episode psychosis. *Schizophr Res*. (2019) 206:318–24. doi: 10.1016/j.schres.2018.10.024

52. Rusterholz T, Hamann C, Markovic A, Schmidt SJ, Achermann P, Tarokh L. Nature and nurture: brain region specific inheritance of sleep neurophysiology in adolescence. *J Neurosci.* (2018) 38:9275–85. doi: 10.1523/JNEUROSCI.0945-18.2018

53. Wamsley EJ, Tucker MA, Shinn AK, Ono KE, McKinley SK, Ely AV, et al. Reduced sleep spindles and spindle coherence in schizophrenia: mechanisms of impaired memory consolidation? *Biol Psychiat*. (2012) 71:154–61. doi: 10.1016/j.biopsych.2011.08.008

54. Purcell S, Manoach D, Demanuele C. Characterizing sleep spindles in 11,630 individuals from the National Sleep Research Resource. *Nat Commun.* (2017) 8:15930. doi: 10.1038/ncomms15930

55. Pakkenberg B. Scheel-Krüger J, Kristiansen LV. Schizophrenia; from structure to function with special focus on the mediodorsal thalamic prefrontal loop. *Acta Psychiatr Scand*. (2009) 120:345–54. doi: 10.1111/j.1600-0447.2009.01447.x

56. Mylonas D, Baran B, Demanuele C, Cox R, Vuper TC, Seicol BJ, et al. The effects of eszopiclone on sleep spindles and memory consolidation in schizophrenia: a randomized clinical trial. *Neuropsychopharmacol*. (2020) 45:2189–97. doi: 10.1038/s41386-020-00833-2

57. Cohen SM, Tsien RW, Goff DC, Halassa MM. The impact of NMDA receptor hypofunction on GABAergic neurons in the pathophysiology of schizophrenia. *Schizophr Res*. (2015) 167:98–107. doi: 10.1016/j.schres.2014.12.026

58. Nakazawa K, Jeevakumar V, Nakao K. Spatial and temporal boundaries of NMDA receptor hypofunction leading to schizophrenia. *NPJ Schizophr*. (2017) 3:98–107. doi: 10.1038/s41537-016-0003-3

Frontiers in Psychiatry

Explores and communicates innovation in the field of psychiatry to improve patient outcomes

The third most-cited journal in its field, using translational approaches to improve therapeutic options for mental illness, communicate progress to clinicians and researchers, and consequently to improve patient treatment outcomes.

Discover the latest Research Topics

See more →

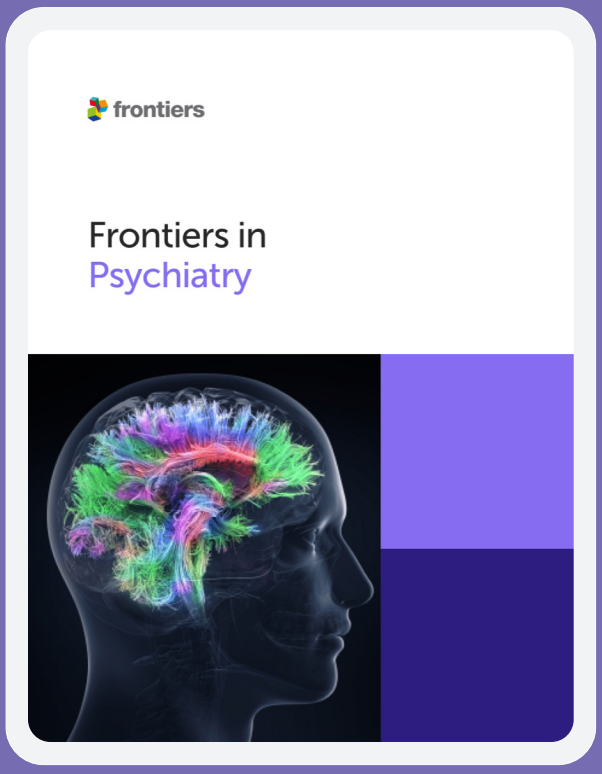

Frontiers

Avenue du Tribunal-Fédéral 34
1005 Lausanne, Switzerland
frontiersin.org

Contact us

+41 (0)21 510 17 00
frontiersin.org/about/contact